The Hong Kong Polytechnic University

Department of Applied Biology and Chemical Technology

Synthesis, Characterization and Applications of Amphiphilic Core-Shell Particles with Polyvinylamine-based Shells

LI WEI YING

A Thesis Submitted in Partial Fulfillment of the Requirements
for the Degree of Doctor of Philosophy

(Aug 2007)

CERTIFICATE OF ORIGINALITY

I hereby declare that this thesis is my own work carried out since my registration for the degree of Doctor of Philosophy in February, 2004 and that, to the best of my knowledge and belief, it reproduces no material previously published or written nor material which has been accepted for the award of any other degree or diploma, except where due acknowledgement has been made in the text.

LI WEI YING

Aug 2007

ABSTRACT

Novel routes have been developed to synthesize various amphiphilic core-shell particles that consist of well-defined hydrophobic polymer cores and polyvinylamine (PVAm)-based shells via direct graft copolymerization of vinyl monomer(s) from PVAm-based water soluble polymers, such as polyvinylamine, poly(vinylalcohol-co-vinylamine) and poly(*N*-vinylacetamide-co-vinylamine) using *tert*-butyl hydroperoxide as an initiator in aqueous system.

The PVAm-based water soluble polymers were synthesized through a two-step reaction: 1) a free-radical polymerization of *N*-vinylacetamide or *N*-vinylformamide with/without vinyl acetate in water to generate a poly(*N*-vinylalkylamide)-based polymer; 2) the hydrolysis of the preformed poly(*N*-vinylalkylamide)-based polymer to a PVAm-based polymer under acidic conditions.

The PVAm-based polymer was then treated with a small amount of *tert*-butyl hydroperoxide (TBHP) to generate free radicals that are able to subsequently initiate both graft- and homo-polymerization of vinyl monomer(s) such as *n*-butyl acrylate (BA), methyl methacrylate (MMA) and styrene to generate the amphiphilic core-shell particles. Stable and highly mono-dispersed particles were produced in high yield with diameters in the range between 100 and 300 nm. The formation of graft copolymers and homopolymers was confirmed by Fourier Transform Infrared spectroscopy (FT-IR). ζ-potential measurement suggested the formation of cationic PVAm-based shells. Transmission Electron Microscopy (TEM) micrographs of the particles revealed that they had well-defined core-shell nanostructures with thick and hairy PVAm shells. Surface morphology studies with Field Emission Scanning Electron Microscopy (FE-SEM) and particle size analysis with dynamic light scattering indicated that the structure of vinyl monomer and water-soluble polymer strongly influenced particle formation, size and morphology.

The reaction conditions were optimized via systematic investigation on reaction pH, initiator concentration, weight ratio of PVAm to MMA, salt concentration and solid content, while tailoring the shell thickness and surface functionality of particles were carried out via the variation of the molecular weight and functionality of PVAm-based polymer as well as their polymeric architectures (crosslinking degree of PVAm) with respect to the particle stability, the monomer conversion, particle size and size distribution, surface charge density, grafting percentage and efficiency, and surface morphology.

The formation of stable particles was strongly dependent on the reaction pH, weight ratio of PVAm to MMA, salt concentration and molecular weight of PVAm. The monomer conversion increased with the increase of the reaction pH, initiator concentration, weight ratio of PVAm to MMA and amination of poly (NVA-PVAm). The particle size and size distribution were able be controlled through the variation of the TBHP concentration and crosslinking degree of PVAm, while the surface functionality of the particles can be controlled by tailoring the functionality of the PVAm-based water soluble polymer. It was also found that the grafting efficiency of

PMMA increased with the increase of reaction pH and decrease of TBHP concentration.

The application of PMMA/PVAm core-shell particles in enzyme immobilization showed that they could immobilize cellulase with high capacity (up to 200 mg/g) and nearly full preservation of its activity (94%).

PUBLICATIONS ARISING FROM THE THESIS

1. Weiying LI, Pei LI. “Synthesis of Well-Defined Amphiphilic Core-Shell Particles Containing Amine-rich Shells”. *Macromolecular Rapid Communications*. **2007**, 28(23), 2267-2271.
2. Weiying LI, Pei LI. “Well-Defined Amphiphilic Core-Shell Particles Containing Amine-rich Shells: Synthesis, Characterization, and Properties”. *Journal of Polymer Science, Part A: Polymer Chemistry*. (In preparation).
3. Weiying LI, Pei LI. “Morphology Control on the Well-Defined Amphiphilic Core-Shell Particles Containing Amine-rich Shells”. *Macromolecules*. (In preparation).
4. Weiying LI, Pei LI. “Well-defined Amphiphilic Core-shell Particles with Polyvinylamine Shells”. *Polymer Preprint*, **2006**, 47(2), 975-976.
5. Weiying LI, Pei LI. “Well-defined Amphiphilic Core-shell Particles with Polyvinylamine Shells", *Abstract of Papers*, The 232nd American Chemical Society National Meeting and Exposition, San Francisco, CA, USA, Sep. 10-14, 2006
6. Weiying LI, Pei LI. “New Route to Core-Shell Particles Containing Polyvinylamine Shells, *Abstract of Papers*, *4th East-Asian Polymer Conference*, Tianjin, P.R. China, May 28-31, 2006, P-E-29.
7. Weiying LI, Pei LI. “Well-defined Amphiphilic Core-shell Nanoparticles with Polyvinylamine Shells”. *Abstract of Papers*, The 13th Symposium on Chemistry Postgraduate Research in Hong Kong, The Hong Kong University of Science and

Technology, Apr. 22, 2006.

8. Weiying LI, Pei LI. “New Route to Amphiphilic PMMA Particles with Polyvinylamine Shells”. *Abstract of Papers*. The 12th Symposium on Chemistry Postgraduate Research in Hong Kong, City University of Hong Kong, Apr. 23, 2005.

ACKNOWLEDGMENTS

First and foremost, I would like to express my deepest gratitude to my supervisor, **Dr. Pei Li**, for her generous guidance, supervision, patience and critical advices throughout my study and her valuable comments and revisions on the manuscript of this thesis. It is a rewarding experience for me under the supervision of Dr. LI.

Dr. Lijun Li and **Dr. Xuepu Mao** helped me doing the measurements on the applications of my project. Here I would like to give my special thanks to them for their hard works and enthusiasm.

I would also like to thank all our group members, **Dr. Yong Jin**, **Dr. Cheng Chen**, **Dr. Xinhua Zhang**, **Dr. Aihua Wu**, **Dr. Man Fei Leung, Dr. Kin Man Ho** and all others**,** for their valuable suggestion, enthusiastic support and assistance during my study. They also have helped me to have a wonderful time in Hong Kong.

I would also like to express my gratitude to all academic and technical staffs of the Department of Applied Biology and Chemical Technology and Department of Applied Physics at The Hong Kong Polytechnic University, who have helped me in various ways during my study.

I must thank my entire family, my wife and my daughter, my parents and parents-in-law, who have given the invaluable support and encouragement over the years of my study. I would get nothing without their physical and mental support.

Finally but not the last, I gratefully acknowledge the Research Committee of The Hong Kong Polytechnic University and University Research Grants Council of the Hong Kong SAR (Project No. PolyU5007/03P) for the financial support of this project and for a grant supporting my conference presentation in the 232nd American Chemical Society National Meeting held in San Francisco in September, 2006.

TABLE OF CONTENTS

Chapter 4 Synthesis of PMMA/PVAm Core-Shell Particles 127

Chapter 9 PMMA/PVAm Core-shell Particles as a Potential Carrier for Enzyme Immobilization 276

ABBREVIATIONS AND SYMBOLS

Abbreviations

AA	acrylic acid
AAm	acrylamide
ATRP	atom transfer radical polymerization
BA	n-butyl acrylate
BSA	bovine serum albumin
CHPO	cumene hydroperoxide
CMC	sodium carbonxy methyl cellulose
DNS	3,5-dinitrosalicylic acid
FS	ferrous sulfate
FT-IR	Fourier transform infrared Spectroscopy
GA	glutaraldehyde
HCl	hydrochloride
HDI	hexamethylene diisocyanate
HEA-Cl	2-(2`-Chloropropionato)ethyl acrylate
HMEM	2-[*p*-(2-hydroxy-2-methylpropiophenone)]-ethylene glycol-methacrylate
HMTETA	1,1,4,7,10,10-hexamethyltriethylenetetramine
KPS	potassium persulfate
MAA	Methacrylic acid
MEA	*N*-(2- methoxyethyl)acrylamide
MF	melamine formaldehyde
NaDC	N,N-diethyldithiocarbamate
NIPAM	*N*-isopropylacrylamide
NMR	Nuclear magnetic resonance
NVA	*N*-vinylacetamide
NVF	*N*-vinylformamide
PAA	polyacrylic acid
PAAm	poly(acrylamide)
PAH	poly(allylamine hydrochloride)
poly(BA-MMA)	poly(*n*-butyl acrylate-methyl methacrylate)
PCEMA	poly(2-cinnamoyethyl methacrylate)
PDI	the polydispersity index
PDMA	poly(N,N-dimethylacrylamide)
PDMAEMA	poly(2-(dimethylamino)ethyl methacrylate)
PEG	poly(ethylene glycol)
PMEA	poly(methoxyethylacrylamide)
PMAA	poly(methacrylic acid)
PMMA	poly(methyl methacrylate)

PNVA	poly(*N*-vinylacetamide)
PNVF	poly(*N*-vinylformamide)
PS	polystyrene
PSS	poly(styrenesulfonic acid)
poly(VA-VAm)	poly(vinyl alcohol-vinylamine)
poly(VAc-NVA)	poly(vinylacetate-*N*-vinylacetamide)
PVAm	polyvinylamine
PVA	poly(vinyl alcohol)
PVAmHCl	poly(vinylammonium chloride)
SEM	Scanning electron microscope
SS	styrenesulfonic acid
SWNT	Single-wall carbon nanotube
MWNT	Multi-wall carbon nanotube
St	styrene
TBHP	*tert*-butyl hydroperoxide
TEM	Transmission electron microscopy
TMTD	tetramethylthiuram disulfide
TPA	terephthal aldehyde
UV	Ultraviolet
V-50	2,2`-azo-bis(2-amidinopropane) dihydrochloride
VBC	vinyl benzylchloride
p-XDC	*p*-xylene dimethyldithiocarbamate

Symbols

Conv.	monomer conversion
D_v	the volume average of particle diameter
D_n	the number average of particle diameter
E_{imm}	efficiency of immobilization
E_{spe}	specific cellulase activity
GP%	grafting percentage
GE%	grafting efficiency
SC%	solid content
ζ	Zeta

Chapter 1 Introduction

1.1 Importance of amphiphilic core-shell polymeric particles

Particles with core-shell structures often exhibit improved physical and chemical properties over their single-component counterparts, and are potentially useful in a broader range of applications. Thus, there have been immense efforts to fabricate core-shell colloidal materials with tailored structural, optical, and surface properties over the last few decades. Among them, amphiphilic particles that consist of well-defined hydrophobic cores and hydrophilic shells or vice versa, have attracted a great deal of attention because of their applicability in modern materials science, and their technological importance in the areas of colloid and interface science. [1] For example, amphiphilic core-shell particles have been utilized in the areas of diagnostics, bioseparations, drug delivery and carrier, gene therapy, coatings, electronics and catalysis.[2] One important advantage of having a polymer shell on the particles is that the shell could provide a charged functional and reactive surface, and improve the stability and dispersibility of the particles. It can also protect the core from extraneous chemical and physical changes. Therefore, much interest has been devoted to the development of methodologies for the engineering of the amphiphilic core-shell particles.

Here, we provide an overview of the various methodologies previously reported for the synthesis of amphiphilic core-shell particles, focusing on those particles that comprise solid polymer cores coated with polymers or biomacromolecules. Other particles that consist of liquid colloidal (e.g., emulsions) and inorganic cores (e.g., SiO_2 or TiO_2) will not be covered here. In addition, conventional routes to core-shell particles through batch or semi-batch emulsion polymerization are not discussed.

1.2 Current methodologies for the preparation of amphiphilic core-shell particles

There are six methodologies developed recently that offer new alternatives for the controlled fabrication of well-defined amphiphilic core-shell particles. They are: 1) the "grafting to" approach, which is the linkage of polymer chains onto a polymer particle through functional groups on both the polymer chain end and particle surface; 2) the "grafting from" approach, which is the graft copolymerization of hydrophilic monomers from the reactive surface of hydrophobic seed particles; 3) the free radical copolymerization of hydrophilic macromonomers or surfmers with hydrophobic monomers in an aqueous medium; 4) the assembling of amphiphilic block copolymer followed by covalent cross-linking of the core or shell part; 5) the stepwise deposition of polyelectrolytes onto charged particle surfaces; and 6) the graft copolymerization of vinyl monomer from a water-soluble polymer containing amino groups, which has been developed in our laboratory.

1.2.1 "Grafting to" approach

The "grafting to" approach is a simple route to fabricate amphiphilic core-shell particles. It involves the reaction between end-functionalized polymer chains and reactive functional groups located on the hydrophobic cores. The grafted polymers on the particle surfaces result in the formation of tethered brushes or corona. For example, Jayachandran and Chatterji[3] used a diisocyanate-coupling reaction to covalently link poly(ethylene glycol) (PEG) chains of a desired molecular weight to the amino-containing surfaces of polystyrene (PS) cores, generating a structurally well-defined PS-PEG core-shell particles (Scheme 1.1). The "grafting to" route can also be performed via the Decker-Forster reaction by grafting poly(ethylene oxide) (PEO) with Schiff's base end group onto chloromethylated PS[4] (Scheme 1.2), or via the carbodiimide chemistry by covalently grafting amino-PEG onto carboxyl PS particles[5] (Scheme 1.3), or via cyclic *trans*-acetalization by grafting PEO grafts bearing a α-bis(hydroxymethyl) chain end onto ω-acetal functionalized branches of PS precursor[6](Scheme 1.4), etc.

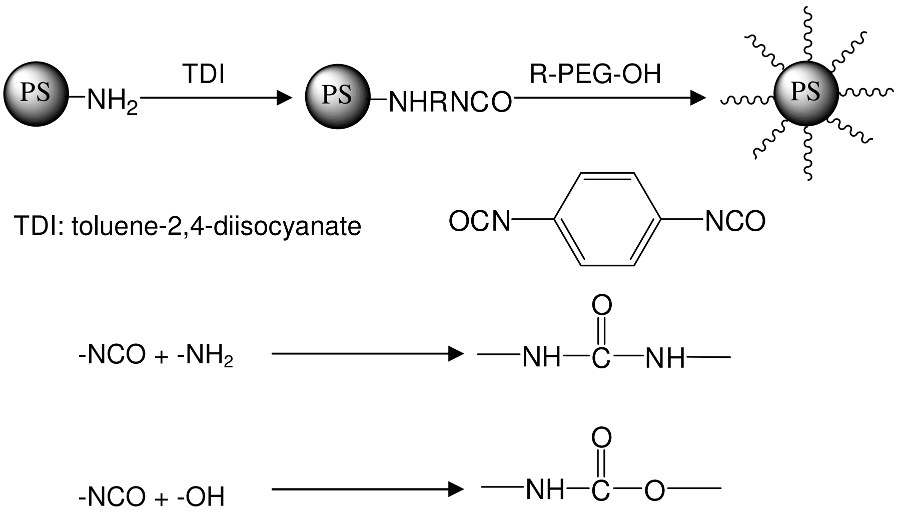

Scheme 1.1 Synthesis of PS-PEG core-shell particles using a diisocyanate-coupling reaction

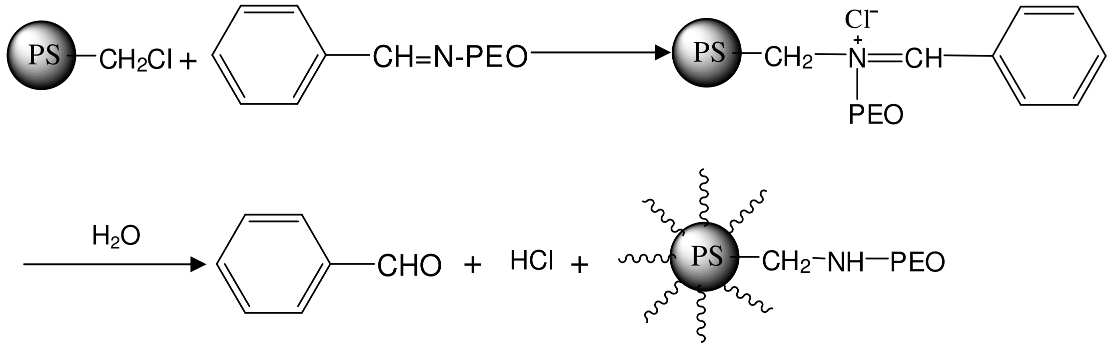

Scheme 1.2 Synthesis of PS-PEG core-shell particles via the Decker-Forster reaction

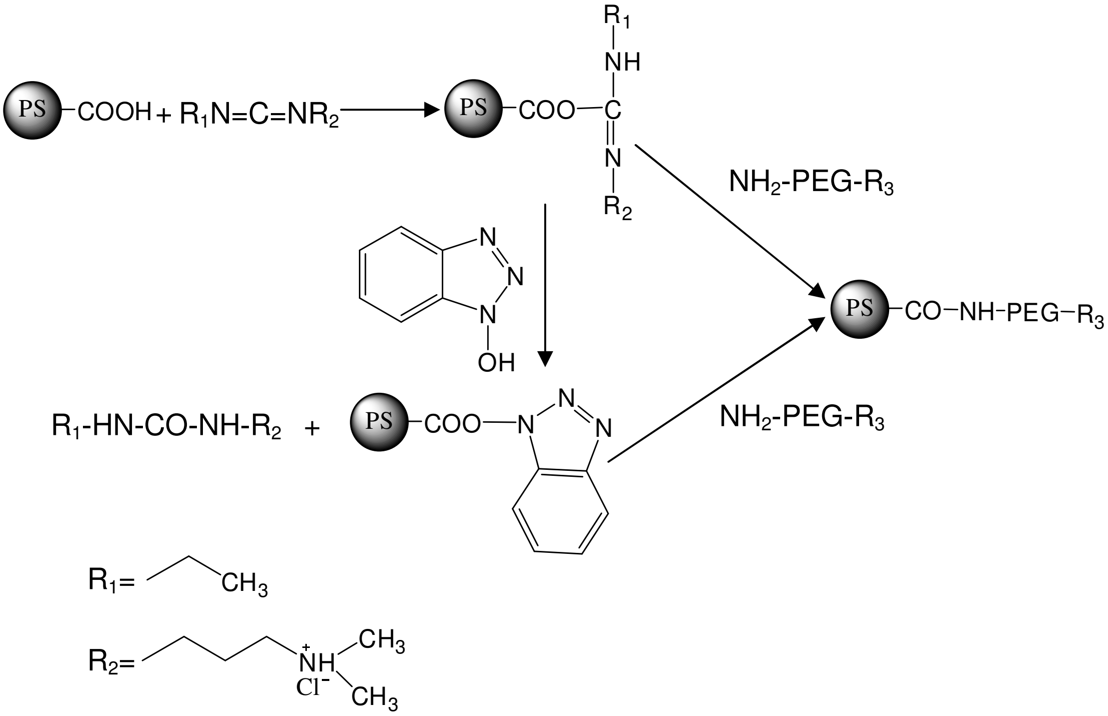

Scheme 1.3 Modification of PS-COOH particles with PEG via carbodiimide chemistry.

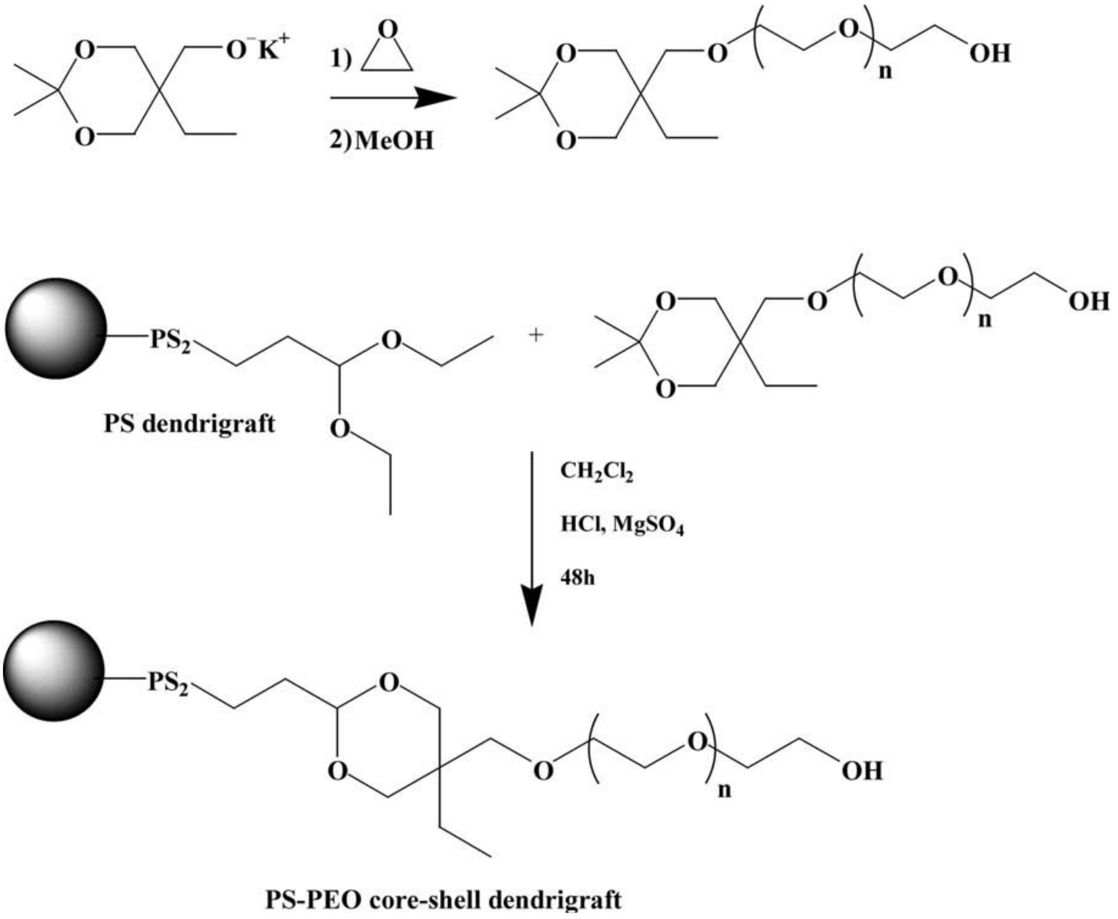

Scheme 1.4 Route to PS–PEO core–shell dendrigraft through cyclic trans-acetalization.

Besides its feature of simplicity, the “graft to” strategy allows an accurate characterization of the resulting copolymers since the attached polymer fractions can be characterized separately. Polymer fractions with narrow molecular weight distributions can be used to graft to the surface. One disadvantage of this method is that it is difficult to achieve high grafting densities because the diffusion of the polymer chains to the particle surfaces for reaction becomes increasingly more difficult as the grafting density increases. Furthermore, the thickness of the corona layer is limited by the molecular weights of the polymer in solution (coronas in the range of 100 nm thickness become inaccessible).[7] Because of this inherent limitation of the “graft to’ approach, there is an increasing attention focusing on “grafting from” technique, in which polymers are directly generated on the particle surface by surface-initiated polymerization.[7, 8]

1.2.2 “Grafting from” approach

The “grafting from” technique is an alternative way to produce “polymer brushes”. Comparing to the “grafting to” technique, it can control the functionality, grafting density and thickness of polymer brushes, which are critical parameters to precisely manipulate the surface properties of well-defined core-shell particles. A review on this subject has been published recently.[7]

The “grafting from” technique can be realized by two methods. One of them is the conventional radical graft copolymerization, by which the average chain length is kept constant, but the density of the polymer brushes increases with the increase of the monomer conversion. Another method is the living radical graft copolymerization, by which the density of the polymer brushes is unchanged, but the length increases with the increase of the monomer conversion. Of the two methods, the living radical graft polymerization has attracted more attention recently because it has a number of advantages such as: 1) a good control over the molecular weight, molecular weight distribution and the structure of the resulting polymer chains; 2) a controllable chain length (i.e., to obtain a controlled shell thickness); 3) a controllable polymer brush density. Therefore, it is widely used in the design and synthesis of well-defined core-shell particles.

A typical procedure for the “grafting from” technique based on the conventional radical graft copolymerization is as follows. A seeded latex containing functional groups is first prepared by the emulsion polymerization of a hydrophobic monomer, followed by the graft radical copolymerization of a water soluble monomer to form amphiphilic core-shell particles. The functional group can be an initiator or a group which can form a redox system with another group to initiate the graft copolymerization. Scheme 1.5 illustrates the general approach.

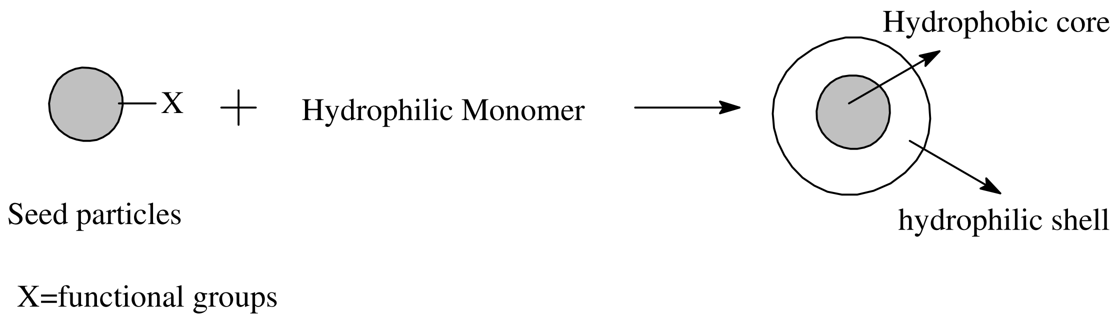

Scheme 1.5 The living radical graft copolymerization of a hydrophilic monomer onto reactive seeded particles.

A number of initiating systems based on the “grafting from” approach to synthesize amphiphilic core-shell particles have been developed. These include photo-initiator[9-15], Ce(IV)-initiated system[16-18], cumene hydroperoxide and ferrous sulfate redox system,[16, 19, 20] and ATRP initiator[21-29].

The graft polymerization using the photo-iniiator is composed of two steps: i) the synthesis of core particles having the photo-initiator groups on the surface; ii) the graft polymerization of monomers onto the core particles via UV-irradiation. For example, R. Saito et al[9] prepared poly(methyl methacrylate)/poly(acrylamide) (PMMA/PAAm) amphiphilic core-shell particles by grafting the second monomer acrylamide (AAm) onto the PMMA seed microspheres in water by UV irradiation via the living radical graft polymerization using the living radical initiators, tetramethylthiuram disulfide(TMTD) or *p*-xylene dimethyldithiocarbamate(*p*-XDC) (Scheme 1.6). Kawaguchi et al[10-12] reported an approach using a photo-initiator, sodium N,N-diethyldithiocarbamate (NaDC) at room temperature to prepare hairy particles consisting of thermo-sensitive poly(*N*-isopropylacrylamide) (PNIPAM) hair (Scheme 1.7). M. Ballauff's group presented a method for the synthesis of well-defined particles having a PS core and a shell of polyacrylic acid (PAA)[13,14] or poly(styrenesulfonic acid) (PSS)[15] chains with 2-[*p*-(2-hydroxy-2-methylpropiophenone)]-ethylene glycol-methacrylate (HMEM) as a photoinitiator (Scheme 1.8). Since the seeded microspheres do not absorb the hydrophilic monomer, grafting could only occur on the surface of the seed microspheres, but not inside the seed microspheres. The particles thus obtained have well-defined core-shell morphology with a narrow size distribution. However, because of the unavoidable chain transfer reaction by the initiator,[30] the efficiency of the living radical polymerization was not high enough, thus a significant amount of the hydrophilic monomer was retained through the dissolution in the aqueous phase[12].

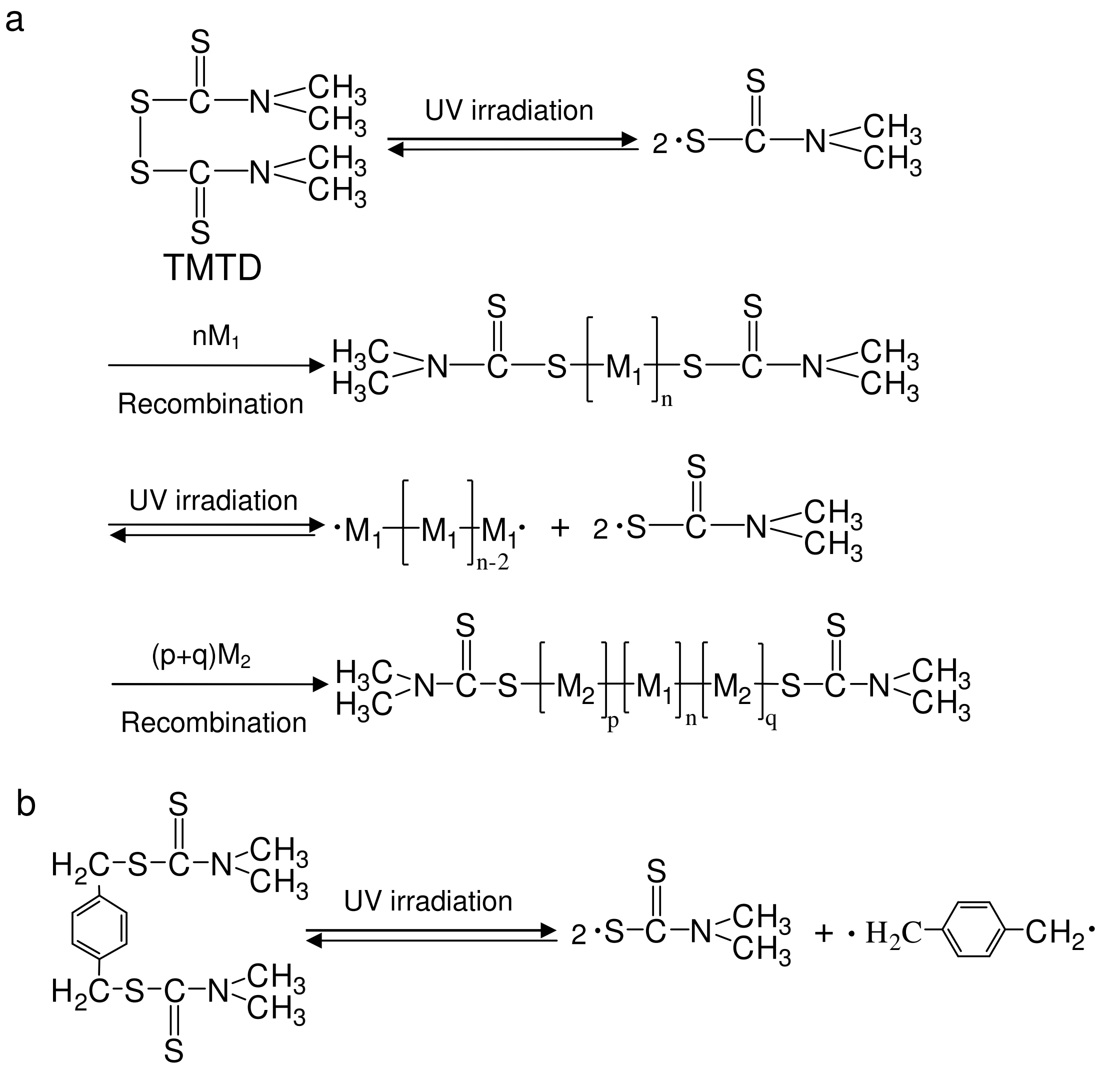

Scheme 1.6 The synthesis of core-shell particles by the UV irradiation via the living radical graft polymerization using the living radical initiators, (a) tetramethylthiuram disulfide(TMTD) or (b) *p*-xylene dimethyldithiocarbamate(*p*-XDC)

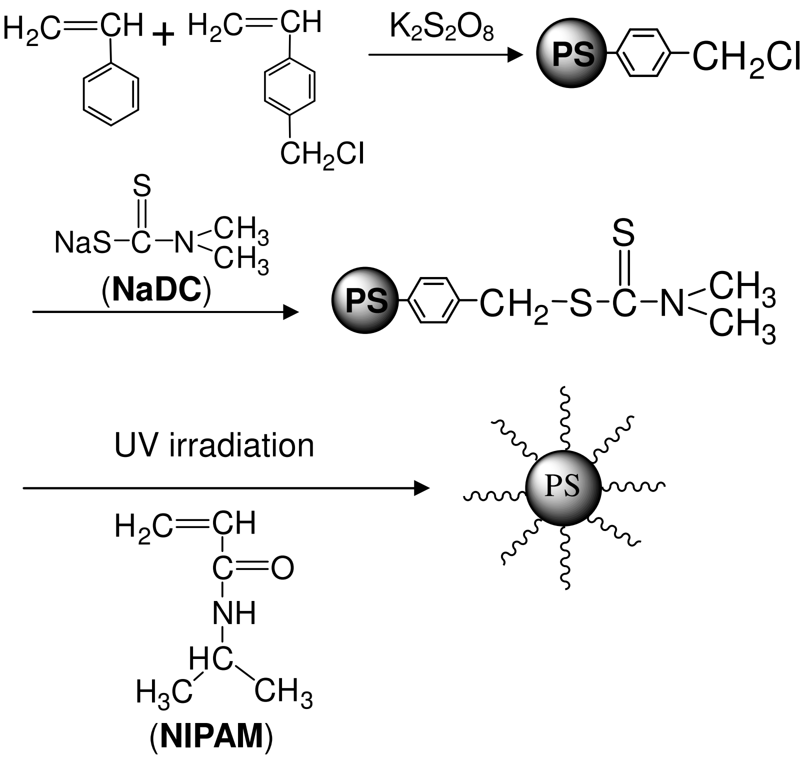

Scheme 1.7 The preparation of PS/PNIPAM hairy particles using sodium *N*,*N*-diethyldithiocarbamate (NaDC) as a photo-initiator.

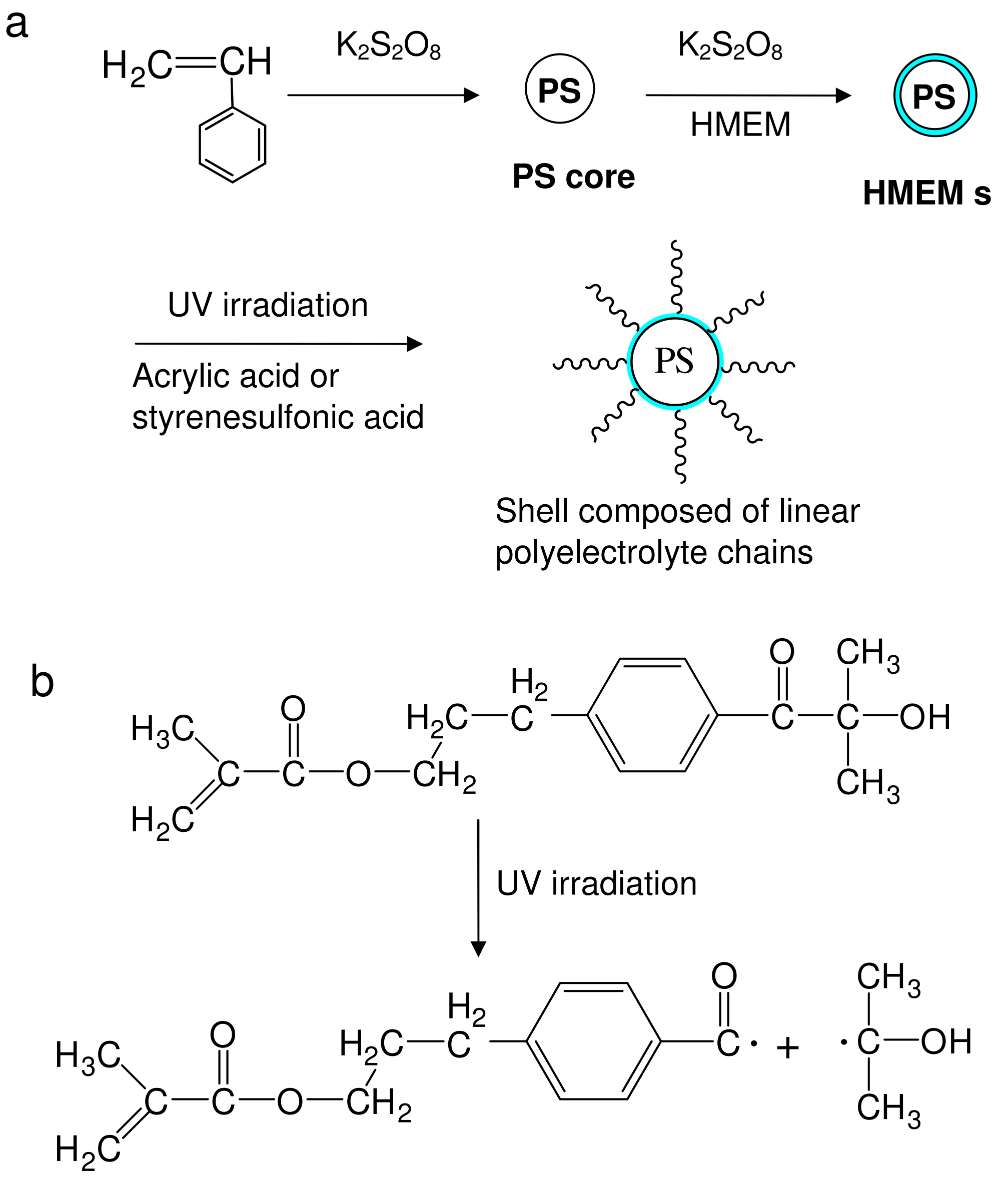

Scheme 1.8 The synthesis of core-shell particles with polyelectrolyte brushes using photoinitiator, HMEM. (a) a general procedure; (b) the decomposition of HMEM into radicals during the photo-initiation

Another method is the graft polymerization of a monomer from OH-containing core particles using ceric ion through a redox initiation mechanism at room temperature. In this initiation system, the hydroxyl groups react efficiently with Ce(IV) ions in an aqueous media[16]. The polymerization mechanism involves a complex formation between Ce(IV) ions and reducing groups such as –OH, followed by the generation of a free radical which initiates the polymerization of vinyl monomer[17](Scheme 1.9). For instance, a Ce(IV)-initiated grafting of *N*-(2-methoxyethyl acrylamide) (MEA) to a shell of poly(styrene-co-2-hydroxyethyl acrylate) on PS seed particles has been reported by Brooks et al[18, 31], as shown in Scheme 1.10. Cationic PS particles were first covered with a shell containing poly(styrene-*co*-2-hydroxyethyl acrylate) by a seed copolymerization using an azo initiator. In the second step, grafted chains anchored to the surface were produced by the polymerization of MEA, in the presence of Ce(IV) as a redox initiator.

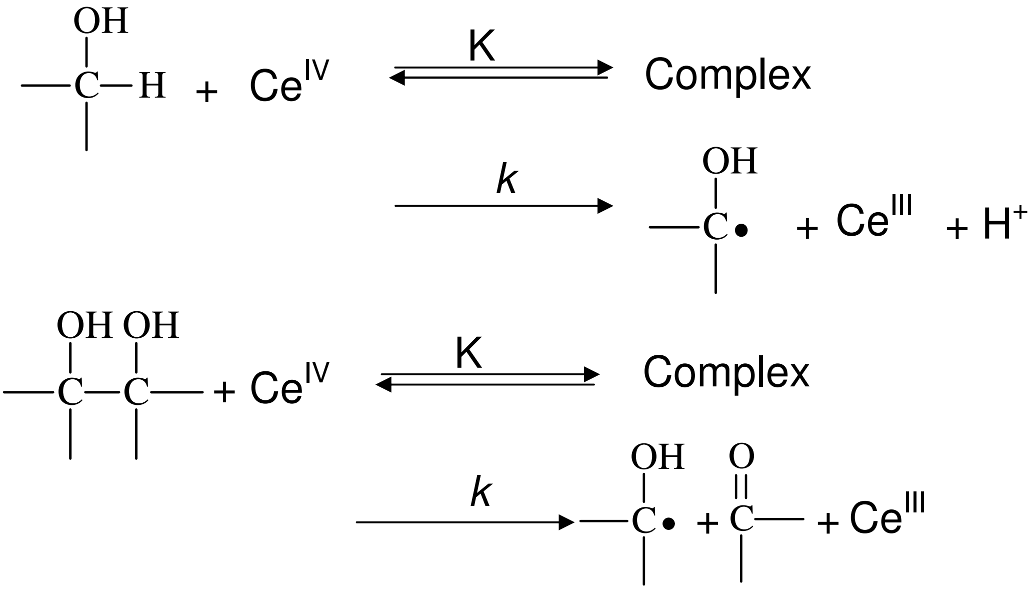

Scheme 1.9 The generation of free radicals from the reaction between Ce(IV) ions and –OH groups

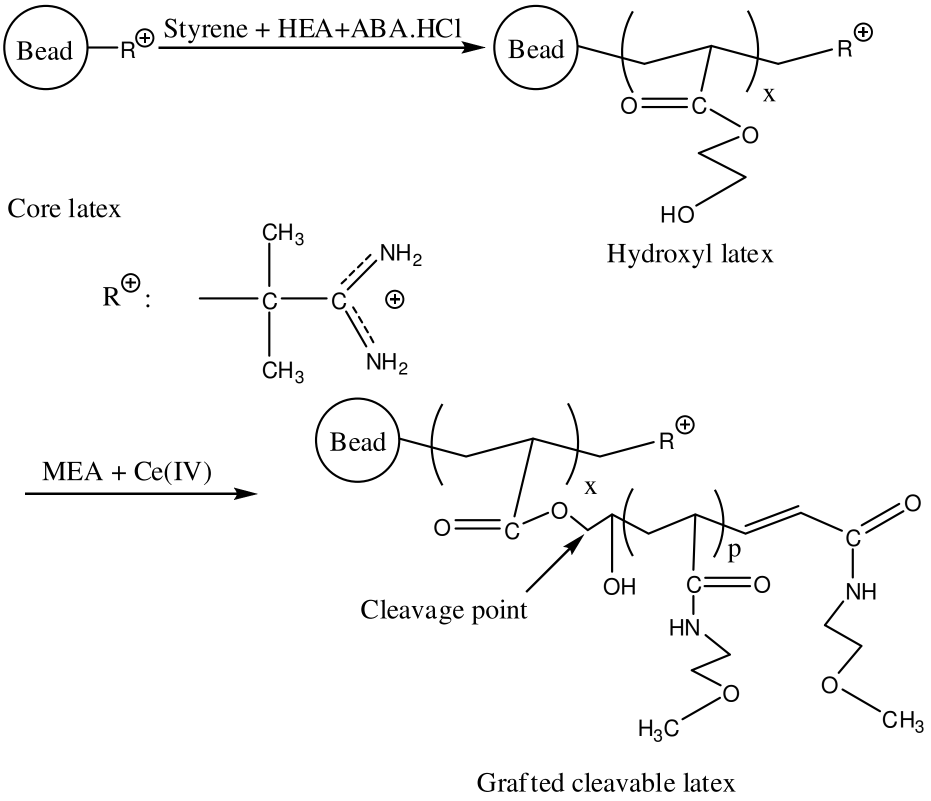

Scheme 1.10 The synthesis of poly(syrene) latex carrying cleavable grafted chains.(Reproduced from reference[18])

A major problem associated with this approach is its extremely low grafting percentage onto the particle surface. Mass balance calculations indicate that two kinds of polymer were formed during the reaction. One dissolved in solution and the other grafted polymer on the beads. The percentage of MEA covalently attached to the surface was only 0.3-2.1% of the total amount of polymerized MEA. Such low grafting efficiency may be attributed to the hydroxyl-containing polymer chains desorbed from the beads during grafting, resulting in the homopolymerization of MEA in water, and forming MEA homopolymer. In other words, there is a large amount of MEA homopolymer dissolving in water, thus an extra purification process is required.

Another redox system to prepare amphiphilic colloidal particles with hydrophobic cores and hydrophilic shells contains cumene hydroperoxide(CHPO) and iron(II) ions[19, 32] (Scheme 1.11). The polymerization includes a two step procedure. First, PS cores were obtained through an emulsion polymerization. A mixture of Styrene (St), ethyl benzene, divinyl benzene, and CHPO was partially polymerized using azobisisobutyronitrile as an initiator and subsequently used as a dispersed phase of a concentrated emulsion in water. The concentrated emulsion was subjected to complete polymerization and colloidal particles of crosslinked PS were thus obtained. In the second step, the PS particles were dispersed in water followed by the addition of acrylamide, *N,N'*-methylenebisacrylamide and ferrous sulfate (FS). Then the polymerization of the hydrophilic monomers was conducted via the CHPO present on the surface of the PS particles and the FS present in the aqueous phase (they together constitute a redox initiator). The bi-phase reaction ensured that initiation occurred mostly on the surface of the particles. The hydrophilic polymer obtained formed shells of the particles. With a crosslinking agent, a porous outer shell could be generated, making the hydrophobic core accessible to the outside medium.

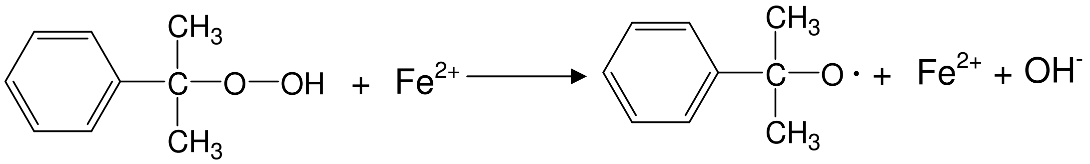

Scheme 1.11 The generation of free radicals from the reaction between CHPO and iron (II) irons

Atom transfer radical polymerization (ATRP), a living radical graft polymerization, is of particular interest because of its tolerance to different reaction conditions and monomer functionality, its ability to produce narrowly distributed polymer chains and the possibility of synthesizing controlled block copolymers. Although ATRP in organic systems has been reported extensively, investigations of aqueous ATRP at room temperature have only been reported recently and attracted increasing interest[33-36].

Brooks et al first reported the controlled synthesis of PNIPAM brushes by aqueous ATRP at room temperature.[26-29] PNIPAM was grown from negatively charged PS particle surfaces, which were functionalized with ATRP initiators, to achieve high molecular weights and a narrow polydispersity (Scheme 1.12). This method involved the following steps: i) PS seed particles with narrow polydispersity were synthesized in a batch reaction by a surfactant-free emulsion polymerization of styrene; ii) An ATRP layer was synthesized on the PS seed particles through a shell polymerization of styrene and 2-(2`-Chloropropionato)ethyl acrylate (HEA-Cl) using potassium persulfate (KPS) as an initiator; iii) NIPAM was grafted from the above particles containing the ATRP layer with 1,1,4,7,10,10-hexamethyltriethylenetetramine (HMTETA)/CuCl/$CuCl_2$/Cu powder under stirring at room temperature. Using this approach, lparticles bearing well-defined temperature-responsive polymer brushes consisting of poly(N,N-dimethylacrylamide) (PDMA), poly(methoxyethylacrylamide) (PMEA), PNIPAM, PMEA-*b*-PNIPAM[24-26] and poly(2-(dimethylamino)ethyl methacrylate) (PDMAEMA) [21] in aqueous media were prepared.

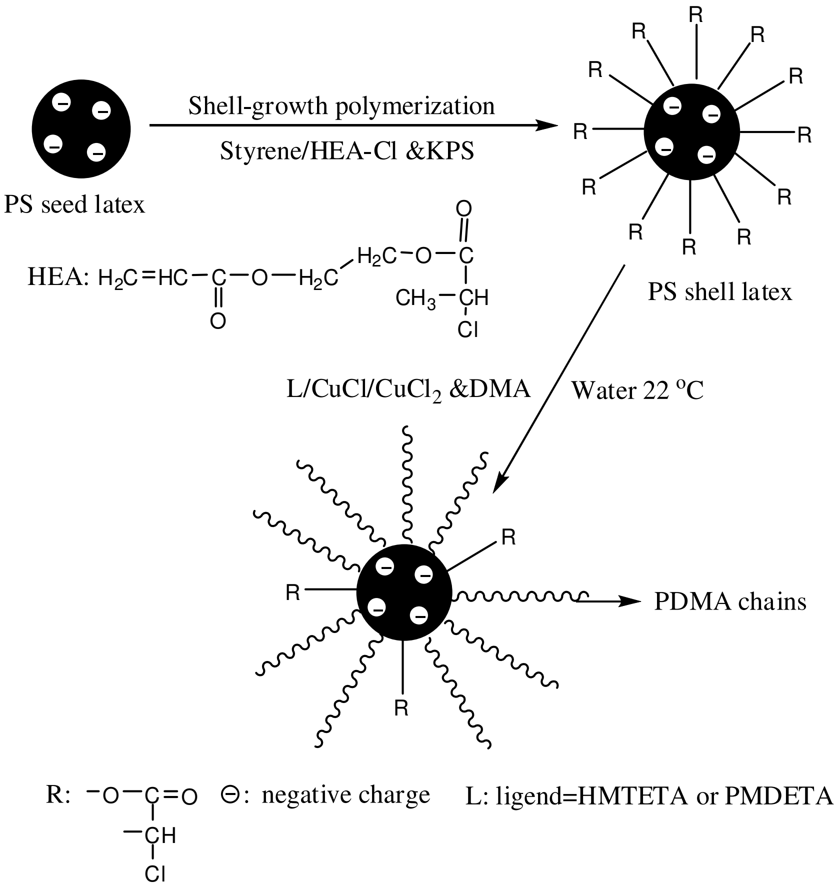

Scheme 1.12 Surface functionalization and aqueous ATRP on PS latex particles. (Reproduced from reference [28])

A problem existing in this approach is that extra cleaning procedures are needed after the grafting reaction. The grafted latex has to be purified by repeated centrifugation-decantation-re-suspension cycles with water and $NaHSO_3$ solution to remove adsorbed copper complexes (8-10 cycles) until there is no detectable amount of polymer, monomer, or catalyst in the supernatant.

1.2.3 Copolymerization of reactive macromonomer with hydrophobic monomer

The preparation of amphiphilic core-shell particles using the macromonomer method was first developed by Akashi and his co-workers[37]. It was achieved by free radical dispersion polymerization or emulsion copolymerization of a hydrophilic vinyl-terminated macromonomer and a hydrophobic monomer in a polar solvent (Scheme 1.13). The macromonomer is a chemical substance containing highly reactive terminal vinyl groups. Its molecular weight is of the magnitude of 10^3 or 10^4. This method allows us to synthesize well-defined novel structure and multiphase composite particles composed of macromonomers and other polymers. In addition, the stability of the latexes can also be improved because the macromonomer are not desorbed from the particle surface, even after washing.

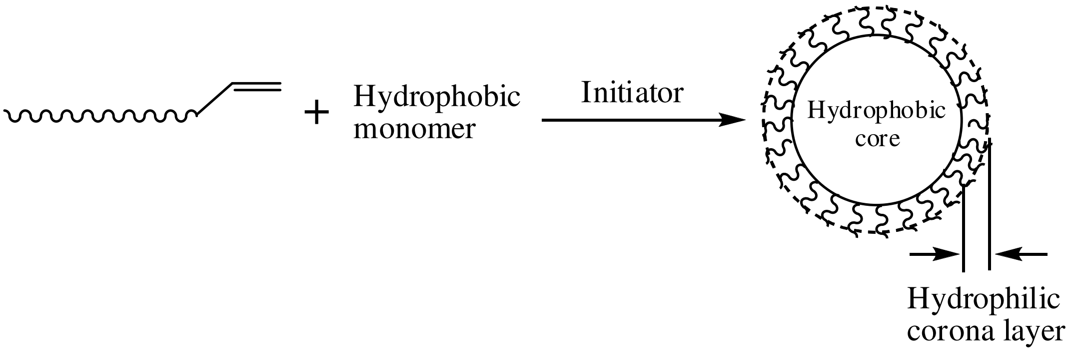

Scheme 1.13 The preparation of amphiphilic core-shell particles via macromonomer methods.

Various amphiphilic core-shell polymeric particles with functional polymeric coronas have been prepared via the macromonomer method by designing and synthesizing various functional hydrophilic macromonomers, such as oligovinylpyrrolidone[37], poly(ethylene glycol)[38-49], poly(2-oxazoline)[50, 51], poly(2-ethyl-2-oxazoline)[52] poly(*N*-isopropylacrylamide)[53-57], poly(4-vinyl-N-n-butylpyridinium bromide)[58], poly(tert-butyl methacrylate)[59], poly(methacrylic acid)[60-62], poly(vinyl alcohol)[63], poly(vinylamine)[64], poly(acrylic acid)[65, 66], poly(N-vinylisobutyramide)[67], poly(2-methacryloyloxyethyl phosphorylcholine)[68], poly(N-vinylformamide)[69], glucosyloxyethyl methacrylate (GEMA) oligomer[70], α-*tert*-butoxy-ω-vinylbenzyl-polyglycidol[71, 72], polyurethane[73-78], etc.

In spite of the success of this approach, there are still some major drawbacks. For example, only very thin hydrophilic shell layers could be prepared because fine, monodispersed amphiphilic particles could only be obtained when macromomonomers with a relatively low molecule weight were used. macromonomers with a high molecule weight are often not suitable due to extensive particle aggregation.[79]

1.2.4 Self-assembly processes of amphiphilic block copolymers

1.2.4.1 Shell crosslinked knedel-like nanoparticles

Shell-crosslinked knedel-like particles (SCKs) are a class of well-defined, polymeric nanostructured materials, which have an amphiphilic core-shell morphology composed of hydrophobic cores and hydrophilic shells.[80-120] The general synthetic approach for the preparation of SCKs involves the supramolecular assembly of block copolymers into polymer micellars, followed by a covalent intramicellar crosslinking reaction throughout the shell layer. The general chemical process is depicted in Scheme 1.14.[111] The uniqueness of the SCK synthesis is that the incorporation of cross-linkable functional groups along the peripheral block of micelles allows for the polymerization of the exterior layer and gives stability to the micellar assembly.

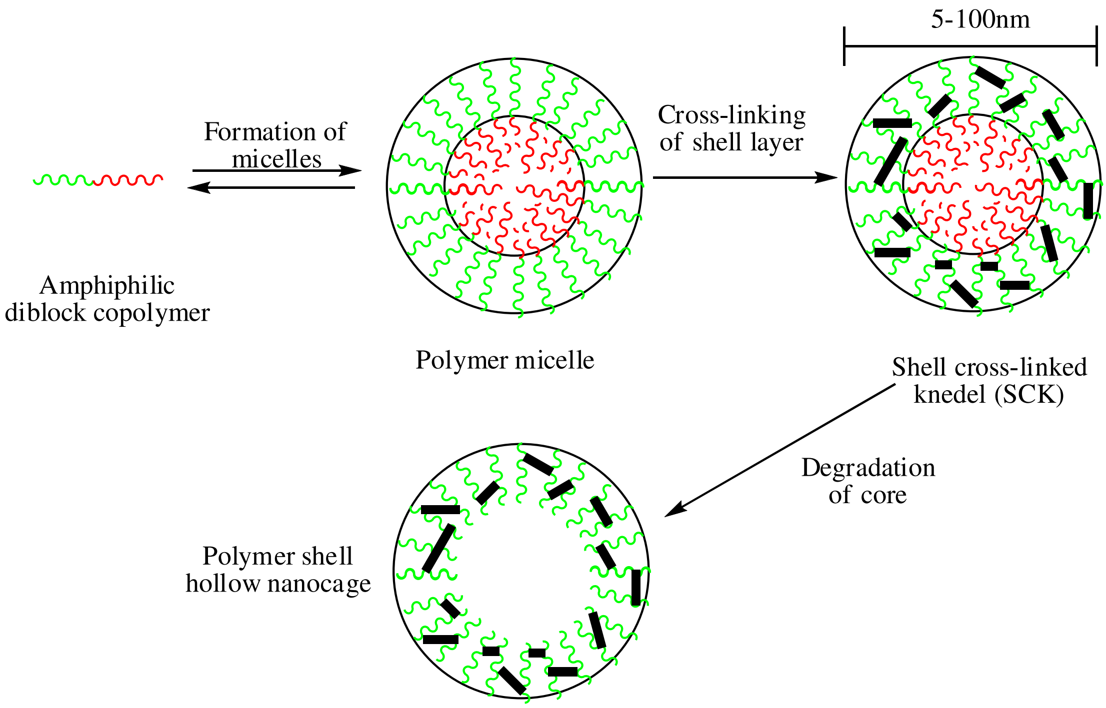

Scheme 1.14 The general synthetic approach for the preparation of shell crosslinked knedel-like (SCK) polymer assemblies involves a combination of self-assembly and covalent stabilization

There are several important properties of the SCK nanoparticles: 1) The dimensions of the core-shell particles range from 5 to 100 nm in diameter with a narrow size distributions. 2) The core and shell of the SCKs are chemically attached while possessing different physical and chemical properties. 3) The rigidity, reactivity, size, shell thickness, core diameter, penetrability, and stability of the structures of SCKs can be easily tailored through variations of the cross-link density, the crosslinkable-block length, and the composition and properties of the block copolymers. 4) The lack of crosslinks in the core region maintains chain mobility and access to the core volume. Because of the stability that the crosslinked shell provides, the core domain can be of dramatically different compositions and properties. For example, glassy, fluidlike and crystalline polymer chains have been employed for the core materials. 5) The most significant aspect of the shell crosslinking is that it provides the opportunities to subsequently modify the initial SCK nanostructures. Scheme 1.14 shows the removal of the core to generate hollow nanoscale cage-like structures[94, 121, 122].

Block copolymers with hydrophobic and hydrophilic segments have been employed in this approach. The assembling process occurs in an aqueous solution. The structure and composition of the amphiphilic block copolymer play a critical role because they determine the nature of the assembly of the polymer that serves as the precursor, as well as the physical and chemical properties of the SCKs. Diblock and triblock copolymers are the common ones to be used. They are prepared through either living anionic[119] or living free radical[103, 108, 123-127] polymerization methods.

After the assembly of the micellar nanoparticles, the crosslinking of the shell is an important step to provide the assembled nanoparticles stability. Various methods utilizing different cross-linking chemistries have been developed to generate SCK nanoparticles with a broad range of compositions, dimensions, and properties. For example, shell crosslinking is through the radical polymerization of styrenyl side groups of *p*-chloromethylstyrene-quaternized poly(4-vinylpyridine) throughout the shell of poly(styrene-*b*-4-vinylpyridine) micelles (Scheme 1.15).[113, 120, 128] No change was observed in dimension of the polymer micelles upon cross-linking, and the diameters of the polymer micelles and SCKs were equivalent. The positively charged, quaternized sites throughout the shell of the SCKs are advantageous for the stability of the nanoparticle suspension. They also facilitate the electrostatic binding interactions of the SCKs with small (e.g. dye molecules) and large (e.g. DNA) negatively charged species.

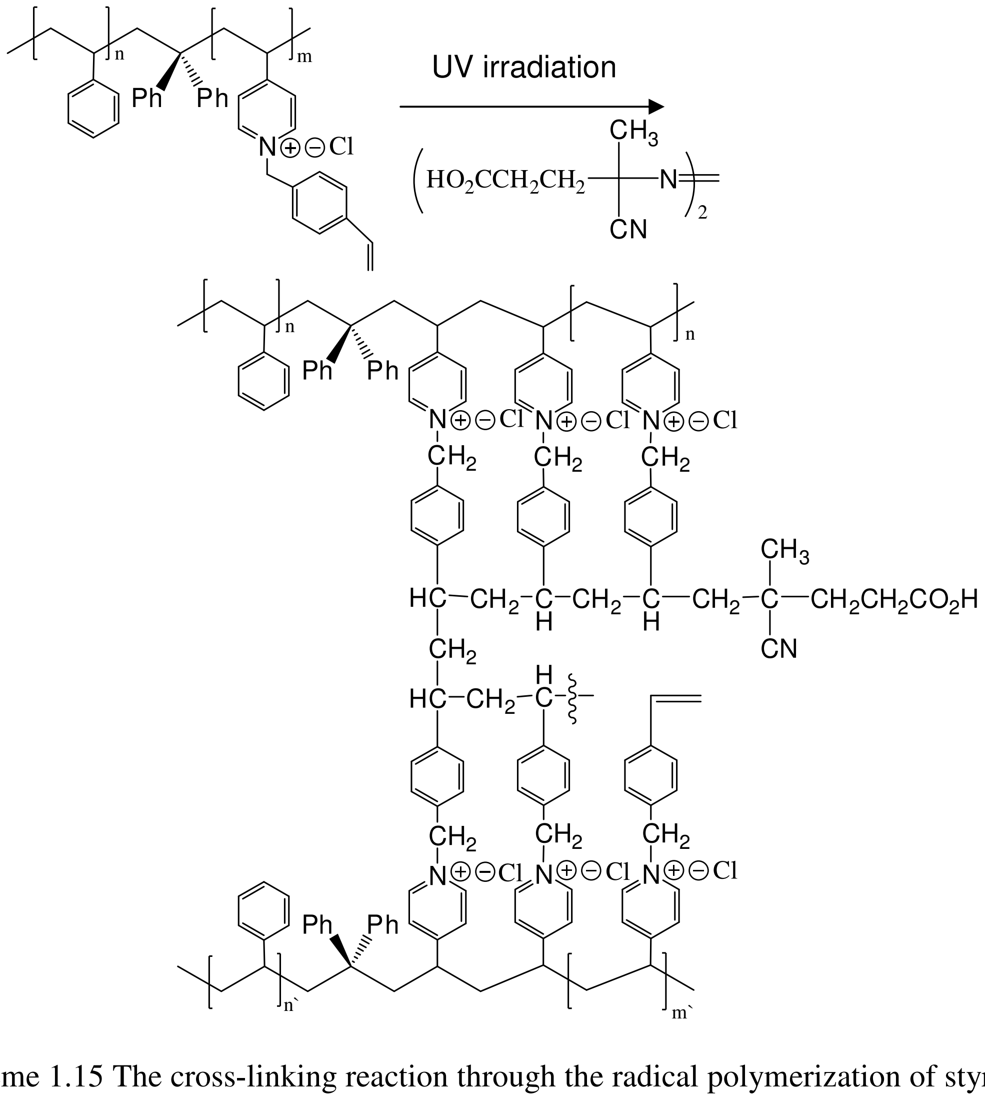

Scheme 1.15 The cross-linking reaction through the radical polymerization of styrenyl side groups of *p*-chloromethylstyrene-quaternized poly(4-vinylpyridine) throughout the shell of poly(styrene- *b*-4-vinylpyridine) micelles.

(Reproduced from reference [120])

Another shell crosslinking approach involves the reaction of multifunctional cross-linking reagents within the polymer micelle shell layer. For example, Wooley's group uses carbodiimide coupling chemistry to link carboxylic acid groups through diamines.[110, 115, 119, 129] Several di- and multi-amino linkers such as 2,2'-(ethylenedioxy)bis(ethylamine), hexakis(ethylene glycol) diamine, hexamethylenediamine, and triethylenetetramine), difunctional poly(ethylene oxide) amd polyacrylamide have been used. The composition of the diamino cross-linker and the extent of cross-linker incorporation dictate the shell composition and properties. Therefore, a variety of SCK nanospheres could be prepared from the same block copolymer precursor. Unlike the shell cross-linking reactions that are accomplished by polymerization of the side chain functional groups, the incorporation of cross-linkers allows for the alteration of the shell properties and increases shell (and overall particle) dimensions. For example, the use of a relatively long chain cross-linker, 2,2`-(ethylenedioxy)bis(ethylamine), imparts a hydrogel-like character to the shell, which causes the swelling of the shell to 2–3-fold increase in thickness in water. The hydrogel character and the shell thickness increase with the increase of the chain length of the cross-linker [e.g., hexakis(ethylene glycol) diamine, and even further to diamino-terminated poly(ethylene glycol)].[115] Furthermore, only a fraction of the acrylic acid sites is required to react with the crosslinking agent in order to form a stabilizing network. The remaining functional groups are available for surface modifications to specific binding, recognition, etc. However, This approach has two major drawbacks: 1) Tedious synthetic procedures to prepare block copolymers and crosslinking of the shells; 2) It can only be performed at very low solid cotents (<1%). Thus it is not a commercially viable approach.

To address these limitations, new SCK particles using 1,2-bis-(2-iodoethoxy)ethane (BIEE) as a bifunctional cross-linker for the covalent stabilization of SCK micelles have been investigated by other groups.[114, 116, 130, 131] The shell crosslinking is achieved by reacting partially quaternized 2-(dimethylamino)ethyl methacrylate-*N*-(morpholino)ethyl methacrylate (DMAEMA-MEMA) diblock copolymer micelles with a bifunctional quaternizing agent, BIEE, in aqueous solution at 60 ℃. Upon cooling to 25 ℃, the hydrophobic MEMA micelle cores become hydrated. Thus, the micelle cores of these new SCK particles could be reversibly hydrated or dehydrated, depending on the solution temperature and/or electrolyte concentration. This ability to control the degree of hydration of the micelle cores suggests possible uptake/release applications. However, in view of its cost, toxicity, limited water solubility, and likely mutagenicity, BIEE is unlikely to be employed in the commercial applications of SCK micelles, particularly in the biomedical field.

Another new method for synthesizing SCK micelles is based on polyelectrolyte complexation by using either an anionic homopolymer or diblock copolymer as an ionic cross-linker in conjunction with a cationic ABC triblock copolymer in which the cationic charge density resides in the central B block (Scheme 1.16).[93, 132] This ionic crosslinking approach involves polymeric reagents that form physical complexes rapidly in aqueous solution at ambient temperature. Ionic cross-linking is readily reversible as the SCL micelles dissociate in the presence of sufficient added electrolyte. Moreover, the product is surprisingly tolerant to added electrolyte. However, a simple homopolyelectrolyte cross-linker only leads to flocculated micelles and it is necessary to use excess diblock copolymer for effective ionic cross-linking.

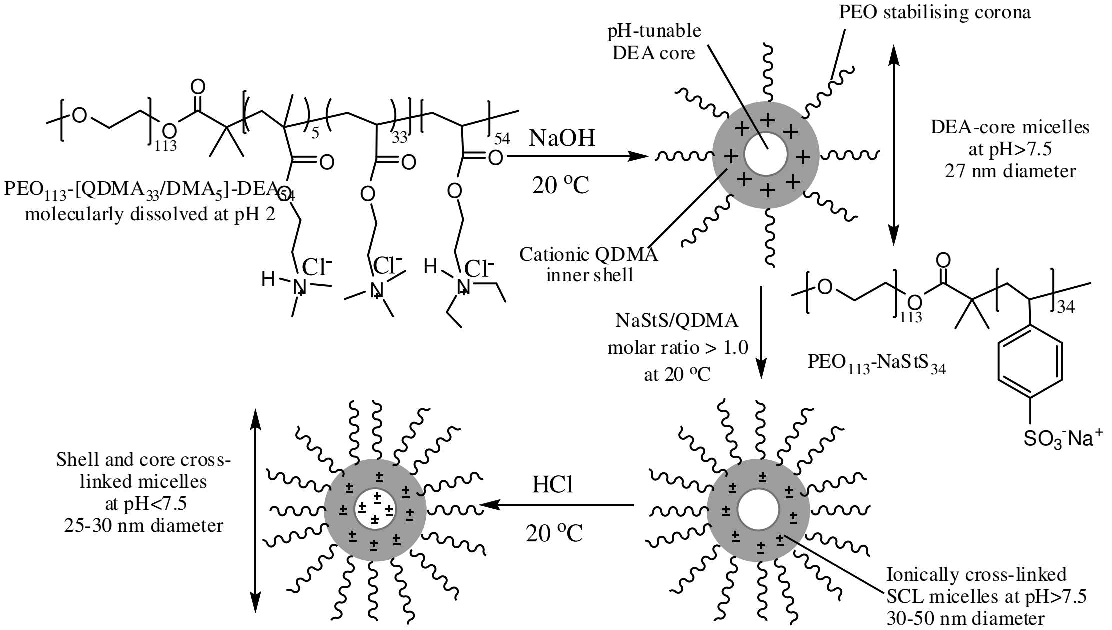

Scheme 1.16 The formation of shell cross-linked micelles by using an ionic crosslinking strategy. Conventional micelles formed by a PEO_{113} – $[QDMA_{33}/DMA_5]$ – DEA_{50} triblock copolymer are stabilized by the addition of an anionic PEO_{113} – $NaStS_{34}$ diblock copolymer. At low pH the conventional micelles dissociate to form individual chains but the ionically cross-linked micelles remain intact, provided that an excess of the anionic diblock copolymer cross-linker is employed.(Reproduced from reference[93])

One of the major barriers that prevent the synthesis of SCK micelles on an industrial scale is that the shell crosslinking must be carried out at high dilution (typically 0.1-0.5% solids) in order to prevent extensive intermicellar cross-linking. To address this problem, ABC triblock copolymers were used to prepared well-defined SCK micelles.[102-104, 108, 112] The first synthesis of the SCK micelles at high solid (10% solid) in aqueous media was done by Armes and co-workes[112] using a poly[ethylene oxide-*block*-2-(dimethylamino)ethyl methacrylate-*block*-2-(N-morpholino)ethyl methacrylate] (PEO-DMA-MEMA) triblock copolymer. Inner shell crosslinking was achieved in 1.0 M Na_2SO_4 at 20℃ for 3-7 days using BIEE. The BIEE can selectively quaternize the more reactive DMA residues in the presence of the sterically hindered MEMA residues. Intermicellar crosslinking was negligible, because the coronal PEO chains ensured minimal interpenetration of the micelles due to steric stabilization. The Chemical structure of the PEO-DMA-MEMA triblock copolymer and the schematic formation of SCK micelles are shown in Scheme 1.17b.

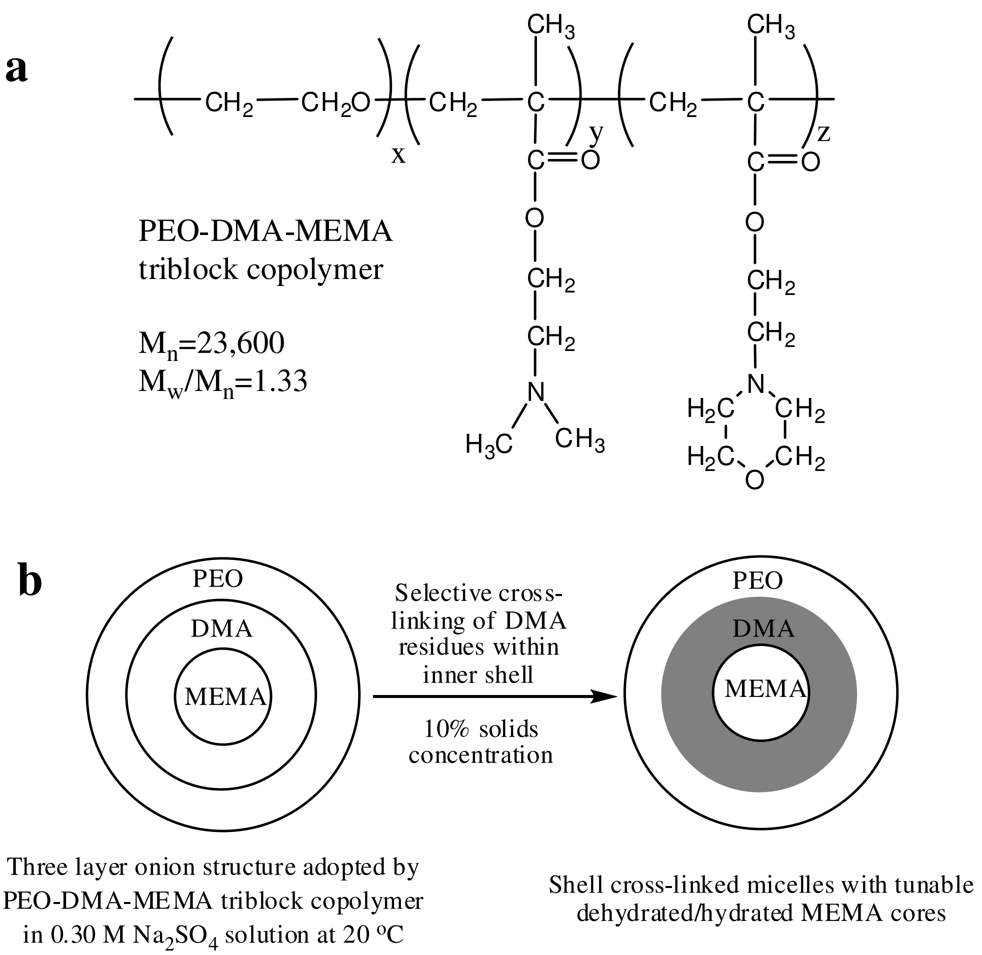

Scheme1.17 (a) Chemical structure of the PEO-DMA-MEMA triblock copolymer; (b) Schematic formation of SCK micelles at high solids using the PEO-DMA-MEMA triblock copolymer.(Reproduced from reference[112])

Most recently, Click chemistry has been employed in SCK synthesis. It combines the crosslinking and functionalization of nanoparticles, which would expand the types of chemistry that could be performed on the nanoparticles, and be tolerant to the functional groups present in the SCKs as well as any further chemistry performed on the SCKs.[87, 90, 127, 133, 134] The Huisgen 1,3-dipolar cycloaddition click reaction was first used for the functionalization of the shells of SCKs.[87, 127, 133](Scheme 1.18a) Thus a new strategy for shell click-crosslinked nanoparticles was developed to allow the reaction between click-readied functional groups in the shell of block copolymer micelles and click-readied termini of a dendrimer to effect a crosslinking. The non-consumed dendrimer termini were then available for reaction with the click-readied active molecules that would be attached to the nanoparticles.[90](Scheme 1.18b) This strategy provides a facile route for the future attachment of biologically important molecules such as reporter molecules, therapeutics, and targeting ligands onto the nanoparticles.

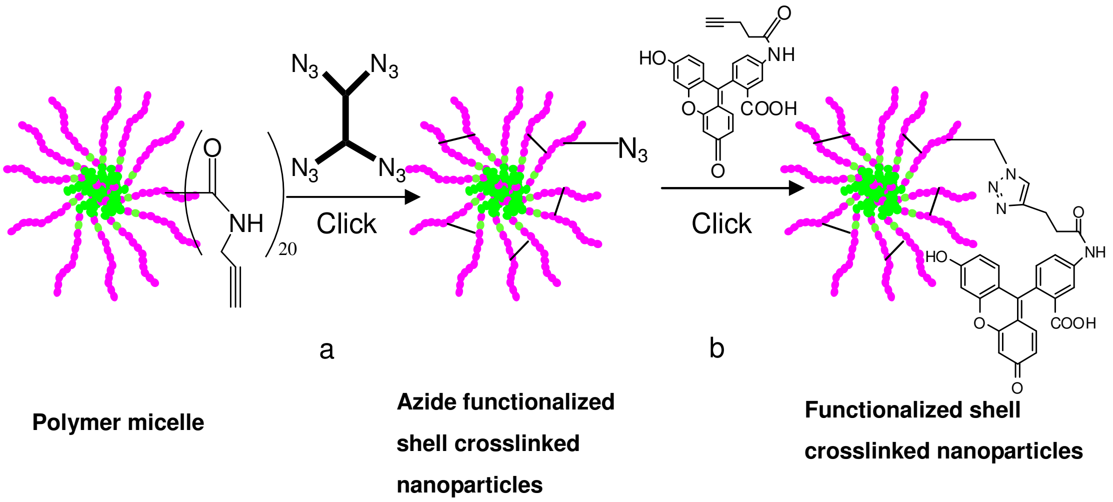

Scheme 1.18 Crosslinking and functionalization of the shells of SCKs via Huisgen 1,3-dipolar cycloaddition click reaction. (Reproduced from reference [90])

1.2.4.2 Core Crosslinkeded Structure

Well-defined core-shell particles with a cross-linked core and hairy shell have also been synthesized by the cross-linking of spherical microdomains in a matrix formed by diblock or triblock copolymers.[9, 135-158] Two features are required to synthesize particles with this method: First, the microdomains, which are crosslinked, should be isolated in a matrix. Second, the sequence formation of a matrix should not generate a bridge structure.[138] It is well known that block and graft copolymers with incompatible sequences form the microphase separation structures in solid state and in solution. When the volume fraction of microdomains of the B sequence of AB diblock copolymer is less than 30 vol% in the polymer volume, a sequence forms a spherical domain.

If the assemblies of block copolymers can be fixed by crosslinking the spherical parts (the spherical microdomains in the solid state and the core in solution), the crosslinked products should form core-shell type polymer microspheres, as shown in Scheme 1.19. The crosslinking of core domains was carried out in micelles formed in solvents selected for block and graft copolymers.[138, 139, 154, 158] The microphase-separated structures in bulk film are more stable than the micelle in solution. Therefore, crosslinking of the spherical microdomains in a film is likely to be a superior preparation method for the core-shell type microspheres. Using this approach, a series of amphiphilic core-shell type polymer microspheres with PS shells were prepared with different cores including poly(methacrylic acid)(PMAA)[149], poly(vinyl alcohol)(PVA)[155] and polypyrrole[154], etc. The PMAA spheres in the solid film were crosslinked with hexamethylene diisocyanate (HDI) by soaking the film of block copolymer in a HDI/hexane solution (Scheme 1.20a) and the PVA cores were crosslinked with terephthal aldehyde (TPA) in solution (Scheme 1.20b). The obtained microspheres have a narrow particle size distribution. However, the crosslinking was done only in a very diluted solution and the yield of the microspheres was low.

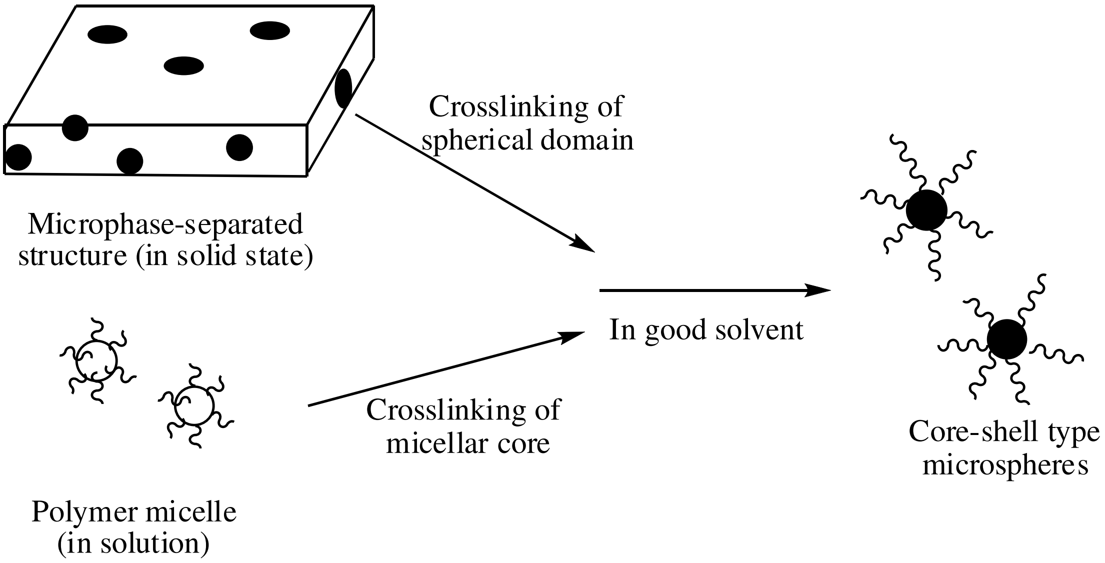

Scheme 1.19 Core-shell polymeric particles synthesized by crosslinking of self-assemblies. (Reproduced from reference[154])

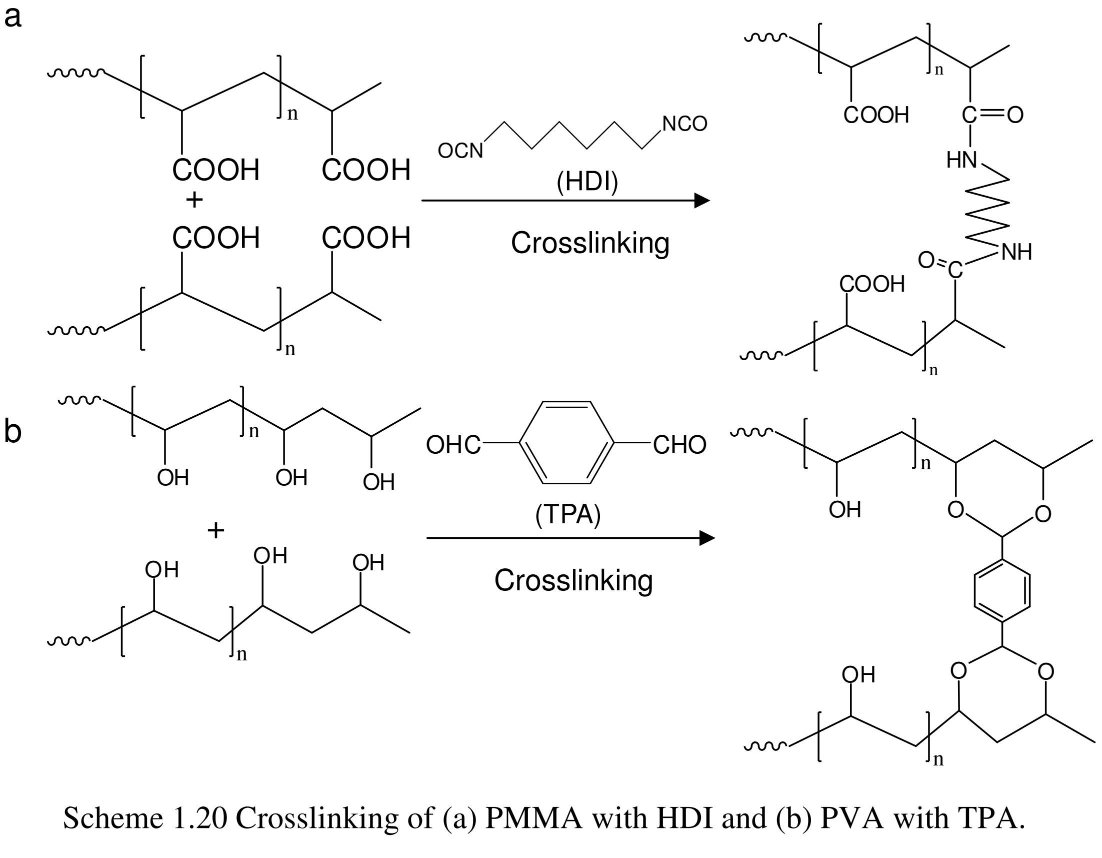

Scheme 1.20 Crosslinking of (a) PMMA with HDI and (b) PVA with TPA.

1.2.5 Stepwise deposition of polyelectrolytes onto charged particle surface

The Stepwise deposition through an electrostatic layer-by-layer (LBL) self-assembly is a well established and highly versatile method to construct multilayers of polyelectrolytes.[1, 159-167] This method involves consecutive adsorption of oppositely charged polyelectrolytes onto a substrate. The irreversible electrostatic attraction is the main driving force for stable film assembly. Thus, the design and preparation of films or coatings with various physical and chemical properties can be achieved through tailing the chemical and physical properties of the layer constituents.

Various strategies to stepwise deposition of polyelectrolytes on to charged colloidal particles have been developed recently.[168-174] Scheme 1.21 illustrates the route for the stepwise deposition onto a polystyrene particle. The polymer used has an opposite charge to that on the particle. Hence it is predominantly adsorbed through electrostatic interactions. For example, polycation/polyanion system such as poly(allylamine hydrochloride) (PAH)/ poly(styrenesulfonate) (PSS), poly(diallyldimethyl ammonium chloride)(PDADMAC)/PSS and PDADMAC/Deoxyribonucleic acid (DNA) have been deposited alternately on the PS colloidal core particles.[169-171, 174, 175]

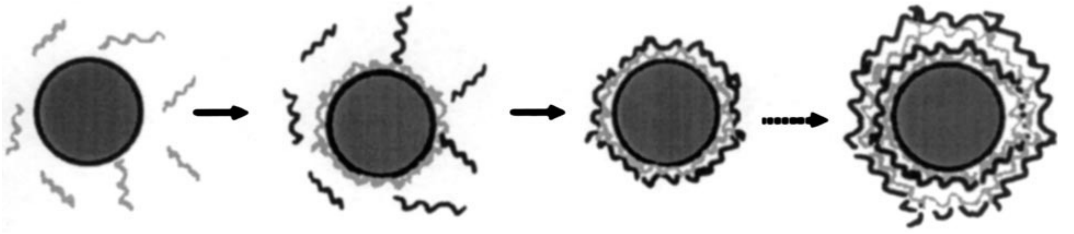

Scheme 1.21 Stepwise deposition of polyelectrolytes onto colloid particles. The grey and black molecules represent polycations and anions, respectively. (Reproduced from reference[171])

There are two methods that have been used in the formation of multiple layers of polyelectrolytes on the particle surface in a controlled fashion: each layer of polyelectrolytes is adsorbed onto the colloidal particles under either a high concentration (excess in solution) or just sufficient to form a saturated layer.[171] In the first case, the remaining non-adsorbed polyelectrolyte molecules is removed by repeated centrifugation washings in water prior to the next coating cycle. The changes in ζ-potential are between positive and negative values, as shown in Figure 1.1. The alternation of ζ-potential values indicates the successful coating of the particle with the polyelectrolyte multilayer upon each layer deposition. In the second approach, it is assumed that most of the polyelectrolyte molecules have been adsorbed to the surface of the particle under the condition of the onset of ζ-potential saturation. Thus, it avoids the time-consuming centrifugation, particle loss during washings and particle interaction in the resulting pellet. However, a larger number of particle aggregates are produced, as compared with a centrifugation-based technique.

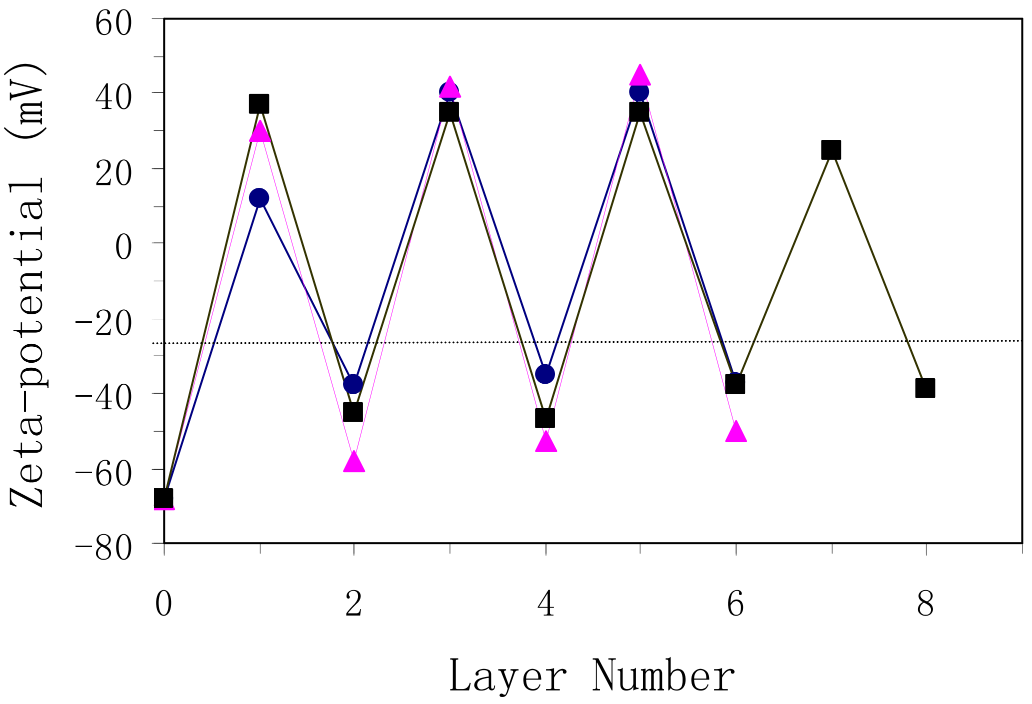

Figure 1.1 ζ-potential as a function of layer number for coated PS sulfate latex particles, Φ 640 nm. ■ =PDADMAC/PSS; ● =PAH/PSS; ▲ =PDADMAC/DNA. Ionic strength=1 mM KNO_3, pH=6.2 ± 0.2, polyelectrolyte deposition in water (PDADMAC/PSS, PDADMACIDNA) and in 0.5 M NaC1 (PAH/PSS).(Reproduced from reference[170])

The main advantage of the LBL technique is that it allows the production of composite colloidal materials with tailored compositions, functions and well-defined morphologies. Colloids of different sizes, shapes and compositions can be employed as templates since polyelectrolytes self-assemble onto numerous surfaces. The thickness of the polymer coatings can be well-defined by altering the number of layers deposited and the solution conditions from which the polymers are adsorbed. In addition, multi-composite polymer films can be assembled through the choice of a large variety of polymers. For example, pure polyelectrolyte[167, 176-180], biological material-polyelectrolyte[181-186], inorganic nanoparticle-polyelectrolyte[168, 187-190] and dendrimer-polyelectrolyte[191-195] multilayer films have been fabricated on colloids using this method. Furthermore, the use of decomposable colloidal cores as templates for the sequential deposition of alternately charged polymers or nanoparticles and polymers, allows the fabrication of novel three-dimensional, hollow polymer capsules[176, 184, 196-202], and hollow inorganic or composite inorganic-organic hybrid capsules[189, 190, 203], respectively (Scheme 1.22).

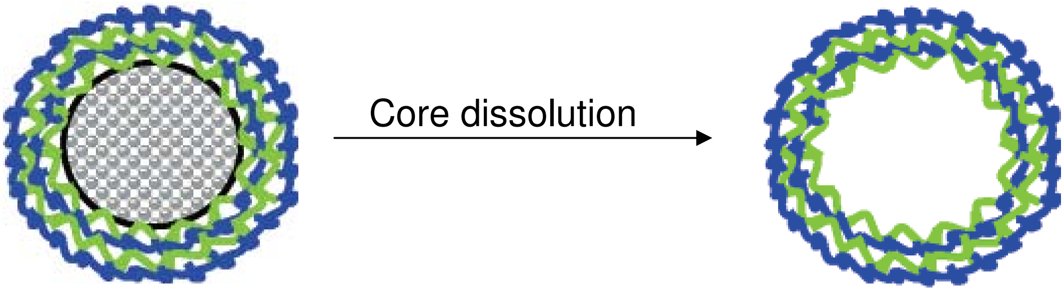

Scheme 1.22 Removal of decomposable cores to fabricate hollow capsules

However, there are still some limitations associated with the LBL strategy. A major barrier is that it requires the time-consuming sequential polyelectrolyte deposition cycles and purification steps. Thus filtration-based purification methods might be used to simplify and speed up the process, in order to allow for a scaling-up production.

1.2.6 Graft copolymerization of vinyl monomer from a water-soluble polymer containing amino groups

The synthesis of well-defined amphiphilic core-shell particles through graft copolymerization of vinyl monomer from a water-soluble polymer containing amino groups is a newly developed approach by Li et al.[204, 205] This approach is based on the reaction between alkyl hydroperoxide and the amino group of the water soluble polymer in water. Amphiphilic graft copolymers and hydrophobic homopolymers are generated concurrently, forming highly monodispersed particles with an amphiphilic core-shell structure. Scheme 1.23 illustrates the formation mechanism of amphiphilic core-shell particles and Scheme 1.24 shows the chemistry of the grafting copolymerization and homopolymerization. The hydroperoxide (ROOH) initially interacts with amino groups on the polymer backbone, forming redox pairs. Electrons transfer and loss of protons result in the formation of amino radicals and alkoxyl radicals (RO·). The amino radicals are capable of initiating the graft copolymerization of vinyl monomers. The RO· generated can either initiate homopolymerization of vinyl monomer or abstract a hydrogen atom from the polymer backbone, thus generating a backbone radical that can also initiate the graft copolymerization of vinyl monomer. The amphiphilic graft copolymers generated *in situ* act like polymeric surfactants, self-assembling to form micelle-like microdomains. These polymeric micelles are able to assist the emulsion polymerization of the vinyl monomer. Therefore, the hydrophobic vinyl monomer can undergo polymerization within the hydrophobic domains of the micelles to form core-shell particles with the water-soluble polymer as the shells.

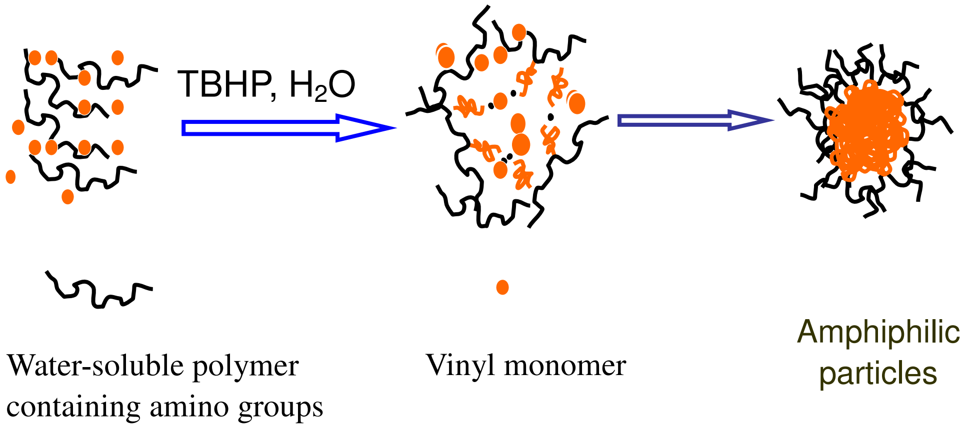

Scheme 1.23 Schematic representation of the formation of amphiphilic core-shell nanospheres. (Reproduced from reference[205])

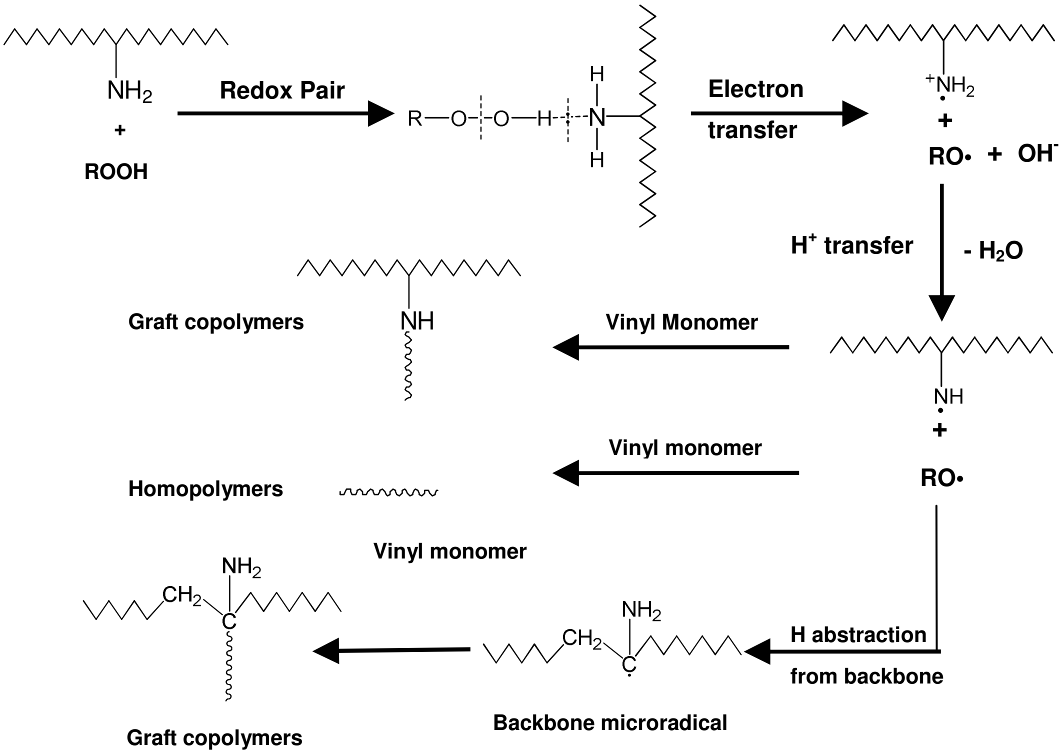

Scheme 1.24 Proposed mechanism for the graft copolymerization of vinyl monomer from water-soluble polymers.

This is a versatile approach to prepare a wide range of core-shell particles with shells from natural biopolymers such as casein, gelatin, albumine bovine serum and chitosan, etc., to synthetic polymers such as polyethyleneimine (PEI), polyallylamine (PAAm), polyvinylamine (PVAm), etc. Thus, various amine-rich core-shell particles can be easily prepared. These types of particles containing highly reactive amine groups are very useful materials because they can electrostatically bind to or covalently link with small (e.g. drug or dye molecules) or large molecules (negatively charged DNA, enzyme). Therefore, they have a great potential in diverse applications including enzyme immobilization, drug and gene deliveries.[206-209] In addition, the composition, functionality, rigidity, reactivity, shell thickness, core diameter, particle size and stability of the particles could be easily tailored through variations of the composition and structure of the shell polymers and the hydrophobic monomers. A series of amphiphilic core-shell particles designed for specific applications have been synthesized using this approach, for example, PMMA/Chitosan[205, 210], poly(*n*-butyl acrylate) (PBA)/Chitosan[211], PMMA/PEI and PMMA/PAAm[212], PNIPAM/PEI and PNIPAM/Chitosan[213, 214] core-shell particles etc. The important properties of the particles obtained include well-defined core-shell structures, nanosphere diameters ranging from 60 to 300 nm, narrow particle size distributions, the ability to tailor the core diameter and shell thickness, and the use of aqueous-based chemistry. A very important feature of this approach is that it can produce particles with a solid content up to 22 wt%. Therefore, it can be amenable to the commercial production of a wide variety of novel amphiphilic core-shell nanomaterials with different sizes, compositions, structures and functions.

1.3. Applications of amphiphilic core-shell particles

Applications of amphiphilic core-shell particles are considerably being explored in various fields because of their promising features such as nanoscale dimensions, different compositions and properties, various core diameters and shell thickness, and most importantly, surface functionalities provided by the hydrophilic shells. Several examples of the use of amphiphilic core-shell particles in different fields are discussed below.

1.3.1 Metallic nanoparticle nanoreactor

Metallic nanoparticles have been widely applied in optics, microelectronics, surface-enhanced Raman scattering, ultrasensitive chemical sensors, information storage and electronics due to their unique properties that are very different from their bulk materials.[215-217] However, the metallic nanoparticles are difficult to handle and may aggregate due to their nano-size and high surface-to-volume ratio. Thus suitable carrier systems may be used as a 'nanoreactor' to immobilize the metallic nanoparticles so that they can be easily handled. A suitable carrier system should meet the following requirements: (1) the carrier system should be totally inert; (2) the stabilizing agent should be not alter or block the surface of the metallic nanoparticles; (3) the carrier system should be sufficiently stable to enable the recycle of the metallic nanoparticles; (4) the formation of well-defined metallic nanoparticles with a narrow size distribution should take place directly on the support.[218]

There are a number of advantages for the use of amphiphilic core-shell particles as nanoreactors. The particle sizes are in nano-dimension and the size distribution is uniform. The core and shell thickness of the particles are well-defined. Most importantly, most of the metallic ions can be confined in the shell layer, thus preventing the metal particles from aggregating in the aqueous phase. Moreover, the immobilization of metallic nanoparticles on the surface of "nanoreactor" is able to retain the high activity of the nanoparticles and allow easy recycling. The properties of the metallic nanoparticles can also be tuned. For example, the catalytic activity of the metallic nanoparticles can be modulated by temperature over a wide range when thermal-sensitive core-shell particles are used as a nanoreactor.[219, 220]

There are two major ways to prepare metallic nanoparticles on the surface of amphiphilic core-shell particles. One is through the immobilization of metallic ions on the surface of preformed amphiphilic core-shell particles, followed by the reduction of the metallic ions to metallic nanoparticles (Scheme 1.25).[103, 218, 221-223] This method includes three steps: (1) Synthesis of core-shell particles via a suitable approach; (2) immobilization of metallic ions onto/into the shell of the particles via complexation[219]or ion exchange[218]; (3) reduction of metallic ions and formation of metallic nanoparticles. The advantages of this procedure are that the properties of the core-shell particles are easily controlled and the metallic nanoparticles obtained have high activity.

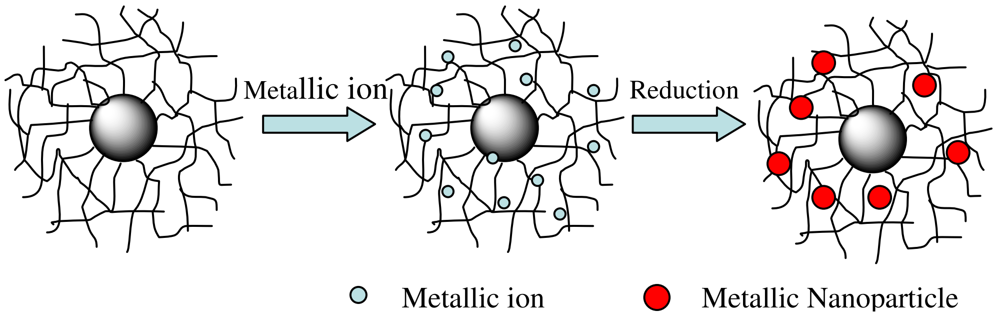

Scheme 1.25 Formation of metallic nanoparticles on/in the shells of core-shell particles

Another method is the *in-situ* formation of metallic nanoparticles on the shells of core-shell particles (Scheme 1.26).[56, 215, 224] The metal salt, hydrophilic micromonomer and organic monomers are first mixed homogeneously in the solution. Then metal ions are reduced to yield free atoms that subsequently coalesce to form larger particles by radicals directly generated from AIBN or by the oligomeric radicals during dispersion polymerization. During the process, the hydrophilic micromonomer chains not only serve as steric stabilizers, but also adsorb the metallic nanopartices onto the surfaces of the core-shell particles.[215] The particle size of the core-shell particles can be changed by variation of the concentration of metal salt. High conversion of up to 96% of metal ions to metal atoms can be achieved and immobilized on the polymeric particles.[56]

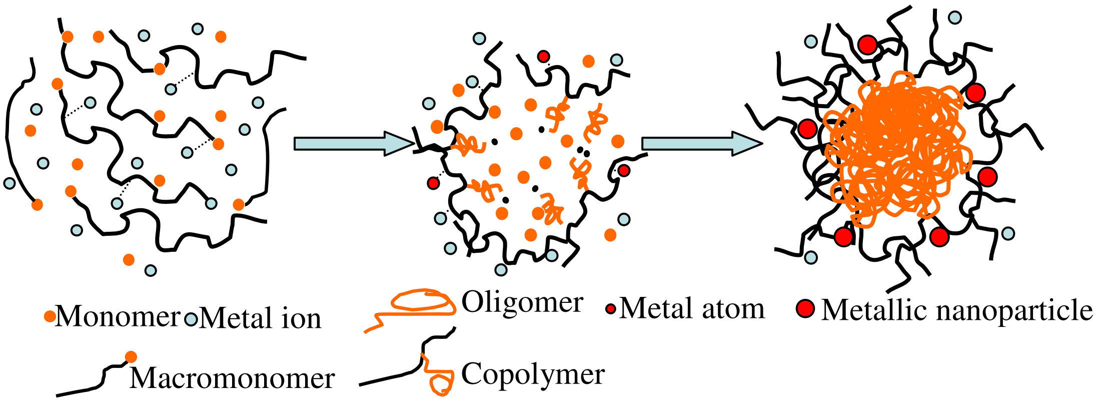

Scheme 1.26 *In-situ* formation of metallic nanoparticles onto/into the shells

1.3.2 Drug delivery

For medical applications, particles should fulfill several requirements relating to their handling and storage: (1) the suspensions should be chemically and colloidally stable over a broad range of pH, ionic strength and temperature; (2) biomolecules are bound onto the particles by adsorption or by covalent immobilization;(3) for many applications, particles should have a tailored diameter and with a narrow size distribution; (4) the adventitious rather than selective adsorption of other molecules, usually proteins, from analyzed liquids should be eliminated or strongly reduced.[225] Amphiphilic core-shell particles with hydrophobic cores and hydrophilic shells cater to the properties mentioned above. The hydrophilic shells provide the stability and functionalities to bond the biomolecules, while the hydrophobic cores hold sufficient strength and durability.

There are several advantages in the use of the amphiphilic core-shell particles as a drug carrier: (1) the bioavailability of drugs with poor absorption characteristics can be improved; (2) the drug can stay at the delivered site for a long time due to the large size of molecules; (3) the release of drugs is slow or can be controlled by diffusion from the carrier or by decomposition of the carrier; (4) the drugs can target with functional components; (5) the side reaction of drugs can be reduced; (6) the stability of drugs in vivo can be assured. [2, 226]

Various amphiphilic core-shell particles have been developed for drug delivery. For example, particles with PEO shells were used for site-specific drug delivery[227] and for target-specific delivery of paclitaxel[228]; particles with polyglycidol (PGL) shells were prepared for adsorption of human serum albumin, human g-globulins, and human fibrinogen[229] and for an immunoassay[71]; particles with polysaccharides shells were applied in the biomedical diagnostic field for the adsorption of bovine serum albumin, and for the covalent binding of antibodies and single-stranded DNA fragments[230]; particles with PNIPAM, PNVA, or PVAm shells were used as carriers for the oral delivery of salmon calcitonin[231-233] etc. In addition, particles with a magnetic property were fabricated for use as a controlled drug delivery system[234], lipid-core particles was applied for target drug delivery[235]. Several comprehensive articles on the applications of particles for drug delivery have been published.[225, 236-242]

1.3.3 Enzyme immobilization

Immobilized enzymes have several benefits compared to their soluble counterparts such as easy recovery, reusability and stability.[243] Thus, they have been widely applied in diverse areas including reusable heterogeneous biocatalysts, stable and reusable devices for analytical and medical applications, selective adsorbents for purification of proteins and enzymes, solid-phase protein chemistry and effective micro-device for the controlled release of protein drugs, etc.[244]

Amphiphilic core-shell particles are very suitable for enzyme and protein immobilization because of their large surface area, nanoscale demensions and surface functionality.[245, 246] The immobilization can be done by various methods, for example, adsorption, entrapment or encapsulation, covalent bonding, crosslinking or a combination of these methods.[247] In general, adsorption and entrapment give less stress and less activity loss to the enzyme, but may give less selectivity on immobilization than covalent bonding or crosslinking.[2] For instance, Caruso et al[248] encapsulated enzyme by the sequential adsorption of oppositely charged polyelectrolytes onto enzyme crystal templates and found that the activity of the encapsulated enzyme was well preserved and their stability against protease degradation was improved. Haupt et al[249] investigated the enzymic activity of glucoamylase and β-glucosidase adsorbed on colloidal particles with spherical polyelectrolyte brushes. Their results showed that up to 600 mg of enzyme was adsorbed per g of the carrier particles and both enzymes kept nearly their full activity. Kang et al[250] studied the properties of covalently immobilized trypsin on P(MMA-EA-AA) latex particles and their results revealed that the immobilized trypsin exhibited much better thermal and chemical stabilities than its free counterpart and maintained over 63% of its initial activity after reusing ten times.

1.3.4 Other applications

Amphiphilic core-shell particles have also been used in numerous applications such as gene delivery[208, 209, 251], bioseparations[252, 253], identification of drug receptors[254, 255], immunodiagnostic assay[225, 256], dye loading[257], antibacterial coating[211], fabrication of novel materials[258], etc. It is foreseeable that the amphiphilic core-shell particles will play more and more important roles in science and technology and their application will be more and more diverse as time goes on.

1.4 Conclusions and Outlooks

Science and technology of polymeric core-shell particles have been developed rapidly in the last decade and the progress seems to be accelerated more and more because of the urgent needs of era to fine materials, mesoscopic science and nanotechnology. Approaches developed recently have demonstrated their effectiveness in design and controlled fabrication of amphiphilic core-shell particles with functional properties. However, many of these approaches still suffer from many drawbacks which have hindered their commercial applications. Thus further development of new approaches to address these problems and possibly open up new applications is highly desired. Therefore, it is foreseen that the realm of design, fabrication and application of amphiphilic core-shell particles will rapidly expand, and foster more and more multidisciplinary research in the future.

References:

1. Caruso, F., Engineering of core-shell particles and hollow capsules. *Nano-Surface Chemistry* **2002**, 505-525.

2. Kawaguchi, H., Functional polymer microspheres. *Progress in Polymer Science* **2000,** 25, (8), 1171-1210.

3. Jayachandran, K. N.; Chatterji, P. R., Grafted polymeric microspheres: a synthetic approach to structurally well-defined brush polymers. *Journal of Macromolecular Science, Pure and Applied Chemistry* **1998,** A35, (12), 1971-1986.

4. Wang, Y.; Du, Q.; Huang, J., Grafting of poly(ethylene oxide) with Schiff's base end group onto chloromethylated polystyrene via Decker-Forster reaction. *Macromolecular Rapid Communications* **1998,** 19, (5), 247-250.

5. Meng, F.; Engbers, G., H. M. ; Feijen, J., Polyethylene glycol-grafted polystyrene particles. *Journal of Biomedical Materials Research Part A* **2004,** 70A, (1), 49-58.

6. Bernard, J.; Schappacher, M.; Viville, P.; Lazzaroni, R.; Deffieux, A., Synthesis and properties of PS-PEO core-shell amphiphilic dendrigrafts. *Polymer* **2005,** 46, (18), 6767-6776.

7. Edmondson, S.; Osborne, V. L.; Huck, W. T. S., Polymer brushes via surface-initiated polymerizations. *Chemical Society Reviews* **2004,** 33, (1), 14-22.

8. Bian, K.; Cunningham, M. F., Synthesis of polymeric microspheres from a Merrifield resin by surface-initiated nitroxide-mediated radical polymerization.

Journal of Polymer Science Part A: Polymer Chemistry **2005,** 43, (10), 2145-2154.

9. Saito, R.; Ni, X.; Ichimura, A.; Ishizu, K., Synthesis of core-shell type microsphere with reactive seed microspheres. *Journal of Applied Polymer Science* **1998,** 69, (2), 211-216.
10. Kawaguchi, H.; Isono, Y.; Tsuji, S., Hairy particles prepared by living radical graft-polymerization. *Macromolecular Symposia* **2002,** 179, (15th Bratislava International Conference on Polymers, Non-Conventional Polymer Dispersions, 2001), 75-87.
11. Horie, K.; Yamada, S.; Machida, S.; Takahashi, S.; Isono, Y.; Kawaguchi, H., Dansyl Fluorescence and Local Structure of Dansyl-Labeled Core-Shell and Core-Hair Type Microspheres in Solution. *Macromolecular Chemistry and Physics* **2003,** 204, (1), 131-138.
12. Tsuji, S.; Kawaguchi, H., Temperature-Sensitive Hairy Particles Prepared by Living Radical Graft Polymerization. *Langmuir* **2004,** 20, (6), 2449-2455.
13. Guo, X.; Weiss, A.; Ballauff, M., Synthesis of Spherical Polyelectrolyte Brushes by Photoemulsion Polymerization. *Macromolecules* **1999,** 32, (19), 6043-6046.
14. Guo, X.; Ballauff, M., Spatial Dimensions of Colloidal Polyelectrolyte Brushes As Determined by Dynamic Light Scattering. *Langmuir* **2000,** 16, (23), 8719-8726.
15. Guo, X.; Ballauff, M., Spherical polyelectrolyte brushes: Comparison between

annealed and quenched brushes. *Physical Review E: Statistical, Nonlinear, and Soft Matter Physics* **2001,** 64, (5-1), 051406/1-051406/9.

16. Xia, R.-K.; He, W.-D.; Pan, C.-Y., Amphiphilic particles prepared by grafting acrylamide onto the surface of styrene-rich copolymer/2-hydroxyethyl acrylate rich copolymer particles. *Colloid and Polymer Science* **2002,** 280, (9), 865-872.
17. Storey, R. F.; Goff, L. J., Ceric ion initiation of vinylidene chloride from poly(vinyl alcohol). *Macromolecules* **1989,** 22, (3), 1058-1064.
18. Hritcu, D.; Mueller, W.; Brooks, D. E., Poly(styrene) Latex Carrying Cerium(IV)-Initiated Terminally Attached Cleavable Chains: Analysis of Grafted Chains and Model of the Surface Layer. *Macromolecules* **1999,** 32, (3), 565-573.
19. Yun, Y.; Li, H.; Ruckenstein, E., Hydrophobic Core/Hydrophilic Shell Amphiphilic Particles. *Journal of Colloid and Interface Science* **2001,** 238, (2), 414-419.
20. Yun, Y.; Li, H.-q., Core-shell particles prepared via concentrated emulsion interface initiation. *Gaofenzi Cailiao Kexue Yu Gongcheng* **2001,** 17, (5), 144-148, 152.
21. Zhang, M.; Liu, L.; Zhao, H.; Yang, Y.; Fu, G.; He, B., Double-responsive polymer brushes on the surface of colloid particles. *Journal of Colloid and Interface Science* **2006,** 301, (1), 85-91.
22. Min, K.; Lan, J.; Hu, J.; Wang, C., Preparation and characterization of

self-dispersible polymeric microspheres. *Polymers for Advanced Technologies* **2006,** 17, (7-8), 491-493.

23. Liu, P.; Su, Z., Surface-initiated atom transfer radical polymerization (SI-ATRP) of styrene from chitosan particles. *Materials Letters* **2006,** 60, (9-10), 1137-1139.
24. Kizhakkedathu, J. N.; Norris-Jones, R.; Brooks, D. E., Synthesis of Well-Defined Environmentally Responsive Polymer Brushes by Aqueous ATRP. *Macromolecules* **2004,** 37, (3), 734-743.
25. Kizhakkedathu, J. N.; Kumar, K. R.; Goodman, D.; Brooks, D. E., Synthesis and characterization of well-defined hydrophilic block copolymer brushes by aqueous ATRP. *Polymer* **2004,** 45, (22), 7471-7489.
26. Goodman, D.; Kizhakkedathu, J. N.; Brooks, D. E., Attractive Bridging Interactions in Dense Polymer Brushes in Good Solvent Measured by Atomic Force Microscopy. *Langmuir* **2004,** 20, (6), 2333-2340.
27. Goodman, D.; Kizhakkedathu, J. N.; Brooks, D. E., Molecular Weight and Polydispersity Estimation of Adsorbing Polymer Brushes by Atomic Force Microscopy. *Langmuir* **2004,** 20, (8), 3297-3303.
28. Kizhakkedathu, J. N.; Brooks, D. E., Synthesis of Poly(N,N-dimethylacrylamide) Brushes from Charged Polymeric Surfaces by Aqueous ATRP: Effect of Surface Initiator Concentration. *Macromolecules* **2003,** 36, (3), 591-598.
29. Jayachandran, K. N.; Brooks, D. E., Aqueous ATRP grafting of acrylamides

from latex surfaces: Molecular weight control by a non-classical mechanism. *Polymer Preprints (American Chemical Society, Division of Polymer Chemistry)* **2002,** 43, (2), 247-248.

30. Otsu, T., Iniferter concept and living radical polymerization. *Journal of Polymer Science, Part A: Polymer Chemistry* **2000,** 38, (12), 2121-2136.

31. Hritcu, D.; Brooks, D. E.; Muller, W., Poly(styrene) latex carrying Ce(IV) initiated terminally attached water soluble chains. *Polymeric Materials Science and Engineering* **1999,** 80, 558-559.

32. Liu, W.-J.; He, W.-D.; Wang, Y.-M.; Wang, D.; Zhang, Z.-C., Interfacial-initiated seeded emulsion polymerization: preparation of polystyrene/poly(methacrylic acid) core/shell particles in the absence of surfactant. *Polymer International* **2006,** 55, (5), 520-524.

33. Perruchot, C.; Khan, M. A.; Kamitsi, A.; Armes, S. P.; von Werne, T.; Patten, T. E., Synthesis of Well-Defined, Polymer-Grafted Silica Particles by Aqueous ATRP. *Langmuir* **2001,** 17, (15), 4479-4481.

34. Wang, X. S.; Jackson, R. A.; Armes, S. P., Facile Synthesis of Acidic Copolymers via Atom Transfer Radical Polymerization in Aqueous Media at Ambient Temperature. *Macromolecules* **2000,** 33, (2), 255-257.

35. Wang, X. S.; Armes, S. P., Facile Atom Transfer Radical Polymerization of Methoxy-Capped Oligo(ethylene glycol) Methacrylate in Aqueous Media at Ambient Temperature. *Macromolecules* **2000,** 33, (18), 6640-6647.

36. Wang, X. S.; Lascelles, S. F.; Jackson, R. A.; Armes, S. P., Facile synthesis of

well-defined water-soluble polymers via atom transfer radical polymerization (ATRP) in aqueous media at ambient temperature. *Chemical Communications* **1999**, (18), 1817-1818.

37. Mitsuru Akashi, I. K. N. M., Synthesis and polymerization of a styryl terminated oligovinylpyrrolidone macromonomer. *Angewandte Makromolekulare Chemie* **1985,** 132, (1), 81-89.

38. Kaneda, I.; Vincent, B., Swelling behavior of PMMA-g-PEO microgel particles by organic solvents. *Journal of Colloid and Interface Science* **2004,** 274, (1), 49-54.

39. Shen, R.; Akiyama, C.; Senyo, T.; Ito, K., Emulsion and dispersion polymerization of styrene in the presence of PEO macromonomers with p-vinylphenylalkyl end groups. *Comptes Rendus Chimie* **2003,** 6, (11-12), 1329-1335.

40. Liu, Z.; Xiao, H.; Wiseman, N.; Zheng, A., Poly(ethylene oxide) macromonomer-grafted polymer nanoparticles synthesised by emulsifier-free emulsion polymerisation. *Colloid and Polymer Science* **2003,** 281, (9), 815-822.

41. Ahmad, H.; Tauer, K., Poly(ethylene glycol)-Coated Monodisperse Micron-Sized Composite Polymer Particles. *Macromolecules* **2003,** 36, (3), 648-653.

42. Liu, X.-Y.; Ding, X.-B.; Zheng, Z.-H.; Zhang, W.-C.; Peng, Y.-X.; Chan Albert, S. C.; Yip, C. W.; Long, X.-P., Characterization of Fe3O4/P(St-MPEO)

amphiphilic magnetic polymer microspheres. *Chemical Research in Chinese Universities* **2002,** 18, (4), 458-461.

43. Li, W.; Ding, X.-B.; Zheng, Z.-H.; Zhang, W.-C.; Deng, J.-G.; Peng, Y.; Chan, A. S. C.; Yip, C. W., Synthesis of amphiphilic microspheres by suspension copolymerization of styrene and poly(ethylene oxide) macromonomer. *Journal of Applied Polymer Science* **2001,** 81, (2), 333-339.

44. Gibanel, S.; Heroguez, V.; Forcada, J., Surfactant characteristics of polystyrene/poly(ethylene oxide) macromonomers in aqueous solution and on polystyrene latex particles: two-step emulsion polymerizations. *Journal of Polymer Science, Part A: Polymer Chemistry* **2001,** 39, (16), 2767-2776.

45. Wu, C.; Akashi, M.; Chen, M.-Q., A Simple Structural Model for the Polymer Microsphere Stabilized by the Poly(ethylene oxide) Macromonomers Grafted on Its Surface. *Macromolecules* **1997,** 30, (7), 2187-2189.

46. Liu, J.; Gan, L. M.; Chew, C. H.; Quek, C. H.; Gong, H.; Gan, L. H., The particle size of latexes from dispersion polymerization of styrene using poly(ethylene oxide) macromonomer as a polymerizable stabilizer. *Journal of Polymer Science, Part A: Polymer Chemistry* **1997,** 35, (16), 3575-3583.

47. Capek, I.; Riza, M.; Akashi, M., Dispersion copolymerization of poly(oxyethylene) macromonomers and styrene. *Journal of Polymer Science, Part A: Polymer Chemistry* **1997,** 35, (15), 3131-3139.

48. Capek, I.; Riza, M.; Akashi, M., Effects of the initiator type on the dispersion copolymerization of poly(ethylene glycol) macromonomer and styrene.

Polymer Journal (Tokyo, Japan) **1992,** 24, (9), 959-970.

49. Akashi, M.; Chao, D.; Yashima, E.; Miyauchi, N., Graft copolymers having hydrophobic backbone and hydrophilic branches. V. Microspheres obtained by the copolymerization of poly(ethylene glycol) macromonomer with methyl methacrylate. *Journal of Applied Polymer Science* **1990,** 39, (9), 2027-2030.

50. Uyama, H.; Honda, Y.; Kobayashi, S., Synthesis and emulsion copolymerization of amphiphilic poly(2-oxazoline) macromonomer possessing a vinyl ester group. *Journal of Polymer Science, Part A: Polymer Chemistry* **1993,** 31, (1), 123-128.

51. Kobayashi, S.; Uyama, H.; Chio, J. H.; Matsumoto, Y., Preparation of micron-size monodisperse poly(methyl methacrylate) particles using poly(2-oxazoline) macromonomer. *Polymer International* **1993,** 30, (2), 265-270.

52. Uyama, H.; Kato, H.; Kobayashi, S., Dispersion polymerization of N-vinylformamide in polar media. Preparation of monodisperse hydrophilic polymer particles. *Polymer Journal (Tokyo, Japan)* **1994,** 26, (7), 858-863.

53. Zhao, H.; Chen, H.; Li, Z.; Su, W.; Zhang, Q., The synthesis of temperature-sensitive PMMA-coating PNIPAM particles via a rapid microwave-assisted polymerization. *European Polymer Journal* **2006,** 42, (9), 2192-2198.

54. Mori, T.; Maeda, M., Temperature-Responsive Formation of Colloidal Nanoparticles from Poly(N-isopropylacrylamide) Grafted with

Single-Stranded DNA. *Langmuir* **2004,** 20, (2), 313-319.

55. Chen, M.-q.; Serizawa, T.; Li, M.; Wu, C.; Akashi, M., Thermosensitive behavior of poly(N-isopropylacrylamide) grafted polystyrene nanoparticles. *Polymer Journal (Tokyo, Japan)* **2003,** 35, (12), 901-910.

56. Chen, C.-W.; Serizawa, T.; Akashi, M., Synthesis and Characterization of Poly(N-isopropylacrylamide)-Coated Polystyrene Microspheres with Silver Nanoparticles on Their Surfaces. *Langmuir* **1999,** 15, (23), 7998-8006.

57. Chen, C.-W.; Chen, M.-Q.; Serizawa, T.; Akashi, M., In-situ formation of silver nanoparticles on poly(N-isopropylacrylamide)-coated polystyrene microspheres. *Advanced Materials (Weinheim, Germany)* **1998,** 10, (14), 1122-1126.

58. Riza, M.; Tokura, S.; Kishida, A.; Akashi, M., Graft copolymers having a hydrophobic backbone and hydrophilic branches. Part IX. Preparation of water-dispersible microspheres having polycationic branches on their surfaces. *New Polymeric Materials* **1994,** 4, (3), 189-198.

59. Riza, M.; Tokura, S.; Iwasaki, M.; Yashima, E.; Kishida, A.; Akashi, M., Graft copolymers having hydrophobic backbone and hydrophilic branches. X. Preparation and properties of water-dispersible polyanionic microspheres having poly(methacrylic acid) branches on their surfaces. *Journal of Polymer Science, Part A: Polymer Chemistry* **1995,** 33, (8), 1219-1225.

60. Ishizu, K.; Kim, S.; Ichimura, A., Microsphere synthesis by emulsion copolymerizations of styrene with poly(methacrylic acid) macromonomers.

Journal of Applied Polymer Science **2002,** 85, (4), 900-905.

61. Chen, M.-q.; Liu, X.-y.; Yang, C.; Akashi, M., Preparation and characterization of polymeric microspheres having isotactic poly(methacrylic acid) on their surfaces. *Chemical Research in Chinese Universities* **2002,** 18, (1), 61-64.

62. Ishizu, K.; Tahara, N., Microsphere synthesis by emulsion copolymerization of methyl methacrylate with poly(methacrylic acid) macromonomers. *Polymer* **1996,** 37, (13), 2853-2856.

63. Ishizu, K.; Tahara, N., Microsphere synthesis by emulsion copolymerization of methyl methacrylate with binary macromonomer blends. *Polymer* **1996,** 37, (9), 1729-1734.

64. Serizawa, T.; Uchida, T.; Akashi, M., Synthesis of polystyrene nanospheres having lactose-conjugated hydrophilic polymers on their surfaces and carbohydrate recognition by proteins. *Journal of Biomaterials Science, Polymer Edition* **1999,** 10, (3), 391-401.

65. Ishizu, K.; Yamashita, M.; Ichimura, A., Microsphere synthesis by emulsion copolymerization of methyl methacrylate with poly(acrylic acid) macromonomers. *Polymer* **1997,** 38, (21), 5471-5474.

66. Ishizu, K.; Yamashita, M.; Ichimura, A., Microsphere synthesis by dispersion copolymerization of methyl methacrylate with poly(acrylic acid) macromonomers. pH effect on microsphere formation. *Macromolecular Rapid Communications* **1997,** 18, (8), 639-642.

67. Chen, M.-q.; Chen, Y.; Liu, X.-y.; Yang, C.; Ni, Z.-b.; Yao, B.-l., Preparation of thermosensitive polymer grafted polystyrene microspheres. *Gongneng Gaofenzi Xuebao* **2002,** 15, (3), 266-270.

68. Uchida, T.; Furuzono, T.; Ishihara, K.; Nakabayashi, N.; Akashi, M., Graft copolymers having hydrophobic backbone and hydrophilic branches. XXX. Preparation of polystyrene-core nanospheres having a poly(2-methacryloyloxyethyl phosphorylcholine) corona. *Journal of Polymer Science, Part A: Polymer Chemistry* **2000,** 38, (17), 3052-3058.

69. Xie, X.; Fan, X., Synthesis of thermo-sensitive functional polymer microspheres using macromonomer poly(N-vinylformamide) and styrene. *Gaofenzi Xuebao* **2001**, (3), 347-350.

70. Serizawa, T.; Yasunaga, S.; Akashi, M., Synthesis and Lectin Recognition of Polystyrene Core-Glycopolymer Corona Nanospheres. *Biomacromolecules* **2001,** 2, (2), 469-475.

71. Basinska, T.; Wisniewska, M.; Chmiela, M., Principle of a new immunoassay based on electrophoretic mobility of poly(styrene/a-tert-butoxy-w-vinylbenzyl-polyglycidol) microspheres: Application for the determination of Helicobacter pylori IgG in blood serum. *Macromolecular Bioscience* **2005,** 5, (1), 70-77.

72. Basinska, T.; Slomkowski, S.; Kazmierski, S.; Dworak, A.; Chehimi, M. M., Studies on the surface layer structure and properties of poly(styrene/a-t-butoxy-w-polyglycidol) microspheres by carbon nuclear

magnetic resonance, X-ray photoelectron spectroscopy, and the adsorption of human serum albumin and g-globulins. *Journal of Polymer Science, Part A: Polymer Chemistry* **2004,** 42, (3), 615-623.

73. Jung, H.; Kim, S. Y.; Lee, K.; Lee, B. H.; Shim, S. E.; Choe, S., High molecular weight monodisperse polystyrene microspheres prepared by dispersion polymerization, using a novel bifunctional macromonomer. *Journal of Polymer Science, Part A: Polymer Chemistry* **2005,** 43, (16), 3566-3573.

74. Jung, H.; Lee, K.; Shim, S. E.; Yang, S.; Lee, J. M.; Lee, H.; Choe, S., Novel macromonomer as a reactive stabilizer in the dispersion polymerization of methyl methacrylate. *Macromolecular Research* **2004,** 12, (5), 512-518.

75. Zhang, H.; Duan, L.; Chen, L.; Huang, H., Stability and copolymerization of concentrated emulsion of styrene and butyl acrylate in the presence of polyurethane macromonomer. *Journal of Applied Polymer Science* **2007,** 103, (3), 1992-1999.

76. Chambon, P.; Chemtob, A.; Cloutet, E.; Cramail, H.; Gibanel, S.; Gnanou, Y.; Heroguez, V.; Quemener, D.; Radhakrishnan, B., Design and use of macromonomers as steric stabilizers for the synthesis of novel functional particles in dispersed media. *Polymer International* **2006,** 55, (10), 1146-1154.

77. Lee, K.; Jung, H.; Kim, S. Y.; Lee, B. H.; Choe, S., Synthesis and characterization of cross-type vinylurethane macromonomer (C-VUM) and their application in the dispersion polymerization of styrene. *Polymer* **2006,** 47, (6), 1830-1836.

78. Kim, S. Y.; Lee, K.; Jung, H.; Shim, S. E.; Lee, B. H.; Choe, S., Macromonomers having different molecular weights of polyethylene glycol and end group functionalities in dispersion polymerization of styrene. *Polymer* **2005,** 46, (19), 7974-7981.

79. Uchida, T.; Kawaguchi, S.; Ito, K., Dispersion (co)polymerization of styrene in polymeric media to prepare polymer micro blends. *Designed Monomers and Polymers* **2002,** 5, (2,3), 285-296.

80. Pilon, L. N.; Armes, S. P.; Findlay, P.; Rannard, S. P., Synthesis and characterization of new shell cross-linked micelles with amine-functional coronas. *European Polymer Journal* **2006,** 42, (7), 1487-1498.

81. O'Reilly, R. K.; Hawker, C. J.; Wooley, K. L., Cross-linked block copolymer micelles: functional nanostructures of great potential and versatility. *Chemical Society Reviews* **2006,** 35, (11), 1068-1083.

82. Hu, F.-Q.; Ren, G.-F.; Yuan, H.; Du, Y.-Z.; Zeng, S., Shell cross-linked stearic acid grafted chitosan oligosaccharide self-aggregated micelles for controlled release of paclitaxel. *Colloids and Surfaces, B: Biointerfaces* **2006,** 50, (2), 97-103.

83. Buetuen, V.; Top, R. B.; Ufuklar, S., Synthesis and Characterization of Novel "Schizophrenic" Water-Soluble Triblock Copolymers and Shell Cross-Linked Micelles. *Macromolecules* **2006,** 39, (3), 1216-1225.

84. Berndt, I.; Pedersen, J. S.; Lindner, P.; Richtering, W., Influence of Shell Thickness and Cross-Link Density on the Structure of Temperature-Sensitive

Poly-N-Isopropylacrylamide-Poly-N-Isopropylmethacrylamide Core-Shell Microgels Investigated by Small-Angle Neutron Scattering. *Langmuir* **2006,** 22, (1), 459-468.

85. Pilon, L. N.; Armes, S. P.; Findlay, P.; Rannard, S. P., Synthesis and Characterization of Shell Cross-Linked Micelles with Hydroxy-Functional Coronas: A Pragmatic Alternative to Dendrimers? *Langmuir* **2005,** 21, (9), 3808-3813.

86. Perkin Kris, K.; Turner Jeffrey, L.; Wooley Karen, L.; Mann, S., Fabrication of hybrid nanocapsules by calcium phosphate mineralization of shell cross-linked polymer micelles and nanocages. *Nano Letters* **2005,** 5, (7), 1457-1461.

87. O'Reilly, R. K.; Joralemon, M. J.; Wooley, K. L.; Hawker, C. J., Functionalization of Micelles and Shell Cross-linked Nanoparticles Using Click Chemistry. *Chemistry of Materials* **2005,** 17, (24), 5976-5988.

88. Matsumoto, K.; Hirabayashi, T.; Harada, T.; Matsuoka, H., Synthesis of shell cross-linked block copolymer micelles with poly(p-styrenesulfonic acid) in the micelle core. *Macromolecules* **2005,** 38, (24), 9957-9962.

89. Joralemon, M. J.; Smith, N. L.; Holowka, D.; Baird, B.; Wooley, K. L., Antigen-decorated shell cross-linked nanoparticles: Synthesis, characterization, and antibody interactions. *Bioconjugate Chemistry* **2005,** 16, (5), 1246-1256.

90. Joralemon, M. J.; O'Reilly, R. K.; Hawker, C. J.; Wooley, K. L., Shell Click-crosslinked (SCC) nanoparticles: A new methodology for synthesis and

orthogonal functionalization. *Journal of the American Chemical Society* **2005,** 127, (48), 16892-16899.

91. Harrisson, S.; Wooley, K. L., Shell-crosslinked nanostructures from amphiphilic AB and ABA block copolymers of styrene-alt-(maleic anhydride) and styrene: polymerization, assembly and stabilization in one pot. *Chemical Communications* **2005**, (26), 3259-3261.
92. Fujii, S.; Cai, Y.; Weaver Jonathan, V. M.; Armes Steven, P., Syntheses of shell cross-linked micelles using acidic ABC triblock copolymers and their application as pH-responsive particulate emulsifiers. *Journal of the American Chemical Society* **2005,** 127, (20), 7304-7305.
93. Weaver, J. V. M.; Tang, Y.; Liu, S.; Iddon, P. D.; Grigg, R.; Billingham, N. C.; Armes, S. P.; Hunter, R.; Rannard, S. P., Preparation of shell cross-linked micelles by polyelectrolyte complexation. *Angewandte Chemie, International Edition* **2004,** 43, (11), 1389-1392.
94. Turner, J. L.; Wooley, K. L., Nanoscale cage-like structures derived from polyisoprene-containing shell cross-linked nanoparticle templates. *Nano Letters* **2004,** 4, (4), 683-688.
95. Tang, C. B.; Qi, K.; Wooley, K. L.; Matyjaszewski, K.; Kowalewski, T., Well-defined carbon nanoparticles prepared from water-soluble shell cross-linked micelles that contain polyacrylonitrile cores. *Angewandte Chemie-International Edition* **2004,** 43, (21), 2783-2787.
96. Qi, K.; Ma, Q. G.; Remsen, E. E.; Clark, C. G.; Wooley, K. L., Determination

of the bioavailability of biotin conjugated onto shell cross-linked (SCK) nanoparticles. *Journal of the American Chemical Society* **2004,** 126, (21), 6599-6607.

97. Pan, D. J.; Turner, J. L.; Wooley, K. L., Shell cross-linked nanoparticles designed to target angiogenic blood vessels via alpha(v)beta(3) receptor-ligand interactions. *Macromolecules* **2004,** 37, (19), 7109-7115.

98. Hales, M.; Barner-Kowollik, C.; Davis, T. P.; Stenzel, M. H., Shell-Cross-Linked Vesicles Synthesized from Block Copolymers of Poly(D,L-lactide) and Poly(N-isopropyl acrylamide) as Thermoresponsive Nanocontainers. *Langmuir* **2004,** 20, (25), 10809-10817.

99. Becker, M. L.; Remsen, E. E.; Pan, D.; Wooley, K. L., Peptide-derivatized shell-cross-linked nanoparticles. 1. Synthesis and characterization. *Bioconjugate Chemistry* **2004,** 15, (4), 699-709.

100. Becker, M. L.; Bailey, L. O.; Wooley, K. L., Peptide-derivatized shell-cross-linked nanoparticles. 2. Biocompatibility evaluation. *Bioconjugate Chemistry* **2004,** 15, (4), 710-717.

101. Murthy, K. S.; Ma, Q. G.; Remsen, E. E.; Kowalewski, T.; Wooley, K. L., Thermal shaping of shell-crosslinked (SCK) nanoparticles, facilitated by nanoconfinement of fluid-like cores. *Journal of Materials Chemistry* **2003,** 13, (11), 2785-2795.

102. Liu, S.; Weaver, J. V. M.; Tang, Y.; Billingham, N. C.; Armes, S. P.; Tribe, K., Synthesis of Shell Cross-Linked Micelles with pH-Responsive Cores Using

ABC Triblock Copolymers. *Macromolecules* **2002,** 35, (16), 6121-6131.

103. Liu, S.; Weaver, J. V. M.; Save, M.; Armes, S. P., Synthesis of pH-Responsive Shell Cross-Linked Micelles and Their Use as Nanoreactors for the Preparation of Gold Nanoparticles. *Langmuir* **2002,** 18, (22), 8350-8357.

104. Liu, S.; Ma, Y.; Armes, S. P.; Perruchot, C.; Watts, J. F., Direct Verification of the Core-Shell Structure of Shell Cross-Linked Micelles in the Solid State Using X-ray Photoelectron Spectroscopy. *Langmuir* **2002,** 18, (21), 7780-7784.

106. Ma, Q. G.; Remsen, E. E.; Kowalewski, T.; Schaefer, J.; Wooley, K. L., Environmentally-responsive, entirely hydrophilic, shell cross-linked (SCK) nanoparticles. *Nano Letters* **2001,** 1, (11), 651-655.

107. Ma, Q.; Remsen, E. E.; Kowalewski, T.; Wooley, K. L., Two-Dimensional, Shell-Cross-linked Nanoparticle Arrays. *Journal of the American Chemical Society* **2001,** 123, (19), 4627-4628.

108. Liu, S.; Armes, S. P., The facile one-pot synthesis of shell cross-linked micelles in aqueous solution at high solids. *Journal of the American Chemical Society* **2001,** 123, (40), 9910-9911.

109. Becker, M. L.; Remsen, E. E.; Wooley, K. L., Diblock copolymers, micelles, and shell-crosslinked nanoparticles containing poly(4-fluorostyrene): Tools for detailed analyses of nanostructured materials. *Journal of Polymer Science Part a-Polymer Chemistry* **2001,** 39, (23), 4152-4166.

110. Zhang, Q.; Remsen, E. E.; Wooley, K. L., Shell Cross-Linked Nanoparticles

Containing Hydrolytically Degradable, Crystalline Core Domains. *Journal of the American Chemical Society* **2000,** 122, (15), 3642-3651.

111. Wooley, K. L., Shell crosslinked polymer assemblies: Nanoscale constructs inspired from biological systems. *Journal of Polymer Science Part A: Polymer Chemistry* **2000,** 38, (9), 1397-1407.

112. Buetuen, V.; Wang, X. S.; Banez, M. V. d. P.; Robinson, K. L.; Billingham, N. C.; Armes, S. P.; Tuzar, Z., Synthesis of Shell Cross-Linked Micelles at High Solids in Aqueous Media. *Macromolecules* **2000,** 33, (1), 1-3.

113. Thurmond, K. B.; Huang, H. Y.; Clark, C. G.; Kowalewski, T.; Wooley, K. L., Shell cross-linked polymer micelles: stabilized assemblies with great versatility and potential. *Colloids and Surfaces B-Biointerfaces* **1999,** 16, (1-4), 45-54.

114. Buetuen, V.; Lowe, A. B.; Billingham, N. C.; Armes, S. P., Synthesis of Zwitterionic Shell Cross-Linked Micelles. *Journal of the American Chemical Society* **1999,** 121, (17), 4288-4289.

115. Huang, H. Y.; Remsen, E. E.; Wooley, K. L., Amphiphilic core-shell nanospheres obtained by intramicellar shell crosslinking of polymer micelles with poly(ethylene oxide) linkers. *Chemical Communications* **1998**, (13), 1415-1416.

116. Buetuen, V.; Billingham, N. C.; Armes, S. P., Synthesis of Shell Cross-Linked Micelles with Tunable Hydrophilic/Hydrophobic Cores. *Journal of the American Chemical Society* **1998,** 120, (46), 12135-12136.

117. Wooley, K. L., From dendrimers to knedel-like structures. *Chemistry-a European Journal* **1997,** 3, (9), 1397-1399.

118. Thurmond, K. B., II; Kowalewski, T.; Wooley, K. L., Shell Cross-Linked Knedels: A Synthetic Study of the Factors Affecting the Dimensions and Properties of Amphiphilic Core-Shell Nanospheres. *Journal of the American Chemical Society* **1997,** 119, (28), 6656-6665.

119. Huang, H. Y.; Kowalewski, T.; Remsen, E. E.; Gertzmann, R.; Wooley, K. L., Hydrogel-coated glassy nanospheres: A novel method for the synthesis of shell cross-linked knedels. *Journal of the American Chemical Society* **1997,** 119, (48), 11653-11659.

120. Thurmond, K. B., II; Kowalewski, T.; Wooley, K. L., Water-Soluble Knedel-like Structures: The Preparation of Shell-Cross-Linked Small Particles. *Journal of the American Chemical Society* **1996,** 118, (30), 7239-7240.

121. Sanji, T.; Nakatsuka, Y.; Ohnishi, S.; Sakurai, H., Preparation of nanometer-sized hollow particles by photochemical degradation of polysilane shell crosslinked micelles and reversible encapsulation of guest molecules. *Macromolecules* **2000,** 33, (23), 8524-8526.

122. Huang, H.; Remsen, E. E.; Kowalewski, T.; Wooley, K. L., Nanocages Derived from Shell Cross-Linked Micelle Templates. *Journal of the American Chemical Society* **1999,** 121, (15), 3805-3806.

123. Becker, M. L.; Liu, J. Q.; Wooley, K. L., Functionalized micellar assemblies prepared via block copolymers synthesized by living free radical

polymerization upon peptide-loaded resins. *Biomacromolecules* **2005,** 6, (1), 220-228.

124. Ma, Y.; Tang, Y.; Billingham, N. C.; Armes, S. P.; Lewis, A. L.; Lloyd, A. W.; Salvage, J. P., Well-Defined Biocompatible Block Copolymers via Atom Transfer Radical Polymerization of 2-Methacryloyloxyethyl Phosphorylcholine in Protic Media. *Macromolecules* **2003,** 36, (10), 3475-3484.
125. Ma, Q. G.; Wooley, K. L., The preparation of t-butyl acrylate, methyl acrylate, and styrene block copolymers by atom transfer radical polymerization: Precursors to amphiphilic and hydrophilic block copolymers and conversion to complex nanostructured materials. *Journal of Polymer Science Part A: Polymer Chemistry* **2000,** 38, 4805-4820.
126. Li, Y.; Lokitz, B. S.; McCormick, C. L., RAFT Synthesis of a Thermally Responsive ABC Triblock Copolymer Incorporating N-Acryloxysuccinimide for Facile in Situ Formation of Shell Cross-Linked Micelles in Aqueous Media. *Macromolecules* **2006,** 39, (1), 81-89.
127. O'Reilly, R. K.; Joralemon, M. J.; Hawker, C. J.; Wooley, K. L., Fluorogenic 1,3-dipolar cycloaddition within the hydrophobic core of a shell cross-linked nanoparticle. *Chemistry--A European Journal* **2006,** 12, (26), 6776-6786.
128. Remsen, E. E.; Thurmond, K. B., II; Wooley, K. L., Solution and Surface Charge Properties of Shell Cross-Linked Knedel Nanoparticles. *Macromolecules* **1999,** 32, (11), 3685-3689.

129. Wang, M.; Jiang, M.; Ning, F.; Chen, D.; Liu, S.; Duan, H., Block-Copolymer-Free Strategy for Preparing Micelles and Hollow Spheres: Self-Assembly of Poly(4-vinylpyridine) and Modified Polystyrene. *Macromolecules* **2002,** 35, (15), 5980-5989.

130. Luo, S.; Xu, J.; Zhang, Y.; Liu, S.; Wu, C., Double Hydrophilic Block Copolymer Monolayer Protected Hybrid Gold Nanoparticles and Their Shell Cross-Linking. *Journal of Physical Chemistry B* **2005,** 109, (47), 22159-22166.

131. Zhang, Z.; Liu, G.; Bell, S., Synthesis of Poly(solketal methacrylate)-block-poly(2-(dimethylamino)ethyl methacrylate) and Preparation of Nanospheres with Cross-Linked Shells. *Macromolecules* **2000,** 33, (21), 7877-7883.

132. Chen, Q.; Hu, Y.; Chen, Y.; Jiang, X.; Yang, Y., Microstructure formation and property of chitosan-poly(acrylic acid) nanoparticles prepared by macromolecular complex. *Macromolecular bioscience* **2005,** 5, (10), 993-1000.

133. O'Reilly, R. K.; Joralemon, M. J.; Hawker, C. J.; Wooley, K. L., Facile syntheses of surface-functionalized micelles and shell cross-linked nanoparticles. *Journal of Polymer Science, Part A: Polymer Chemistry* **2006,** 44, (17), 5203-5217.

134. Joralemon, M. J.; O'Reilly, R. K.; Matson, J. B.; Nugent, A. K.; Hawker, C. J.; Wooley, K. L., Dendrimers clicked together divergently. *Macromolecules*

2005, 38, (13), 5436-5443.

135. Zhang, L.; Katapodi, K.; Davis, T. P.; Barner-Kowollik, C.; Stenzel, M. H., Using the reversible addition-fragmentation chain transfer process to synthesize core-crosslinked micelles. *Journal of Polymer Science, Part A: Polymer Chemistry* **2006,** 44, (7), 2177-2194.

136. Zheng, G.; Pan, C., Facile one-pot synthesis of nano core crosslinked micelles via RAFT polymerization in selective solvent. *Gaofenzi Xuebao* **2005**, (5), 664-668.

137. Yoshida, E.; Tanaka, M.; Takata, T., Direct preparation of core cross-linked micelles in a nonselective solvent. *Colloid and Polymer Science* **2005,** 284, (1), 51-57.

138. Saito, R., Synthesis of Discotic Microgels by Cross-Linking of Poly(styrene-block-4-vinylpyridine)/3-n-Pentadecylphenol Blend Film. *Macromolecules* **2001,** 34, (13), 4299-4301.

139. Saito, R.; Fujita, A.; Ichimura, A.; Ishizu, K., Synthesis of microspheres with microphase-separated shells. *Journal of Polymer Science, Part A: Polymer Chemistry* **2000,** 38, (11), 2091-2097.

140. Emoto, K.; Iijima, M.; Nagasaki, Y.; Kataoka, K., Functionality of Polymeric Micelle Hydrogels with Organized Three-Dimensional Architecture on Surfaces. *Journal of American Chemical Society* **2000,** 122, (11), 2653-2654.

141. Won, Y.-Y.; Davis, H. T.; Bates, F. S., Giant Wormlike Rubber Micelles. *Science* **1999,** 283, (5404), 960-963.

142. Saito, R.; Akiyama, Y.; Tanaka, M.; Ishizu, K., Synthesis of the flower type microgels. *Colloids and Surfaces, A: Physicochemical and Engineering Aspects* **1999,** 153, (1-3), 305-310.

143. Kim, J.-H.; Emoto, K.; Iijima, M.; Nagasaki, Y.; Aoyagi, T.; Okano, T.; Sakurai, Y.; Kataoka, K., Core-stabilized polymeric micelle as potential drug carrier: increased solubilization of taxol. *Polymers for Advanced Technologies* **1999,** 10, (11), 647-654.

144. Kakizawa, Y.; Harada, A.; Kataoka, K., Environment-sensitive stabilization of core-shell structured polyion complex micelle by reversible cross-linking of the core through disulfide bond. *Journal of the American Chemical Society* **1999,** 121, (48), 11247-11248.

145. Iijima, M.; Nagasaki, Y.; Okada, T.; Kato, M.; Kataoka, K., Core-Polymerized Reactive Micelles from Heterotelechelic Amphiphilic Block Copolymers. *Macromolecules* **1999,** 32, (4), 1140-1146.

146. Emoto, K.; Nagasaki, Y.; Kataoka, K., Coating of Surfaces with Stabilized Reactive Micelles from Poly(ethylene glycol)-Poly(DL-lactic acid) Block Copolymer. *Langmuir* **1999,** 15, (16), 5212-5218.

147. Saito, R.; Akiyama, Y.; Ishizu, K., Flower shaped microgel. 3: Synthesis of poly(2-hydroxyethylmethacrylate) core-polystyrene shell type microgels. *Polymer* **1998,** 40, (3), 655-660.

148. Saito, R.; Yoshida, S.; Ishizu, K., Synthesis of poly(vinyl alcohol) core-polystyrene shell-type flower microgels. *Journal of Applied Polymer*

Science **1997,** 63, (7), 849-854.

149. Saito, R.; Tanaka, S.; Ishizu, K., Synthesis of poly(methacrylic acid) core/polystyrene shell type polymer microspheres. *Polymer* **1997,** 38, (7), 1725-1729.

150. Saito, R.; Sugita, M.; Ishizu, K., Hierarchical structure of lattices in film formation of core-shell type polymer microspheres. 2. Microsphere/homopolymer blends. *Journal of Colloid and Interface Science* **1997,** 187, (2), 515-519.

151. Saito, R.; Ishizu, K., Flower type microgels. 1. Synthesis of the microgels. *Polymer* **1997,** 38, (1), 225-229.

152. Saito, R.; Ishizu, K., Effects of different core densities on the diffusibility of microspheres. *Polymer* **1997,** 39, (2), 335-338.

153. Henselwood, F.; Liu, G., Water-Soluble Nanospheres of Poly(2-cinnamoylethyl methacrylate)-block-poly(acrylic acid). *Macromolecules* **1997,** 30, (3), 488-493.

154. Ishizu, K.; Honda, K.; Saito, R., Synthesis of polymer microspheres with polypyrrole core. *Polymer* **1996,** 37, (17), 3965-3970.

155. Saito, R.; Okamura, S.-i.; Ishizu, K., Synthesis of poly(vinyl alcohol) core-polystyrene shell type microspheres. *Polymer* **1995,** 36, (23), 4515-4520.

156. Saito, R.; Kotsubo, H.; Ishizu, K., Synthesis of microspheres with 'hairy-ball' structures from poly(styrene-b-2-vinyl pyridine) diblock copolymers. *Polymer* **1992,** 33, (5), 1073-1076.

157. Fukutomi, T.; Imori, Y.; Saito, R.; Shizu, K., The synthesis of microgels composed of polyelectrolytes. *Journal of Applied Polymer Science* **1992,** 44, (4), 737-741.

158. Saito, R.; Kotsubo, H.; Ishizu, K., Core-shell type polymer microspheres prepared from poly(styrene-b-methacrylic acid). 1. Synthesis of microgel. *European Polymer Journal* **1991,** 27, (10), 1153-1159.

159. Angelatos, A. S.; Katagiri, K.; Caruso, F., Bioinspired colloidal systems via layer-by-layer assembly. *Soft Matter* **2006,** 2, (1), 18-23.

160. Zhu, Y.; Yang, X.; Li, P.; Hu, Y., From Layer-by-layer assembled core-shell particles to medical/biochemical diagnostics and drug delivery. *Huaxue Jinzhan* **2003,** 15, (6), 512-517.

161. Caruso, F.; Sukhorukov, G., Coated colloids: preparation, characterization, assembly and utilization. *Multilayer Thin Films* **2003**, 331-362.

162. Grieve, K.; Grieser, F.; Furlong, D. N., Formation of nanoparticles in organized amphiphilic films. *Surfactant Science Series* **2001,** 100, (Reactions and Synthesis in Surfactant Systems), 639-665.

163. Caruso, F., Nanoengineering of particle surfaces. *Advanced Materials (Weinheim, Germany)* **2001,** 13, (1), 11-22.

164. Mohwald, H.; Lichtenfeld, H.; Moya, S.; Voigt, A.; Baumler, H.; Sukhorukov, G.; Caruso, F.; Donath, E., From polymeric films to nanoreactors. *Macromolecular Symposia* **1999,** 145, (Polymer Sorption Phenomena), 75-81.

165. Mohwald, H., From Langmuir monolayers to nanocapsules. *Colloids and*

Surfaces A: Physicochemical and Engineering Aspects **2000,** 171, (1-3), 25-31.

166. Biggs, S.; Sakai, K.; Addison, T.; Schmid, A.; Armes, S. P.; Vamvakaki, M.; Butun, V.; Webber, G., Layer-by-layer formation of smart particle coatings using oppositely charged block copolymer micelles. *Advanced Materials (Weinheim, Germany)* **2007,** 19, (2), 247-250.

167. Wong, J. E.; Richtering, W., Surface modification of thermoresponsive microgels via layer-by-layer assembly of polyelectrolyte multilayers. *Progress in Colloid and Polymer Science* **2006,** 133, 45-51.

168. Caruso, F.; Moehwald, H., Preparation and Characterization of Ordered Nanoparticle and Polymer Composite Multilayers on Colloids. *Langmuir* **1999,** 15, (23), 8276-8281.

169. Caruso, F.; Caruso, R. A.; Donath, E.; Mohwald, H.; Sukhorukov, G. Fabrication of multilayer-coated particles and hollow shells by electrostatic self-assembly of nanocomposite multilayers on decomposable colloidal templates. WO 9947253, 1999.

170. Sukhorukov, G. B.; Donath, E.; Lichtenfeld, H.; Knippel, E.; Knippel, M.; Budde, A.; Mohwald, H., Layer-by-layer self assembly of polyelectrolytes on colloidal particles. *Colloids and Surfaces, A: Physicochemical and Engineering Aspects* **1998,** 137, (1-3), 253-266.

171. Sukhorukov, G. B.; Donath, E.; Davis, S.; Lichtenfeld, H.; Caruso, F.; Popov, V. I.; Mohwald, H., Stepwise polyelectrolyte assembly on particle surfaces: a

novel approach to colloid design. *Polymers for Advanced Technologies* **1998,** 9, (10-11), 759-767.

172. Donath, E.; Sukhorukov, G. B.; Caruso, F.; Davis, S. A.; Mohwald, H., Novel hollow polymer shells by colloid-templated assembly of polyelectrolytes. *Angewandte Chemie, International Edition* **1998,** 37, (16), 2202-2205.

173. Chen, T.-y.; Somasundaran, P., Preparation of novel core-shell nanocomposite particles by controlled polymer bridging. *Journal of the American Ceramic Society* **1998,** 81, (1), 140-144.

174. Caruso, F.; Niikura, K.; Furlong, D. N.; Okahata, Y., Assembly of Alternating Polyelectrolyte and Protein Multilayer Films for Immunosensing. *Langmuir* **1997,** 13, (13), 3427-3433.

175. Donath, E.; Walther, D.; Shilov, V. N.; Knippel, E.; Budde, A.; Lowack, K.; Helm, C. A.; Moehwald, H., Nonlinear Hairy Layer Theory of Electrophoretic Fingerprinting Applied to Consecutive Layer by Layer Polyelectrolyte Adsorption onto Charged Polystyrene Latex Particles. *Langmuir* **1997,** 13, (20), 5294-5305.

176. Kim, B.-S.; Vinogradova, O. I., pH-Controlled Swelling of Polyelectrolyte Multilayer Microcapsules. *Journal of Physical Chemistry B* **2004,** 108, (24), 8161-8165.

177. Park, M.-K.; Onishi, K.; Locklin, J.; Caruso, F.; Advincula, R. C., Self-Assembly and Characterization of Polyaniline and Sulfonated Polystyrene Multilayer-Coated Colloidal Particles and Hollow Shells. *Langmuir* **2003,** 19,

(20), 8550-8554.

178. Quinn, J. F.; Caruso, F., Facile Tailoring of Film Morphology and Release Properties Using Layer-by-Layer Assembly of Thermoresponsive Materials. *Langmuir* **2004,** 20, (1), 20-22.

179. Johnston, A. P. R.; Zelikin, A. N.; Lee, L.; Caruso, F., Approaches to Quantifying and Visualizing Polyelectrolyte Multilayer Film Formation on Particles. *Analytical Chemistry* **2006,** 78, (16), 5913-5919.

180. Wang, Y.; Caruso, F., Template Synthesis of Stimuli-Responsive Nanoporous Polymer-Based Spheres via Sequential Assembly. *Chemistry of Materials* **2006,** 18, (17), 4089-4100.

181. Caruso, F.; Moehwald, H., Protein Multilayer Formation on Colloids through a Stepwise Self-Assembly Technique. *Journal of the American Chemical Society* **1999,** 121, (25), 6039-6046.

182. Shenoy, D. B.; Antipov, A. A.; Sukhorukov, G. B.; Mohwald, H., Layer-by-Layer Engineering of Biocompatible, Decomposable Core-Shell Structures. *Biomacromolecules* **2003,** 4, (2), 265-272.

183. Zhou, D.; Bruckbauer, A.; Batchelor, M.; Kang, D.-J.; Abell, C.; Klenerman, D., Influence of the foundation layer on the layer-by-layer assembly of poly-L-lysine and poly(styrenesulfonate) and its usage in the fabrication of 3D microscale features. *Langmuir* **2004,** 20, (21), 9089-9094.

184. Zhang, Y.; Guan, Y.; Zhou, S., Single Component Chitosan Hydrogel Microcapsule from a Layer-by-Layer Approach. *Biomacromolecules* **2005,** 6,

(4), 2365-2369.

185. Radeva, T.; Kamburova, K.; Petkanchin, I., Formation of polyelectrolyte multilayers from polysaccharides at low ionic strength. *Journal of Colloid and Interface Science* **2006,** 298, (1), 59-65.

186. Wang, Y.; Caruso, F., Nanoporous protein particles through templating mesoporous silica spheres. *Advanced Materials (Weinheim, Germany)* **2006,** 18, (6), 795-800.

187. Tieke, B.; Toutianoush, A.; Jin, W., Selective transport of ions and molecules across layer-by-layer assembled membranes of polyelectrolytes, p-sulfonato-calix[n]arenes and Prussian Blue-type complex salts. *Advances in colloid and interface science* **2005,** 116, (1-3), 121-131.

188. Wang, D.; Caruso, R. A.; Caruso, F., Synthesis of macroporous titania and inorganic composite materials from coated colloidal spheres - A novel route to tune pore morphology. *Chemistry of Materials* **2001,** 13, (2), 364-371.

189. Caruso, F.; Caruso, R. A.; Moehwald, H., Nanoengineering of inorganic and hybrid hollow spheres by colloidal templating. *Science (Washington, D. C.)* **1998,** 282, (5391), 1111-1114.

190. Nelson, K.; Deng, Y., The shape dependence of core-shell and hollow titania nanoparticles on coating thickness during layer-by-layer and sol-gel synthesis. *Nanotechnology* **2006,** 17, (13), 3219-3225.

191. Crespo-Biel, O.; Dordi, B.; Reinhoudt, D. N.; Huskens, J., Supramolecular Layer-by-Layer Assembly: Alternating Adsorptions of Guest- and

Host-Functionalized Molecules and Particles Using Multivalent Supramolecular Interactions. *Journal of the American Chemical Society* **2005,** 127, (20), 7594-7600.

192. Sukhorukov, G. B., Multilayer hollow microspheres. *Microspheres, Microcapsules & Liposomes* **2002,** 5, (Dendrimers, Assemblies, Nanocomposites), 111-147.

193. Khopade, A. J.; Caruso, F., Stepwise Self-Assembled Poly(amidoamine) Dendrimer and Poly(styrenesulfonate) Microcapsules as Sustained Delivery Vehicles. *Biomacromolecules* **2002,** 3, (6), 1154-1162.

194. Khopade, A. J.; Caruso, F., Surface-modification of polyelectrolyte multilayer-coated particles for biological applications. *Langmuir* **2003,** 19, (15), 6219-6225.

195. Sauer, M.; Meier, W., Colloidal nanoreactors and nanocontainers. *Colloids and Colloid Assemblies* **2004**, 150-174.

196. Zhao, Q.; Zhang, S.; Tong, W.; Gao, C.; Shen, J., Polyelectrolyte microcapsules templated on poly(styrene sulfonate)-doped $CaCO_3$ particles for loading and sustained release of daunorubicin and doxorubicin. *European Polymer Journal* **2006,** 42, (12), 3341-3351.

197. Mauser, T.; Dejugnat, C.; Moehwald, H.; Sukhorukov, G. B., Microcapsules Made of Weak Polyelectrolytes: Templating and Stimuli-Responsive Properties. *Langmuir* **2006,** 22, (13), 5888-5893.

198. De Geest, B. G.; Dejugnat, C.; Verhoeven, E.; Sukhorukov, G. B.; Jonas, A.

M.; Plain, J.; Demeester, J.; De Smedt, S. C., Layer-by-layer coating of degradable microgels for pulsed drug delivery. *Journal of Controlled Release* **2006,** 116, (2), 159-169.

199. Zhu, H.; McShane Michael, J., Macromolecule encapsulation in diazoresin-based hollow polyelectrolyte microcapsules. *Langmuir* **2005,** 21, (1), 424-430.

200. Zheng, S.; Tao, C.; He, Q.; Zhu, H.; Li, J., Self-assembly and Characterization of Polypyrrole and Polyallylamine Multilayer Films and Hollow Shells. *Chemistry of Materials* **2004,** 16, (19), 3677-3681.

201. Shi, X.; Briseno, A. L.; Sanedrin, R. J.; Zhou, F., Formation of Uniform Polyaniline Thin Shells and Hollow Capsules Using Polyelectrolyte-Coated Microspheres as Templates. *Macromolecules* **2003,** 36, (11), 4093-4098.

202. Glinel, K.; Sukhorukov, G. B.; Moehwald, H.; Khrenov, V.; Tauer, K., Thermosensitive hollow capsules based on thermoresponsive polyelectrolytes. *Macromolecular Chemistry and Physics* **2003,** 204, (14), 1784-1790.

203. Shchukin, D. G.; Ustinovich, E. A.; Sukhorukov, G. B.; Moehwald, H.; Sviridov, D. V., Metallized polyelectrolyte microcapsules. *Advanced Materials (Weinheim, Germany)* **2005,** 17, (4), 468-472.

204. Li, P.; Zhu, J. M.; Harris, F. W. Amphiphilic core-shell latexes. US. Patent 6,573,313, 2002.

205. Li, P.; Zhu, J.; Sunintaboon, P.; Harris, F. W., New Route to Amphiphilic Core-Shell Polymer Nanospheres: Graft Copolymerization of Methyl

Methacrylate from Water-Soluble Polymer Chains Containing Amino Groups. *Langmuir* **2002,** 18, (22), 8641-8646.

206. Feng, M.; Li, P., Amine-containing core-shell nanoparticles as potential drug carriers for intracellular delivery. *J Biomed Mater Res A FIELD Full Journal Title:Journal of biomedical materials research. Part A* **2007,** 80, (1), 184-193.

207. Mao, X.; Guo, G.; Huang, J.; Du, Z.; Huang, Z.; Ma, L.; Li, P.; Gu, L., A novel method to prepare chitosan powder and its application in cellulase immobilization. *Journal of Chemical Technology and Biotechnology* **2006,** 81, (2), 189-195.

208. Feng, M.; Lee, D.; Li, P., Intracellular uptake and release of poly(ethyleneimine)-co-poly(methyl methacrylate) nanoparticle/pDNA complexes for gene delivery. *International Journal of Pharmaceutics* **2006,** 311, (1-2), 209-214.

209. Zhu, J.; Tang, A.; Law, L. P.; Feng, M.; Ho, K. M.; Lee, D. K. L.; Harris, F. W.; Li, P., Amphiphilic core-shell nanoparticles with poly(ethylenimine) shells as potential gene delivery carriers. *Bioconjugate Chemistry* **2005,** 16, (1), 139-146.

210. Zhu, J.; Li, P., Synthesis and characterization of poly(methyl methacrylate)/casein nanoparticles with a well-defined core-shell structure. *Journal of Polymer Science, Part A: Polymer Chemistry* **2003,** 41, (21), 3346-3353.

211. Ye, W.; Leung, M. F.; Xin, J.; Kwong, T. L.; Lee, D. K. L.; Li, P., Novel

core-shell particles with poly(n-butyl acrylate) cores and chitosan shells as an antibacterial coating for textiles. *Polymer* **2005,** 46, (23), 10538-10543.

212. Li, P.; Zhu, J.; Sunintaboon, P.; Harris, F. W., Preparation of latexes with poly(methyl methacrylate) cores and hydrophilic polymer shells containing amino groups. *Journal of Dispersion Science and Technology* **2003,** 24, (3 & 4), 607-613.

213. Leung, M. F.; Zhu, J.; Harris, F. W.; Li, P., Novel synthesis and properties of smart core-shell microgels. *Macromolecular Symposia* **2005,** 226, (Polymer Chemistry, Reactions and Processes), 177-185.

214. Leung, M. F.; Zhu, J.; Harris, F. W.; Li, P., New route to smart core-shell polymeric microgels: Synthesis and properties. *Macromolecular Rapid Communications* **2004,** 25, (21), 1819-1823.

215. Chen, C.-W.; Chen, M.-Q.; Serizawa, T.; Akashi, M., In-situ formation of silver nanoparticles on poly(N-isopropylacrylamide)-coated polystyrene microspheres. *Advanced Materials* **1998,** 10, (14), 1122-1126.

216. Sharma, G.; Mei, Y.; Lu, Y.; Ballauff, M.; Irrgang, T.; Proch, S.; Kempe, R., Spherical polyelectrolyte brushes as carriers for platinum nanoparticles in heterogeneous hydrogenation reactions. *Journal of Catalysis* **2007,** 246, (1), 10-14.

217. Lu, Y.; Mei, Y.; Walker, R.; Ballauff, M.; Drechsler, M., Nano-tree'-type spherical polymer brush particles as templates for metallic nanoparticles. *Polymer* **2006,** 47, (14), 4985-4995.

218. Mei, Y.; Sharma, G.; Lu, Y.; Ballauff, M.; Drechsler, M.; Irrgang, T.; Kempe, R., High Catalytic Activity of Platinum Nanoparticles Immobilized on Spherical Polyelectrolyte Brushes. *Langmuir* **2005,** 21, (26), 12229-12234.

219. Lu, Y.; Mei, Y.; Drechsler, M.; Ballauff, M., Thermosensitive core-shell particles as carriers for Ag nanoparticles: modulating the catalytic activity by a phase transition in networks. *Angewandte Chemie, International Edition* **2006,** 45, (5), 813-816.

220. Lu, Y.; Mei, Y.; Ballauff, M.; Drechsler, M., Thermosensitive Core-Shell Particles as Carrier Systems for Metallic Nanoparticles. *Journal of Physical Chemistry B* **2006,** 110, (9), 3930-3937.

221. Turner, J. L.; Pan, D. P. J.; Plummer, R.; Chen, Z. Y.; Whittaker, A. K.; Wooley, K. L., Synthesis of gadolinium-labeled shell-crosslinked nanoparticles for magnetic resonance imaging applications. *Advanced Functional Materials* **2005,** 15, (8), 1248-1254.

222. Sharma, G.; Ballauff, M., Cationic spherical polyelectrolyte brushes as nanoreactors for the generation of gold particles. *Macromolecular Rapid Communications* **2004,** 25, (4), 547-552.

223. Jungmann, N.; Schmidt, M.; Maskos, M., Amphiphilic Poly(organosiloxane) Nanospheres as Nanoreactors for the Synthesis of Topologically Trapped Gold, Silver, and Palladium Colloids. *Macromolecules* **2003,** 36, (11), 3974-3979.

224. Chen, C. W.; Serizawa, T.; Akashi, M., In Situ Formation of Au/Pt Bimetallic Colloids on Polystyrene Microspheres: Control of Particle Growth and

Morphology. *Chemistry of Materials* **2002,** 14, (5), 2232-2239.

225. Basinska, T., Hydrophilic core-shell microspheres: A suitable support for controlled attachment of proteins and biomedical diagnostics. *Macromolecular Bioscience* **2005,** 5, (12), 1145-1168.

226. Sakuma, S.; Hayashi, M.; Akashi, M., Design of nanoparticles composed of graft copolymers for oral peptide delivery. *Advanced Drug Delivery Reviews* **2001,** 47, (1), 21-37.

227. Brindley, A.; Davis, S. S.; Davies, M. C.; Watts, J. F., Polystyrene colloids with surface-grafted polyethylene oxide as model systems for site-specific drug delivery. I. Preparation and surface chemical characterization using SIMS and XPS. *Journal of Colloid and Interface Science* **1995,** 171, (1), 150-161.

228. Bae, K. H.; Lee, Y.; Park, T. G., Oil-Encapsulating PEO-PPO-PEO/PEG Shell Cross-Linked Nanocapsules for Target-Specific Delivery of Paclitaxel. *Biomacromolecules* **2007,** 8, (2), 650-656.

229. Basinska, T., Adsorption studies of human serum albumin, human g-globulins, and human fibrinogen on the surface of P(S/PGL) microspheres. *Journal of Biomaterials Science, Polymer Edition* **2001,** 12, (12), 1359-1371.

230. Charreyre, M. T.; Revilla, J.; Elaissari, A.; Pichot, C.; Gallot, B., Surface functionalization of polystyrene nanoparticles with liposaccharide monomers: Preparation, characterization and applications. *Journal of Bioactive and Compatible Polymers* **1999,** 14, (1), 64-90.

231. Sakuma, S.; Ishida, Y.; Sudo, R.; Suzuki, N.; Kikuchi, H.; Hiwatari, K.-i.;

Kishida, A.; Akashi, M.; Hayashi, M., Stabilization of salmon calcitonin by polystyrene nanoparticles having surface hydrophilic polymeric chains, against enzymic degradation. *International Journal of Pharmaceutics* **1997,** 159, (2), 181-189.

232. Sakuma, S.; Sudo, R.; Suzuki, N.; Kikuchi, H.; Takamori, H.; Sato, T.; Minamitake, Y.; Hayashi, Y.; Sugita, O.; Hiwatari, K.-i.; Kishida, A.; Akashi, M., Human calcitonin delivered orally by means of nanoparticles composed of novel graft copolymers. *Journal of Dispersion Science and Technology* **2003,** 24, (3 & 4), 623-632.

233. Sakuma, S.; Suzuki, N.; Sudo, R.; Hiwatari, K.-i.; Kishida, A.; Akashi, M., Optimized chemical structure of nanoparticles as carriers for oral delivery of salmon calcitonin. *International Journal of Pharmaceutics* **2002,** 239, (1-2), 185-195.

234. Zhang, Y.; Li, L.; Tang, F.; Ren, J., Controlled drug delivery system based on magnetic hollow spheres/polyelectrolyte multilayer core-shell structure. *Journal of Nanoscience and Nanotechnology* **2006,** 6, (9/10), 3210-3214.

235. Torchilin, V. P., Lipid-core micelles for targeted drug delivery. *Current Drug Delivery* **2005,** 2, (4), 319-327.

236. Malik, D. K.; Baboota, S.; Ahuja, A.; Hasan, S.; Ali, J., Recent advances in protein and peptide drug delivery systems. *Current Drug Delivery* **2007,** 4, (2), 141-151.

237. Degim, I. T.; Celebi, N., Controlled delivery of peptides and proteins. *Current*

Pharmaceutical Design **2007,** 13, (1), 99-117.

238. Kim, K. K.; Pack, D. W., Microspheres for drug delivery. *BioMEMS and Biomedical Nanotechnology* **2006,** 1, 19-50.

239. Bramwell, V. W.; Perrie, Y., Particulate delivery systems for vaccines: what can we expect? *Journal of Pharmacy and Pharmacology* **2006,** 58, (6), 717-728.

240. Sarker, D. K., Engineering of nanoemulsions for drug delivery. *Current Drug Delivery* **2005,** 2, (4), 297-310.

241. Sukhorukov, G. B., From polyelectrolyte capsules to drug carriers. *ACS Symposium Series* **2004,** 879, (Carrier-Based Drug Delivery), 249-266.

242. Freiberg, S.; Zhu, X. X., Polymer microspheres for controlled drug release. *International Journal of Pharmaceutics* **2004,** 282, (1-2), 1-18.

243. Wilhelm, T.; Frank, W., *Immobilized Enzymes: Methods and Applications*. 1999; p 95-126.

244. Cao, L., Immobilized enzymes: science or art? *Current Opinion in Chemical Biology* **2005,** 9, (2), 217-226.

245. Neumann, T.; Haupt, B.; Ballauff, M., High activity of enzymes immobilized in colloidal nanoreactors. *Macromolecular Bioscience* **2004,** 4, (1), 13-16.

246. Yasuda, M.; Kobayashi, M.; Kotani, T.; Kawahara, K.; Nikaido, H.; Ueda, A.; Ogino, H.; Ishikawa, H., Synthesis of amphiphilic polymer particles by seed polymerization and their application for lipase immobilization. *Macromolecular Chemistry and Physics* **2002,** 203, (2), 284-293.

247. Panesar, P. S.; Kennedy, J. F., *Carrier-bound Immobilized Enzymes: Principles, Application and Design, by L. Cao, Wiley-VCH Verlag, GmbH & Co. KGaA, Weinheim, Germany: 2005*. 2006; Vol. 64, p 603.

248. Caruso, F.; Trau, D.; Moehwald, H.; Renneberg, R., Enzyme Encapsulation in Layer-by-Layer Engineered Polymer Multilayer Capsules. *Langmuir* **2000,** 16, (4), 1485-1488.

249. Haupt, B.; Neumann, T.; Wittemann, A.; Ballauff, M., Activity of Enzymes Immobilized in Colloidal Spherical Polyelectrolyte Brushes. *Biomacromolecules* **2005,** 6, (2), 948-955.

250. Kang, K.; Kan, C.; Yeung, A.; Liu, D., The properties of covalently immobilized trypsin on soap-free P(MMA-EA-AA) latex particles. *Macromolecular Bioscience* **2005,** 5, (4), 344-351.

251. Thurmond, K. B.; Remsen, E. E.; Kowalewski, T.; Wooley, K. L., Packaging of DNA by shell crosslinked nanoparticles. *Nucleic Acids Research* **1999,** 27, (14), 2966-2971.

252. Kawaguchi, H.; Fujimoto, K., Smart latexes for bioseparation. *Bioseparation* **1998,** 7, (4/5), 253-258.

253. Kawaguchi, H.; Fujimoto, K., Smart latexes for bioseparation and bioprocessing. *Smart Polymers for Bioseparation and Bioprocessing* **2004**, 191-206.

254. Matsuya, T.; Tashiro, S.; Hoshino, N.; Shibata, N.; Nagasaki, Y.; Kataoka, K., A Core-Shell-Type Fluorescent Nanosphere Possessing Reactive

Poly(ethylene glycol) Tethered Chains on the Surface for Zeptomole Detection of Protein in Time-Resolved Fluorometric Immunoassay. *Analytical Chemistry* **2003,** 75, (22), 6124-6132.

255. Shimizu, N.; Sugimoto, K.; Tang, J.; Nishi, T.; Sato, I.; Hiramoto, M.; Aizawa, S.; Hatakeyama, M.; Ohba, R.; Hatori, H.; Yoshikawa, T.; Suzuki, F.; Oomori, A.; Tanaka, H.; Kawaguchi, H.; Watanabe, H.; Handa, H., High-performance affinity beads for identifying drug receptors. *Nature Biotechnology* **2000,** 18, (8), 877-881.

256. Radomska-Galant, I.; Basinska, T., Poly(styrene/-tert-butoxy-vinylbenzyl-polyglycidol) Microspheres for Immunodiagnostics. Principle of a Novel Latex Test Based on Combined Electrophoretic Mobility and Particle Aggregation Measurements. *Biomacromolecules* **2003,** 4, (6), 1848-1855.

257. Jungmann, N.; Schmidt, M.; Ebenhoch, J.; Weis, J.; Maskos, M., Dye loading of amphiphilic poly(organosiloxane) nanoparticles. *Angewandte Chemie, International Edition* **2003,** 42, (15), 1714-1717.

258. Sunintaboon, P.; Ho, K. M.; Li, P.; Cheng, S. Z. D.; Harris, F. W., Formation of Nanostructured Materials via Coalescence of Amphiphilic Hollow Particles. *Journal of the American Chemical Society* **2006,** 128, (7), 2168-2169.

Chapter 2 Objectives

2.1 Amine-rich polymeric particles

Polymer particles containing reactive surface functional groups have attracted much interest because of their wide range of applications, including additives for paints, adhesives, coatings, carriers for covalent immobilization of catalysts, antibodies, enzymes, drugs and other biomolecules.[1] Common reactive functional groups include carboxyl, hydroxyl, aldehyde, acetal, chloromethyl and amino groups.[2] The amino group provides the particles with a cationic nature, which is capable of binding particles with anionic materials like nucleotide or enzymes. It also provides the particles with a nucleophilicity, thus the particles can be used for crosslinking, covalent bonding of biomaterials or modified to other functional particles through various post-derivatizations with specific functional groups such as aldehyde, epoxy, carboxy or isocyanate, as shown in Figure 2.1.

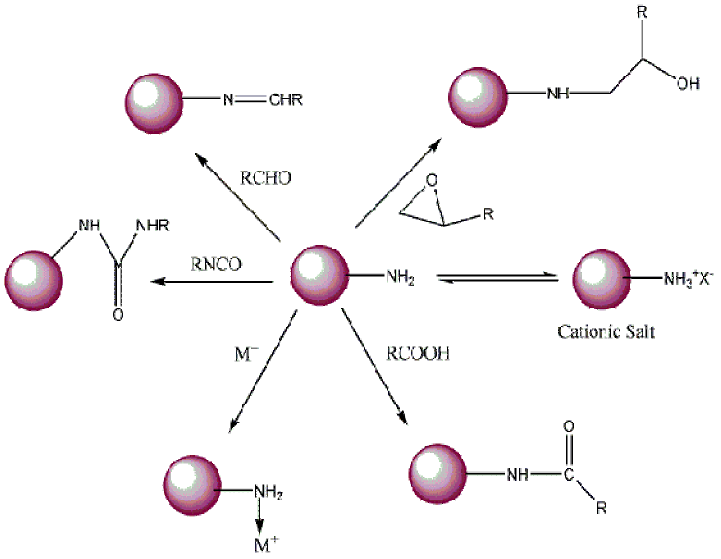

Figure 2.1 Derivatization of amine-containing particle to other functionalities

There are several approaches to synthesize amine-rich polymer particles: 1) The batch emulsion copolymerization of amino-functionalized monomers with conventional monomers such as styrene.[3, 4] However, the use of ionic co-monomers or highly water-soluble amino monomers leads to a broad particle size distribution and the formation of water-soluble polyelectrolytes. 2) The two- or multi- step seeded emulsion polymerization, where the amino-functional monomer is copolymerized in the presence of polystyrene seed particles.[5-9] 3) The chemical modifications of other surface functional groups to amino groups such as the post-polymerization reactions on crosslinked polystyrene and polychloromethylstyrene particles (Eq. 2.1 and 2.2)[10], the modification of carbonyl surface groups (Eq. 2.3)[11] or hydroxyl and carboxyl groups (Eq. 2.4)[12, 13], the nitration of polystyrene and reduction to amino groups (Eq. 2.5)[14, 15], or Hofmann degradation of amide groups (Eq. 2.6)[16]. However, these methods suffer from the side reactions and the poor particle stability due to the changes in the medium conditions in different reactions used to produce the amino functionality.[2]

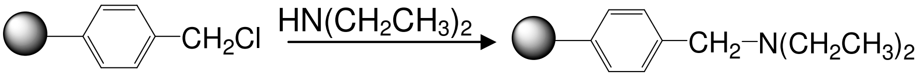

(Eq. 2.1)

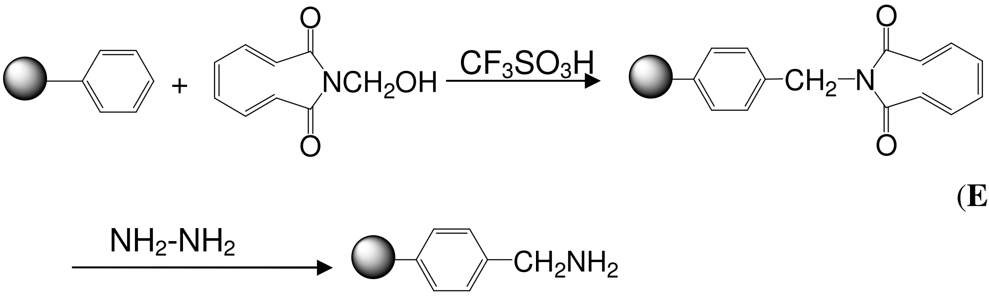

(Eq. 2.2)

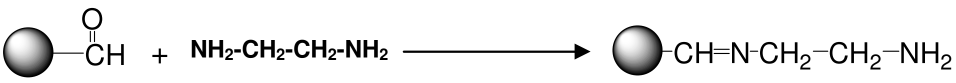

(Eq. 2.3)

(Eq. 2.4)

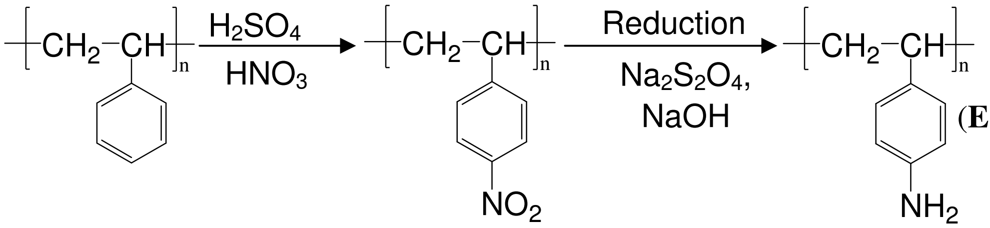

(Eq.2.5)

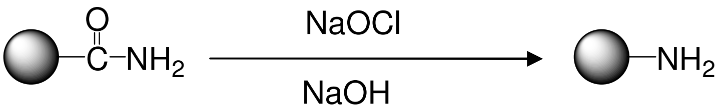

(Eq. 2.6)

2.2. Polyvinylamine-based amphiphilic core-shell particles

Polyvinylamine (PVAm), [-CH_2-CH(NH_2)-]$_n$, is an important water-soluble functional and linear polymer with all primary amino groups bonded directly to the main chain. Owing to the rapid absorption of carbon dioxide from air, PVAm is not stable in the atmosphere. Thus it is commonly stored in the form of poly(vinylammonium chloride) (PVAmHCl). PVAmHCl possesses the highest known charge density along the polymer backbone.[17] As one of the simplest polycationic polymers, it is in principle an ideal model for the simplest representative of a group of weak poly-bases in polyelectrolyte studies. Because of its pH-dependent nature, it is possible to easily control the ionic properties, such as the charge density and acid-base strength, by simple protonation. Thus it has been used in a variety of applications, for example, as chelating ligands for various heavy metal ions[18, 19], carriers for the immobilization of enzymes[20, 21], flocculants in wastewater treatment[22-24], additives in papermaking[25-28], finishing agents in textile modification[29, 30], components in personal care products[31-34], crosslinkers in adhesives[35-37] and coatings[38-41], oil field chemicals[42-44], and a pretreatment for the salt-free dyeing of cotton with reactive dyes[45], etc.

PVAm is also of interest because of its nucleophilic nature. The high activity of the amino groups provides the polymer significant modification possibilities, which make it suitable to be used as a starting material for the preparation of a variety of important functional materials[46-48]. For instance, PVAm has been modified with various reactions to prepare nitrogenous resins[46], water-soluble polymeric dyes[49-53], thermo-sensitive and/or pH-sensitive polymers[54-56], photo-sensitive polymers[57, 58], chromophoric water-soluble polymers[17, 59], polymeric catalysts[60-64], polymer surfactants[65], and so on. Hence, PVAm is not only of theoretical importance, but also of practical significance.

2.3. Current methodologies to prepare PVAm-based particles

Nano- or micro-particles are emerging materials because they possess many important features such as the large specific surface area, high mobility, easy recovery from the dispersion and reversible dispersibility, etc. Thus the synthesis of functional particles with PVAm shells has received an increasing interest. Unfortunately, because the most convenient monomer for PVAm, *N*-vinylamine, is not available, PVAm-based particles can not be synthesized directly via the conventional heterogenerous polymerization, e.g. emulsion polymerization and dispersion polymerization. As a result, various indirect approaches have been developed for the synthesis of PVAm-based particles.

2.3.1 Emulsion polymerization of styrene using poly[(vinyl alcohol)-co-(vinyl amine)] [poly(VA-VAm)] as a stabilizer

Campbell et al[66] used poly(VA-VAm) as a stabilizer for the batch emulsion polymerization of styrene using persulfate-ion as an initiator to give a cationic latex. The particles were relatively uniform with particle size ranging from 100 to 500 nm in diameter. Separation of the stabilizer from the latexes via extraction and centrifugation indicated that only 20% of the poly(VA-VAm) remained after four extraction/decantation cycles. The result suggested that the predominant mechanism of stabilization of the polystyrene particles was through the physical adsorption rather than the grafting of the stabilizer to the particles.

2.3.2 Hydrolysis of performed particles with poly(*N*-vinylalkylamide) shells

Another approach to synthesize particles with PVAm shells is the hydrolysis of performed particles with poly(*N*-vinylalkylamide) shells.

For example, Serizawa *et al*[67] first prepared poly(*N*-vinylacetamide) (PNVA) macromonomers with terminal methylstyrene groups, then copolymerized them with styrene by a dispersion polymerization to obtain polystyrene (PS)/PNVA microspheres. The microspheres were subsequentyly hydrolyzed in 4 N HCl at 80 °C for 48 hours to obtain cationic microspheres with PVAm coronas, as shown in Figure 2.2.

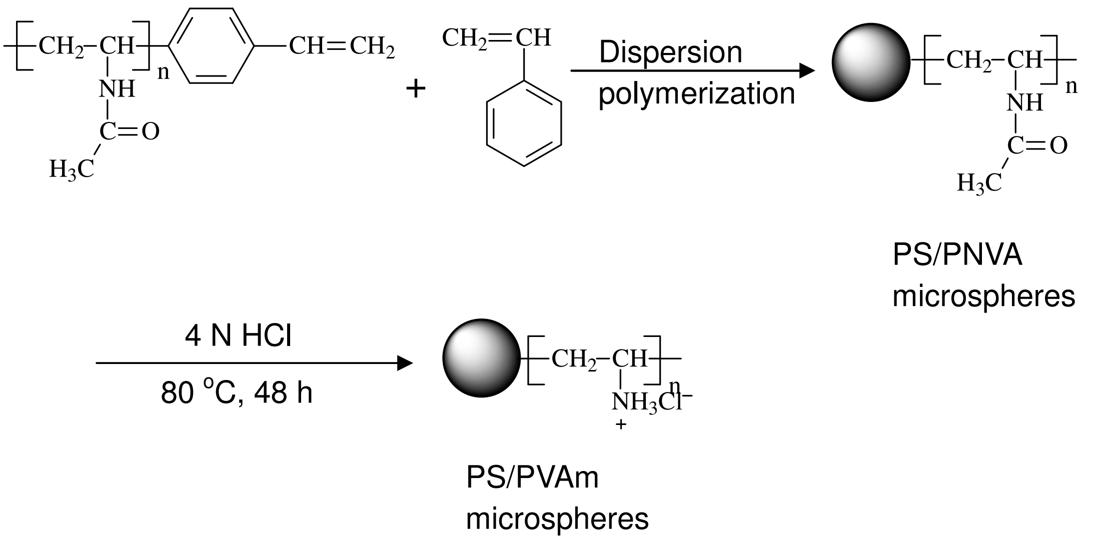

Figure 2.2 Synthesis of PS/PVAm microspheres from PNVA micromonomers

Figure 2.3 shows another procedure reported by Xu *et al*[68]. They first prepared poly(*N*-isopropylacrylamide) (PNIPAM) microgels or PS particles containing poly(*N*-vinylformamide) (PNVF) by a semi-batch surfactant-free emulsion polymerization of *N*-isopropylacrylamide (NIPAM) or styrene with *N*-vinylformamide (NVF). Then the microgels or composite particles were hydrolyzed with HCl at 70 °C to obtain PNIPAM/PVAm microgels or PS/PVAm core-shell particles (Figure 2.3, step 1). Despite its success, the yields of the incorporated NVF were less than 50% and the acidic hydrolysis of the NIPAM/NVF microgel was also low (only 39%).

To concentrate the amine groups on the exterior surface of the PNIPAM/PVAm microgels, a new route was proposed by coupling iodine-terminated poly(*N*-vinylformamide) (PNVF) oligomers to the microgel amines, followed by a second hydrolysis of the PNVF corona to give the corresponding polyvinylamine[69] (Figure 2.3, step 2 and 3). However, this procedure is too complicated and the yields of both NVF incorporation and the formamide conversion to amines were only about 50%. In addition, degradation of the polymers under rigorous hydrolysis conditions is another major disadvantage.

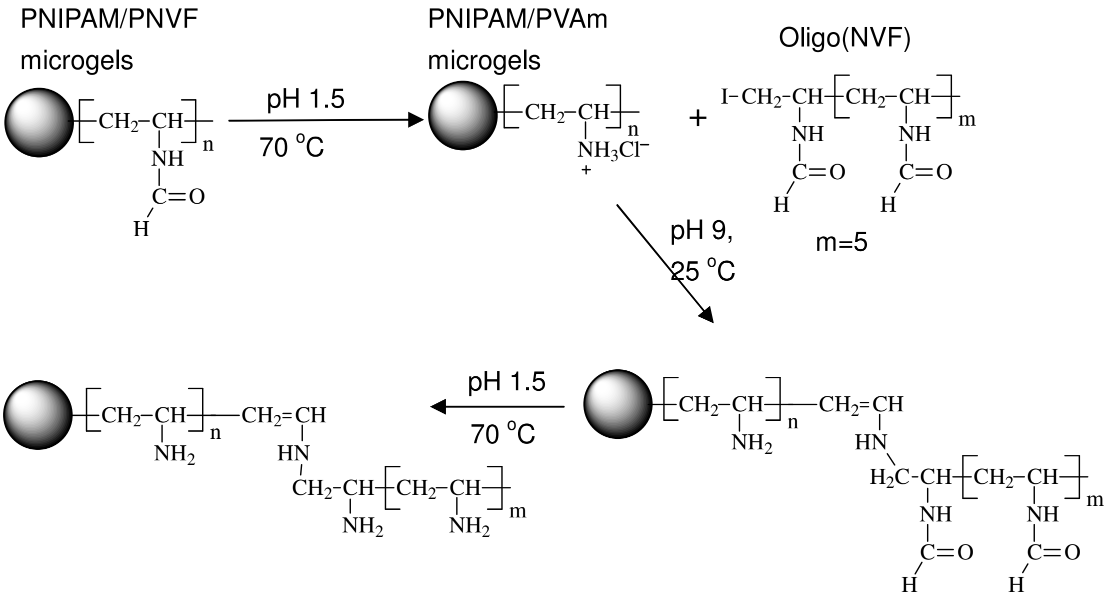

Figure 2.3 Coupling of oligo(NVF) followed by a second hydrolysis to concentrate the amine groups on the exterior surface of the microgels

2.3.3 Step-deposition between anionic polyelectrolytes and PVAm

Another approach to prepare core-shell particles bearing PVAm shells is step deposition, or the so called layer by layer (LBL) assemblies between anionic polyelectrolytes and PVAm. For example, Serizawa *et al* fabricated ultrathin hydrogels via a two step procedure: 1) Fabrication of ultrathin films on a solid substrate through sequential formation of amide linkages in LBL assemblies between PVAm and poly(acrylic acid-co-acrylamide)[70] or poly(acrylic acid-co-*N*-isopropylacrylamide)[71] in the presence of a water-soluble carbodiimide hydrochloride, 1-ethyl-3-(3-dimethylaminopropyl)carbodidmide hydrochloride; 2) Formation of ultrafine hydrogels by immersing the films into an aqueous phase. Various *N*-vinylalkylamide copolymers containing primary amine groups, such as poly(vinylamine-co-*N*-vinylisobutyramide)[72] or poly(vinylamine-co-*N*-vinylformamide)[73-75], have also been used with poly(acrylic acid)[72-74] or poly(sodium styrene sulfonate)[75]. These ultrathin hydrogels have been found potential applications for the loading and release of charged drugs.[76] However, the tedious procedure involving step deposition and repeating washing/drying cycles are major drawbacks which limit their production and applications. Thus, there is a strong demand for the development of a simple and versatile method to synthesize PVAm-based core-shell particles.

2.4. Objectives of the research

In this research, we aim to develop a novel, simple and versatile approach to synthesize well-defined PVAm-based particles with diameters in nano-demensions, a narrow size distribution, a controllable core-shell structure and tailored functionalities. This research is an extension of our previous studies[77, 78] on the preparation of well-defined amphiphilic core-shell particles, which is based on the reaction between *tert*-butyl hydroperoxide (TBHP) and the amino groups of water soluble polymers in water in the presence of dispersed vinyl monomer(s).

The PVAm-based particles are prepared by a direct graft copolymerization of vinyl monomer(s) from PVAm induced by TBHP in the absence of surfactant. The major challenges in this project are: (1) to synthesize and purify PVAms having a desired molecule weight and functionalities; (2) to optimize the reaction conditions and understand those factors affecting the particle properties; (3) to apply the method to the synthesis of different types of particles.

This thesis is composed of three major parts regarding to the synthesis, characterization and application of PVAm-based core-shell particles:

1. *Synthesis and characterization of PVAm with different molecule weights and functionalities*

   PVAms with different molecule weights and functionalities are prepared by a solution polymerization of NVA or NVF, followed by an acidic hydrolysis in a HCl solution. The polymers are characterized by FTIR, ^{1}H NMR and viscometer.

2. *Synthesis and characterization of PVAm-based core-shell particles*

The effects of various reaction parameters, such as the reaction pH, initiator concentration, weight ratio of monomer to PVAm, salt concentration in medium, molecular weight of PVAm, functionalities of PVAm and crosslinking degree of PVAm on the particle formation, particle size and size distribution, surface charge density and morphologies are examined. Methyl methacrylate (MMA) is first used as a model monomer to carry out the effect studies. Then various PVAm-based core-shell particles using other monomers are synthesized based on the optimal conditions determined in the PMMA system.

3. *Exploration of applications of the PVAm-based core-shell particles*

The application of the PVAm-based particles in the enzyme immobilization is investigated.

References:

1. Kawaguchi, H., Functional polymer microspheres. *Progress in Polymer Science* **2000,** 25, (8), 1171-1210.
2. Forcada, J.; Hidalgo-C lvarez, R., Functionalized Polymer Colloids: Synthesis and Colloidal Stability. *Current Organic Chemistry* **2005,** 9, (11), 1067-1084.
3. Ganachaud, F.; Sauzedde, F.; Elaissari, A.; Pichot, C., Emulsifier-free emulsion copolymerization of styrene with two different amino-containing cationic monomers. I. Kinetic studies. *Journal of Applied Polymer Science* **1997,** 65, (12),

2315-2330.

4. Delair, T.; Marguet, V.; Pichot, C.; Mandrand, B., Synthesis and characterization of cationic amino functionalized polystyrene latexes. *Colloid and Polymer Science* **1994,** 272, (8), 962-970.
5. Miraballes-Martínez, I.; Martín-Molina, A.; Galisteo-González, F.; Forcada, J., Synthesis of amino-functionalized latex particles by a multistep method. *Journal of Polymer Science Part A: Polymer Chemistry* **2001,** 39, (17), 2929-2936.
6. Miraballes-Martínez, I.; Forcada, J., Synthesis of latex particles with surface amino groups. *Journal of Polymer Science Part A: Polymer Chemistry* **2000,** 38, (23), 4230-4237.
7. Charreyre, M.-T.; Razafindrakoto, V.; Veron, L.; Delair, T.; Pichot, C., Radically initiated copolymers of styrene with 4-vinylbenzylamine and its trifluoroacetamide derivative. 1. Kinetic studies of solution polymerization. *Macromolecular Chemistry and Physics* **1994,** 195, (6), 2141-2152.
8. Charreyre, M.-T.; Razafindrakoto, V.; Veron, L.; Delair, T.; Pichot, C., Radically initiated copolymers of styrene with 4-vinylbenzylamine and its trifluoroacetamide derivative. 2. Preparation of latex particles bearing amino groups. *Macromolecular Chemistry and Physics* **1994,** 195, (6), 2153-2167.
9. Ramos, J.; Martín-Molina, A.; Sanz-Izquierdo, M. P.; Rus, A.; Borque, L.; Hidalgo-Álvarez, R.; Galisteo-González, F.; Forcada, J., Amino-functionalized latex particles obtained by a multi-step method: Development of a new immunoreagent. *Journal of Polymer Science Part A: Polymer Chemistry* **2003,** 41,

(15), 2404-2411.

10. Cousin, P.; Smith, P., Synthesis and characterization of styrene-based microbeads possessing amine functionality. *Journal of Applied Polymer Science* **1994,** 54, (11), 1631-1641.

11. Basinska, T.; Slomkowski, S., Attachment of horseradish peroxidase (HRP) onto the poly(styrene/acrolein) latexes and onto their derivatives with amino groups on the surface; activity of immobilized enzyme. *Colloid and Polymer Science* **1995,** 273, (5), 431-438.

12. Quash, G.; Roch, A.-M.; Niveleau, A.; Grange, J.; Keolouangkhot, T.; Huppert, J., The preparation of latex particles with covalently bound polyamines, IgG and measles agglutinins and their use in visual agglutination tests. *Journal of Immunological Methods* **1978,** 22, (1-2), 165-174.

13. Molday, R. S.; Dreyer, W. J.; Rembaum, A.; Yen, S. P. S., New immunolatex spheres: visual markers of antigens on lymphocytes for scanning electron microscopy. *The Journal of Cell Biology* **1975,** 64, (1), 75-88.

14. Page, J. D.; Derango, R.; Huang, A. E., Chemical modification of polystyrene's surface and its effect on immobilized antibodies. *Colloids and Surfaces A: Physicochemical and Engineering Aspects* **1998,** 132, (2-3), 193-201.

15. Covolan, V. L.; Innocentini Mei, L. H.; Rossi, C. L., Chemical Modifications on Polystyrene Latex: Preparation and Characterization for Use in Immunological Applications. *Polymers for Advanced Technologies* **1997,** 8, (1), 44-50.

16. Kawaguchi, H.; Hoshino, H.; Amagasa, H.; Ohtsuka, Y., Modifications of a

polymer latex. *Journal of Colloid and Interface Science* **1984,** 97, (2), 465-475.

17. Roth, I.; Spange, S., Nucleophilic substitution of 4-fluoronitrobenzene with polyvinylamine in water mediated by cyclodextrins. *Macromolecular Rapid Communications* **2001,** 22, (15), 1288-1291.
18. Kobayashi, S.; Suh, K. D.; Shirokura, Y., Chelating ability of poly(vinylamine): effects of polyamine structure on chelation. *Macromolecules* **1989,** 22, (5), 2363-2366.
19. Tbal, H.; Le Maguer, D.; Morcellet, J.; Delporte, M.; Morcellet, M., Chelating resins based on polyvinylamine and divinylbenzene or ethylene glycol dimethacrylate. *Reactive Polymers* **1992,** 17, (2), 207-217.
20. Johansen, C. Synergistic microbicides, especially for laundry detergents, comprising a polycationic compound and an enzyme. WO 9,732,480, 1997.
21. Wang, L.; Yang, S.; Jiang, Y., Study on immobilization of cellulase by interpolymer complexes. *Gaofenzi Xuebao* **1989**, (1), 117-120.
22. Dubin, P. L. High-molecular-weight poly(vinylamine hydrochloride) as a flocculant. USP 4,217,214, 1980.
23. Hund, R.; Jehn-Rendu, C. Novel methods for synthesizing polyvinylamine-type flocculating and coagulating agents, novel agents thus obtained, uses thereof, and improved paper thus obtained. WO 2,000,058,378, 2000.
24. Sommese, A. G.; Chung, D. K. Use of polymers containing vinylamine/vinylformamide for the treatment of food processing wastewater. USP 6,610,209, 2003.

25. Murao, Y.; Sawayama, S.; Sato, K. Powdered poly(vinylamine). JP 61,190,508, 1986.
26. Itagaki, T.; Shiraga, M.; Sawayama, S.; Satoh, K. Manufacture of vinylamine copolymers as flocculants and papermaking additives. EP 251,182, 1988.
27. Natsuhara, E.; Murata, N.; Tanimoto, S.; Saikai, H. Strength agents for papermaking. JP 06,093,594, 1994.
28. Linhart, F., Some thoughts on the mode of action of wet-strength and dry-strength agents: are our theories of the mode of action of these chemicals still valid? *Professional Papermaking* **2006**, (1), 20-25.
29. Detering, J.; Grimm, G.; Freund, T. Hydrophobically modified polyethyleneimines and polyvinylamines for wrinkle-resistant finishing of cellulose textiles. WO 2,002,095,122, 2002.
30. Wittke, R.; Knittel, D.; Schollmeyer, E. Permanent equipment and modification of polymer surfaces with linear polyvinyl amine to improve coloring and antibacterial characteristics. DE 102,005,026,596, 2006.
31. McAndrew, T. P.; Nordquist, A. F.; Pinschmidt, R. K., Jr.; Eichelberger, D. P. Amine functional polymers as thickening agents. USP 5,270,379, 1993.
32. Niessner, M.; Rubenacker, M.; Nilz, C.; Hossel, P. Water-soluble polymers and their use in cosmetic formulations. WO 9,804,596, 1998.
33. Yamamoto, T. Hair preparations containing nitrogen-contg. polymers and film-forming polymers. JP 09,087,151, 1997.
34. Hoover, M. F.; Guilbault, L. J. Preparation of polymers containing primary

pendant amino groups and their use in hair conditioning products. USP 4,713,236, 1987.

35. Vratsanos, L. A.; Kuphal, J. A.; Renz, W. L. Use of vinylamine homopolymers and copolymers in film lamination. EP 644,247, 1995.
36. Arthur, S. D. Bioadhesives made from acetoacetate polyols crosslinked with amines and polyamines for wound healing and surgical closure. USP 2,006,079,599, 2006.
37. Lenney, W. E.; Campbell, K. D.; Bott, R. H.; Kuphal, J. A.; Mao, C. L. Vinyl alcohol-vinyl amine copolymers as stabilizing protective colloids in aqueous emulsion polymerization. EP 599,245, 1994.
38. Champ, S.; Seyffer, H. Biocidal polymer coatings. DE 102,005,021,364, 2006.
39. Pinschmidt, R. K., Jr.; Chen, N., New N-vinylformamide derivatives and their use in radiation cure coatings. *Polymer Preprints* **1998,** 39, (1), 639-640.
40. Hosoda, K.; Enome, M.; Kamio, K.; Kawashima, M.; Morya, M. Antifouling agents for coating materials. JP 07,165,522, 1995.
41. Roser, J.; Mohr, J.; Lange, A.; Oppenlaender, K.; Denzinger, W.; Loerzer, T. Polyethylenimine and poly(vinylamine) derivatives for coating of aluminum for offset printing plates. EP 490,231, 1992.
42. Lai, T. W.; Vijayendran, B. R. Compositions containing high molecular weight poly(vinylamines) for enhanced oil recovery. EP 295,615, 1988.
43. Pinschmidt, R. K., Jr.; Vijayendran, B. R. Crosslinked vinylamine polymer in enhanced oil recovery. USP 4,973,410, 1990.

44. Pinschmidt, R. K., Jr.; Lai, T. W. Enhanced oil recovery with high molecular weight polyvinylamine formed in-situ. USP 4,931,194, 1990.

45. Ma, W.; Zhang, S.; Tang, B.; Yang, J., Pretreatment of cotton with poly(vinylamine chloride) for salt-free dyeing with reactive dyes. *Coloration Technology* **2005,** 121, (4), 193-197.

46. Reynolds, D. D.; Kenyon, W. O., Preparation of polyvinylamine, polyvinylamine salts, and related nitrogenous resins. *Journal of the American Chemical Society* **1947,** 69, 911-915.

47. Pinschmidt, R. K., Jr.; Renz, W. L.; Carroll, W. E.; Yacoub, K.; Drescher, J.; Nordquist, A. F.; Chen, N., *N*-Vinylformamide-building block for novel polymer structures. *Journal of Macromolecular Science, Pure and Applied Chemistry* **1997,** A34, (10), 1885-1905.

48. Badesso, R. J.; Nordquist, A. F.; Pinschmidt, R. K., Jr.; Sagl, D. J., Synthesis of amine functional homopolymers with *N*-ethenylformamide. *Advances in Chemistry Series* **1996,** 248, (Hydrophilic Polymers), 490-504.

49. Wingard, R. E.; Dawson, D. J. Water-soluble polymeric dye. DE 2,751,262, 1978.

50. Dawson, D. J.; Otteson, K. M.; Davis, R. Water-soluble polymeric yellow dye. DE 2,754,485, 1978.

51. Gless, R. D., Jr.; Dawson, D. J.; Wingard, R. E. Polyvinylamine and salts thereof. USP 4018826, 1977.

52. Dawson, D.; Gless, R.; Wingard, R. E., Jr., Polymeric dyes from polyvinylamine.

Chemtech **1976,** 6, (11), 724-726.

53. Dawson, D. J.; Gless, R. D.; Wingard, R. E., Jr., Poly(vinylamine hydrochloride). Synthesis and utilization for the preparation of water-soluble polymeric dyes. *Journal of the American Chemical Society* **1976,** 98, (19), 5996-6000.
54. Akashi, M.; Nakano, S.; Kishida, A., Synthesis of poly(*N*-vinylisobutyramide) from poly(N-vinylacetamide) and its thermosensitive property. *Journal of Polymer Science, Part A: Polymer Chemistry* **1996,** 34, (2), 301-3.
55. Yamamoto, K.; Imamura, Y.; Nagatomo, E.; Serizawa, T.; Muraoka, Y.; Akashi, M., Synthesis and functionalities of poly(*N*-vinylalkylamide). XIV. Polyvinylamine produced by hydrolysis of poly(*N*-vinylformamide) and its functionalization. *Journal of Applied Polymer Science* **2003,** 89, (5), 1277-1283.
56. Chen, X.; Wang, Y.; Pelton, R., pH-Dependence of the Properties of Hydrophobically Modified Polyvinylamine. *Langmuir* **2005,** 21, (25), 11673-11677.
57. El Achari, A.; Coqueret, X., Photocrosslinkable vinylamine copolymers. I. Synthesis and photosensitivity of cinnamoylated polyvinylamine. *Journal of Polymer Science, Part A: Polymer Chemistry* **1997,** 35, (12), 2513-2520.
58. Mori, K.; Ueno, N. Photosensitive vinylamine polymer compositions. JP 2,000,344,991, 2000.
59. Roth, I.; Simon, F.; Bellmann, C.; Seifert, A.; Spange, S., Fabrication of Silica Particles Functionalized with Chromophores and Amino Groups Using Synergism of Poly(vinylamine) Adsorption and Nucleophilic Aromatic

Substitution with Fluoroaromatics. *Chemistry of Materials* **2006,** 18, (20), 4730-4739.

60. Crini, G.; Morcellet, M.; Torri, G., HPLC of structural isomers with cyclodextrin-poly(vinylamine)-coated silica columns, Part I: synthesis and characterization of cyclodextrin-bonded stationary phases by NMR solid state. *Journal of Chromatographic Science* **1996,** 34, (11), 477-484.
61. Martel, B.; Pollet, A.; Morcellet, M., *N*-Benzylated Poly(vinylamine): Synthesis, Characterization, and Catalytic Activity in Ester Cleavage. *Macromolecules* **1994,** 27, (19), 5258-5262.
62. Roth, I.; Spange, S., Kinetic Studies on the Nucleophilic Aromatic Substitution of Fluoronitrobenzene Derivatives with Polyvinylamine in Water Mediated by 2,6-O-Dimethyl-b-cyclodextrin. *Macromolecules* **2005,** 38, (24), 10034-10041.
63. Martel, B.; Morcellet, M., Cyclodextrin-poly(vinylamine) systems. II. Catalytic hydrolysis of p-nitrophenyl acetate. *European Polymer Journal* **1995,** 31, (11), 1089-1093.
64. Crini, G.; Lekchiri, Y.; Janus, L.; Morcellet, M.; Morin, N., Beta-cyclodextrin-copolymers coated on silica beads: synthesis, characterization and retention behavior in HPLC. *Chromatographia* **1999,** 50, (11/12), 661-669.
65. Qiu, Y.; Zhang, T.; Ruegsegger, M.; Marchant, R. E., Novel nonionic oligosaccharide surfactant polymers derived from poly(vinylamine) with pendant dextran and hexanoyl groups. *Macromolecules* **1998,** 31, (1), 165-171.
66. Campbell, K. D.; Sagl, D. J.; Vanderhoff, J. W., Polystyrene particles with

surface amino groups. *Journal of Dispersion Science and Technology* **1998,** 19, (6 & 7), 785-804.

67. Serizawa, T.; Taniguchi, K.; Akashi, M., Hetero-coagulation of polymeric core-corona microspheres. *Colloids and Surfaces, A: Physicochemical and Engineering Aspects* **2000,** 169, (1-3), 95-105.
68. Xu, J.; Barros Timmons, A.; Pelton, R., *N*-Vinylformamide as a route to amine-containing latexes and microgels. *Colloid and Polymer Science* **2004,** 282, (3), 256-263.
69. Xu, J.; Pelton, R., A new route to poly(*N*-isopropylacrylamide) microgels supporting a polyvinylamine corona. *Journal of Colloid and Interface Science* **2004,** 276, (1), 113-117.
70. Serizawa, T.; Wang, Z.-J.; Tateishi, T.; Akashi, M., Ultrathin hydrogels prepared from poly(acrylic acid-co-acrylamide) and poly(vinylamine) on a solid substrate. *Polymer Journal (Tokyo, Japan)* **2004,** 36, (1), 54-58.
71. Serizawa, T.; Matsukuma, D.; Nanameki, K.; Uemura, M.; Kurusu, F.; Akashi, M., Stepwise Preparation and Characterization of Ultrathin Hydrogels Composed of Thermoresponsive Polymers. *Macromolecules* **2004,** 37, (17), 6531-6536.
72. Serizawa, T.; Nanameki, K.; Yamamoto, K.; Akashi, M., Thermoresponsive Ultrathin Hydrogels Prepared by Sequential Chemical Reactions. *Macromolecules* **2002,** 35, (6), 2184-2189.
73. Serizawa, T.; Kawanishi, N.; Akashi, M., Polyelectrolyte multilayers of poly(vinylamine hydrochloride-co-N-vinylformamide) with variable primary

amine content and a weak polyacid poly(acrylic acid). *Journal of Applied Polymer Science* **2006,** 102, (4), 3927-3933.

74. Serizawa, T.; Nakashima, Y.; Akashi, M., Stepwise Fabrication and Characterization of Ultrathin Hydrogels Prepared from Poly(vinylamine-co-*N*-vinylformamide) and Poly(acrylic acid) on a Solid Substrate. *Macromolecules* **2003,** 36, (6), 2072-2078.
75. Serizawa, T.; Kawanishi, N.; Akashi, M., Layer-by-Layer Assembly between Poly(vinylamine hydrochloride-co-*N*-vinylformamide) with Variable Primary Amine Content and Poly(sodium styrene sulfonate). *Macromolecules* **2003,** 36, (6), 1967-1974.
76. Serizawa, T.; Matsukuma, D.; Akashi, M., Loading and Release of Charged Dyes Using Ultrathin Hydrogels. *Langmuir* **2005,** 21, (17), 7739-7742.
77. Li, P.; Zhu, J. M.; Harris, F. W. Amphiphilic core-shell latexes. USP 6,573,313, **2002**.
78. Li, P.; Zhu, J.; Sunintaboon, P.; Harris, F. W., New Route to Amphiphilic Core-Shell Polymer Nanospheres: Graft Copolymerization of Methyl Methacrylate from Water-Soluble Polymer Chains Containing Amino Groups. *Langmuir* **2002,** 18, (22), 8641-8646.

Chapter 3 Synthesis of Polyvinylamine

3.1 Introduction

It is impossible to prepare polyvinylamine (PVAm) directly from the polymerization of *N*-vinylamine ($CH_2{=}CHNH_2$) because this monomer is unstable due to its tautomerization to ethanimine ($CH_3CH{=}NH$). Therefore, PVAm can only be synthesized via indirect routes.

One way to synthesize PVAm is the Hofmann degradation of polyacrylamide (PAAm) (Eq. 3.1) [1-3]. It is an economic way to produce PVAm. However, it must be carried out under drastic reaction conditions, which leads to considerable side-reactions. Thus PVAm with high purity cannot be easily obtained in this way.

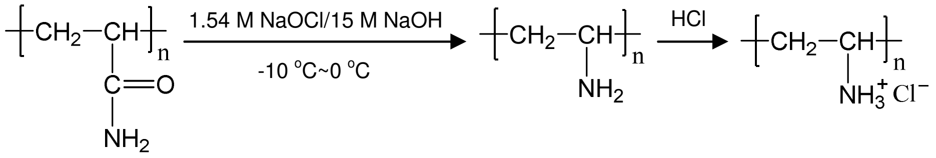

(Eq. 3.1)

Another way is the hydrolysis of preformed poly(*N*-vinylalkylamide) such as poly(*N*-vinylphthalimide)[4](Eq. 3.2), poly(*tert*-butyl-*N*-vinylcarbamate)[5](Eq.3.3), poly(*N*-vinylacetamide) (PNVA)[6] and poly(*N*-vinylformamide) (PNVF)[7-10]. The hydrolysis of poly(*N*-vinylphthalimide) or poly(*tert*-butyl-*N*-vinylcarbamate) must be carried out under very drastic conditions such as in concentrated HCl solution, thus their applications are limited. The hydrolysis of PNVA or PNVF can be performed under milder conditions, thus they are more competitive in the synthesis of PVAm.

However, it is only after *N*-vinylacetamide (NVA) and *N*-vinylformamide (NVF) have become commercially available recently that the hydrolysis of poly(*N*-vinylacetamide) (PNVA)[11] or poly(*N*-vinylformamide) (PNVF) [10, 12, 13] become the most commonly used methods in the preparation of high purity PVAm.

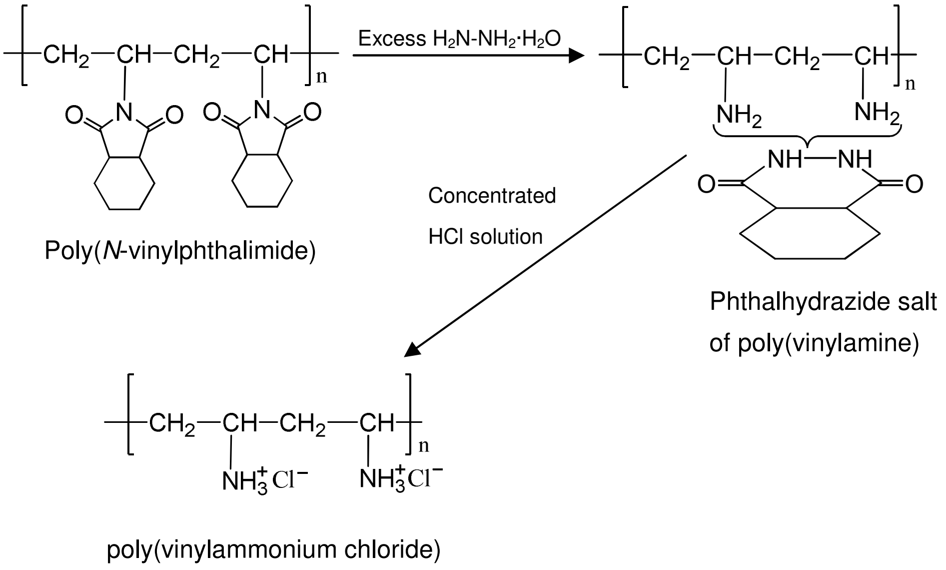

(Eq. 3.2)

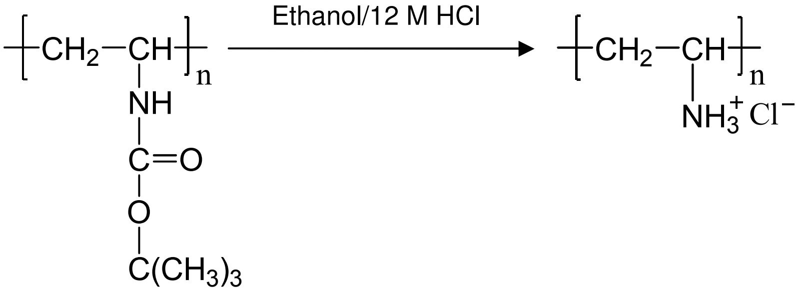

(Eq. 3.3)

Since NVA is a less toxic reagent than NVF, and can be used for polymerization without further purification, it was chosen to be the precursor for our synthesis of PVAm in this study. The polymerization of NVA was carried out in an aqueous medium using V-50 as an initiator.

Lai *et al*[14] reported that PNVA could be converted into PVAm by hydrolyzed in either an acidic or alkaline aqueous solution as illustrated in Scheme 3.1. The difference between the acidic and the basic hydrolysis is that the acidic hydrolysis produces cationic polymers, whereas the basic hydrolysis yields polymers with free amine functional groups. The acidic hydrolysis is conducted in a mixture of methanol and aqueous solvent, and produces methyl acetate which can be easily removed as a light component. However, the electrostatic repulsion between cationic amine groups and proton ions hinders the acidic hydrolysis to a complete conversion. In contrast, basic hydrolysis is usually a more effective approach, giving almost complete hydrolysis. On the other hand, by-product from the basic hydrolysis such as sodium acetate salt, has to be removed by dialysis or precipitation.

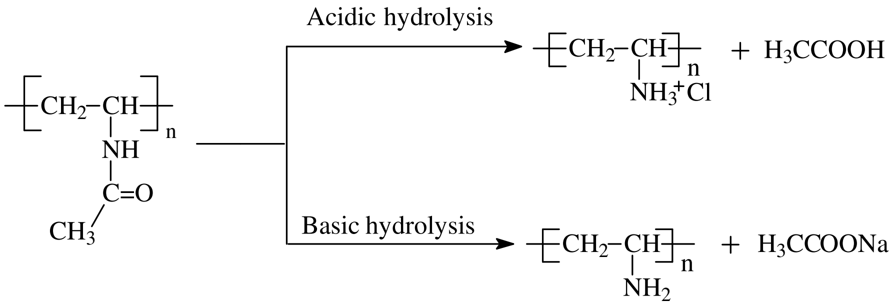

Scheme 3.1 Acidic and basic hydrolysis of PNVA

Synthesis of PVAm through both the acidic and basic hydrolysis of PNVA was studied. When hydrolysis of PNVA was carried out using 2 M NaOH aqueous solution at 100 °C for 48 hours, only little hydrolysis occurred according to the results from ^{1}H NMR measurement of the final product. A phase separation was observed when the mixture of PNVA and NaOH solution was heated, which indicated that PNVA had a thermal-sensitive nature in the hot concentrated alkaline solution. Hong *et al*[15] reported that aqueous PNVA solution exhibited a cloud point in the presence of salt. The cloud point was corresponding to a liquid-liquid phase separation, which was induced by the repulsive interaction between the salt and the polymer as characterized with the polymer-rich top phase and the salt-rich bottom phase. Thus the poor hydrolysis of PNVA in alkaline solution might be caused by the poor solubility of PNVA in the hot alkaline solutions, which is due to the thermal-sensitive nature of PNVA in concentrated NaOH soluiton and the salting-out effect. When the hydrolysis of PNVA was carried out in 3 M HCl aqueous solution, high purity of PVAm could be obtained if the hydrolysis was carried out with sufficient reaction time. Here we report the successful synthesis of polyvinylamine under acidic hydrolysis.

3.2 Experimental

3.2.1 Materials

N-vinylacetamide (NVA) (97%, white crystal, hygroscopic, MW=85.11, Aldrich), 2,2’-Azobis(2-amidinopropane) dihydrochloride (97%, faint yellow crystal, free radical initiator, $T_{1/2}$=56℃, MW=271.2, Wako) (V-50), reagent grade of acetone, methanol, hydrochloric acid (HCl) and NaOH were all used as received.

N-vinylacetamide

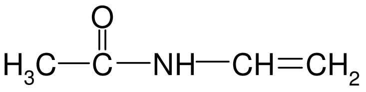

$$H_3C-\overset{\overset{\displaystyle O}{\|}}{C}-NH-CH=CH_2$$

2,2’-Azobis(2-amidinopropane) dihydrochloride

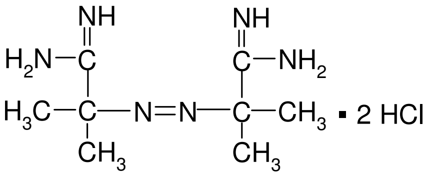

3.2.2 Synthesis of PNVA from NVA

Scheme 3.2 shows the chemical reaction of free radical solution polymerization of NVA. The polymerization was carried out at 60 °C for 24 hours using V-50 as a free radical initiator. In a typical experiment, NVA (10 g, 0.1175 mol) was dissolved in DI water (100 g) in a three-necked flask equipped with a condenser and a nitrogen inlet. The solution was purged with nitrogen for 30 minutes to remove oxygen since the oxygen may act as a strong inhibitor to form stable peroxy radicals. A given amount of initiator was subsequently added into the solution and the solution was heated at 60 °C under nitrogen atmosphere for 24 hours. A transparent and viscous mixture was obtained, which contains unreacted monomer (NVA), PNVA, unreacted initiator and oligomer of NVA. Because the monomer, initiator and oligomer of NVA are soluble in acetone, while PNVA is not, the crude products were purified by repeated dissolution-decantation-precipitation cycles with acetone and DI H_2O. For example, 330 mL of acetone was poured slowly into 100 mL of reaction mixture under stirring to get a white precipitate. The precipitate was then dissolved in water and re-precipitated twice in acetone and dried in a vacuum oven at 50 °C for 3 days. The yield of PNVA was calculated in terms of Eq. 3.4.

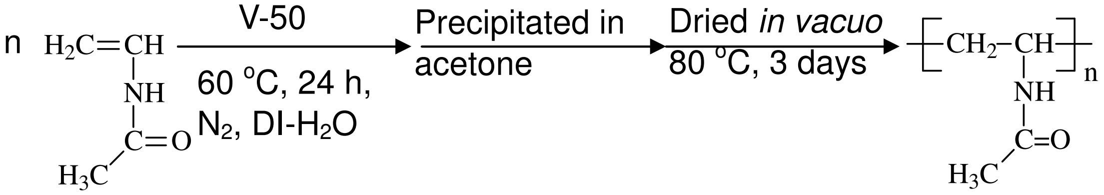

Scheme 3.2 Synthesis of PNVA

$$\text{Yield (\%)} = \frac{\text{The weight of polymer obtained}}{\text{The weight of monomer added}} \times 100\% \qquad \textbf{(Eq. 3.4)}$$

3.2.3 Acidic hydrolysis of PNVA to PVAmHCl

Scheme 3.3 shows that PNVA was hydrolyzed in 3 M HCl solution at 100 °C for 48 h after degassing with nitrogen. In a typical reaction, PNVA (5.04 g, amide groups: 0.0592 mol) was dissolved in 3 M HCl solution (40 ml) in a three-necked flask equipped with a condenser and a nitrogen inlet. After purging N_2 for 30 minutes, the solution was heated at 85 °C and kept for 3 days. Since PVAmHCl is insoluble in any organic solvent, it can be purified by precipitation in a water-miscible organic solvent. Thus, the reaction product was precipitated directly from water by dropwise addition of 12 M HCl solution. The precipitate was further purified by repeated dissolution-decantation-precipitation cycles with water and acetone. Finally, the precipitate was dried at 50 °C *in vacuo* for 3 days to afford an almost completely hydrolyzed PVAmHCl. The product yield was calculated based on Eq. 3.5.

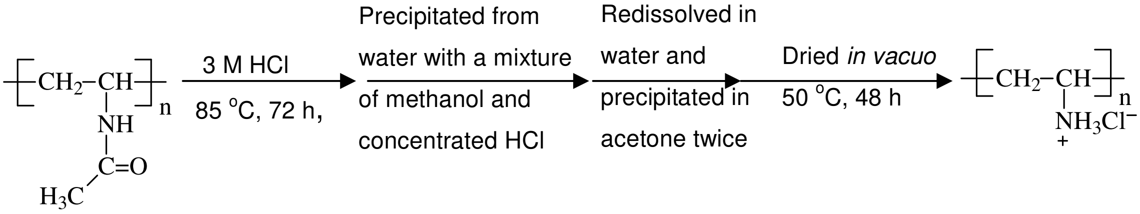

Scheme 3.3 acidic hydrolysis of PNVA to PVAmHCl

$$\text{Yield (\%)} = \frac{\text{The weight of the polymer obtained}}{\text{The theoretical yield}} \times 100\% \quad \textbf{(Eq.3.5)}$$

3.2.4 Preparation of PVAm from PVAmHCl

The preparation of PVAm from PVAmHCl is illustrated in Scheme 3.4. PVAmHCl (70g) was dissolved in DI water and mixed with about equivalent mole of NaOH (50g) for about 10 minutes to produce PVAm (pH >12). The resulting PVAm was first purified by repeated cycles of precipitation-decantation-dissolution using freshly distilled acetone and DI water, and then concentrated by vacuum distillation to give a slightly yellow and viscous liquid. The use of freshly distilled acetone and DI water is in order to remove any dissolved CO_2 in them. Solid content of the solution was measured gravimetrically.

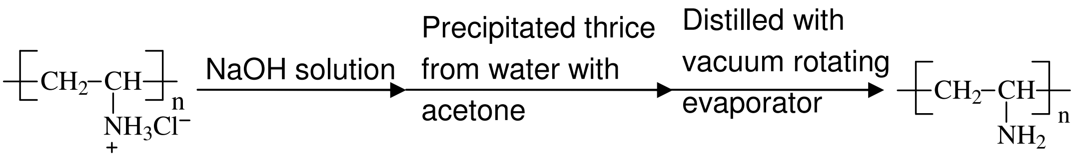

Scheme 3.4 synthesis of PVAm from PVAmHCl

3.2.5 Characterization of PNVA, PVAmHCl and PVAm

FT-IR spectra were recorded on a Nicolet Avatar 360 FT-IR spectrophotometer using KBr disks. ^{1}H NMR spectra were recorded on a Bruker advance DPX-400 using D_2O as solvent.

The number average Mw ($\bar{M}_n$) of PNVA and PVAm were measured viscometrically. The experiments were performed in a thermo-constant water bath using an Ubbelohde viscometer. The $\bar{M}_n$ of PNVA was calculated based on a Mark-Houwink equation according to a literature[16]:

$$[\eta]_{H_2O,30℃}=1.6\times 10^{-3}\times \bar{M}_n^{0.52} \qquad (\textbf{Eq.3.6})$$

Wherein the [η] is expressed in dl/g.

The $\bar{M}_n$ of PVAm was calculated based on a Mark-Houwink relation published by Treslong and Morra[17], which is suitable for PVAm (free base) with $1.5\times 10^4 < \bar{M}_n < 1.6\times 10^5$ in 0.01 M NaOH/0.1 M NaCl solution at 25 ℃:

$$[\eta]=6.2\times 10^{-3}\times \bar{M}_n^{0.88} \qquad (\textbf{Eq.3.7})$$

Wherein the [η] is expressed in ml/g.

The amination degree of PVAm, i.e., the hydrolysis degree of PNVA, was calculated from the intensity ratio of the methylene protons of poly(NVA-co-VAm) at 3.0-3.6 ppm and the methlyne proton of poly(NVA) at 3.8-4.2 ppm[11].

3.3 Results and Discussions

3.3.1 Synthesis of PNVA

A series of experiments based on free radical polymerization of NVA in various solvents at 60 ^{o}C in the presence of KPS, VA-044, BPO, or AIBN have been studied by Akashi *et al.*[11]. Results showed that the polymerization proceeded well in both water and organic solvent regardless of the solubility of NVA, but the conversion was extremely low when peroxides were used, which is consistent with those results reported by Stackman[18]. Therefore, V-50 was chosen in our system to prepare PNVA via free radical polymerization of NVA at 60 ^{o}C for 24 hours in water.

Purification of PNVA could be done by either dialysis in DI-water or repeated precipitation-decantation-dissolution cycles with acetone and DI-water. Dialysis could give high purity PNVA without using any organic solvent. However, it was time-consuming and the solution obtained was very dilute. Thus dialysis was not suitable for large quantity production. Repeated precipitation-decantation-dissolution cycles with acetone and DI-water was, therefore, used in our system.

The chemical structure of the purified PNVA was identified by IR analysis. It was expected that the absorbance of C=C double bond in NVA would be greatly reduced or disappeared in PNVA. Figure 3.1 shows IR spectra of NVA and PNVA, and Table 3.1 summarizes the interpretations of the spectra.

Comparing the spectra of NVA (Figure 3.1a) and PNVA (Figure 3.1b), the peak at

1640 cm^{-1}, representing C=C double bond from NVA disappears in the spectrum of PNVA, indicating that there is no unreacted NVA monomer in the purified PNVA sample. For PNVA spectrum (Figure 3.1b), the peak at 3275 cm^{-1} is attributed to the N-H stretching vibration, the peak at 1672 cm^{-1} is assigned to C=O stretching vibration, the peaks at 1554 and 1305 cm^{-1} are donated by the combination of N-H and C-N, and the peak at 1374 cm^{-1} is caused by the CH_3 attached to a C atom. All these peaks indicate the existence of amide groups.

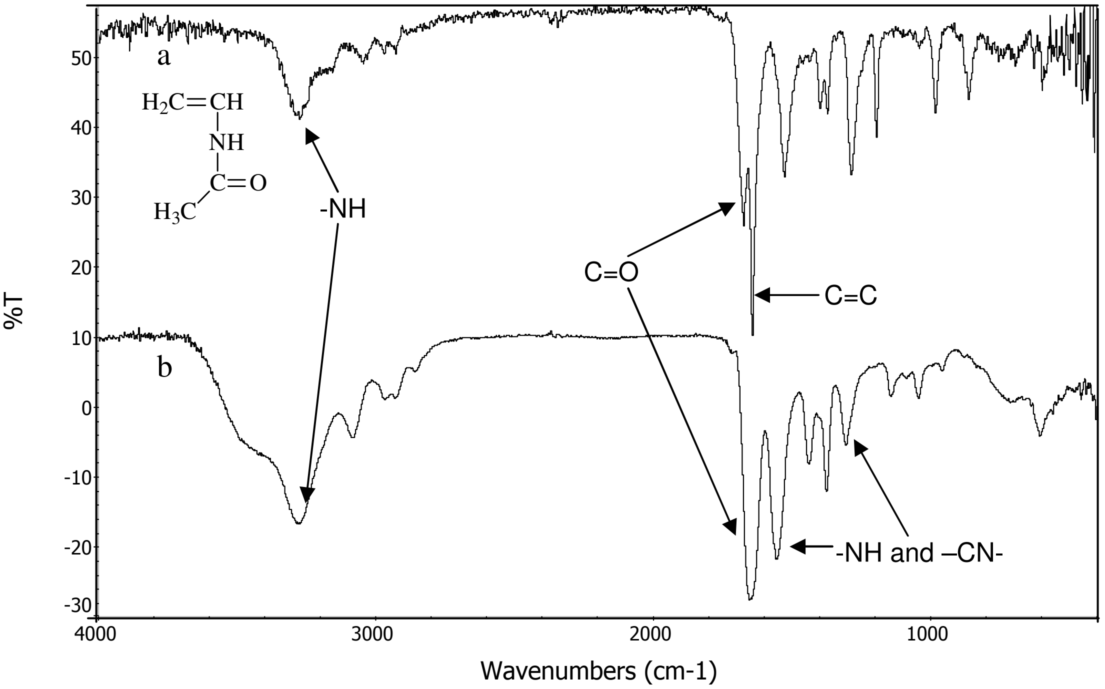

Figure 3.1 IR spectra of a) NVA and b) PNVA

Table 3.1 Interpretations of IR spectra

NVA		PNVA	
Wavenumber (cm^{-1})	Interpretation	Wavenumber (cm^{-1})	Interpretation
3274	-NH stretching	3276	-NH stretching
3045	=CH stretching	1647	C=O stretching
1672	C=O stretching	1554	-NH deformation C-N stretching
1640	C=C stretching	1374	-CH$_3$ bending
1526	-NH deformation	1305	-NH bending C-N stretching

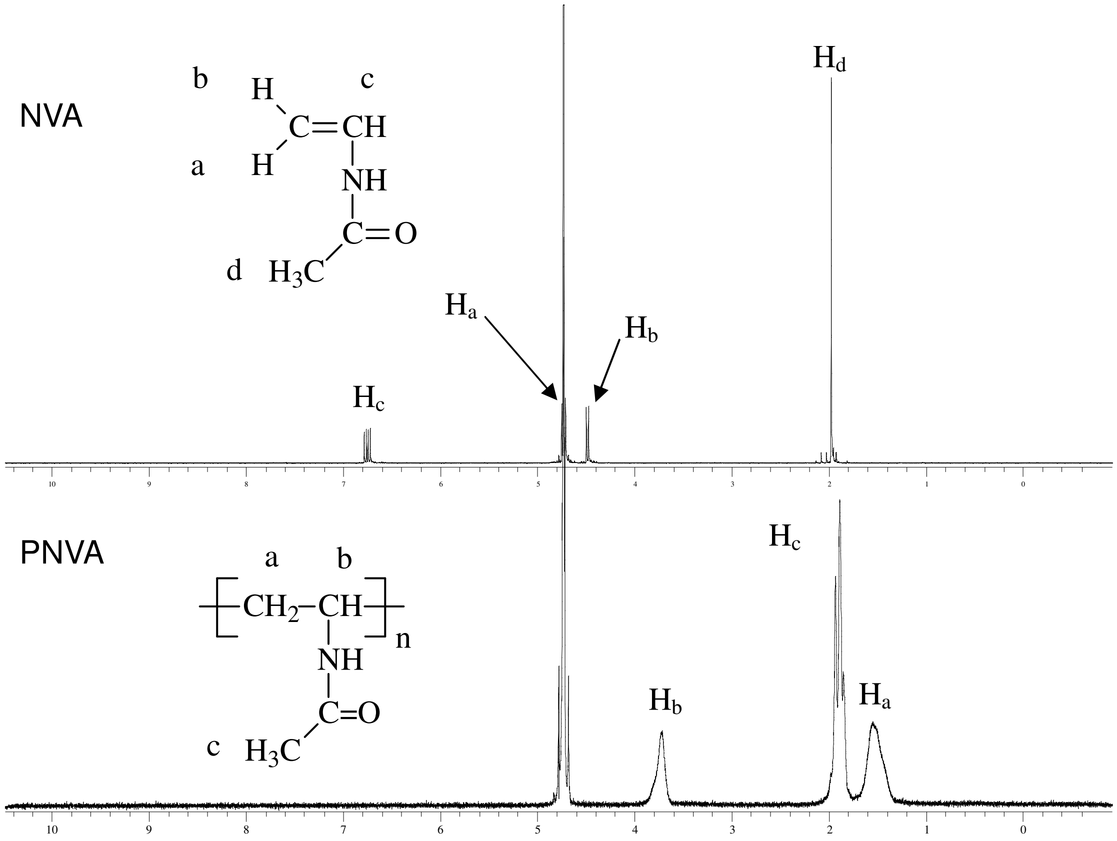

Figure 3.2 ^{1}H NMR spectra of NVA and PNVA

The formation of PNVA was further identified with ^{1}H NMR spectroscopy. Figure 3.2 shows the NMR spectra of NVA and PNVA in D_2O. In the spectrum of NVA

(Figure 3.2a), four peaks at 6.72-6.78, 4.71-4.75, 4.47-4.50 and 1.97 ppm are assigned to the protons of H_c, H_a, H_b and H_d according to the literature[6, 11], whereas the resonance of the H_a overlaps with the peak of H_2O at 4.80 ppm. These peaks disappears in the spectrum of PNVA, while new peaks at 1.54, 3.71 ppm, which are donated by the protons on $–CH_2$ and –CH- groups of PNVA respectively[19], are observed. The results clearly show that there is no unreacted monomer in the polymer sample. These results are in accordance with the results obtained from FT-IR spectra. In the spectrum of PNVA, the resonance of the acetamide methyl protons appears at 1.85-1.93 ppm, which splits into three peaks due to the triad tacticity of PNVA, syndiotactic structure, atactic structure and isotactic structure[11]. In both of the spectra, the peak attributed to H on –NH- was not observed because of the quick hydrogen-deuterium exchange in D_2O.[20]

3.3.2 Hydrolysis of PNVA to PVAm

Dawson et al[6] reported an acidic hydrolysis of PNVA at a high acidic concentration (6 M HCl solution) for a long time (27 h) to achieve complete hydrolysis. The use of such drastic conditions may be mainly due to the generation of numerous positive charges in close proximity along the polymer backbone, not to any intrinsic difficulty in the hydrolysis of the amide groups[18]. Akashi *et al*[19] also hydrolyzed PNVA at 95 °C in 0.2 M HCl solution for 24 hours. However, only 67% hydrolysis was obtained. Gless[21] pointed out that the suitable acid concentration for the hydrolysis of PNVA should be from 1.05 to 3 equivalents of acid per equivalent of polymer. An excess amount of acid could cause the hydrolyzed product to precipitate prematurely. High temperature was also required for the hydrolysis of PNVA. However, a brown color developed during the hydrolysis. The higher the temperature, the darker the color was. Therefore, the hydrolysis of PNVA was carried out at 85 °C for 3 days in 3 M HCl solution with 2 equivalents of acid per equivalent of polymer. It was found that the hydrolysis product precipitated prematurely after the hydrolysis was carried out for 36 hours. In this case, extra DI H_2O had to be added in order to dissolve the precipitates. The product generated was purified and identified with FT-IR and ^{1}H NMR spectroscopes.

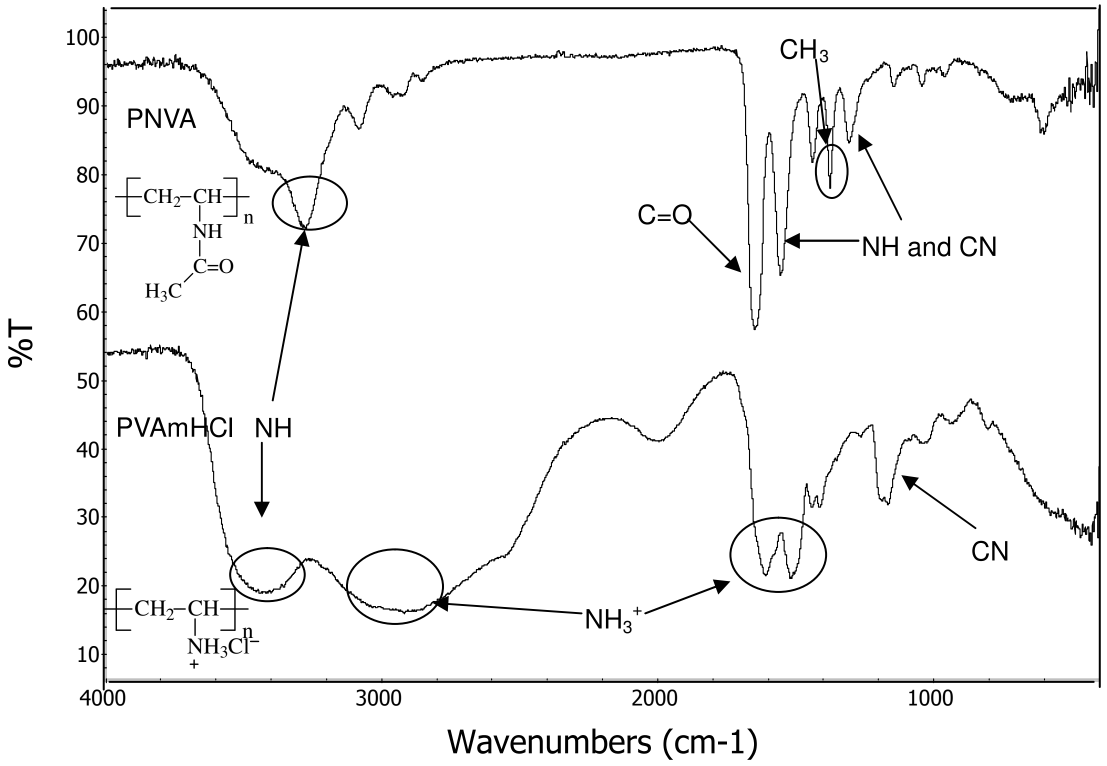

Figure 3.3 IR spectra of PNVA and PVAmHCl

The IR spectra of PNVA and the acid-hydrolyzed product are shown in Figure 3.3.

Comparing the two spectra, the peaks which indicate the existence of the amide group of PNVA include peaks at 3278 cm^{-1} (N-H stretching vibration), 1653 cm^{-1} (C=O stretching vibration), 1553 and 1303 cm^{-1} (combination of N-H and C-N), and 1374 cm^{-1} (-CH_3 attached to a C atom). All these peaks disappear in the IR spectrum of the product obtained. The results suggest that PNVA has been substantially hydrolyzed. The IR spectrum of PVAmHCl shows the typical characteristics of the primary amine salts. The broad absorption at 3200-2400 is attributed to the NH_3^+ asymmetric stretching, while the peaks at about 1621 and 1519 cm^{-1} are donated by NH_3^+ asymmetric and symmetric deformation respectively. The peaks at 3433 and 1160 cm^{-1} are corresponding to -NH_2 and C-N stretching, respectively.

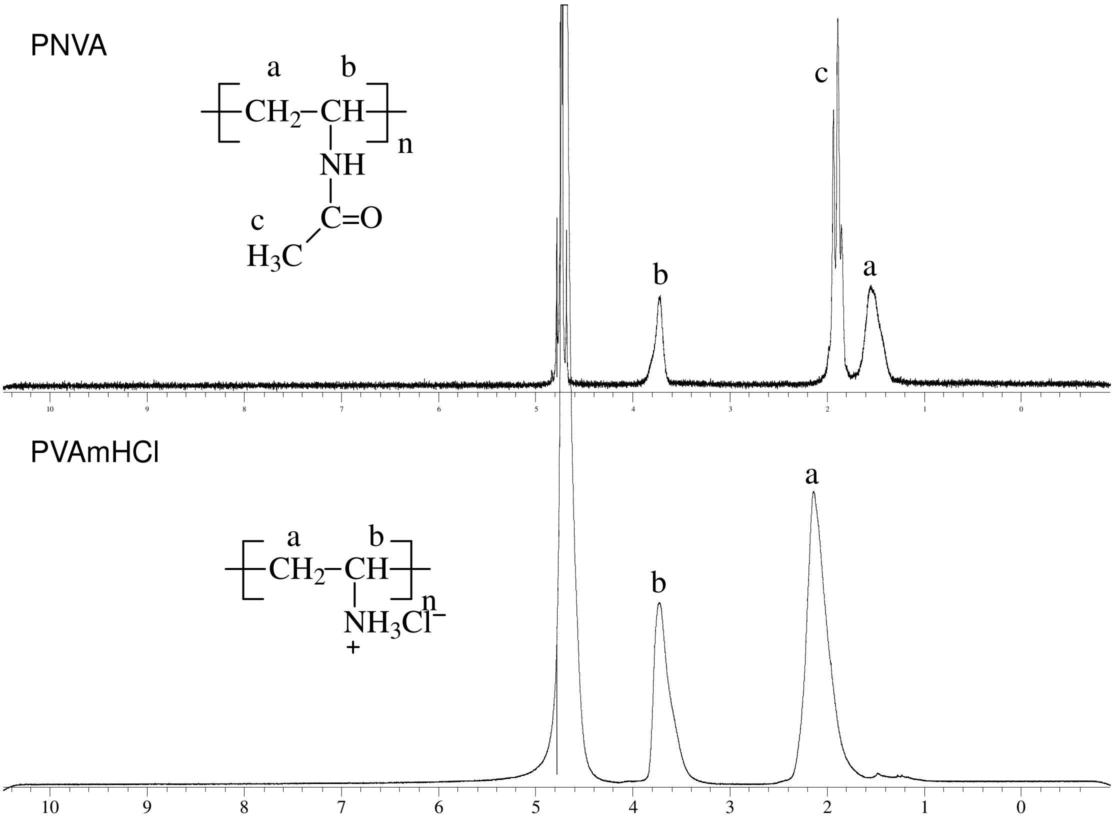

Figure 3.4 ^1H NMR spectra of PNVA and PVAmHCl

The ^{1}H NMR spectra of PNVA and the acid-hydrolyzed product are shown in Figure 3.4. After hydrolysis, significant changes are observed in the ^{1}H NMR spectrum of the product. The peak attributed to the protons of -CH_2- in the backbone of PNVA shifts downfield to 2.14 ppm in the spectrum of PVAmHCl, while the peak donated to the proton in –CH- also shifts downfield to 3.72 ppm. Most importantly, the peaks at 1.85-1.93 ppm assigned to the acetamide methyl protons disappear in the spectrum of PVAmHCl, indicating that the hydrolysis degree of the PVAm obtained is nearly 100%, giving the protonated polyvinylamine (PVAmHCl).

The PVAmHCl can be easily converted to PVAm via an acid-base reaction with NaOH. However, Reynolds[4] reported that it was difficult to prepare a PVAm in its free form because of the formation of the corresponding carbonate salt due to its rapid absorption of carbon dioxide from the air. Thus the conversion of PVAmHCl to PVAm must be carried out carefully in a CO_2-free system. Therefore the PVAm was prepared by first reacting PVAmHCl with NaOH, followed by purification with repeated precipitation-decantation-dissolution cycles using freshly distilled DI water and acetone. NaOH pellets used in this reaction should not contain any impurities of carbonate. The PVAm obtained should be stored immediately in nitrogen atmosphere to prevent it from being carbonated. In spite of trying all possible ways to obtain pure PVAm, it was still unavoidable that some of the amino groups were carbonated during the production and storage. It is also difficult to remove all the inorganic salt from the reaction mixture due to the co-precipitation of salt with PVAm.

The structure of the product was identified with ^1H NMR spectroscopy. Here, the crude product obtained by reacting PVAmHCl with excess NaOH without further purification was compared with the PVAm being treated with CO_2 to form a carbonated PVAm. Figure 3.5 shows ^1H NMR spectra of PVAmHCl, PVAm, and carbonated PVAm.

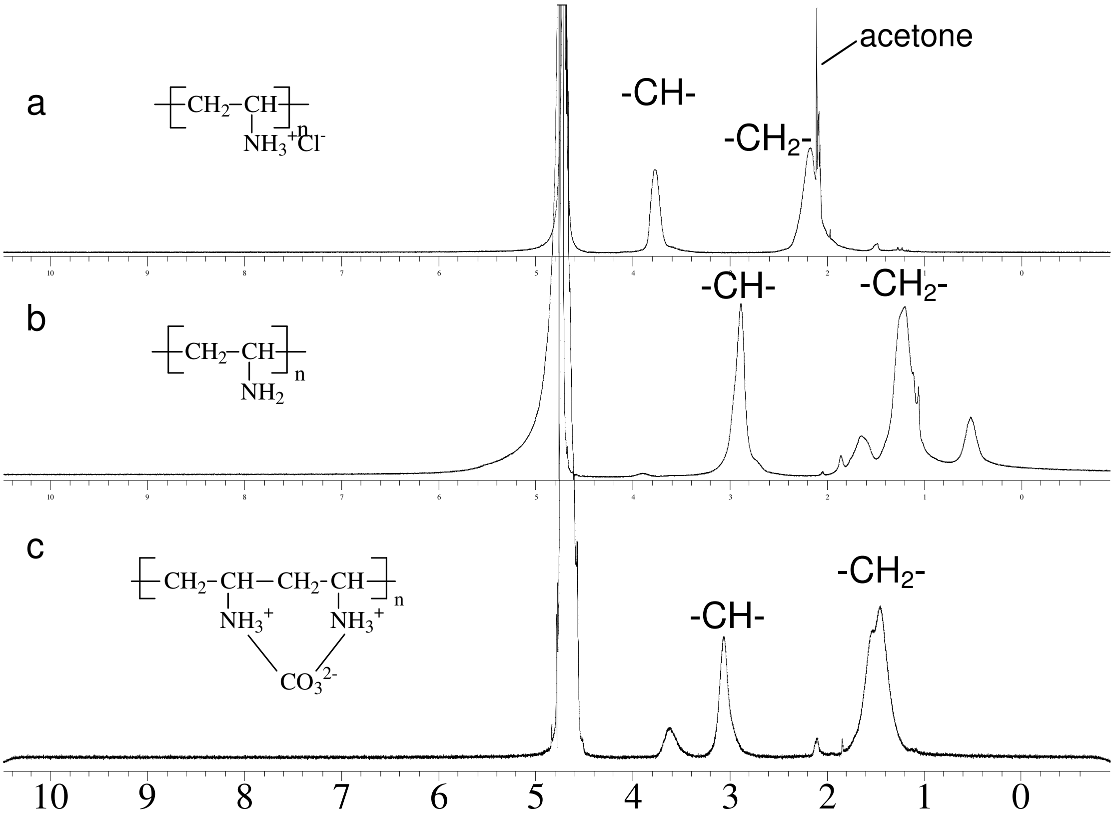

Figure 3.5 ^1H NMR spectra of (a) PVAmHCl, (b) PVAm, and (c) carbonated PVAm.

Table 3.2 summarizes chemical shifts of above spectra. After converting PVAmHCl to PVAm, both the proton peaks of $–CH_2$- and -CH- shift slightly upfield because of the absence of strong electron withdrawing groups.

Table 3.2 Summary of chemical shifts of various polyvinylamine derivatives

Product	PVAmHCl	PVAm	Carbonated PVAm
Chemical shifts of –CH_2- protons (ppm)	2.17	1.22	1.47
Chemical shifts of –CH- protons (ppm)	3.77	2.89	3.07

Although complete conversion of PVAmHCl to PVAm can be achieved, the PVAm is not very stable in air and is easily carbonated during the transformation. Thus it is better to store the polymer in the form of PVAmHCl, and convert it to the PVAm when needed.

3.3.3 Synthesis of PVAms with different molecular weights (Mw)

Various PVAms with different Mws were prepared via the hydrolysis of the preformed PNVAs with different Mws. It is well known that Mw of polymer through a free radical polymerization is dependant upon monomer structure and concentration, reaction temperature, concentration and type of initiators, as well as chain transfer agent. Among these parameters, varying the mole ratio of monomer to initiator, reaction temperature and use of chain transfer agents are common approaches to control the Mw of the polymer produced. In our experiments, PNVAs with different Mws from 5.4×10^5 to 2.6×10^5 were prepared by varying mole ratio of monomer to initiator from 200:1 to 50:1. Detailed reaction conditions and results are listed in Table 3.3.

Table 3.3 Reaction conditions and PNVAs obtained

Entry	The mole ratio of monomer to initiator	Reaction Temp. (℃)	Total weight (g)	Solid content (%)	Yield (%)	Mw[a] (×10^5)
PNVA1	200:1	60	110	9	--	5.4
PNVA2	200:1	60	220	9	97	4.2
PNVA3	150:1	60	100	10	78	3.4
PNVA4	100:1	60	100	10	98	2.7
PNVA5	50:1	60	100	10	90	2.6
PNVA6	30:1	80	100	10	--	--
PNVA7[b]	200:1	60	110	9	70	0.19

[a] The Mw were measured viscometrically.

[b] The polymerization was performed in a mixture of isopropyl alcohol and DI water (V/V=10:1)

It was noted that the Mw of PNVA2 was much lower than that of PNVA1 when the concentration was doubled. The higher monomer concentration resulted in higher polymerization rate, which then causes the higher temperature of the reaction system due to exothermic polymerization of the monomer. The result indicates that the polymerization temperature is also a key factor affecting the Mw of the polymer produced.

To obtain PNVA with a lower Mw, the polymerization was performed at a higher temperature (80 ℃ instead of 60 ℃) with a lower monomer to initiator ratio (30:1, Table 3.3, PNVA6). Higher reaction temperature aimed to accelerate the decomposition rate of initiator, thus increasing the radical concentration in the polymerization system. In this case, Mw of the product was not measured because it was hydrolyzed directly. But the formation of lower Mw product was reflected by the lower viscosity of the reaction mixture.

With the same purpose, another polymerization was carried out at 60 ℃ with the mole ratio of 200:1 in a mixture of isopropyl alcohol and DI water (V/V=10:1) (Table 3.3, PNVA7). Isopropyl alcohol is considered to be a good chain transfer agent with a transfer constant about 200 times higher than water.[22] Thus, it could reduce the Mw of the polymer produced. Our result indicates that the PNVA had a Mw of 1.9×10^5, which is the lowest among all PNVAs produced. However, the yield was only 70%, which was considerably lower than other entries.

A series of PVAms were obtained through the hydrolysis of their corresponding PNVAs. The Mws of the PVAms were measured viscometrically at 25 ^{o}C in viscometers of the Ubbelohde type in an aqueous solution of 0.01 M NaOH/0.1 M NaCl. Figure 3.6 shows the results of viscometric measurements. The calculated $[\eta]$ and Mw of the PVAms from Eq. 3.7 are recorded in Table 3.4. The Mw of PVAm ranged from 4.0×10^5 to 3.5×10^4. It does not theoretically agree with the Mw of PNVA, which might be because the facts that: (1) the Eq. 3.6 for calculating the Mw of PNVAs is from an unpublished thesis, which does not show the valid range of Mw; (2) the valid Mw for Eq. 3.7 ranges from 1.5×10^4 to1.6×10^5, while most of the Mw of PVAms are out of the range. However, they do give us the relative information on the Mw of the polymers.

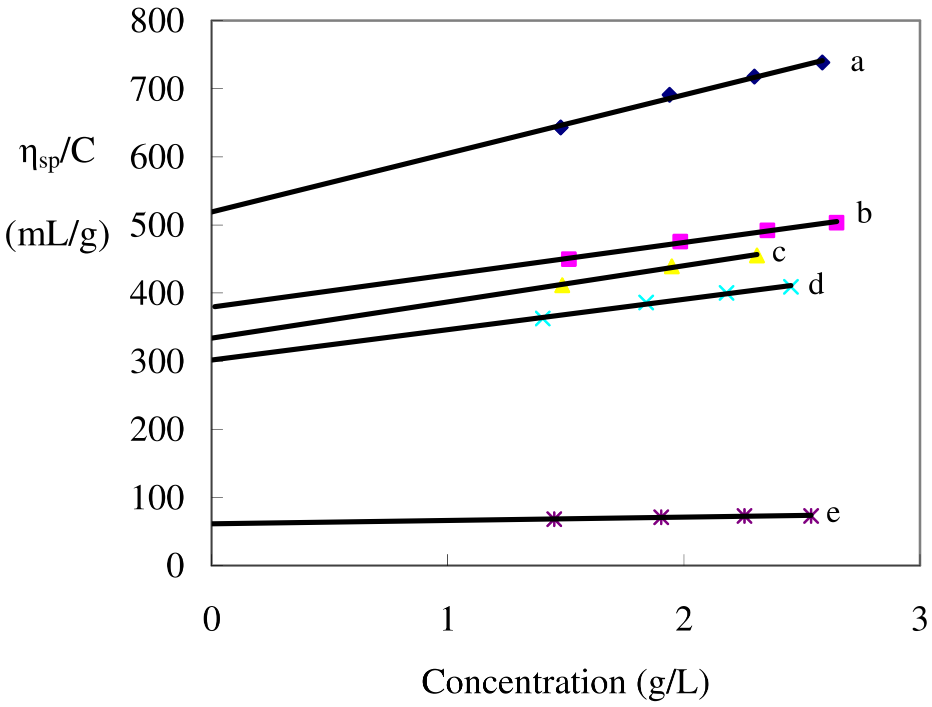

Figure 3.6 Viscometric measurements of PVAm samples. (a) a5; (b) a7; (c) a8; (d) a9; (e) a10.

Table 3.4 The hydrolysis of PNVA to PVAm[a]

Entry	Oil bath Temp. (℃)	PNVA	Mw of PNVA	Yield (%)	[η] (mL/g)	Mw of PVAm
a5	100	PNVA2	4.2×10^5	82	523	4.0×10^5
a7	112	PNVA3	3.4×10^5	88	379	2.7×10^5
a8	112	PNVA4	2.7×10^5	88	333	2.4×10^5
a9	112	PNVA5	2.6×10^5	98	301	2.1×10^5
a10	112	PNVA6	--	76	61	3.5×10^4

[a] The hydrolysis of PNVA was performed for 48 h in 3 M HCl solution.

3.4 Conclusions

PVAm was synthesized by a three-step reaction: (1) The preparation of PNVA via a free radical polymerization of NVA in water using V-50 as an initiator; (2) The hydrolysis of the preformed PNVA in 3 M HCl aqueous solution; (3) The conversion of PVAmHCl to PVAm with NaOH solution in the absence of carbon dioxide. The successful synthesis was confirmed by IR and ^{1}H NMR spectroscopes. The NMR spectrum of PVAmHCl produced indicates that the hydrolysis was nearly complete. However, when converting PVAmHCl to PVAm, it was unavoidable that a small amount of carbonated product was formed. Thus the storage in the form of PVAmHCl is preferred because of its good stability..

A series of PVAmHCls with different Mw were prepared through the hydrolysis of PNVAs with different Mw. The PNVAs were synthesized via free radical polymerization of NVA at different initiator concentration, temperature or in the presence of chain transfer agent. The results suggested that initiator concentration, temperature and chain transfer agent affected the Mw of the polymer produced.

References:

1. El Achari, A.; Coqueret, X.; Lablache-Combier, A.; Loucheux, C., Preparation of poly(vinylamine) from polyacrylamide: a reinvestigation of the Hofmann reaction. *Makromolekulare Chemie* **1993,** 194, (7), 1879-1891.
2. Tanaka, H., Hofmann reaction of polyacrylamide: relationship between reaction condition and degree of polymerization of polyvinylamine. *Journal of Polymer*

Science, Polymer Chemistry Edition **1979,** 17, (4), 1239-1245.

3. Tanaka, H.; Senju, R., Preparation of cationic polymers and their applications. IV. Preparation of poly(vinylamine) by the Hofmann degradation of poly(acrylamide). *Bulletin of the Chemical Society of Japan* **1976,** 49, (10), 2821-2823.
4. Reynolds, D. D.; Kenyon, W. O., Preparation of polyvinylamine, polyvinylamine salts, and related nitrogenous resins. *Journal of the American Chemical Society* **1947,** 69, 911-915.
5. Hart, R., New method for the synthesis of polyvinylamine. *Journal of Polymer Science* **1958,** 29, 629-636.
6. Dawson, D. J.; Gless, R. D.; Wingard, R. E., Jr., Poly(vinylamine hydrochloride). Synthesis and utilization for the preparation of water-soluble polymeric dyes. *Journal of the American Chemical Society* **1976,** 98, (19), 5996-6000.
7. Uchino, N.; Machida, S. *N*-Vinylamine polymers and their quaternary ammonium salts. JP 51100188, **1976**.
8. Brunnmueller, F.; Schneider, R.; Kroener, M.; Mueller, H.; Linhart, F.; Burkert, H.; Beyer, K. H. Linear, basic polymers and their use. EP 71050, **1983**.
9. Dawson, D. J.; Otteson, K. M. Ethylidenebisformamide, and its use in preparing poly(vinylamine) and its salts. USP 4490557, **1984**.
10. Badesso, R. J.; Nordquist, A. F.; Pinschmidt, R. K., Jr.; Sagl, D. J., Synthesis of amine functional homopolymers with *N*-ethenylformamide. *Advances in Chemistry Series* **1996,** 248, (Hydrophilic Polymers), 490-504.
11. Akashi, M.; Yashima, E.; Yamashita, T.; Miyauchi, N.; Sugita, S.; Marumo, K., A

novel synthetic procedure of vinylacetamide and its free radical polymerization. *Journal of Polymer Science, Part A: Polymer Chemistry* **1990,** 28, (12), 3487-3497.

12. Yamamoto, K.; Imamura, Y.; Nagatomo, E.; Serizawa, T.; Muraoka, Y.; Akashi, M., Synthesis and functionalities of poly(*N*-vinylalkylamide). XIV. Polyvinylamine produced by hydrolysis of poly(*N*-vinylformamide) and its functionalization. *Journal of Applied Polymer Science* **2003,** 89, (5), 1277-1283.
13. Gu, L.; Zhu, S.; Hrymak, A. N., Acidic and basic hydrolysis of poly(*N*-vinylformamide). *Journal of Applied Polymer Science* **2002,** 86, (13), 3412-3419.
14. Lai, T. W.; Vijayendran, B. R. Manufacture of high-molecular-weight poly(*N*-vinylamides) and poly(vinylamines) by inverse emulsion polymerization. EP 264649, **1988**.
15. Hong, J. S.; Nakahara, T.; Maeda, H.; Kikunaga, Y.; Kishida, A.; Akashi, M., Cloud points and phase separation of aqueous poly(*N*-vinylacetamide) (PNVA) solutions in the presence of salts. *Colloid and Polymer Science* **1996,** 274, (11), 1013-1019.
16. Dubin, P. L.; Levy, I. J., Gel permeation chromatography of cationic polymers on pw gel columns. *Journal of Chromatography A* **1982,** 235, (2), 377-387.
17. Bloys van Treslong, C. J.; Morra, C. F. H., Poly(vinylamine). Synthesis and characterization. *Recueil des Travaux Chimiques des Pays-Bas* **1975,** 94, (5), 101-105.

18. Stackman, R. W.; Summerville, R. H., Synthesis of *N*-vinylacetamide and preparation of some polymers and copolymers. *Industrial & Engineering Chemistry Product Research and Development* **1985,** 24, (2), 242-246.
19. Akashi, M.; Saihata, S.; Yashima, E.; Sugita, S.; Marumo, K., Novel nonionic and cationic hydrogels prepared from *N*-vinylacetamide. *Journal of Polymer Science, Part A: Polymer Chemistry* **1993,** 31, (5), 1153-1160.
20. Hvidt, A.; Corett, R., Kinetics of hydrogen-deuterium exchange in poly(*N*-vinylacetamide) measured by infrared spectroscopy. *Journal of the American Chemical Society* **1970,** 92, (19), 5546-5550.
21. Gless, R. D., Jr.; Dawson, D. J.; Wingard, R. E. Polyvinylamine and salts thereof. USP 4,018,826, **1977**.
22. Brandrup, J.; Immergut, E. H.; Grulke, E. A., *Polymer handbook.* 4th ed.; Wiley: New York, **1999**; p II112.

Chapter 4

Synthesis of Amphiphilic Core-shell PMMA/PVAm Particles

4.1 Introduction

Recently, a novel and efficient method has been developed by our group to prepare well-defined amphiphilic core-shell particles in the absence of surfactant via the direct graft copolymerization of vinyl monomers from water-soluble polymers containing amino groups.[1, 2] This approach is based on the reaction between alkyl hydroperoxides and amino groups of the water-soluble polymer in water in the presence of dispersed vinyl monomers. During the reaction, amphiphilic graft copolymers and hydrophobic homopolymers are generated concurrently. The amphiphilic copolymers self-assemble to form micelle-like micro-domains, which assist the emulsion polymerization of vinyl monomer(s) to form highly mono-dispersed particles with amphiphilic core-shell structures. Using this novel synthetic approach, a series of well-defined amphiphilic core-shell particles have been synthesized such as poly(methyl methacrylate (PMMA)/chitosan[2, 3], poly(*n*-butyl acrylate) (PBA)/chitosan[4], PMMA/poly(ethylenimine) (PEI) and PMMA/poly(allylamine) (PAAm)[5], poly(*N*-isopropylacrylamide) (PNIPAM)/PEI and PNIPAM/chitosan[6, 7] core-shell particles etc.

Based on these findings, here we propose a novel route to synthesize amphiphilic core-shell particles which consist of well-defined hydrophobic polymer cores and polyvinylamine (PVAm) shells by graft copolymerization of vinyl monomer(s) from

PVAm in the absence of surfactant using TBHP as an initiator. These particles are expected to possess several unique properties, such as diameters in nano-dimension with a narrow size distribution, controllable core-shell structure and tailored functionalities.

To achieve these objectives, effects of reaction parameters, such as the initiator concentration, weight ratio of monomer to PVAm, pH and ionic strength of reaction medium, molecular weight, amination degree and crosslinking degree of PVAm have been systematically examined in order to gain insights of those factors which control the properties of the particles such as particle size, core-shell structure and morphologies, etc.

4.2 Experimental

4.2.1 Materials

Methyl methacrylate (MMA) (colorless liquid, Mw=100.12, density=0.936 g/cm^3, Aldrich) was purified by first washing three times with 10 wt.% sodium hydroxide (NaOH) aqueous solution to remove the inhibitor that was added in the monomer for safe storage, then with distilled water until the pH of the water layer to neutral. Finally the monomer was dried with anhydrous calcium chloride, followed by vacuum distillation.[5] *tert*-Butyl hydroperoxide (TBHP) (70% aqueous solution, colorless liquid, MW=90.07, Aldrich) and glutaraldehyde (GA) (50 wt.% aqueous solution, Aldrich), were used as received and diluted to appropriate concentrations prior to usage. Reagent *grade* of hydrochloric acid (HCl) (37%, Aldrich), NaOH (Fluka), chloroform (Aldrich) and acetone (Aldrich) were used as received. De-ionized (DI) water was used as the dispersion medium.

Poly(vinylammonium chloride) (PVAmHCl) and poly(vinylamine) (PVAm) were prepared as described in Chapter 3. For the sake of storage stability, unless stated otherwise, PVAmHCl was used directly without being converted to PVAm in most of the studies. Since each batch of PVAmHCl synthesized might vary in their Mw, it was attempted to carry out each effect study using the same batch of polymer.

4.2.2 Synthesis of PVAm/PMMA core-shell nanoparticles

4.2.2.1 Grafting copolymerization using linear polyvinylamine

For a total of 50 g of solution, an appropriate amount of PVAmHCl (0.125~1g) was dissolved in DI water and the pH of the solution was adjusted to a given value (7~12) with a 1 M NaOH solution. The solution was then mixed with purified MMA (1~2g) in a three-necked water-jacketed flask equipped with a thermometer, a reflux condenser and a nitrogen inlet and purged with nitrogen under stirring for 30 minutes to remove oxygen. The mixture was stirred and heated to 80℃. Then an appropriate amount of TBHP (2.5×10^{-3} ~ 0.1 mmol) was added and the mixture was kept at 80℃ under stirring for 3 hours. After the reaction, the particle dispersion was carefully purified by repeated centrifugation-decantation-dispersion cycles using DI water to remove unreacted water-soluble polymer.

4.2.2.2 Grafting copolymerization using crosslinked polyvinylamine

PVAm was prepared by neutralizing PVAmHCl with NaOH to pH 12, followed by purification with repeated cycles of precipitation-decantation-dissolution using freshly distilled acetone and DI water. The PVAm was first slightly crosslinked by using an appropriate amount of glutaraldehyde prior to polymerization. A detailed procedure is as follows. For a solution of total 50 g, PVAm (0.5 g) was dissolved in DI water and the pH of the solution was adjusted to 8.0 with 3 M of HCl solution. The solution was then stirred and mixed with an appropriate amount of GA solution (0-5 ml of 5 wt.% aqueous solution) for 12 hrs at room temperature in a water-jacketed flask equipped with a thermometer, a condenser, a magnetic stirrer and a nitrogen inlet. The solution was then heated to 80 ^{o}C for 2 h. A small amount of MMA (about 0.5 g) was mixed with the solution at 80 ^{o}C for 30 min, followed by addition of the remaining monomers (1.5 g) and diluted TBHP solution (1.0 mL of 10 mM solution). The polymerization was then carried out at 80 ^{o}C for 3 h under nitrogen atmosphere.

4.2.3 Measurement and characterization

4.2.3.1 Conversion

After polymerization, the precipitate, if any, was filtered off, washed, dried and weighed. The solid content of the latex was measured gravimetrically. The monomer conversion for particle formation, which refers to the weight percentage of polymerized MMA in particles based on the total weight of monomer added, was calculated as follows:

$$\text{Monomer conversion for particle formation} = \frac{\text{Weight of total solid in dispersion} - \text{Weight of water soluble polymer added}}{\text{Total weight of MMA added}} \times 100\%$$

The total monomer conversion, which refers to the weight percentage of polymerized MMA based the total weight of monomer added, was calculated as follows:

$$\text{Total monomer conversion} = \frac{\text{Weight of total solid in dispersion} + \text{Weight of precipitate} - \text{Weight of water soluble polymer added}}{\text{Total weight of MMA added}} \times 100\%$$

Unless stated otherwise, the monomer conversion in this thesis refers to the monomer conversion into particles.

4.2.3.2 Grafting percentage and grafting efficiency

The graft copolymers and PMMA homopolymers were isolated from the resulting polymers by Soxhlet extraction with chloroform for 48 hours. The graft copolymers were then collected in the thimble and the homo-PMMA was dissolved in chloroform and collected in the round bottom flask. Grafting percentages (GP%) and the grafting efficiency (GE%) were calculated as follows:

$$\text{GP\%} = \frac{\text{Weight of grafted PMMA}}{\text{Weight of water soluble polymer}} \times 100\%$$

$$\text{GE\%} = \frac{\text{Weight of grafted PMMA}}{\text{Weight of total polymerized MMA}} \times 100\%$$

4.2.3.3 Particle size and size distribution of PMMA/PVAm particles

Unless stated otherwise, the particle size and size distribution were measured on a Coulter LS 230 particle size analyzer.

The purified particle dispersion was added dropwise into the cleaned analyzer. Then the obtained “D_v” and “D_n” (the volume and number average of the particle diameters, respectively,) were used to calculate the polydispersity index (PDI), as shown below. If the PDI value is equal to 1, it indicates monodisperse particle size distribution.

$$\text{PDI} = \frac{D_v}{D_n}$$

In some cases, the particle size and size distribution were measured on a Zetasizer 3000 HSA.

4.2.3.4 Surface charge density

The ξ-potential of the core-shell particles was measured with a Malvern Zetasizer 3000HSA (Malvern, UK). The sample was prepared by diluting the core-shell particle dispersion with a 1 mM NaCl solution to about 1000 ppm, followed by vibrating the dispersion for 10 minutes in an ultrasonic vibrator. Then the particle dispersion was injected into a cleaned sample cell of Zetasizer with a syringe.

4.2.3.5 Composition of PVAm/PMMA core-shell particles

FT-IR spectra were recorded on a Nicolet Avatar 360 FT-IR spectrophotometer using KBr disks. The ^{1}H NMR spectra were recorded on a Bruker advance DPX-400 (400 MHz) instrument using D_2O as solvent.

4.2.3.6 Morphologies of PVAm/PMMA core-shell particles

Transmission Electron Microscopy (TEM) micrographs were obtained with a JEOL 2010 transmission microscope at an accelerating voltage of 200 kV or with a JEM 100 CX transmission microscope at an accelerating voltage of 100 kV. Each sample was prepared by wetting a carbon-coated grid with a small drop of dilute particle dispersion. The dried particles were treated with a small drop of phosphotungstic acid (PTA) solution (0.5 wt.-%) for an appropriate time, then dried at room temperature.

The surface morphologies of the particles were examined by Field Emission Scanning Electron Microscopy (FE-SEM, JEOL JSM 6335F). Each sample was prepared by spreading a drop of dilute particle dispersion on a glass surface and drying in a dust-free environment at room temperature. The dried specimen was then coated with a thin layer of gold to a depth of ca. 5 Å. under vacuum.

4.3 Results and Discussions

4.3.1 Synthesis of the PMMA/PVAm core-shell particles

Our previous studies[3, 5] have shown that the optimum reaction temperature and time for the graft copolymerization of MMA from a water soluble polymer containing amino groups were 80 °C and 2~3 hrs, respectively. Thus the PMMA/PVAm core-shell particles were prepared under these conditions in the absence of surfactants. The polymerization is based on the reaction between alkyl hydroperoxides and the amino groups of the water-soluble polymer, PVAm, in water in the presence of a dispersed hydrophobic monomer, MMA. During the reaction, the hydroperoxides initially interact with amino groups on the polymer backbone, generating macromolecular radicals and alkoxyl radicals. Those two types of radicals then initiate the graft and the homo-polymerization of the monomer, respectively. The alkoxyl radicals might also abstract hydrogen atoms from the water soluble polymer, thus generating macromolecular radicals that could also initiate the graft copolymerization.[2] The amphiphilic PVAm-g-PMMA graft copolymers generated *in situ* act like polymeric surfactants, and self-assemble to form micelle-like microdomains. The micellar domains subsequently promote the emulsion polymerization of MMA. Stable particles were then produced in the absence of surfactant. Thus the water-soluble polymer provides not only reactive points such as amino groups for initiation, but also the electrostatic and steric stabilization (Scheme 4.1).

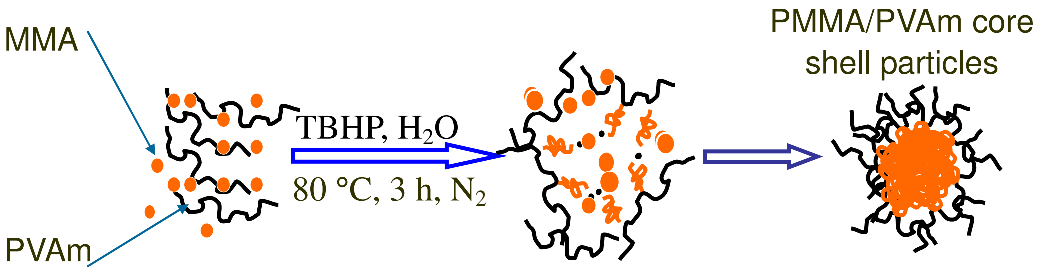

Scheme 4.1 The graft copolymerization of MMA from PVAm

4.3.2 The effect of reaction pH on the graft copolymerization of MMA from PVAm

PVAm is a weak cationic polyelectrolyte, and its charge density can be varied by pH from fully ionized ($pH < 3$) to completely neutral ($pH > 10$).[8] Kirwan[9] observed that PVAm experienced a conformational transition from coil to globule during the change of the solution pH from acidic to basic condition. At a low pH where PVAm is fully ionized ($pH < 3$), it exists in an extended coil conformation. While at a high pH ($pH > 10$), the polyelectrolyte is completely de-protonated and has a globular conformation, as seen in Figure 4.1.

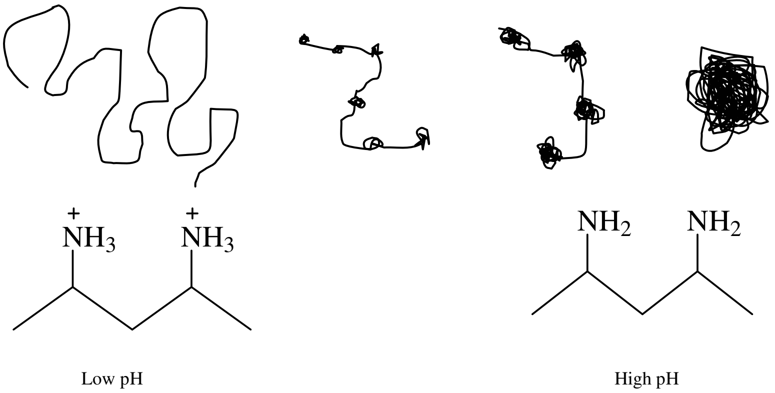

Figure 4.1 Schematic representation of the extended coil-to-globular conformational transition for linear flexible poly(vinylamine).(Reproduced from reference[9])

Since the ionization degree of amine groups depends on the solution pH, it is anticipated that the pH of the reaction medium may strongly affect the polymerization and particle formation due to the differences in available amine groups and solubility of the resulting PVAm. Therefore, the effect of the reaction pH on the graft co-polymerization of MMA from PVAm was studied with respect to the monomer conversion, grafting percentage, grafting efficiency, particle size and particle size distribution, surface charge and morphologies. The reaction pH here refers to the pH of the PVAm solution prior to polymerization.

PVAmHCl was first dissolved in H_2O and the pH of the solution was adjusted to an appropriate value with 2M NaOH solution. The PVAm solution was then treated with a small amount of TBHP (0.1 mM) in the presence of MMA at 80 ^{o}C for 3 hours to generate PMMA/PVAm core-shell particles. The weight ratio between PVAm and MMA was 1:7.5 (PVAmHCl:MMA=1:4). After polymerization, the pH of the dispersion was recorded to monitor the pH changes before and after the polymerization. Average molecular weight of PVAm used was about 390,000 Delton measured viscometrically.

A series of experiments were carried out at different reaction pH and the results are summarized in Table 4.1. When the polymerization was carried at pH 7 and 8, large amounts of precipitates formed during the polymerization. The monomer conversion for particle formation and total conversion were also only 25% and 45% respectively at reaction pH 8. The result indicates that almost half of the polymerized

MMA were unstable and precipitated at pH 8. When the reaction pH increased to higher than 9, the precipitate generated decreased significantly and the monomer conversion for particle formation increased to up to 65% at reaction pH 12. The difference between the conversion for particle formation and the total conversion was little, suggesting that almost all the polymerized MMA was in the particle cores.

Table 4.1 Effect of reaction pH on the graft copolymerization of MMA from PVAm[a]

Entry	Reaction pH	Observation	pH of the dispersion after polymerization	Weight of precipitate (g)	Conversion for particle formation[b] (%)	Total conversion[c] (%)
P172	7	Some precipitate	7	0.23	19	42
P173	8	Some precipitate	7.6	0.20	25	45
P174	9	little precipitate	7.9	0.02	39	42
P175	10	little precipitate	8.4	0.03	34	37
P177	11	little precipitate	8.6	0.07	55	62
P178	12	little precipitate	8.2	0.01	65	66

[a] In all cases, the reactions were all carried out at 80 °C for 3 hrs; TBHP concentration was 0.1 mM; the weight ratio of PVAm to MMA was 1:7.5; the solid content was 2.5% based on the total weight of the reaction mixture, the total weight of the reaction mixture is 50g.

[b] Conversion for particle formation refers to the weight percentage of polymerized monomer in particles based on the total weight of monomer added

[c] Total conversion refers to the weight percentage of polymerized monomer based on the total weight of monomer added.

It is speculated that the strong influence of reaction pH on monomer conversion is because the number of -NH_2 group increases with the increase of pH. Since primary amine groups are highly reactive electron-donating groups towards the redox reaction with alkyl hydroperoxide, the reactivity of PVAm thus is higher at a higher pH. In addition, the PVAm becomes less hydrophilic at a higher pH, thus its grafted copolymers may be easier to form micellar domains, which assists the particle growth via an emulsion polymerization.

At pH 7 and 8, there might be enough NH_2 groups to form redox pairs with TBHP molecules to initiate the polymerization. However, the water soluble polymer is very hydrophilic due to the presence of a large amount of NH_3^+ groups on the polymer chains. Thus it takes a long reaction time to reach the hydrophobic-hydrophilic balance through graft-copolymerization of the hydrophobic monomer from the water-soluble polymer and self-assembling of the graft copolymers to form micellar domains. The homopolymer generated at the same time might grow very large, resulting in homogeneous nucleation without sufficient stabilization before the micellar formation. Another possibility might be that the generated alkoxyl radicals might diffuse into the monomer droplet and initiate the polymerization, causing droplet homogenous nucleation. Both of the two approaches to form homopolymers lead to the generation of precipitation during polymerization because of the lack of stabilization.

When the reaction pH was further increased to a pH higher than 9, more and more $-NH_3^+$ groups are converted to $-NH_2$ groups. As a result, the graft-copolymerization would become faster because of the increased availability of amine groups and PVAm becomes less hydrophilic. Thus the formation of micellar domains would become easier, and the homo-polymerization and graft-copolymerization would take place in the micellar cores. Therefore, the ungrafted homopolymer precipitate generated during the polymerization decreases significantly and the monomer conversion increases with the raising pH. The highest conversion was 65% with above conditions (at pH 12, [TBHP]=0.1 mM, 3 h at 80 °C).

It was noted that the pH of the reaction system decreased after the polymerization, and the higher the reaction pH, the larger in the pH difference. The pH drop after the polymerization may be attributed to three possible side reactions during the polymerization.

1) The Michael addition between primary amine groups of PVAm and vinyl group of MMA[10-13] as shown in Scheme 4.2. An amine group of PVAm acts as an nucleophile, and adds to the *β*-position of the monomer to form an amine ester group.

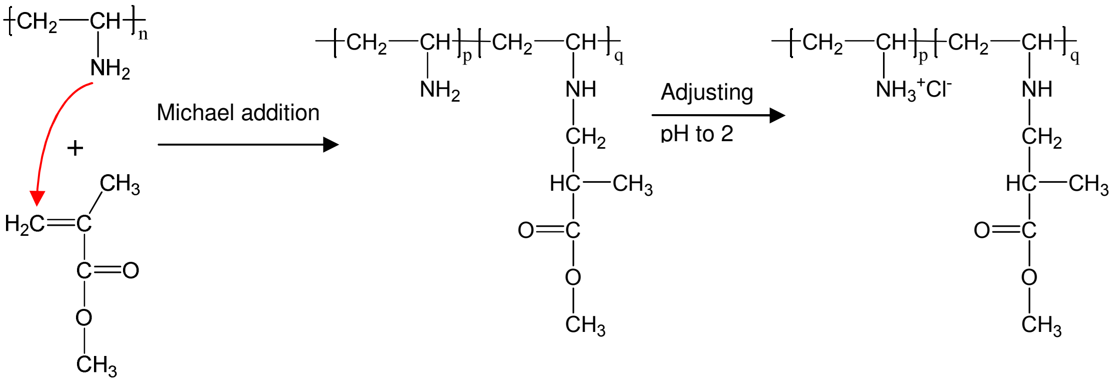

Scheme 4.2 Michael addition of PVAm to MMA.

2) The 1,2-addition between the primary amine group of PVAm and the carbonyl group of MMA (Scheme 4.3). An amine group of PVAm could undergo a

1,2-addition reaction to a carbonyl, forming an amide group.

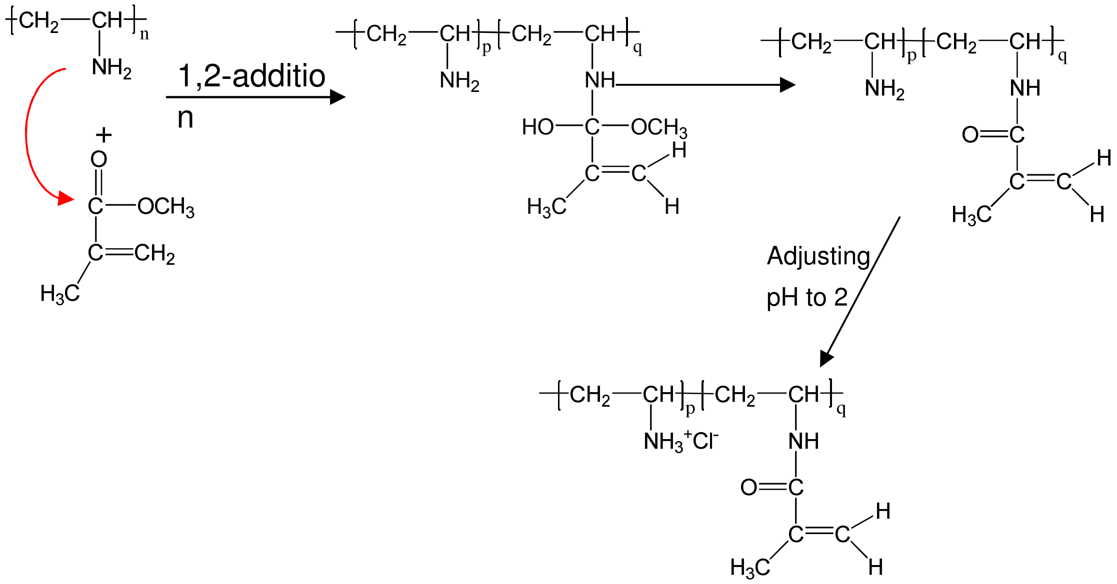

Scheme 4.3 Possible side reaction of 1,2-addition of PVAm to MMA monomer

3) The hydrolysis of MMA under strong alkaline conditions as shown in Scheme 4.4. The MMA monomer might first react with a OH- group to form an intermediate, followed by converting it to methacrylic acid (MAA). The resulting MAA may combine with PVAm to form a weak acid-weak base salt.

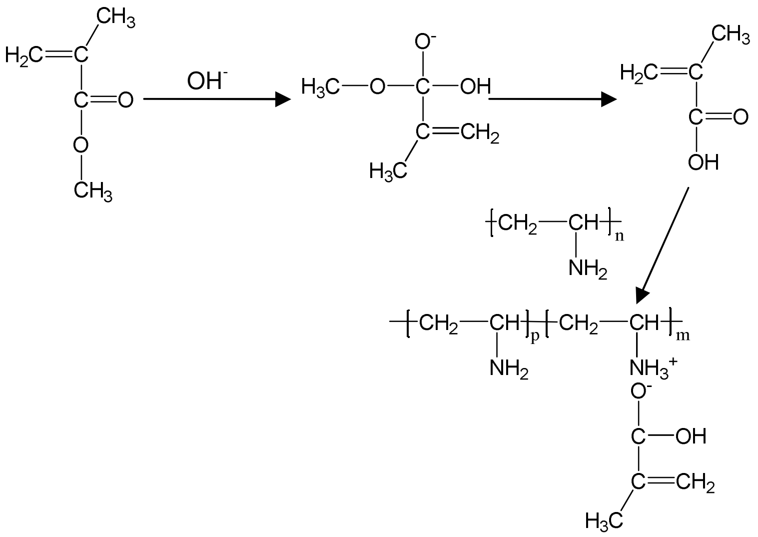

Scheme 4.4 Possible side reaction of the hydrolysis of MMA monomer under alkaline conditions.

The Michael addition and 1,2-addition consume the primary amine groups to covalently linked, neutral N-C bond and the partial hydrolysis of MMA reacts with OH^- anions. All the three reactions would decrease the pH of the reaction system.

To find out the side reactions that occur during the polymerization, three control experiments were carried out. (1) PVAm was mixed with MMA monomer at both pH 12 and pH 7 at 80 ^oC for 3 hours without addition of TBHP solution (Scheme 4.5 for pH 12 and Scheme 4.6 for pH 7). After reaction, the mixture was collected and analyzed to examine the difference before and after the reaction. When the reaction was carried out at pH 12, the pH of the reaction mixture was 7.8 after the reaction, which is much lower than that before the reaction. When the reaction was carried out at pH 7, the pH of the reaction mixture was 6.8 after the reaction, which is almost the same as before. The pH of the mixture was then adjusted to 2 with a 2 M HCl solution, followed by extracted with $CHCl_3$ to remove any unreacted MMA monomer and, if any, PMMA oligomer and dialyzed against DI-water. (2) PVAm was mixed with MAA at pH 10 at 80 ^oC for 2 hrs to find out if the anmino group of PVAm could react with MAA to form amide groups (Scheme 4.7). To make sure that the amount of MAA is comparable with that in the polymerization system of PVAm and MMA, the pH of PVAmHCl solution (original 2.5) was first adjusted to 12 with 10% NaOH solution to convert PVAmHCl to PVAm, then to 6 with MAA, and finally to 10 with 10% NaOH solution. The mixture was then heated to 80 ^oC for 3 hours to carry out the reaction. After cooled down, the pH of the mixture was adjusted to 2, followed by dialysis against DI-H_2O. PVAmHCl was also dialyzed against DI-H_2O for comparison

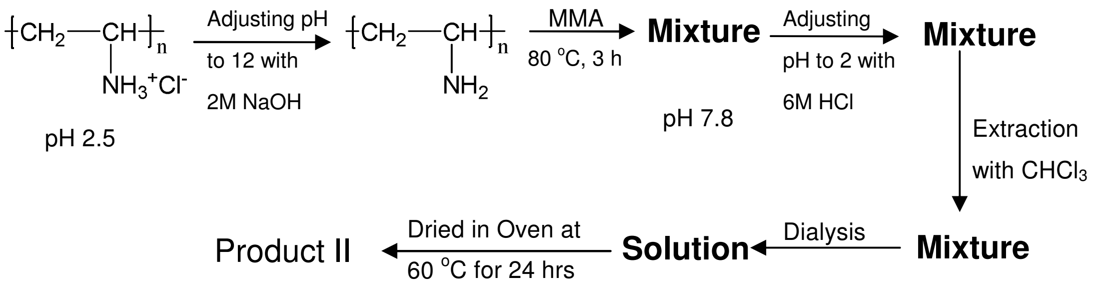

Scheme 4.5 Procedure for reaction between PVAm and MMA at pH 12, followed by dialysis

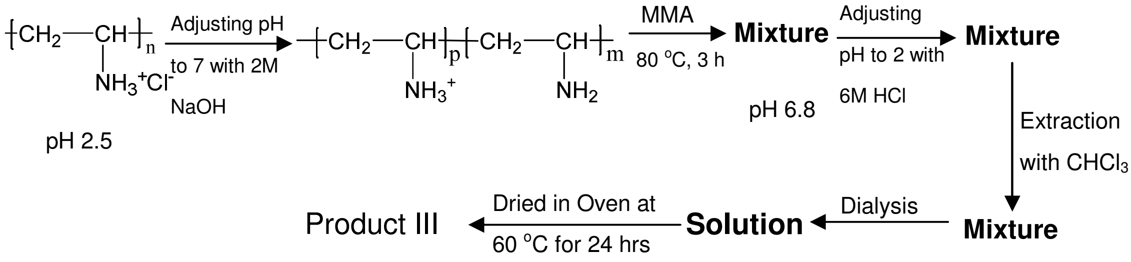

Scheme 4.6 Procedure for reaction between PVAm and MMA at pH 7, followed by dialysis

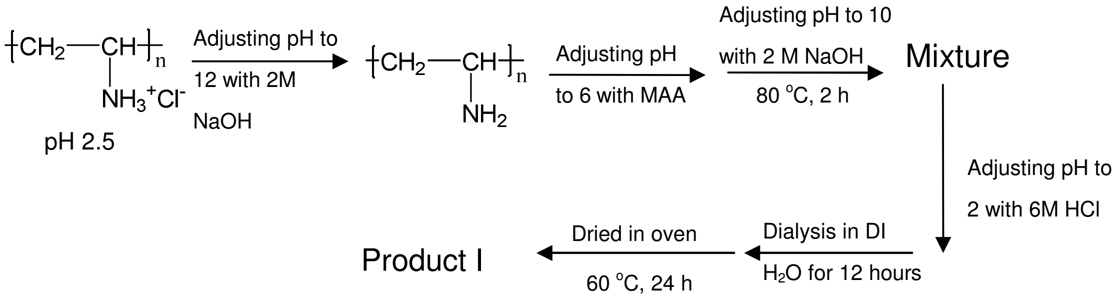

Scheme 4.7 Procedure for reaction between PVAm with MAA, followed by dialysis

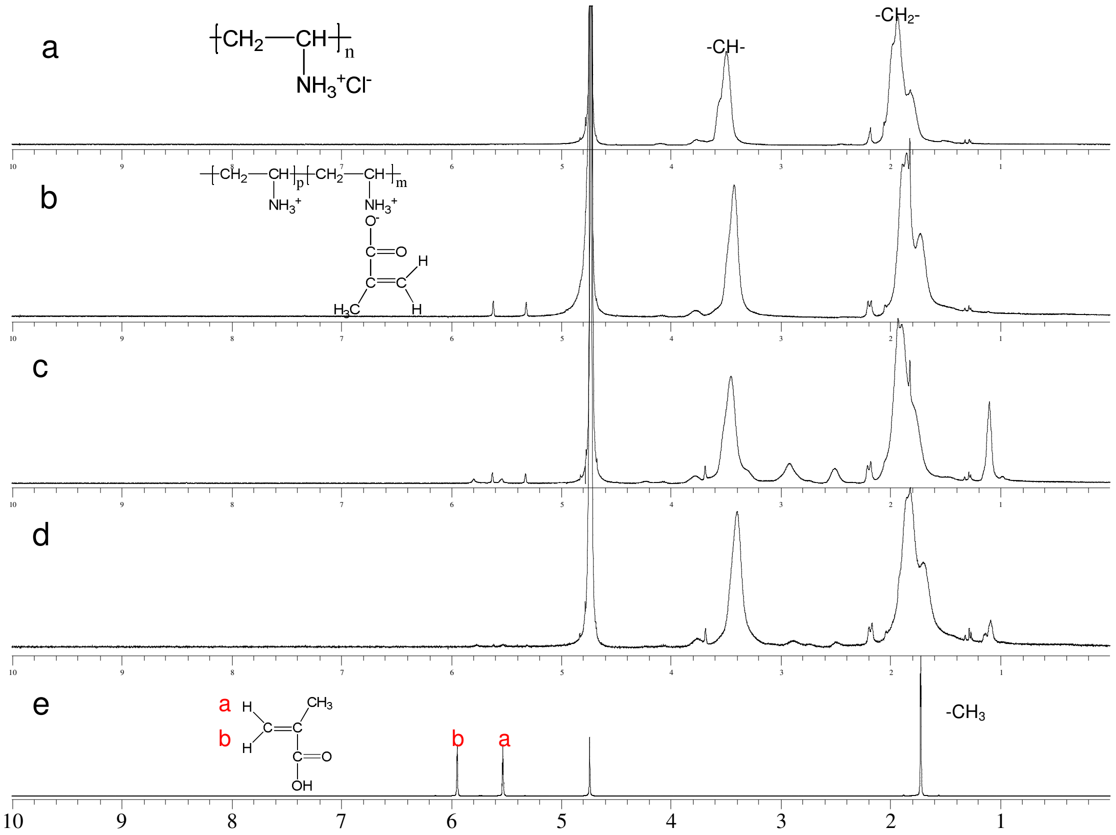

Figure 4.2 ^{1}H NMR spectra of (a) dialyzed PVAmHCl; (b) Product I (product obtained from the reaction between PVAm and MAA), (c) Product II (product from the reaction between PVAm and MMA at pH 12 for 3 hours), (d) Product III (product from the reaction between PVAm and MMA at pH 7 for 3 hours); and (e) MAA in D_2O

The products obtained were characterized by ^{1}H NMR spectroscopy (Figure 4.2). In the spectrum of dialyzed PVAmHCl (Figure 4.2a), the chemical shifts of the protons of $–CH_2$- and -CH- on the main chains of the polymers shift upfield to 1.90 and 3.45 ppm, respectively after dialysis, which is due to the pH difference before and after dialysis (pH 2.5 versus 4.8).

To better interpret the structure of product I (obtained from the reaction between

PVAm and MAA), product II (from the reaction between PVAm and MMA at pH 12) and Product III (product from the reaction between PVAm and MMA at pH 7), their ^{1}H NMR spectra (Figure 4.2b, 4.2c and 4.2d) are shown in Figure 4.3, Figure 4.4 and Fogure 4.5, respectively.

There are some new peaks at 5.62, 5.32 and 1.82 ppm in the ^{1}H NMR spectrum of product I (Figure 4.2b and Figure 4.3) comparing with the spectrum of PVAmHCl (Figure 4.2a). These peaks are exactly the same as the peaks attributed from MAA (Figure 4.2e). This result suggests that there is no conversion between PVAm and MAA. They just form a salt through electrostatic interaction.

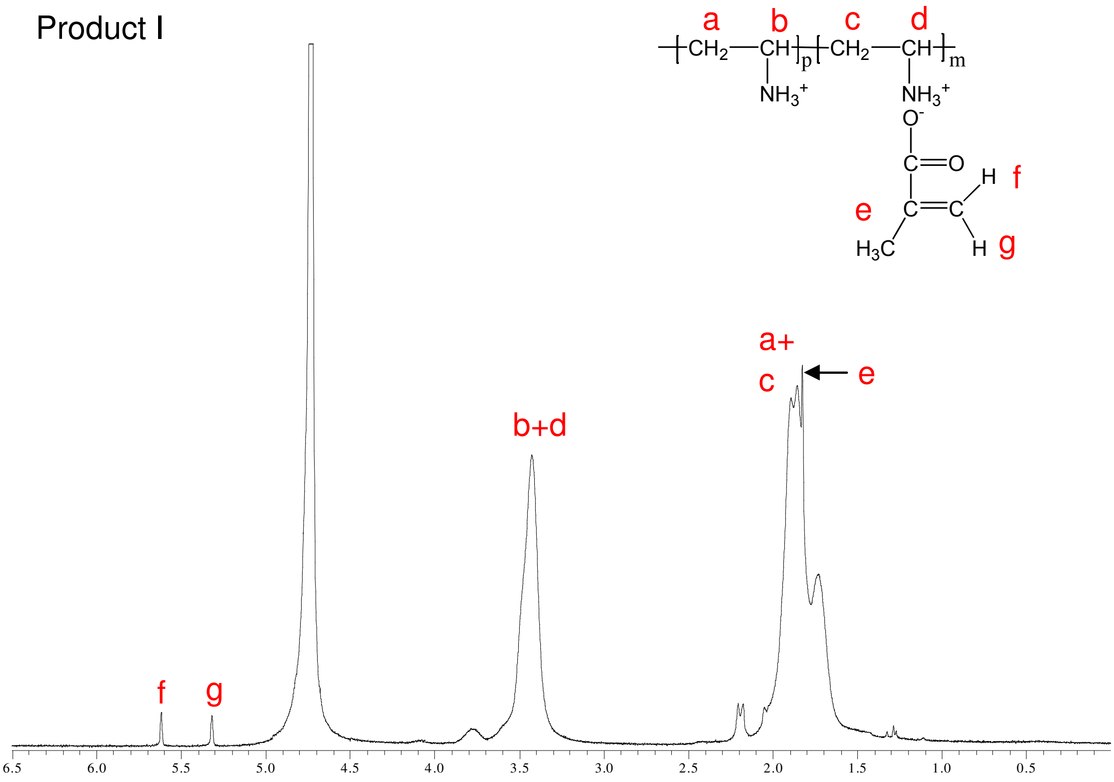

Figure 4.3 ^{1}H NMR spectra of Product I (product obtained from the reaction between PVAm and MAA)

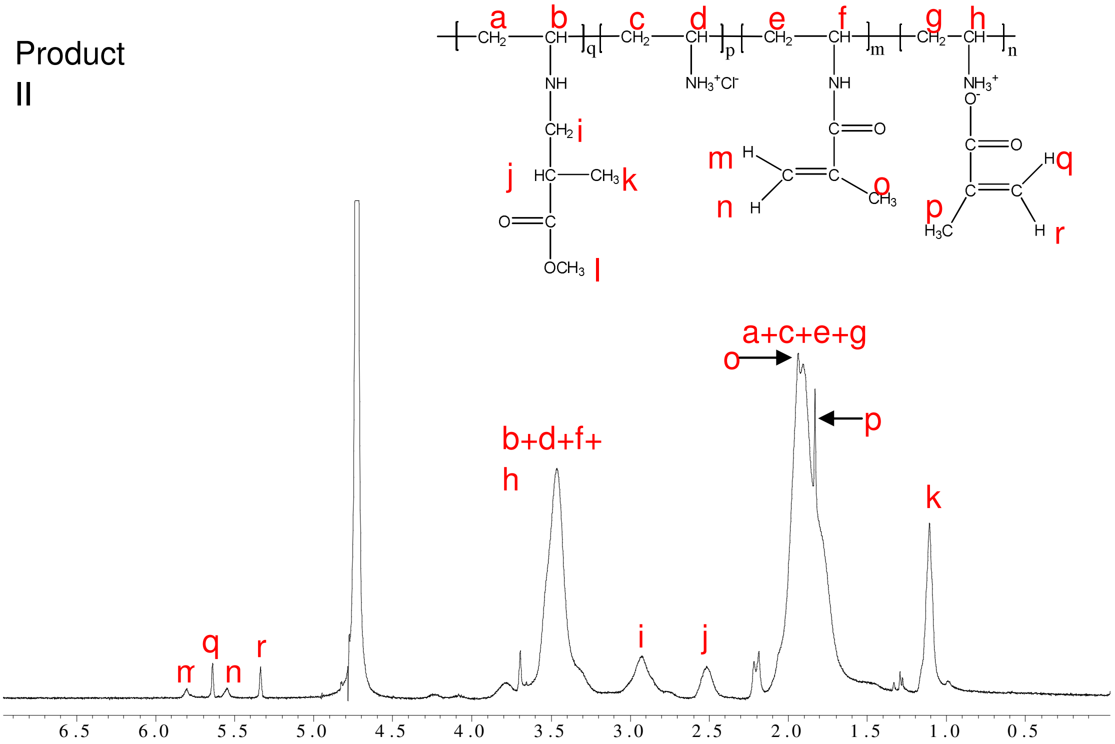

Figure 4.4 ^{1}H NMR spectra of Product II (product obtained from the reaction between PVAm and MMA at pH 12) in D_2O

In the ^{1}H NMR spectrum of product II (Figure 4.2c and Figure 4.4), two little peaks at 5.80 and 5.55 ppm are attributed from the two vinylic protons of methacrylamide. The methacrylamide might be the result of 1,2-additon of PVAm to the carbonyl of MMA or through the reaction between PVAm and MAA which was generated from the hydrolysis of MMA. Because the amino group of PVAm can not react with MAA to form an amide during the experiment, the methacrylamide is introduced through nucleophilic attack of PVAm to the carbonyl, followed by releasing a methanol (Scheme 4.3). The two new peaks at 5.63 and 5.32 ppm are attributed from the protons of MAA, similar to the peaks in the spectrum of product I. These results evidently prove that MMA is hydrolyzed to MAA during the experiment.

The peak attributed from the methyl groups appears at 1.83 ppm, which is overlapped with the peaks of the protons on $–CH_2$- groups on the main chain of the polymer.

In the ^1H NMR spectrum of product II, there are still some other new peaks at about 1.10, 2.51, 2.92 ppm, which are corresponding to the protons on $–CH_3$, -CH- and $–CH_2$- groups in the amine ester structure of product II, respectively. These groups might be formed through the Michael addition. However, the peak attributed to the methoxyl groups was still not found in the spectrum. It may be overlapped with the peaks of –CH- on the main chain of the polymer.

Therefore, there are three types of groups including amine ester, methacrylamide and methacrylic acid in the product according to the ^1H NMR studies when PVAm and MMA reacted at pH 12 in the absence of TBHP. The results reveal that all three reactions including hydrolysis of MMA, Michael addition to double bond and 1,2-addition to carbonyl occur under the polymerization conditions. The peaks attributed to protons on amine ester groups and MAA are much stronger than those of methacrylamide as shown in the NMR spectra. Thus the hydrolysis of MMA and Michael addition of PVAm to MMA are the major side reactions during the polymerization, while 1,2-addition is a minor one.

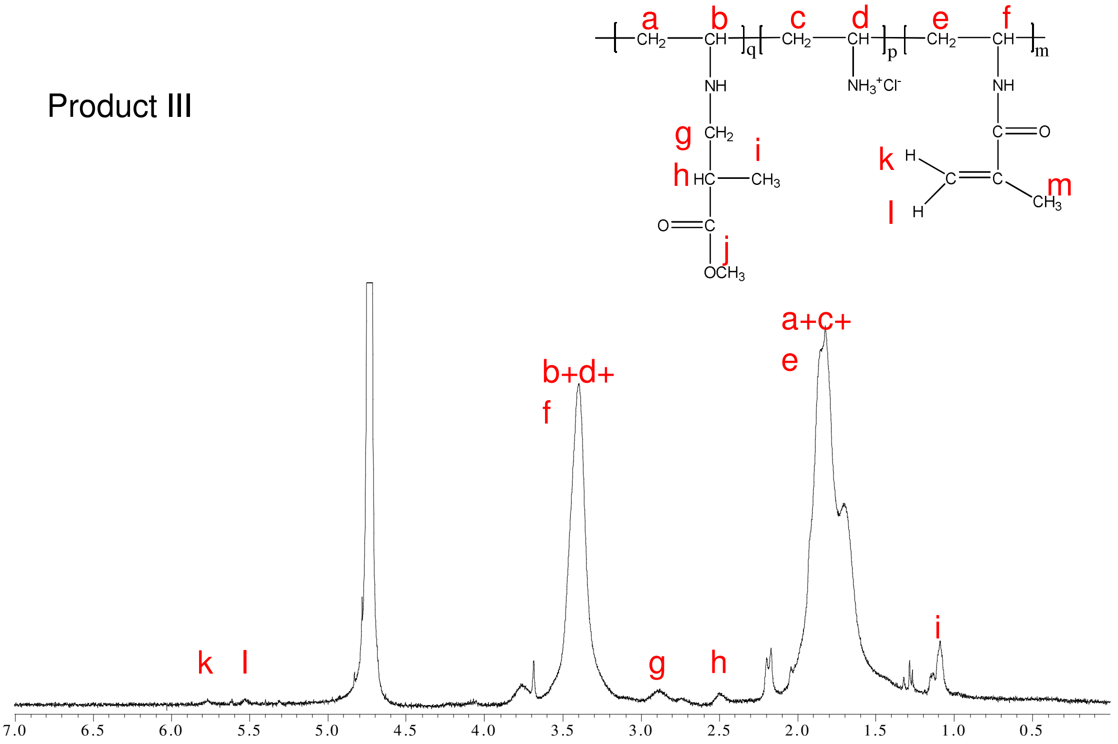

Figure 4.5 ^{1}H NMR spectra of Product III (product obtained from the reaction between PVAm and MMA) in D_2O

In the ^{1}H NMR spectrum of product III (Figure 4.2d and Figure 4.5), the peaks attributed to the products of Michael addition and 1,2-addition can be found. However, they are much weaker than that of product II, which indicates that less side reactions occur at pH 7 than at pH 12. The occurrence of less side reactions at pH 7 than at pH 12 can be attributed to less amino groups, the nucleophilic groups in the reactions, are available at pH 7 than at pH 12. In addition, no peaks attributed to MAA appeared in the spectrum, indicating that no hydrolysis occurs at pH 7.

Figure 4.6 shows the dependence of grafting percentage (GP%) and grafting efficiency (GE%) as a function of reaction pH. It can be seen that both the grafting percentage and grafting efficiency rise considerably as the reaction pH increases. The increase of grafting percentage is attributed to the increase of MMA conversion. Lower grafting efficiency indicates that more homopolymers were formed during the polymerization. The increase of grafting percentage with the increase of reaction pH suggests that the homo-polymerization preferably takes place at a lower pH such as pH 7 or 8, while graft copolymerization at a higher pH such as 11 to 12. These results are in accordance with the results of the effect of reaction pH on conversion and amount of precipitates generated. It also confirms our analysis of the effect of reaction pH on the polymerization.

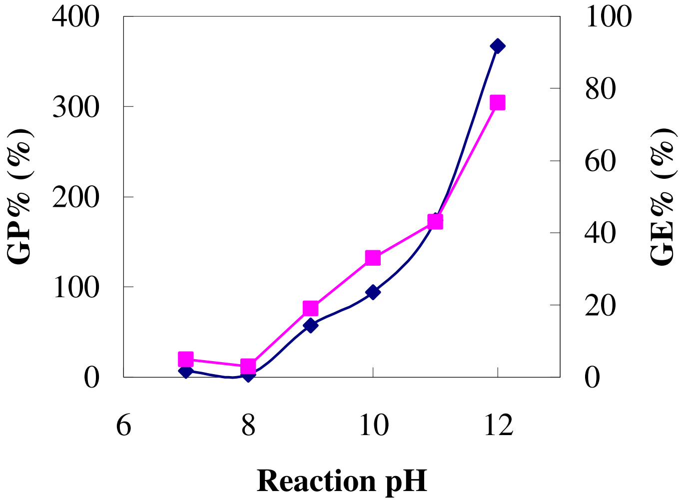

Figure 4.6 Effect of reaction pH on the grafting percentage (GP%) (◆) and grafting efficiency (GE%)(■) of the graft copolymerization of MMA from PVAm.

The effect of reaction pH on the surface charge of the particles was investigated by measuring the ξ-potential of the particles in 1 mM NaCl solution. Figure 4.7 shows that particles synthesized at different pH gave comparable ξ-potential values between 40 and 50 mV. Such high positive surface charges could provide sufficient particle stabilization in water. The ξ-potential results also indicate the presence of PVAm shells in which the amine groups contribute to such high positive surface charge values.

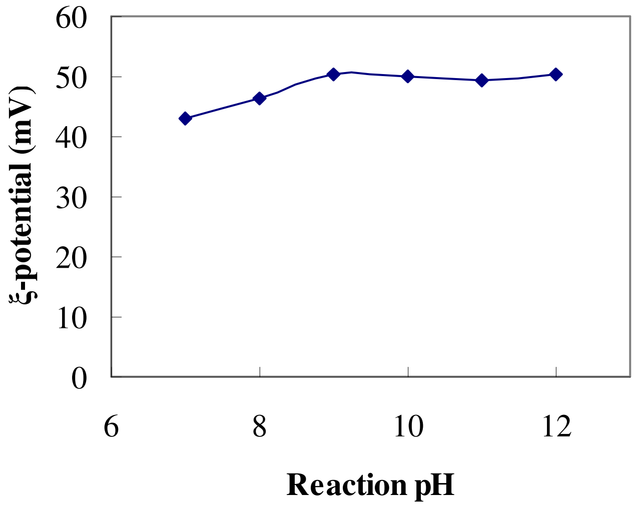

Figure 4.7 Effect of reaction pH on the surface charge of the particles generated.

Figure 4.8 illustrates that the effect of reaction pH on the particle size and size distribution of the latexes. The particle size increases with the increase of reaction pH, while the size distribution becomes narrower. At lower reaction pH such as 7, 8 and 9, a few large particles with diameters larger than 1.5 μm was generated with multi-model size distribution (Figure 4.8a, 4.8b and 4.8c). Such broad size distribution indicated the existence of different nucleation mechanisms during the polymerization. When the reaction pH increased to 11 or 12, the particle size was about 230 nm in diameter and the size distribution was near uniform (Figure 4.8e and 4.8f), indicating that all the particles generated under these reaction conditions were formed according to one type of nucleation mechanism. Higher monomer conversion gave to larger particle size, while the improvement of particle size distribution with the increase of reaction pH was due to the fast formation of micelle at high pH as discussed above.

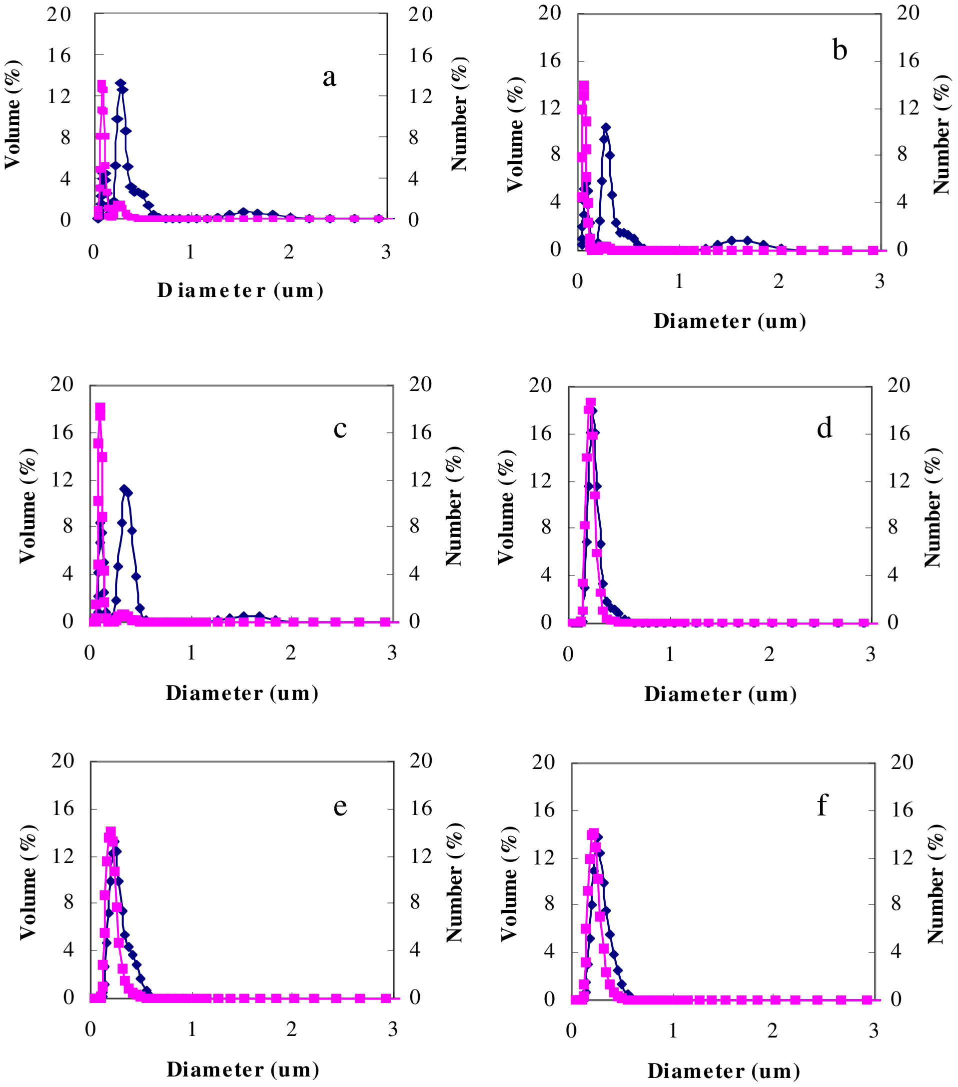

Figure 4.8 Effect of reaction pH on the particle size and size distribution. D_v (◆); D_n (■); PDI=D_v/D_n. Reaction pH a) 7, D_n=98 nm, PDI=2.81; b) 8, D_n=71 nm, PDI=3.55; c) 9, D_n=111 nm, PDI=2.51; d) 10, D_n=227 nm, PDI=1.15; e) 11, D_n=213 nm, PDI=1.29; f) 12, D_n=229 nm, PDI=1.25.

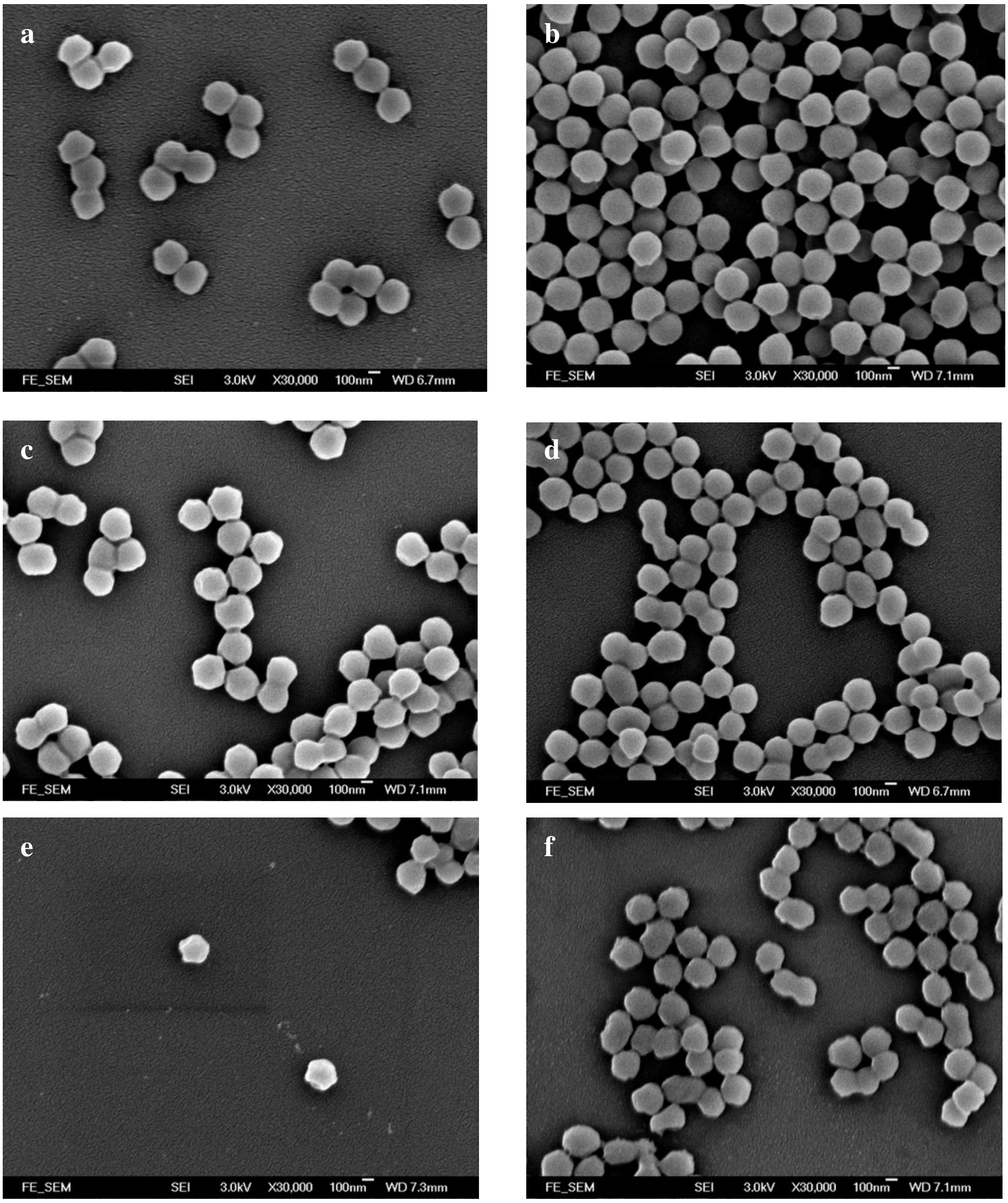

Figure 4.9 FE-SEM micrographs of PMMA/PVAm particles produced by copolymerization of MMA from PVAm at different reaction pH: a) 7; b) 8; c) 9; d) 10; e) 11; f) 12.

The effect of reaction pH on the surface morphology of the PMMA/PVAm particles was studied with Field Emission Scanning Electron Microscopy (FE-SEM). Figure 4.9 illustrates the FE-SEM micrographs of the PMMA/PVAm particles prepared under different reaction pH. It was noted that although particle sizes were quite uniform at various pH, the surface morphologies of the PMMA/PVAm particles were noticeablely different. The surface roughness became more and more obvious with those particles prepared at pH 11 (Figure 4.9e) and 12 (Figure 4.9f). The roughness of the particle shell suggests a phase separation due to the incompatibility of shell materials. The incompatibility may be due to two reasons: (1) The nucleophilic addition of primary amine to terminal double bond of the MMA; (2) The existence of PMMA in the shell. The hydrophobic segment of the methyl methacrylate covalently linked to the PVAm has poor compatibility with the hydrophilic PVAm chains. This interpretation can also explain the fact that the surface roughness increases at higher pH because the Michael addition is more favorable due to the increase of available amine groups. When the pH increases, the increased hydrophobic modification of PVAm via the Michael addition of MMA to PVAm and the salt formation between PVAm and MAA generated from hydrolysis of MMA, together with the increased grafting percentage increase the compatibility between PMMA and PVAm, resulting more PMMA in the shell. The increased amount of PMMA in the shell results in a rougher surface.

4.3.3 The effect of TBHP concentration

The graft copolymerization of MMA from PVAm was induced by a small amount of TBHP which is a water-soluble initiator. TBHP molecules form redox pairs with the amino groups, generating amino and *t*-BuO radicals concurrently. The amino radicals can initiate the graft copolymerization of MMA from PVAm to generate PVAm-graft-PMMA amphiphilic copolymers, while the *t*-BuO radical can initiate the homopolymerization of MMA.[2] Because the amount of TBHP used in the reaction is much less than that of the amino groups on the PVAm chains (molar ratio of TBHP molecules to amino groups: from 1:600~1:1200), the concentration of TBHP determines the number of graft sites when other conditions are kept constant.

To investigate the effect of TBHP concentration on the polymerization of MMA from PVAm, TBHP concentrations ranging from 0.05-2 mM were used in a series of experiments. All the polymerization were carried out at pH 12 at 80℃ for 3 hours with the PVAm to MMA weight ratio of 1:7.5 and the solid content of 2.5 wt.-%. The average molecular weight (M_v) of the PVAm used here was about 390K Delton.

Table 4.2 Effect of TBHP concentration on the graft copolymerization of MMA from PVAm[a]

Entry	[TBHP] (mM)	pH of the dispersion after polymerization	Conv. (%)	GP%	GE%
P180	0.05	7.94	54	377	94
P178	0.1	8.21	65	367	76
P181	0.2	8.45	56	321	78
P182	0.5	8.60	63	335	73
P183	1	8.52	76	357	64
P184	2	8.88	79	265	45

[a] All the reactions were carried out at 80 °C for 3 h; the reaction pH was 12; the weight ratio of PVAm to MMA was 1:7.5; the solid content was 2.5% based on weight; the total weight of reaction mixture was 50 g.

Results in Table 4.2 shows that pH of the reaction mixture dropped from 12 to about 8~9 after polymerization, which was due to the partial hydrolysis of monomer under alkaline condition and the conversion of primary amine groups to neutral covalent C-N bond through the Michael Addition of the amine group to MMA monomer. The monomer conversion fluctuated slightly as the TBHP concentration varied from 0.05 to 0.5 mM, indicating that TBHP concentration had little influence on the conversion in this range. Further increase of the TBHP concentration to 1 or 2 mM increased the monomer conversion to up to 79% (P184). At the same time, the drop in the pH of the reaction system before and after the reaction was less, indicating that higher TBHP concentration increased the rate of polymerization, and reduced the side reactions.

The effect of TBHP concentration on the grafting percentage (GP%) and grafting efficiency (GE%) is shown in Table 4.2. The grafting percentage ranged from 377% to 355% with TBHP concentration from 0.05 to 1 mM. Further increasing TBHP concentration to 2 mM reduced the grafting percentage to 266%. The grafting efficiency was reduced significantly from 94% to 45% with the increase of TBHP concentrations from 0.05 to 2 mM. These results indicate that more PMMA homopolymers are formed at higher TBHP concentrations. This effect may be due to the fact that a higher TBHP concentration would result in higher *t*-butoxy and hydroxyl radical concentrations through the thermal decomposition of TBHP, thus increasing the rate of homopolymerization of MMA.

Figure 4.10 shows the effect of TBHP concentration on the surface charge of the

PMMA/PVAm particles. The surface charge of the particles generated with different TBHP concentration were almost the same, indicating that TBHP concentration has little influence on the surface charge of the particles.

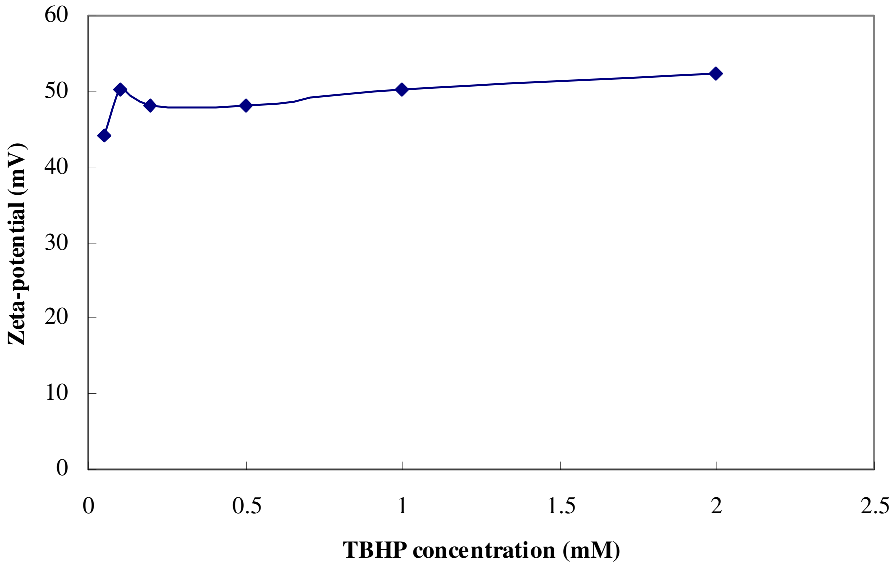

Figure 4.10 Effect of TBHP concentration on the surface charge of the PMMA/PVAm particles.

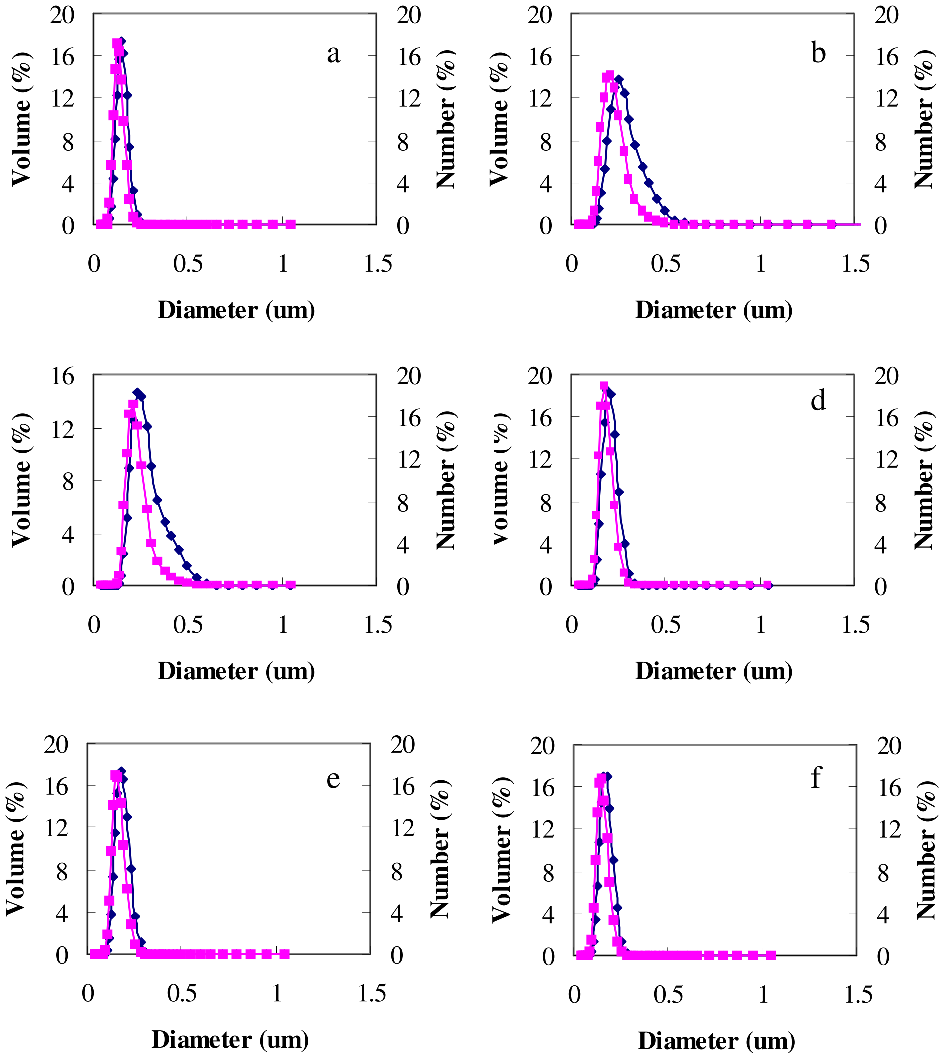

Figure 4.11 Effect of TBHP concentration on the particle size and size distribution of PMMA/PVAm particles. D_v (◆); D_n (■); PDI=D_v/D_n. TBHP concentration (mM): a) 0.05, D_n=137 nm, PDI=1.14; b) 0.1, D_n=229 nm, PDI=1.25; c) 0.2, D_n=237 nm, PDI=1.20; d) 0.5, D_n=192 nm, PDI=1.11; e) 1, D_n=168 nm, PDI=1.14; f) 2, D_n=155 nm, PDI=1.14.

Figure 4.11 shows that the particle size was quite small when the TBHP concentration was 0.05 mM (Table 4.2, P180), which might be due to the low monomer conversion (56%). As the TBHP concentration increased from 0.1 (P178) to 2 mM (P184), the particle size decreased from 230 to 155 nm and the size distribution of the particles became narrower (PDI reduced from 1.25 to 1.14). The decrease of particle size and increase of monomer conversion indicate an increase of particle number in the reaction system. The results clearly suggest that the increase of TBHP concentration increases radical concentration, subsequently promoting the probability of nucleation.

The effect of TBHP concentration on the particle morphology was also investigated. Figure 4.12 shows that all the particles synthesized using different TBHP concentrations have a similar surface morphology with a rough surface, indicating that TBHP has little effect on the surface morphology of the particles. In other words, the key factor affecting the surface morphology of the particle is not TBHP concentration. The FE-SEM images also show that diameter of the particles decreases with increasing TBHP concentration from 0.1 to 2 mM. These results are consistent with the particle size measurements. Thus the particle size can be tailored by changing the TBHP concentration in the reaction system.

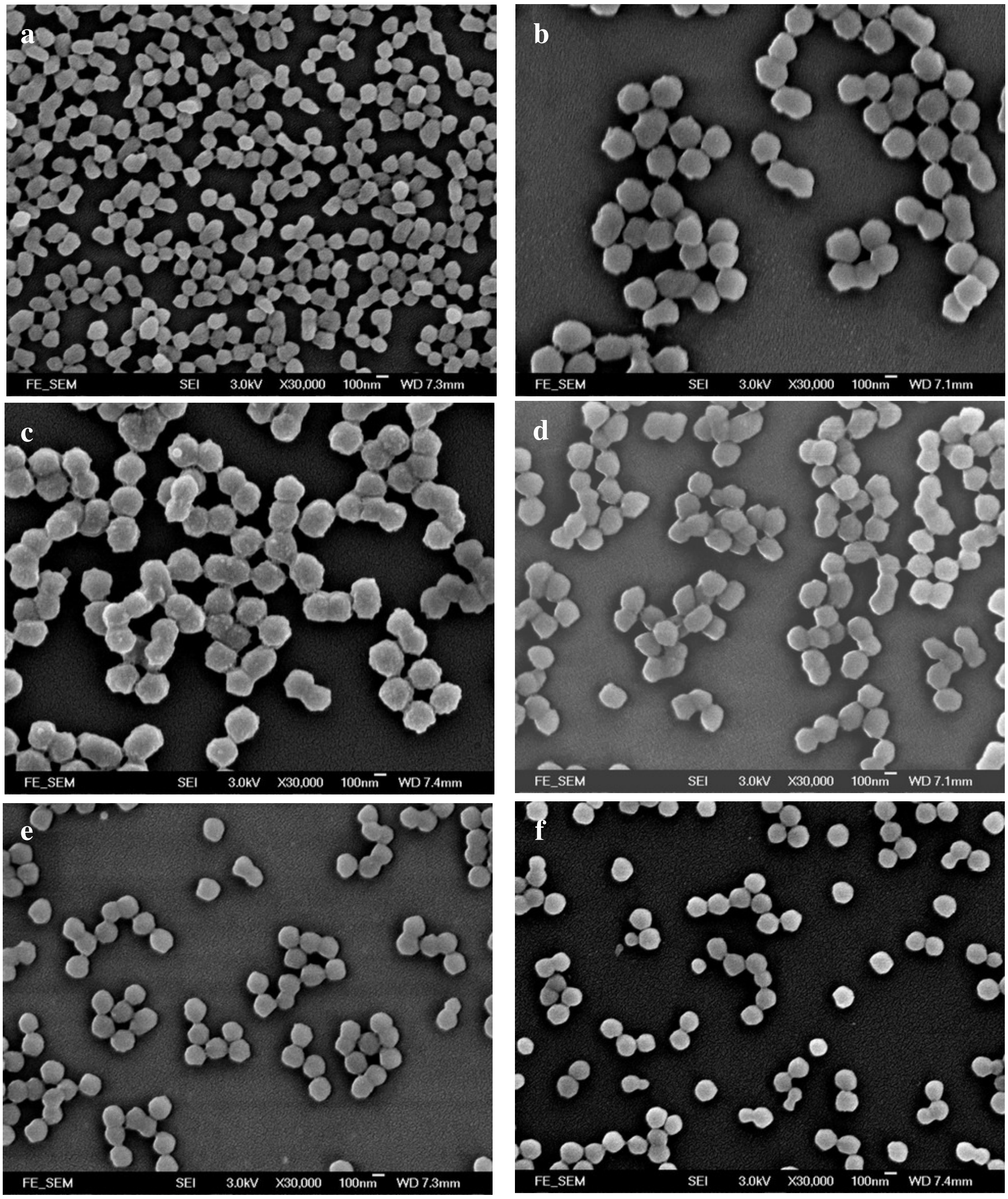

Figure 4.12 FE-SEM micrographs of PMMA/PVAm particles produced by copolymerization of MMA from PVAm with different TBHP concentrations (mM): a) 0.05; b) 0.1; c) 0.2; d) 0.5; e) 1; f) 2.

4.3.4 The effect of weight ratio of MMA to PVAm

The ability to tailor the core diameter and shell thickness is a highly desirable property for the synthesis of core-shell particles. Varying the MMA to PVAm charging ratio is one of the simplest way to control the core diameter and shell thickness of the PMMA/PVAm core-shell particles. Since the change in core-shell composition would affect the stability of the particles, the monomer conversion, particle size and size distribution and morphology of the particles might be affected.

Table 4.3 Effect of charging weight ratio of MMA to PVAm on the polymerization of MMA from PVAm[a]

Entry	Mw of PVAm (×10^5)	W_{PVAm} (g)	W_{MMA} (g)	MMA/ PVAm weight ratio	[TBHP] (mM)	pH	SC (%)	Conv. (%)	D_v (nm)	D_n (nm)	PDI
P27	3.6	0.25	1	4:1	0.1	12	2.5	73	219	198	1.11
P28	3.6	0.125	1	8:1	0.1	12	2.5	60	204	183	1.11
P122	3.4	0.8	3.2	4:1	0.2	11	5	81	279	243	1.15
P125	3.4	0.2	3.2	16:1	0.2	11	5	60	274	237	1.16

[a] All reactions were carried out at 80 ^{0}C for 3 h; The total weight of reaction mixture was 80g for P122 and P125, the others were 50 g.

[b] W_{PVAm} and W_{MMA} are weight of PVAm and MMA respectively; [TBHP] refers to the concentration of TBHP; SC (%) is the abbreviation of solid content based on weight; Conv. (%) is the abbreviation of conversion based on weight..

Table 4.3 shows two sets of results using different MMA to PVAm ratios, while keeping the amount of MMA constant. Comparing results from each set, both MMA conversions were increased significantly with the increase of PVAm concentration. For example, the conversion rose to 81% (P122) from 60% (P125) when the weight ratio of PVAm to MMA increased from 1:16 to 1:4. A similar effect was observed when the polymerization was carried out with a lower solid content (2.5%). This effect may be contributed to the fact that the increase of PVAm concentration provides not only more amine groups for the reaction, but also higher stability. In fact, insufficient amount of PVAm resulted in severe coagulation of the particles. For example, when using a lower concentration of PVAm (MMA to PVAm weight ratio = 16:1), a considerable amount of precipitates were formed after polymerization. On the other hand, varying the weight ratio of PVAm to MMA had little influence on the particle size. The differences between the number average particle diameters of sample P27 and P28, and P122 and P125 were only 17 nm and 6 nm, respectively.

Figure 4.13 illustrates SEM images of PMMA/PVAm particles prepared with two different weight ratio of MMA to PVAm (P122 and P125). These particles are very uniform with similar raspberry-like surface morphology. Therefore, the MMA to PVAm weight ratio has little or no influence on the surface morphology of the particles.

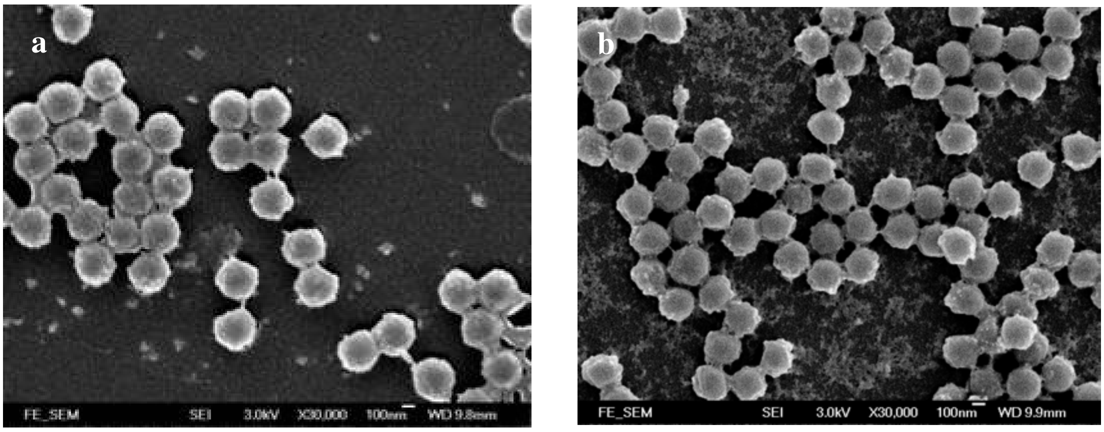

Figure 4.13 FE-SEM images of PMMA/PVAm particles prepared with two different weight ratios of MMA to PVAm. a) Weight ratio of PVAm to MMA = 1:4 (P122); b) Weight ratio of PVAm to MMA = 1:16 (P125).

4.3.5 The effect of salt concentration

It is well known that the existence of salt in the emulsion polymerization system could reduce the solubility of the surfactant, thus promoting the formation of micelles and increasing the polymerization rate. However, if there is too much salt in the emulsion polymerization system, the salt would neutralize the surface charge of the particles and reduce the thickness of the electric double layer of the particles, thus decreasing the stability of the particles and inducing the aggregation of the particles.

Since the pH of PVAmHCl solution is about 3, it has to be neutralized with NaOH solution to either neutral or alkaline pH before polymerization. Thus NaCl salt is formed during this process and remained in the PVAm solution. When a polymerization is carried out at reaction pH 12 with about 0.25 g of PVAm for a total solution of 50 g, the concentration of NaCl is about 0.12 M. It increases with the increase of the amount of PVAm used. Therefore, the effect of the salt concentration on the copolymerization of MMA from PVAm must be taken into account before increasing the amount of PVAm used in the graft copolymerization.

To investigate the effect of salt concentration, a series of polymerizations were carried out under different NaCl concentrations ranging from 0.12 to 1 M. The PVAm used for this study had a M_v of about 3.4×10^5 Delton.

Table 4.4 Effect of NaCl concentration on the polymerization of MMA from PVAm[a]

Entry	[NaCl] (M)	Observation	Conv. (%)	Dv (nm)	Dn (nm)	PDI
P42	0.12	Stable Latex	52	217	196	1.11
P43	0.5	Some precipitates	69	293	226	1.30
P44	1.0	Excessive precipitates	--	411	245	1.68

[a] All the reactions were carried out at 80 °C for 2 h; the weight ratio of PVAm to MMA was 1:4; the amount of MMA was 1g; the initiator concentration was 0.1 mM; The total weight of the reaction mixture was about 50 g; the reaction pH was 12.

Table 4.4 shows the effect of salt concentration on the graft polymerization of MMA from PVAm. A little precipitates appeared when the salt concentration of the reaction mixture was about 0.5 M (P43), while severe precipitates formed at the salt concentration of about 1.0 M (P45). These results indicated that particle stability decreased with the increase of salt concentration. On the other hand, the monomer conversion was increased from 52% to 69% with the increase of salt concentration from 0.12 to 0.5 M. This effect might be caused by the higher salt concentration which promoted the formation of micelles. However, the particle size became larger and size distributions were broader at a higher salt concentration. Results illustrated in Figure 4.14 and listed in Table 4.4 show that the particle size was small and size distribution was very narrow in low salt concentration (P42). However, the size distribution became broader as the salt concentration was increased to 0.5 M. When the salt concentration was about 1 M, stable particles could not be obtained, and the size distribution was a multi-modal distribution with PDI as large as 1.68 (P44). These results indicate that a higher salt concentration has a negative effect on particle stability, thus, extra salt formed during conversion of PVAmHCl to PVAm must be removed, especially when a large amount of PVAm is used. Alternatively, pure PVAm should be prepared separately prior to usage.

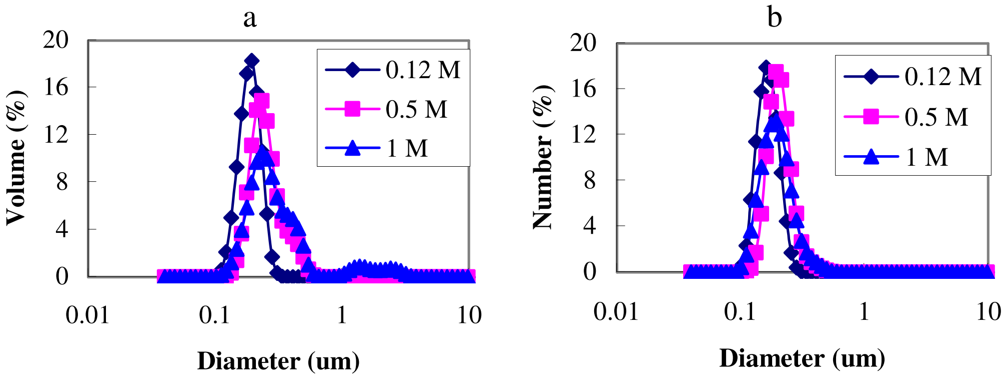

Figure 4.14 Effect of NaCl concentration on particle size and size distribution of PMMA/PVAm particles. a) Particle size distribution based on volume percentage; b) Particle size distribution based on number percentage.

The effect of salt concentration on the surface morphology of PMMA/PVAm particles was investigated with FE-SEM. Figure 4.15 shows that very uniform particles could be generated in the presence of various salt concentrations. In addition, all these particles have similar raspberry-like surface morphology. These results suggest that the salt concentration has little effect on particle formation and their morphology. It mainly affects the particle stability.

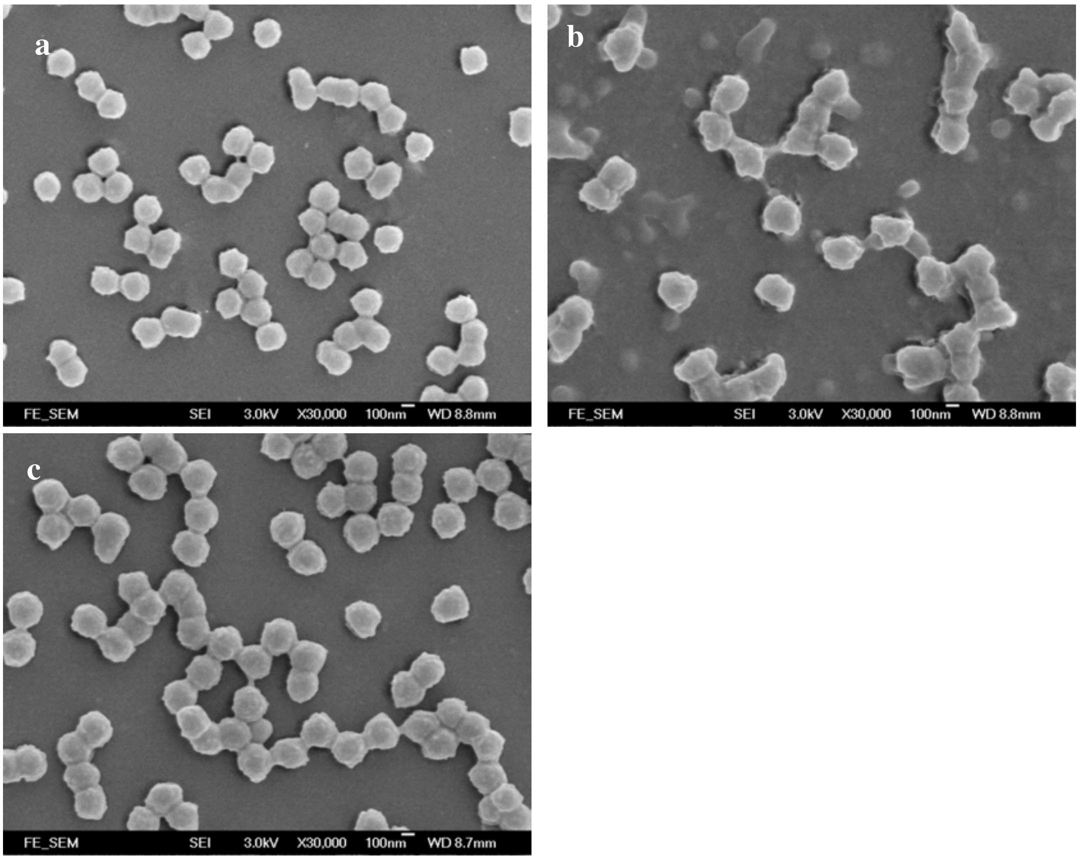

Figure 4.15 FE-SEM pictures of the PMMA/PVAm particles prepared under different NaCl concentrations. a) 0.12 M (P42); b) 0.5 M (P43); c) 1 M (P44).

4.3.6 The effect of the molecular weight of PVAm

In order to obtain stable latexes, an important criterion must be satisfied: the particles must be stabilized in water via electrostatic or steric interaction or a combination of both. For the PMMA/PVAm particles, almost all the amino groups are in the form of primary amine at pH 12, thus there is little electrostatic repulsion between the particles. Therefore, the particles stability in water is mainly relied on the steric repulsion of PVAm chains which is strongly dependant on the molecular weight and architecture of the PVAm. The molecular weight of PVAm might influence the particles in two aspects: 1) The increase in molecular weight of PVAm can enhance the steric effect, thus improving the stability of the particles; 2) The molecular weight may change the shell thickness of the particles, thus varying the surface morphology of the particles.

To investigate the effect of molecular weight on the graft copolymerization of MMA from PVAm, a series of PVAm with different molecular weights ranging from 3.5×10^4 to 4.0×10^5 have been synthesized by varying the molar ratio of the monomer to initiator or changing the reaction medium, as described in Chapter 3.

Table 4.5 summarizes the results of the copolymerization of MMA from PVAms with different molecular weights. When a higher molecular weight sample of PVAm ($M_v = 400$ K) was used in the polymerization, the latex formed (P8) was stable with a high monomer conversion and narrow particle size distribution (PDI=1.09). When the PVAms with molecular weights less than 270 K were used, some precipitates were generated during the polymerization and the particle size distributions became broader ranging from 1.41 to 2.93. The worst results were obtained when PVAm with Mw of 35,000 was used (P14). No latex could be obtained and all the polymerized monomer was precipitated. These results indicated that PVAm with lower molecular weight could not provide enough stability for the particles at pH 12.

The results shown in Table 4.5 also indicate that the molecular weight of PVAm has little effect on the monomer conversion, grafting percentage and efficiency as well as the surface charge.

Table 4.5 Effect of Mw of PVAm on the copolymerization of MMA from PVAm[a]

Entry	M_v of PVAm ($\times 10^5$)	Observation	Conv. (%)	GP %	GE %	ζ-potential (mV)	Dv (nm)	Dn (nm)	PDI
P8	4.0	Stable	76	377	68	42	296	271	1.09
P9	2.7	Some precipitates	70	367	72	43	387	173	2.23
P10	2.5	Some precipitates	69	290	57	41	341	117	2.93
P12	1.9	Some precipitates	69	299	59	45	261	186	1.41
P14	0.35	All precipitated	--	--	--	--	--	--	--

[a] All the reactions were carried out at 80 ℃ for 3 h; the initiator concentrations were 0.1 mM; the weight ratio of PVAmHCl to MMA was 1:4; the solid content was 2.5% based on weight; the reaction pH was 12.

[b] "--" means that the data didn't measured.

Since the PVAms with lower molecular weights could not provide enough stability for the particles generated at pH 12, it was assumed that increase of electrostatic repulsion through converting some amine groups to the corresponding ammonium cations may enhance the particle stability. Therefore, the effect of pH on the graft polymerization of MMA from PVAm using a PVAm with M_v of 35,000 was examined at pH 8, 10 and 12, respectively.

Table 4.6 Effect of reaction pH on the graft copolymerization of MMA from PVAm with M_v of 35,000[a]

Entry	Reaction pH	Initiating time[b] (min)	Observation
P14	12	15	All the products precipitated
P15	10	35	All the products precipitated
P16	8	>60	All the products precipitated

[a] All the reactions were all carried out at 80℃ for 3 h; the initiator concentrations were 0.1 mM in all cases; the weight ratio of PVAm to MMA was 1:7.5; the solid content was 2.5% based on weight.

[b] The initiating time refers to the interval between the time that the polymerization starts and the time when the phase separation can be observed.

It was found that the initiating time (which refers to the interval between the time that the polymerization begins and the time that the phase separation appears) increased from 15 minutes to more than 60 minutes when the reaction pH dropped from 12 to 8. The longer induction time suggests that the initial micellization of the amphiphilic graft copolymers become more and more difficult as the pH decreases. All products were precipitated out in each case, indicating that the particles generated could not be stabilized by a low molecular weight PVAm even with the help of electrostatic interaction. The precipitates in sample P14 was collected and extracted with chloroform. The analysis results showed that up to 86% of the precipitates were PMMA homopolymers, indicating that there was little graft copolymerization took place.

Figure 4.16 shows the morphologies of the PMMA/PVAm particles obtained using PVAms with different molecular weights. These particles have similar morphologies, which means that the molecular weight of PVAm is not a key factor affecting the morphology of the particles.

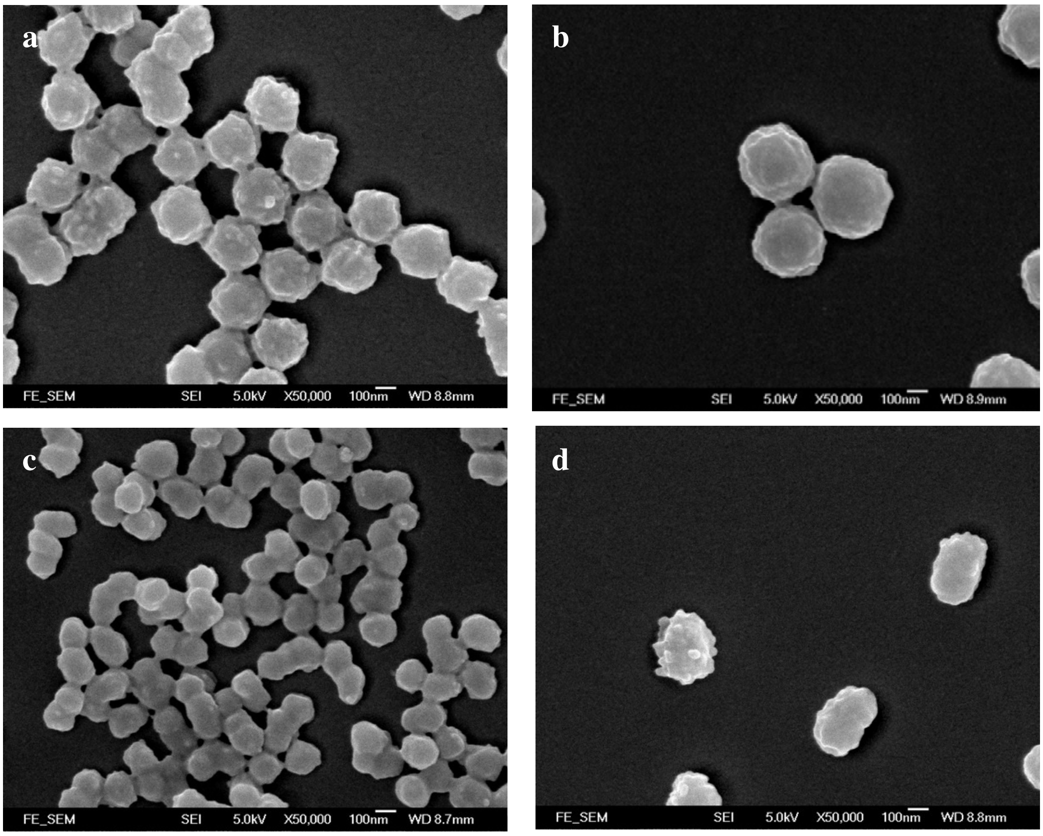

Figure 4.16 FE-SEM pictures of PMMA/PVAm core-shell particles prepared by copolymerization of MMA from different molecular weight of PVAms: a) 400K (P8); b) 250K (P10); c) 210K (P11); d) 190K (P12).

4.3.7 Effect of amination degree

As described in Chapter 2, PVAm has been used as a starting material to synthesize a variety of important functional materials due to its nucleophilic nature. Since only a few amino groups are needed to react with TBHP to initiate the polymerization, it is anticipated that bi- or multi-functional polymers containing amino and other functional groups may be used in our system to synthesize core-shell particles.

An example of the bi-functional polymers is the copolymers containing amino and amide groups. A simple way to obtain the bi-functional polymers containing amino and amide groups is through the partial hydrolysis of poly(*N*-vinylacetamide) (PNVA) to produce copolymers of *N*-vinylacetamide and *N*-vinylammonium chloride [poly(NVA-VAmHCl)] with different amination degree. However, variation of the amination degree of the copolymers changes charge density on the polymer chain and solubility of the polymer in water. Thus the amination degree of the copolymer may influence the particle formation, monomer conversion, particle size and size distribution as well as particle morphology.

The hydrolysis of PNVA to poly(NVA-co-VAmHCl)s with different amination degrees was achieved at 80 °C through carrying out the hydrolysis for 20, 28, 40, 66 hours respectively. After purification, the amination degrees of the copolymers produced were calculated from the intensity ratio between the methlyne protons next to amino groups and the methlyne protons next to amide groups of poly(NVA-co-VAmHCl)s in their ^{1}H NMR spectra according to literature.[14] The amination degrees of poly(NVA-co-VAmHCl)s were 31%, 55%, 70% and 89% respectively.

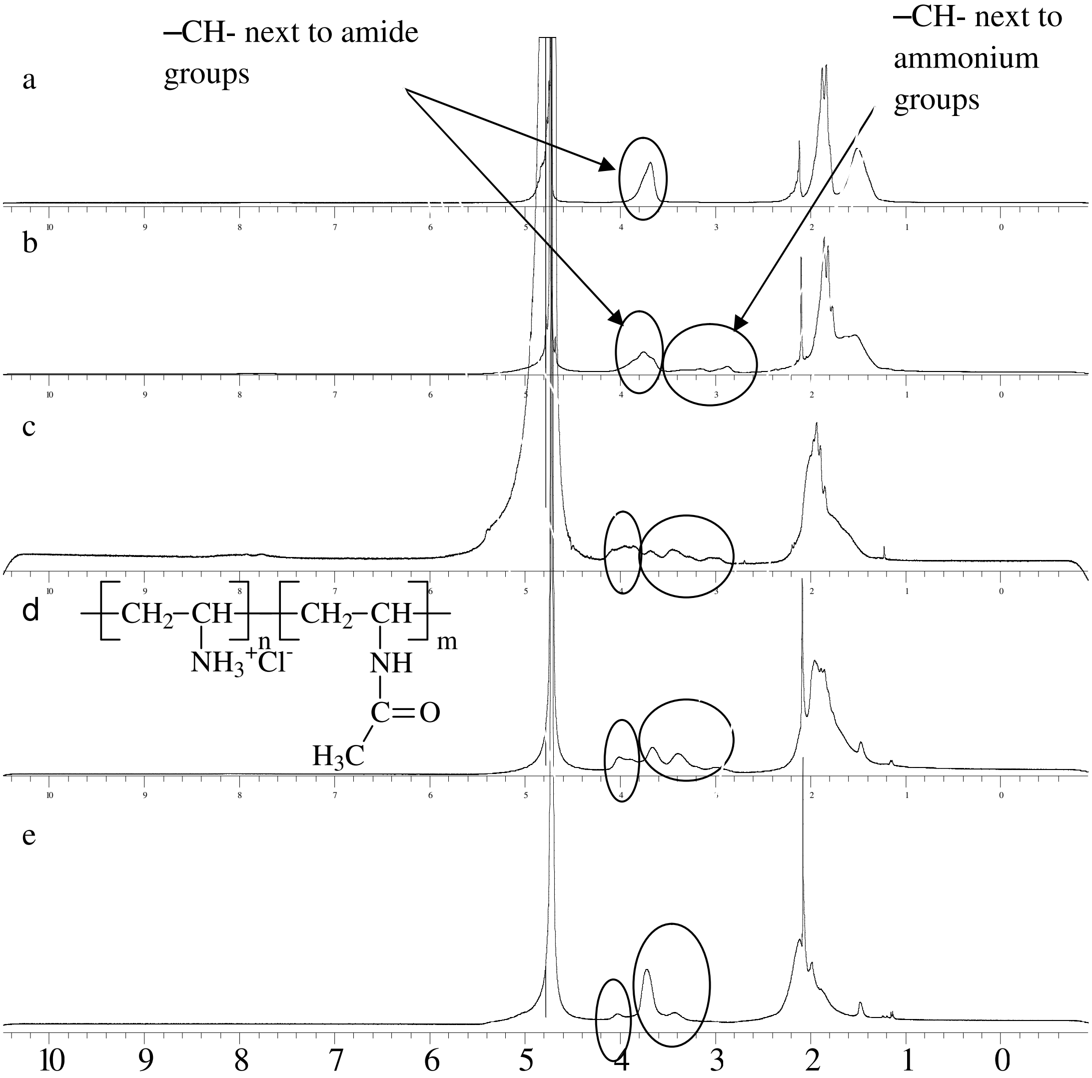

Figure 4.17 ^{1}H-NMR spectra of PNVA and poly(NVA-co-VAmHCl)s with different amination degrees. a) PNVA; b) 31%; c) 55%; d) 70%; e) 89%.

Figure 4.17 shows the ^{1}H-NMR spectra of PNVA and poly(NVA-co-VAmHCl)s with different amination degrees. The peaks of the methlye proton shift a little when the amide groups are converted to the ammonium groups. And their shapes varied with the amination degree of poly(NVA-co-VAmHCl). When PNVA was partially hydrolyzed to poly(NVA-co-VAmHCl), the peaks corresponding to the protons of methlyne next to amide groups are between 3.6-4.1 ppm (31% amination),,3.8-4.2

ppm (55% amination),,3.8-4.1 ppm (70% amination), and 3.9-4.1 ppm (80% amination). The peaks corresponding to the methlyne protons next to ammonium groups are between 2.7-3.6 ppm (31% amination), 2.8-3.8 ppm (55% amination), 2.8-3.8 ppm (70% amination), and 3.2-3.8 ppm (89% amination).

Once the poly(NVA-co-VAmHCl)s with different amination degrees were prepared, they were applied to the graft copolymerization of MMA. To gain in-depth understanding on the effect of amination on the graft copolymerization, each polymer was used to perform a series of graft copolymerizations under different reaction pH (7, 8.5, 10 and 11).

The experimental results are summarized in Table 4.7. No particles were obtained when poly(NVA-co-VAm) with 31% amination was used. Higher amination degree of the copolymers up to 55% resulted in the formation of core-shell particles with an acceptable monomer conversion. These results suggest that it is feasible to use copolymers containing other functional groups for the graft copolymerization as long as the amination degree of the copolymer is higher than a critical degree.

Table 4.7 Effect of amination degree on the graft copolymerization of MMA from poly(NVA-co-VAm) [a]

Entry	Amination (%)	pH	Conv. (%)	Dv (nm)	Dn (nm)	PDI	ζ-potential (mV)
P136	31	7	Negligible	--	--	--	--
P137	31	8.5	Negligible	--	--	--	--
P138	31	10	6	--	--	--	--
P139	31	11	10	--	--	--	--
P155	55	7	18	292	247	1.18	57.7
P156	55	8.5	50	289	91	3.18	57.2
P159	55	10	49	259	69	3.75	56.8
P158	55	11	44	232	214	1.08	55.7
P128	70	7	51	225	208	1.08	47.7
P144	70	8.5	59	300	284	1.06	42.9
P145	70	10	86	300	220	1.36	43.3
P146	70	11	61	301	286	1.05	42.8
P135	89	7	66	246	232	1.06	46.2
P140	89	8.5	69	313	297	1.05	43.2
P141	89	10	71	303	287	1.06	43.1
P143	89	11	65	300	285	1.06	43.8

[a] All the reactions were carried out at 80℃ for 3 h; The weight ratio of poly(NVA-co-VAmHCl) to monomer was 1:2; the amount of monomer was 2g; the TBHP concentration was 0.2 mM; The total weight was about 50 g.

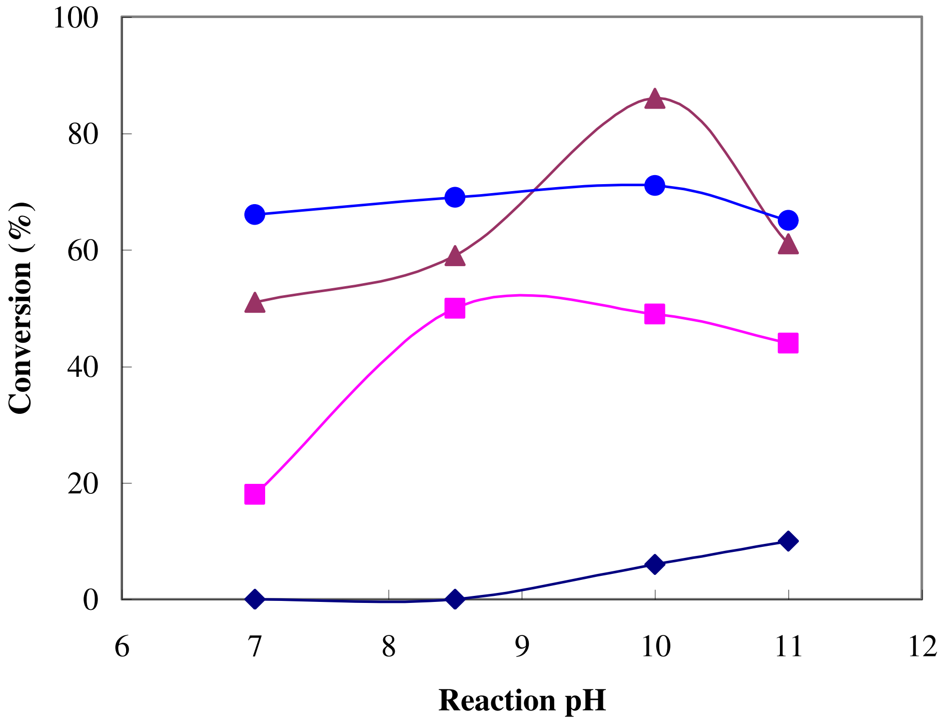

Figure 4.18 Effect of amination degree of poly(NVA-co-VAm) on the graft copolymerization of MMA from poly(NVA-VAm)s. Amination degree of the copolymers: (◆) 31%; (■) 55%; (▲) 70%; (●) 89%

Figure 4.18 demonstrates the effect of amination degree of the poly(NVA-co-VAm) on the graft copolymerization of MMA from poly(NVA-VAm). Generally speaking, the monomer conversion increased significantly from about 0-10% to above 60% when the amination of poly(NVA-co-VAm) increased from 31% to 70%. A further increase of the amination to up to 89% only gave a slightly higher conversion. The higher monomer conversion at a higher amination degree may be attributed to the higher number of available reactive amino groups for the graft copolymerization. In addition, the solubility and charge of the poly(NVA-co-VAm) copolymers increased with the increase of amination degree of the copolymer, resulting in better stabilization of the particles..

Comparing the experimental results at different pH using the copolymer having the same amination degree, the monomer conversion increased when the reaction pH increased from 7 to 10, which is consistent with the results of the effect of reaction pH on the graft copolymerization of MMA from PVAm. However, further increasing the reaction pH to 11 resulted in a slight decreased in conversion. In our previous study with 100% amination degree of the copolymer, pH 12 was found to give the highest conversion. Such difference may be due to the existence of amide groups in poly(NVA-co-VAm) chains which might decrease the pK_b of the copolymer.

Figure 4.19 shows the effect of the amination degree of the poly(NVA-co-VAm)s on the surface charge of the particles. It can be seen that the surface charges of the particles with amination of 70% and 89% are comparable under the same pH. The results indicate that the amination degree of the copolymer has little effect on the surface charge of the particles. Comparing the particles obtained at different pH using the same copolymer, the highest surface charge appeared at pH 7, which is due to the higher degree of protonation of amine groups.

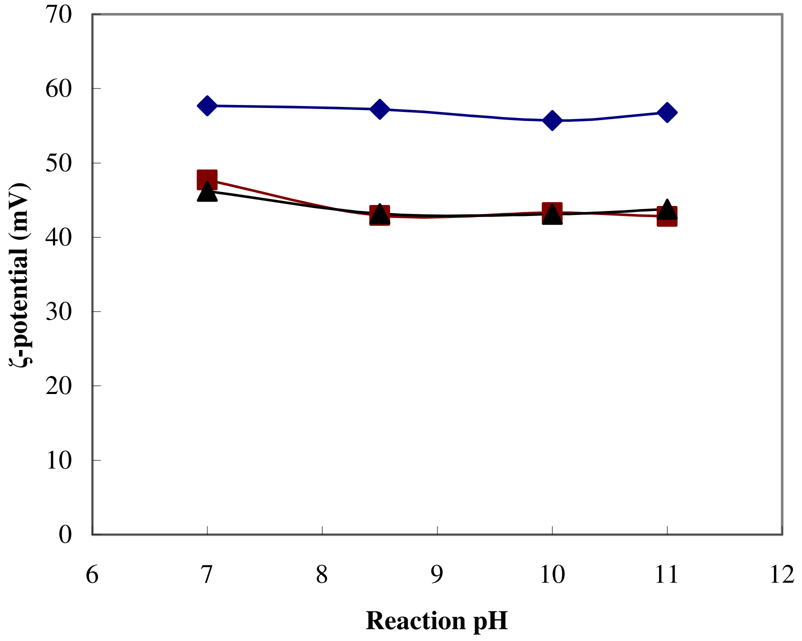

Figure 4.19 Effect of the amination degree of poly(NVA-co-VAm) on the surface charge of the particles. Amination degree: (◆) 55%; (■) 70%; (▲) 89%

Figure 4.20 shows the effect of the amination degree of the copolymers on particle size and size distribution. The volume average diameter of the particles obtained from the copolymer with 55% amination degree was larger than that of the particles produced from the copolymer with amination degrees of 70% and 89%. Furthermore, when the polymerizations were carried out at pH 8 and 10, very broad particle size distributions with PDI=3.18 and 3.75 respectively, were obtained. Particles prepared from copolymers with amination degree of 70% and 89% had very narrow particle size distributions (PDI≈1.1).

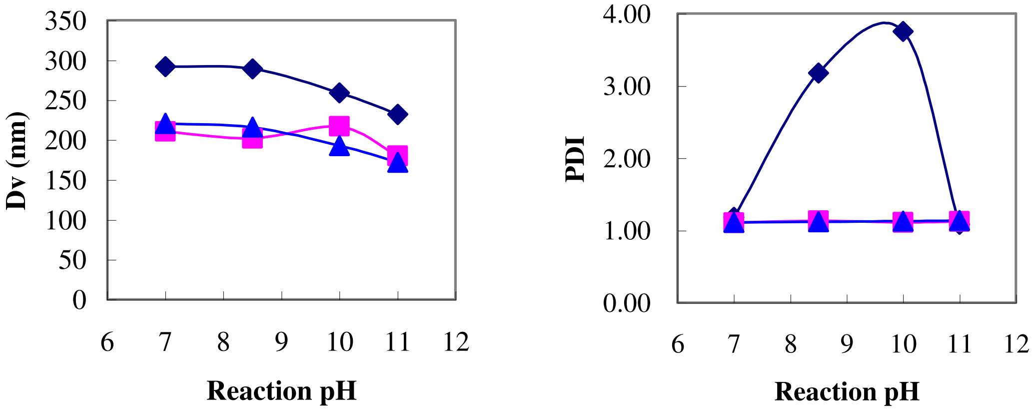

Figure 4.20 Effect of the amination degree of poly(NVA-co-VAm) on particle size and size distribution. Amination: (◆) 55%; (■) 70%; (▲) 89%

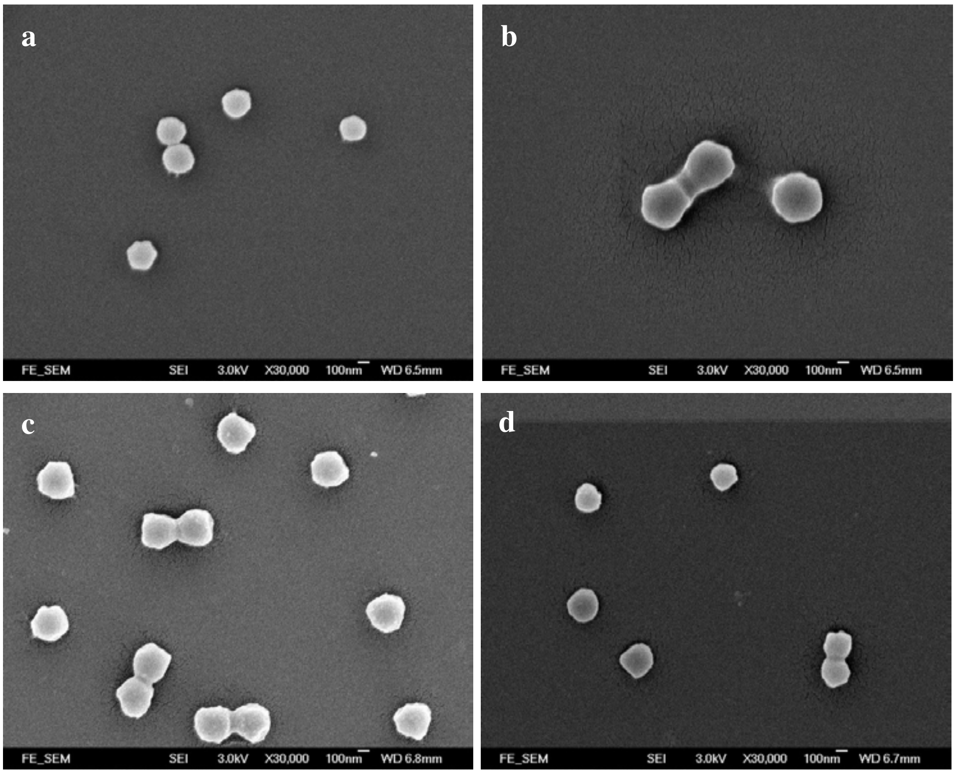

Figure 4.21 Effect of poly(NVA-co-VAm) containing 55% amination degree on particle morphology. Reaction pH: a) 7; b) 8.5; c) 10; d) 11;

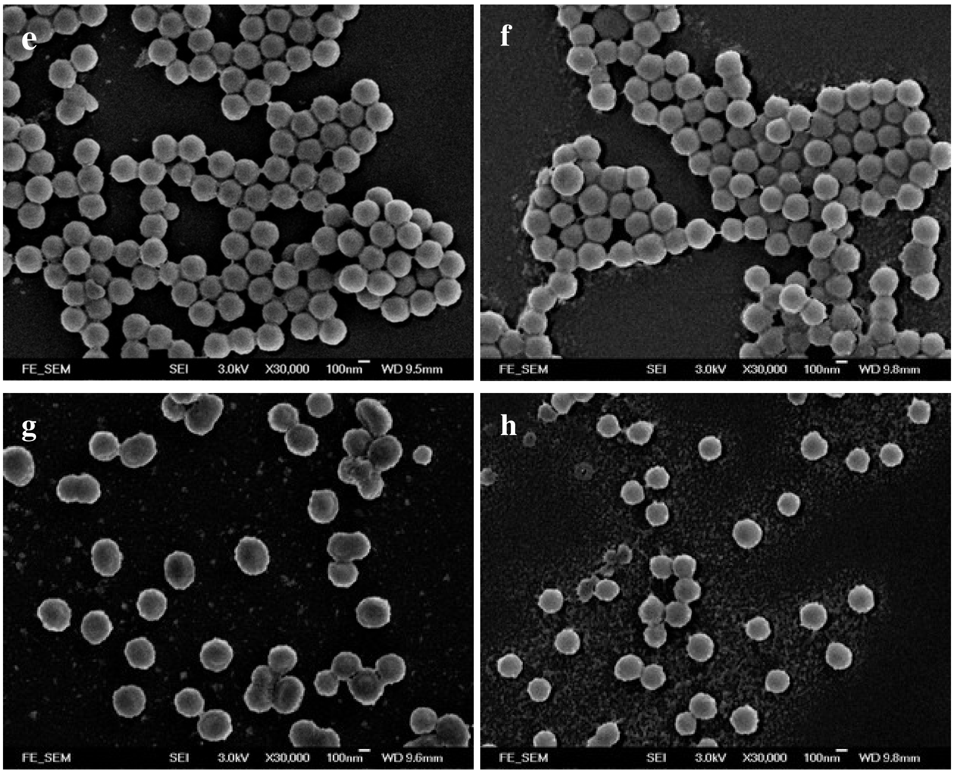

Figure 4.22 Effect of poly(NVA-co-VAm) containing 70% amination degree on particle surface morphology. Reaction pH: e) 7; f) 8.5; g) 10; h) 11.

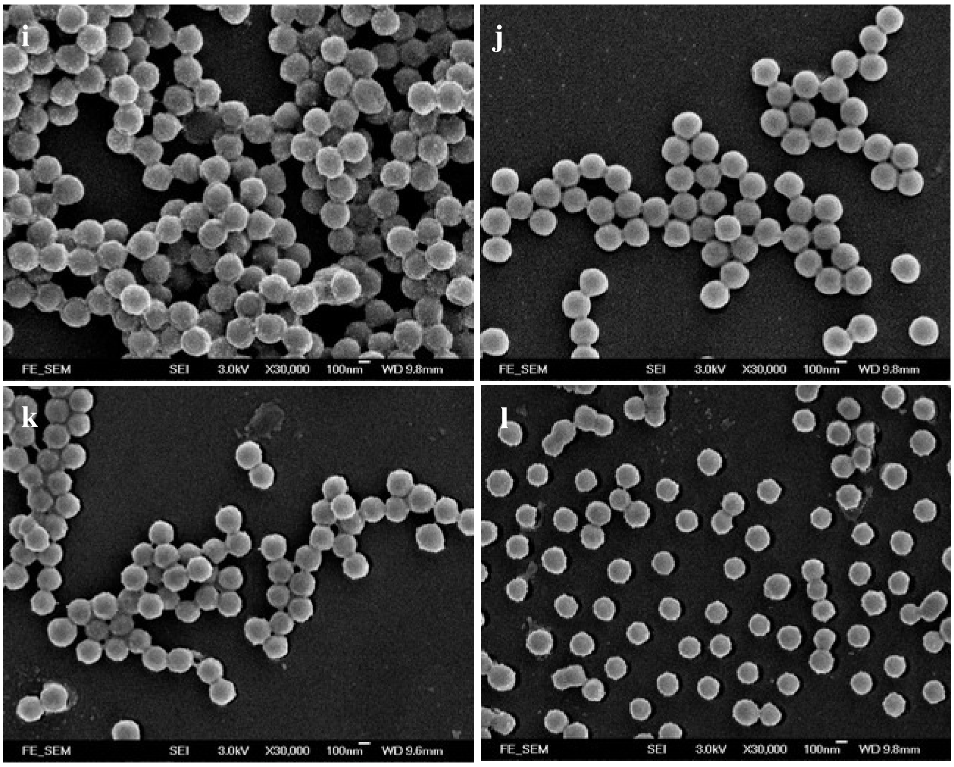

Figure 4.23 Effect of poly(NVA-co-VAm) containing 89% amination degree on particle surface morphology. Reaction pH: i) 7; j) 8.5; k) 10; l) 11

Figure 4.21, 4.22 and 4.23.show the effect of the amination degree on the particle morphology. The surface morphologies of the particles obtained under the same reaction pH using poly(NVA-co-PVAm)s with different amination degree are similar. The particles obtained at pH 7 are spherical, while particles obtained at pH 11 have a raspberry-shaped surface. The surface morphologies of the particles obtained at pH 8.5 and 10 are between these two shapes. These findings are similar to the results of the effect of reaction pH on the surface morphologies described previously.

4.3.8 The effect of crosslinking degree of PVAm

The PVAm used in the previous experiments were linear polymers. The advantages of using linear polymers are that they can be easily produced, purified and applied in the graft copolymerization. However, linear polymers provide poor steric stablization for the particles. Thus, only PVAms with very high Mw can produce stable particles, while lower Mw ones, for example 35,000, can not. In order to enhance the stability of particles through steric stabilization effect, the linear PVAm was pre-treated with a small amount of crosslinker to create branch and slightly crosslinked PVAm. The modified PVAm may also affect the properties of the particles such as size and size distribution, morphologies, etc.

4.3.8.1 Synthesis of crossslinked PVAm

Two approaches were attempted to produce crosslinked PVAm. One is through the synthesis of a crosslinked poly(*N*-vinylalkylamide), then hydrolyzing it to produce a crosslinked PVAm. The other way is through addition of a crosslinking reagent containing multi-functional groups that can react with amino groups on linear PVAm chains to crosslink the polymer.

4.3.8.1.1 Synthesis of crosslinked PVAm through a crosslinked poly(*N*-vinylalkylamide)

Scheme 4.8 shows the reaction steps to synthesis crosslinked PVAm. The crosslinked poly(*N*-vinylformamide) (PNVF) was first synthesized by copolymerization of *N*-vinylformamide (NVF) and *N,N*`-methylene bisacrylamide (MBA, a crosslinker) at 60 °C for 24 hours under nitrogen atmosphere using V-50 as a free-radical initiator. After purification of the products, the crosslinked PNVF was subjected to hydrolysis in a 2 M HCl solution at 80 °C for 4 days. The final product was purified by repeated precipitation in acetone and its structure was identified by ^{1}H NMR spectroscopy.

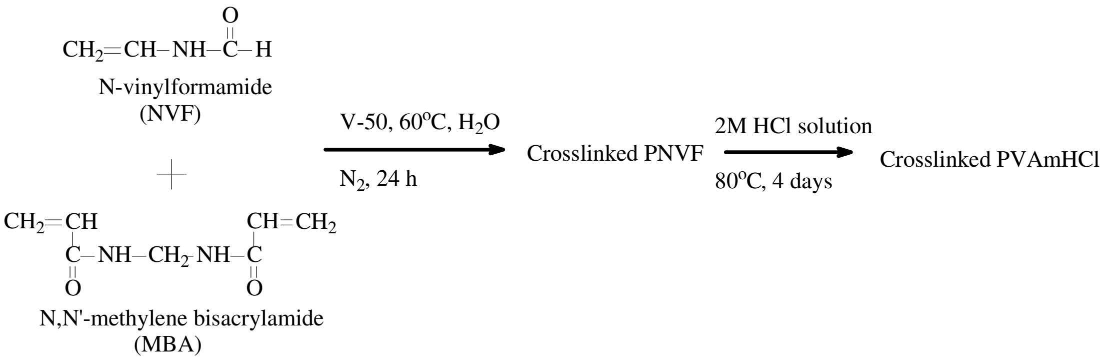

Scheme 4.8 Synthesis of crosslinked PVAm from crosslinked PNVF

Figure 4.24 shows the ^{1}H NMR spectra of crosslinked PNVF and the hydrolysis product. In the spectrum of crosslinked PNVF, the peaks at about 1.6, 3.8 and 8.0 ppm are donated to the protons on methylene (-CH_2-), methlyne (-CH-) and aldehyde (-CHO) groups on PNVF respectively, while the peaks at about 7.6-7.8 and 3.2-3.6 ppm are attributed to the protons on methlyne groups next to carbonyl groups and methylene groups between the two secondary amine groups respectively. In the spectrum of the hydrolysis product, however, the peaks indicating the existence of MBA units in the ^{1}H NMR spectrum of the crosslinked PNVF disappeared. The results suggest that the crosslinked structure was destroyed during hydrolysis. This effect is attributed to the fact that the MBA molecules also contain amide groups, which is similar to the amide structure of NVF. Thus the crosslinking is unstable under the hydrolysis conditions, resulting in breaking crosslinking bondings.

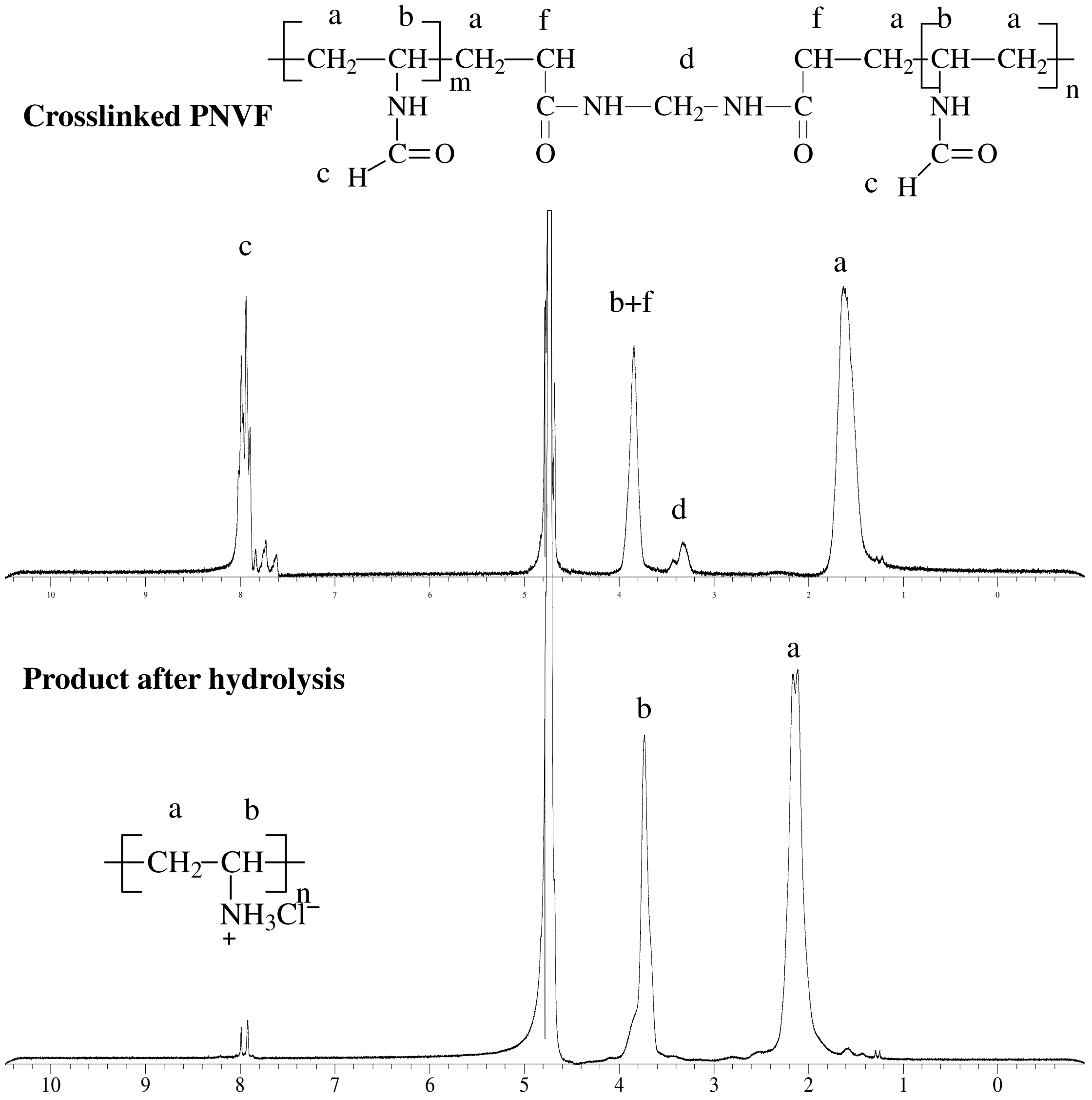

Figure 4.24 ^{1}H NMR spectra of crosslinked PNVF and product after hydrolysis

From the results above, MBA is not suitable for the synthesis of crosslinked PVAm. The crosslinking bonding of the PNVF must not be affected by the drastic hydrolysis conditions. Therefore, butadiene, pentadiene or monomers with similar structures may be used.

4.3.8.1.2 Synthesis of crossslinked PVAm through the reaction between PVAm and a crosslinker

Another way to synthesize slightly crosslinked PVAm is through the reaction between the PVAm and a crosslinker. The advantage of this method is that the crosslinking degree can be controlled easily by varying the amount of the crosslinker..But the disadvantage is that the crosslinking reaction consumes some amine groups, thus less amine groups are available for the graft copolymerization.

Glutaraldehyde (GA) is a commonly used crosslinker for crosslinking of enzymes in biology because it can easily react with amino groups at room temperature to form a crosslinked structure. In our study, GA was used as the crosslinker and the crosslinking mechanism is shown in Scheme 4.9. Aldehyde groups on GA molecules are reacted with amino groups on PVAm to form an imine structure after dehydration. The crosslinking reaction was carried out at a pH between 8 and 8.5 overnight according to a literature report.[15]

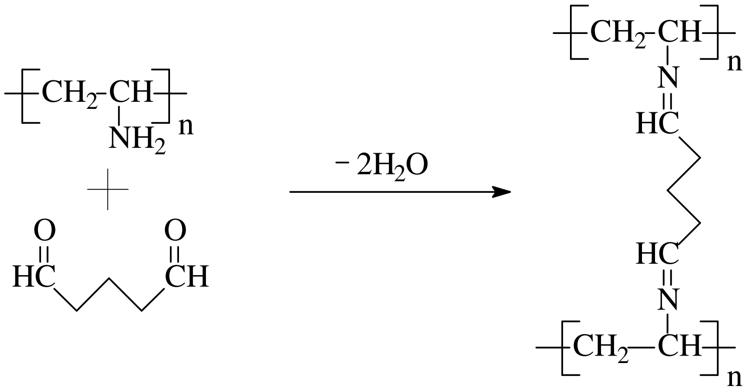

Scheme 4.9 Crosslinking of PVAm with glutaraldehyde

PVAm was crosslinked by 5 mol-% GA (expressed as percentage of a molar ratio of –CHO groups of the GA and $-NH_2$ groups of the PVAm) at pH 8 for from 30 minutes to 12 hours, and the reaction were monitored by UV spectroscopy as shown in Figure 4.25. The maximum absorption of the PVAm appears at about 231 nm and there is no peak at 250 nm. After GA was added into the PVAm solution, a new absorption peak is observed near 250 nm, which is attributed to the formation of C=N bond. The intensity of this C=N peak increased with the increase of the reaction time, indicating that the crosslinking reaction occurred effectively.

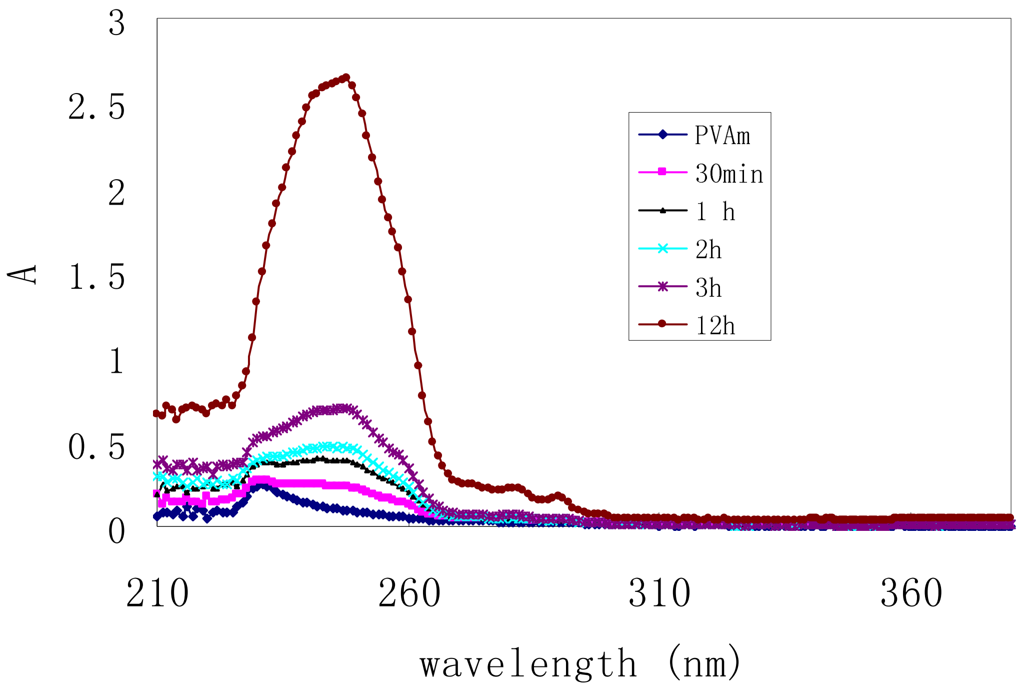

Figure 4.25 UV spectra of PVAm and PVAm crosslined with 5% mol-% GA at different times (The mol-% GA is expressed as percentage of a molar ratio of –CHO groups of the GA and $-NH_2$ groups of the PVAm)

4.3.8.2 Effect of crosslinking degree of the linear PVAm

The effect of crosslinking degree (CD%) on the graft copolymerization of MMA from PVAm has been investigated using pure PVAm instead of its salt form. Average Mw of the PVAm was about 270 K Delton. Scheme 4.10 shows the synthetic steps for producing PMMA/PVAm core-shell nanoparticles. PVAm was first crosslinked by mixing it with GA overnight in water at pH 8 at room temperature, followed by heating the solution at 80 °C for 2 hours. The crosslinked PVAm was then treated directly with a small amount of TBHP in the presence of MMA to generate the PMMA/PVAm core-shell particles.

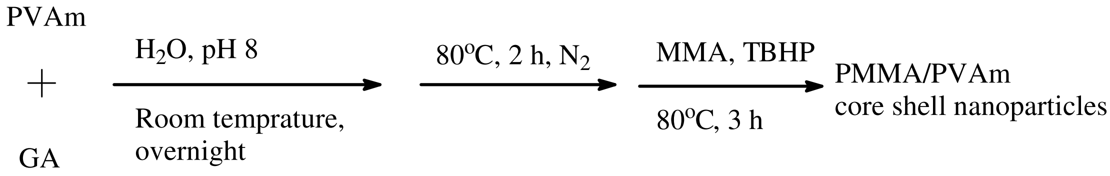

Scheme 4.10 Synthesis of PMMA/PVAm core-shell particles through crosslinking of the PVAm with GA.

Table 4.8 Effect of crosslinking degree of the PVAm on the graft copolymerization[a]

Entry	CD (mol-%)[b]	Conv. (%)	D_V (nm)	D_n (nm)	PDI	ζ-potential (mV)
P154	0	72	237	200	1.18	43.2
P151	5	66	288	234	1.23	45.8
P152	10	57	204	182	1.12	42
P153	20	61	123	115	1.07	29.3

[a] Other conditions: The polymerizations were carried out at 80 ^{0}C for 3 h. Weight ratio of PVAm to MMA=1:4; The monomer weight was 2 g; [TBHP]=0.2 mM; Solid content = 5%; The total weight was about 50g.

[b] The crosslinking degree (CD%) was expressed as percentage of a molar ratio of –CHO groups of the GA and $-NH_2$ groups of the linear PVAm.

A series of PMMA/PVAm particles were synthesized successfully by the graft copolymerization of MMA from PVAms which have been crosslinked with GA with different crosslinking degrees. The experimental results are summarized in Table 4.8. When PVAm was not crosslinked or slightly crosslinked (5 mol-%) with GA, some precipitates were observed at the end of the polymerization, indicating that linear or low-crosslinked (<5% mol-%) PVAm used here could not provide enough stabilization to the particles produced during the copolymerization at pH 8. The increase of crosslinking degree to 10 or 20 mol-% significantly improved the stability of the particles. No precipitate was observed after the polymerization. The improvement in particle stability can be reasonably attributed to the increased steric stabilization effect through crosslinking of PVAm.

Table 4.8 shows that an increase of the crosslinking degree up to 10% decreased the MMA conversion from 72% to 57%. Further increase of the crosslinking degree to 20% had only slightly influence on the MMA conversion. The decrease of MMA conversion with higher crosslinking degree might be attributed to stable free radicals generated from the reaction between –CHO and $–NH_2$ at a high temperature. It has been reported that free radicals can be generated when heating the products of the amino-carbonyl reactions between sugars or related carbonyl compounds and amino acids or amines[16, 17] (Eq. 4.1), or the Maillard reaction between glycolaldehyde or glyceraldehydes and *N, N*-dialkylethylenediamine (alkyl = methyl, ethyl, *iso*-propyl, *tert*-butyl)[18] (Eq.4.2). These radicals may terminate some free radicals during the polymerization, thus decreasing the concentration of the free radicals in the reaction system during the polymerization.

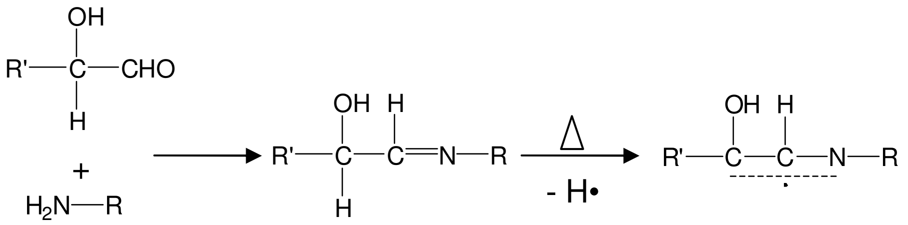

(Eq.4.1)

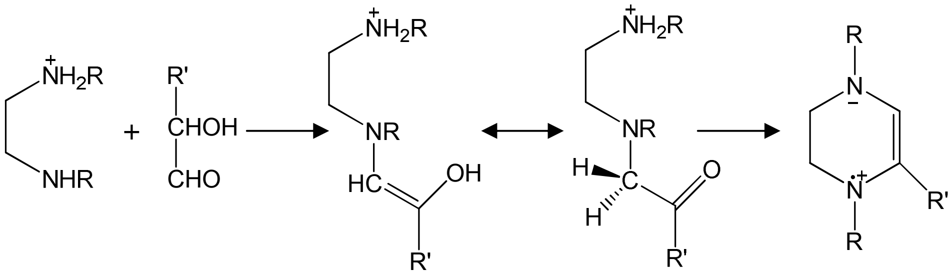

(Eq.4.2)

Figure 4.26 shows the effect of the crosslinking degree of PVAm on the surface charge of PMMA/PVAm particles. The surface charge of the particles had a little fluctuation (~+43 mV) when the crosslinking degree increased from 0% to 10%. Further increasing the crosslinking degree from 10% to 20% resulted in considerable reduction of the surface charge of the particles from +42 to +29.3 mV. These results showed that slight crosslinking of PVAm had little effect on the surface charge of the particles. However, the high crosslinking degree could reduce the surface charge of the particles, which may be due to the conversion of significant quantity of amine groups to imine linkage through the crosslinking reaction.

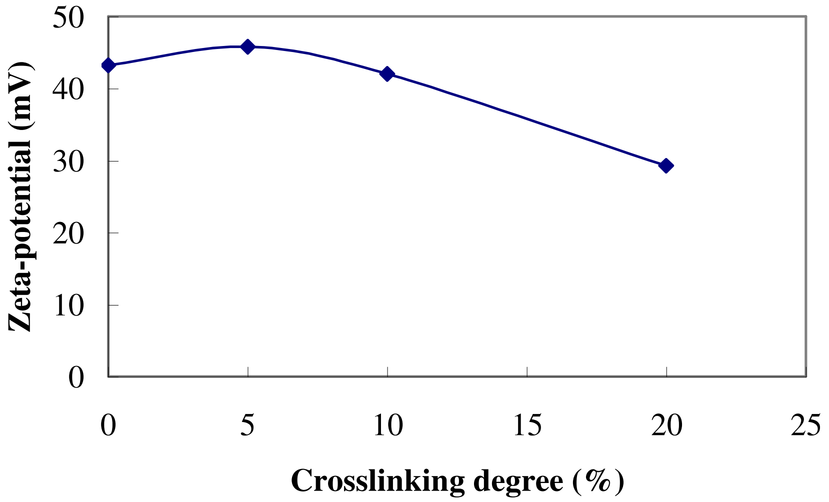

Figure 4.26 Effect of the crosslinking degree of PVAm on the surface charge of PMMA/PVAm particles

Figure 4.27 demonstrates the effect of the crosslinking degree of PVAm on the particle size and size distribution of PMMA/PVAm particles. The average particle size increased slightly when the crosslinking degree increased from 0% to 5%. However, further increasing the crosslinking degree from 10% to 20% significantly decreased the particle diameters from 173 to 111 nm**.** This effect may be attributed to the increase in steric repulsion of the PVAm. Thus the micellar domains which were formed *in-situ* during particle nucleation were smaller. Figure 4.26 also shows that the increase in the crosslinking degree from 10% to 20% results in a narrower particle size distribution. Thus, the particle size of the PVAm-based particles can be tailored simply by the addition of an appropriate amount of crosslinker.

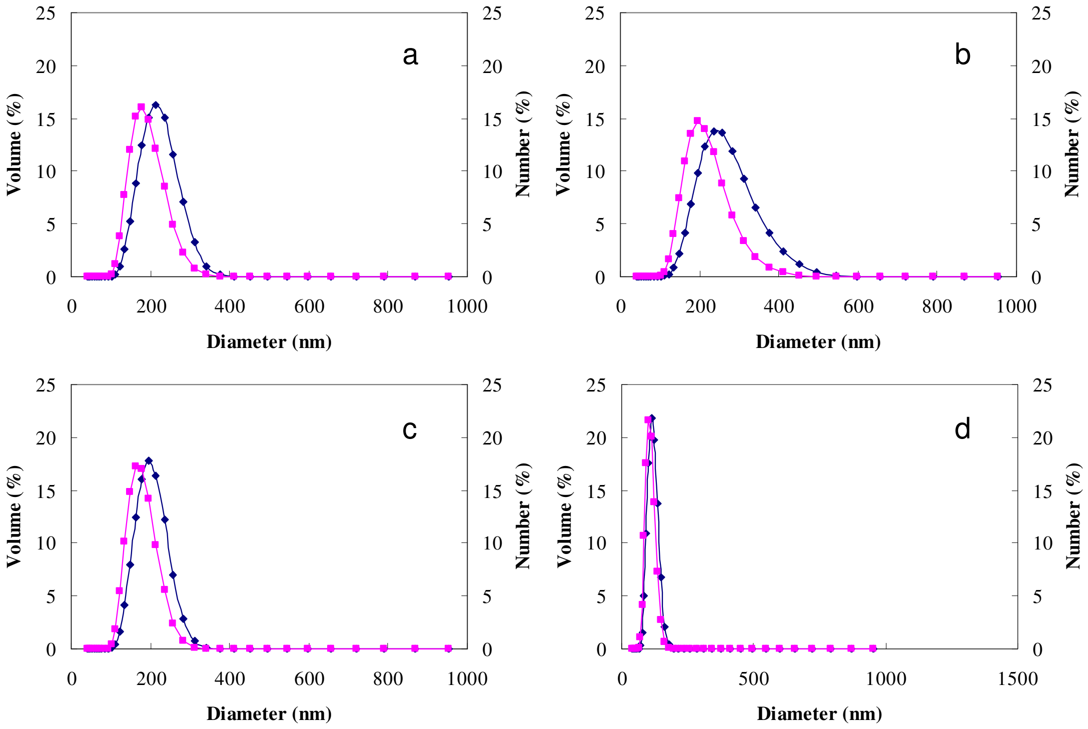

Figure 4.27 Effect of the crosslinking degree of PVAm on the particle size and size distribution of PMMA/PVAm particles. D_v (◆); D_n (■); PDI=D_v/D_n. Crosslinking degree: a) 0%, D_n=200 nm, PDI=1.28; b) 5%, D_n=234 nm, PDI=1.23; c) 10%, D_n=182 nm, PDI=1.12; d) 5%, D_n=115 nm, PDI=1.07.

Figure 4.28 shows FE-SEM images of PMMA/PVAm particles synthesized using PVAms with different crosslinking degrees. The images exhibit that the particle size decreases with the increase of crosslinking degree, while the size distribution becomes narrower. These results are consistent with the results obtained from the particle size measurements. The surface morphology of the particles also changes as the crosslinking degrees of PVAm increase. The particles are spherical and have a smooth surface when using PVAm without crosslinking or with low crosslinking. But the surface of the particles becomes irregular when the crosslinking degree of PVAm increases, and finally appears a raspberry shape when crosslinking degree is 20%.

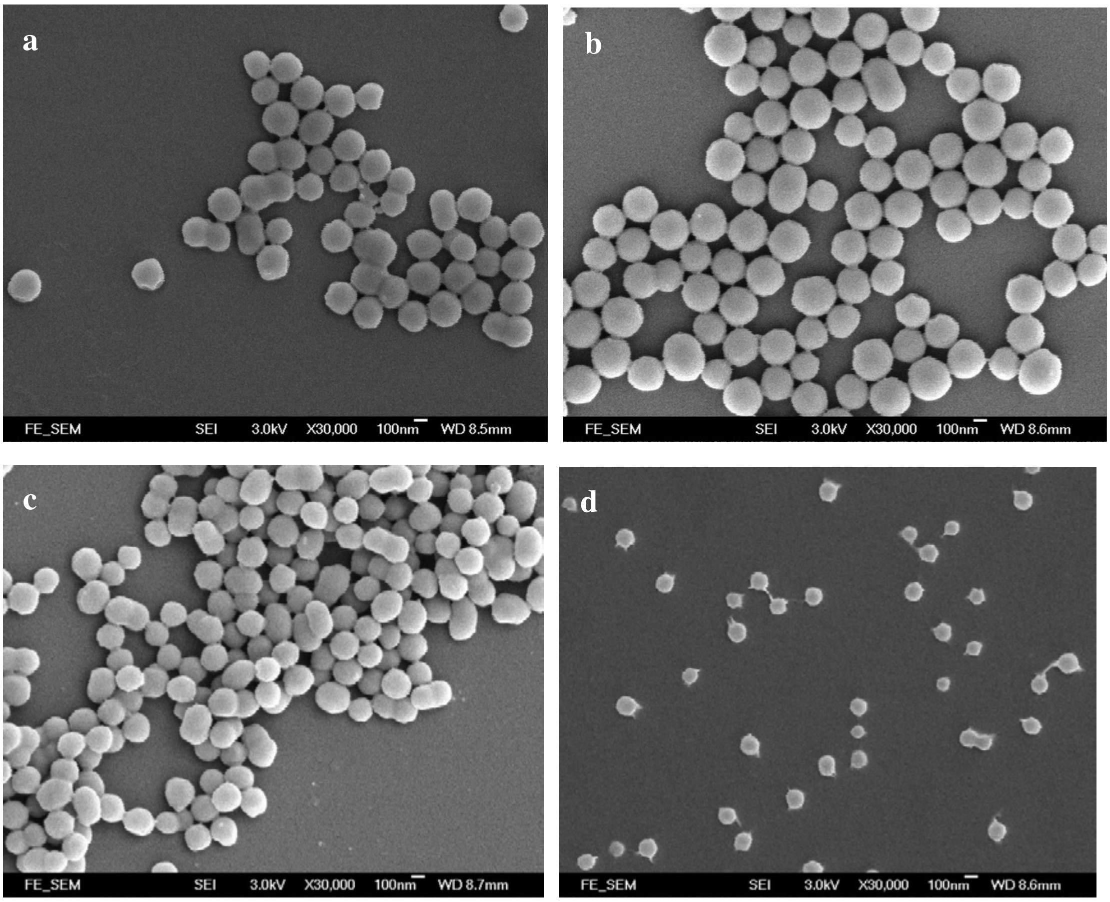

Figure 4.28 FE-SEM pictures of PMMA/PVAm particles using PVAms with different crosslinking degree. a). CD%=0; b). CD%=5; c). CD%=10; d). CD%=20

Although the crosslinking of PVAm with GA was successful, there were still some problems about the use of GA as a crosslinker. One problem is that the imine structure formed is not stable, and it decomposes under high temperature**,** which has negative effect on the graft copolymerization of MMA from PVAm. Another problem is that the crosslinking with GA may generate undesirable yellowing. Thus, other types of crosslinkers which can overcome these negative effects are preferred.

4.3.9 pH-sensitive property of PMMA/PVAm core-shell particles

The pH-sensitive property of PMMA/PVAm core-shell particles was investigated with respect to the stability, surface charge density, particle size and size distribution of the particles. Results are summarized in Table 4.9, wherein the particles used in these studies were prepared by the graft polymerization of MMA from PVAm at reaction pH 10. Particles were stable when the particle dispersion was stored between pH 3 and 8, but became unstable when the pH value was 9. ξ- Potential measurement showed that the positive potential slowly decreased from +63.4 to +45.8 mV with the increase of pH from 3 to 9. Further increasing the pH from 9 to 11 rapidly decreased the positive potential from +45.8 to +22.4 mV. Thus the decrease of the stability of the particle dispersion at a higher pH was attributed to the decrease of positive charges of ammonium ions. The effect of pH value on the particle size and size distribution of the PMMA/PVAm particles were investigated with a dynamic light scattering. There were almost no changes in particle size and size distribution when pH changes between 3 and 8. However, the particle size increased drastically when the pH increased to 9 and the size distribution became very broad. Further increasing pH to 10 or 11 caused the particle unstable and the particle size and size distribution could not be measured. The increase in particle size and broadness of size distribution were attributed to the coagulation of particles at the higher pH due to the decrease of surface charge.

Table 4.9 Effect of pH on the properties of PMMA/PVAm core-shell particles [a]

pH	Stability	ξ- potential (mV)	D_v (nm)	Dn (nm)	PDI[b]
3	stable	59.1	430.6	413.8	1.04
4	stable	63.4	433.6	409.2	1.06
5	stable	60.4	497.3	409.9	1.21
6	stable	54.2	540.7	456.2	1.19
7	stable	50.7	480.7	419.2	1.15
8	stable	47.1	548.0	427.6	1.28
9	medium	45.8	958.8	549.9	1.74
10	unstable	26.6	--	--	--
11	unstable	22.4	--	--	--

[a] Reaction conditions for synthesis of the particles: The polymerizations were carried out at 80 ^{0}C for 3 h. Weight ratio of PVAm to MMA=1:7.5;; [TBHP]=0.1 mM; Solid content = 2.5%; Reaction pH = 10; The total weight was about 50g.

[b] The particle size and size distribution were measured with a Zetasizer. Concentration of the dispersion was 250 ppm based on weight.

Figure 4.29 shows the FE-SEM images of PMMA/PVAm particles in different pH. The PMMA/PVAm particles were prepared by the graft copolymerization of MMA from PVAm at pH 12. There was no apparent difference in the morphology of the particles under different pH (raspberry-like). However, severe aggregation occured when the particles were stored at pH 11, confirming the results of the effect of pH on particles size and size distribution. These results also suggest that PVAm shells are pH-sensitive.

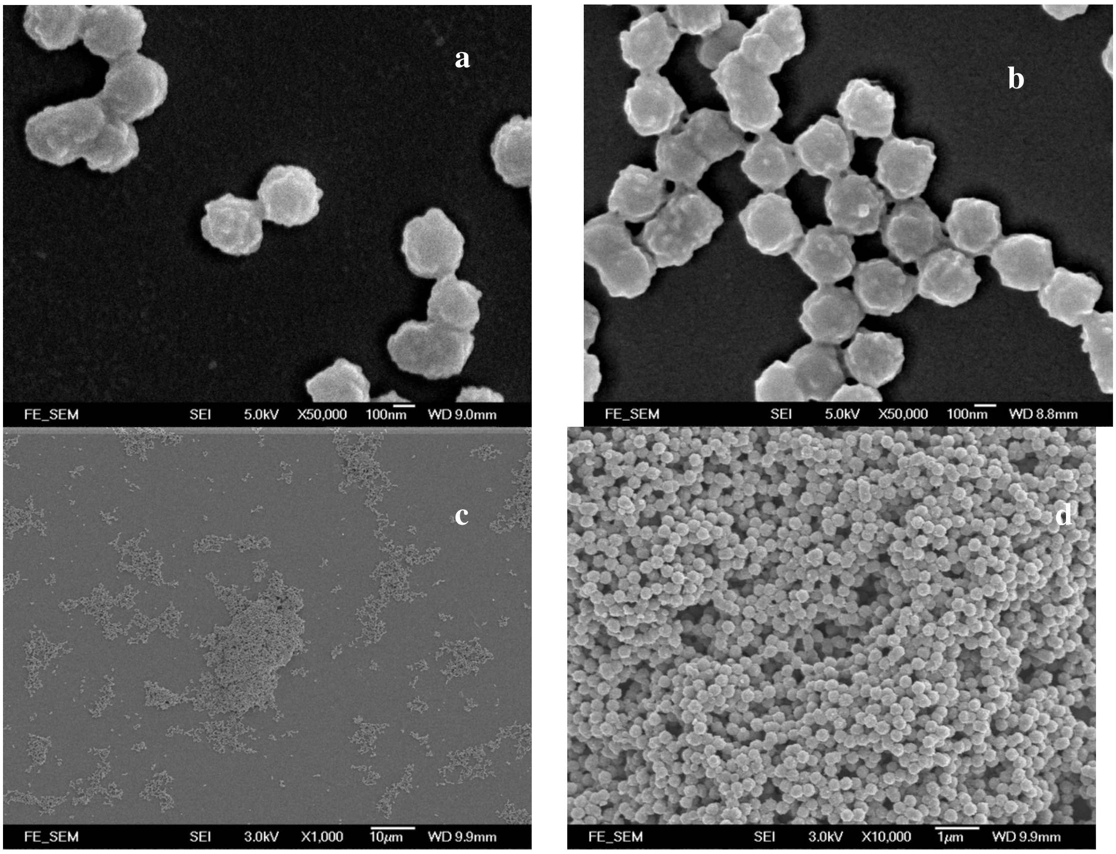

Figure 4.29 FE-SEM pictures of PMMA/PVAm core-shell particles (P8) at different pH context: a) pH=2; b) pH=6; c) and d) pH=11.

4.3.10 Composition of PMMA/PVAm core-shell particles

FT-IR technique was used to identify the composition of the PMMA/PVAm core-shell particles. Because PVAm is not soluble in chloroform while PMMA homopolymers are soluble, the amphiphilic PVAm-g-PMMA copolymers and PMMA homopolymers were isolated by Soxhlet extraction with chloroform. After extraction, the graft copolymers remained in the thimble filter while the PMMA homopolymers dissolved in chloroform.

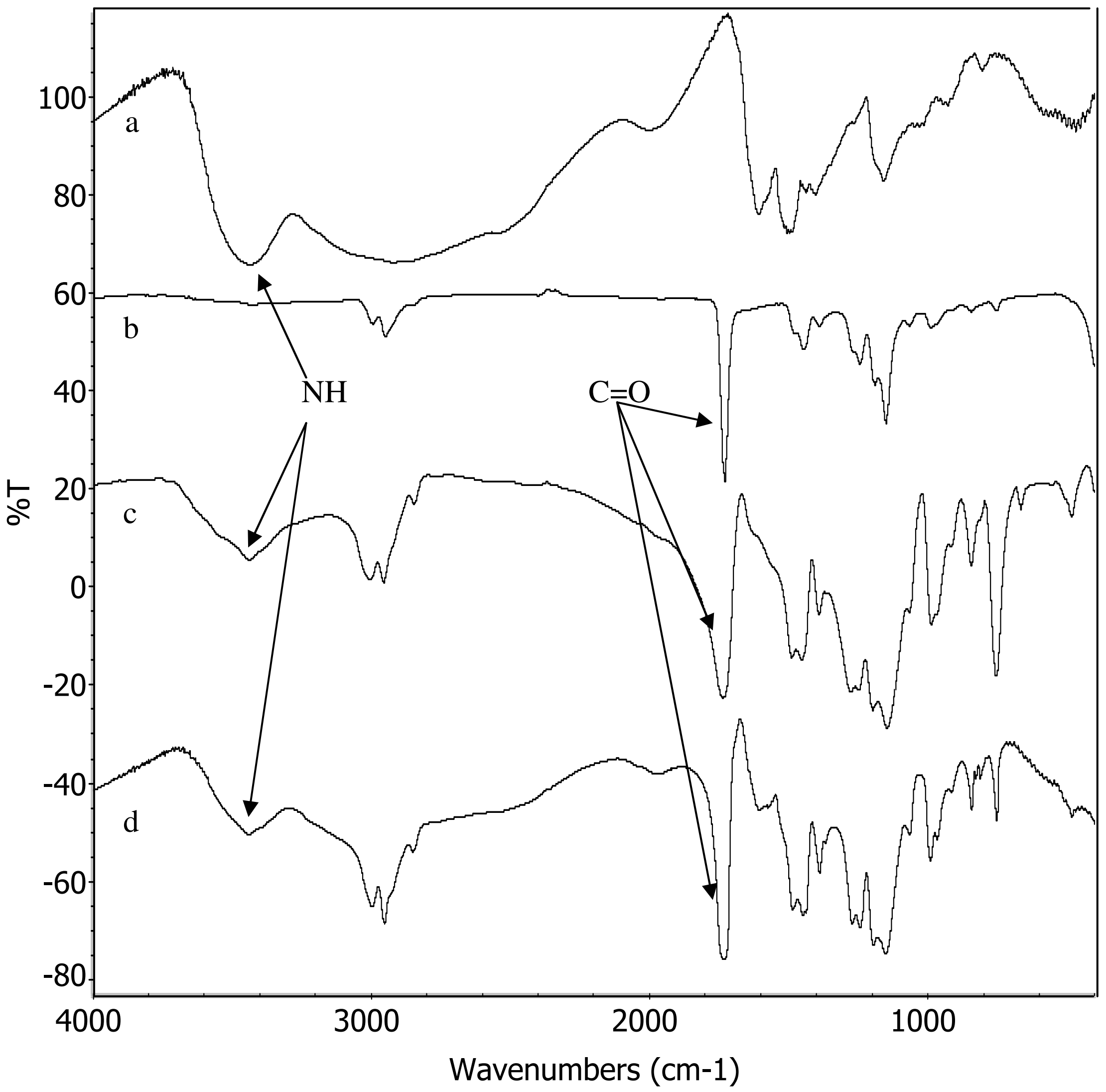

Figure 4.30 FT-IR spectra of (a) PVAmHCl; (b) isolated PMMA homopolymer; (c) PVAm-g-PMMA graft copolymer and (d) physical mixture of PVAmHCl and PMMA homopolymer.

Figure 4.30 shows the FT-IR spectra of PVAmHCl, PMMA isolated from particles, physical mixture of PVAmHCl and PMMA homopolymer and PVAm-g-PMMA. The spectrum of the polymer extracted from particles (Figure 4.30b) is exactly the same as compared with the standard IR spectrum of PMMA, confirming the formation of the PMMA homopolymer. The spectrum of PVAm-g-PMMA (Figure 4.30c) shows strong amine peaks around 3439 cm^{-1} and carbonyl peak at about 1734 cm^{-1}, which clearly indicates that the formation of the graft copolymers. The spectrum of the physical mixture of PVAmHCl and PMMA homopolymer (Figure 4.30d) is similar to the spectrum of the PVAm-g-PMMA copolymer. This result suggests that there is very low grafting point on the PVAm and the grafted PMMA is essentially the same to its homopolymer.

4.3.11 Morphologies of PMMA/PVAm core-shell particles

Figure 4.31 demonstrates the FE-SEM and TEM images of PMMA/PVAm particles produced by the copolymerization of MMA from PVAm at pH 12 with a PVAm to MMA weight ratio of 1:7.5 and TBHP concentration of 0.1 mM. Here the particles for TEM observation were stained with 2% PTA solution for an appropriate time. The micrographs show that the particles are highly monodispersed with a rough surface morphology like raspberry. This surface morphology is of very interesting because it would increase the effective surface area of the particles and hence the ability of the particles on absorption and immobilization. The formation of the raspberry-typed surface morphology might be caused by the nature of the monomer nature, the partially hydrolysis of monomer and other side reactions such as Michael addition during polymerization**,** as described in section 4.3.2**.**

Figure 4.32 shows TEM images of PMMA/PVAm particles. The PMMA/PVAm particles were first stained with a 1 wt.-% phosphotungstic acid solution for 1 min.

The PVAm shells were able to complex with phosphotungstic anion through cation-anion interaction while the polymeric cores could not be stained. Thus the TEM images clearly revealed that the particles had well-defined core-shell structure, where PMMA cores (white part) were coated with thick and hairy PVAm shells (darker part).

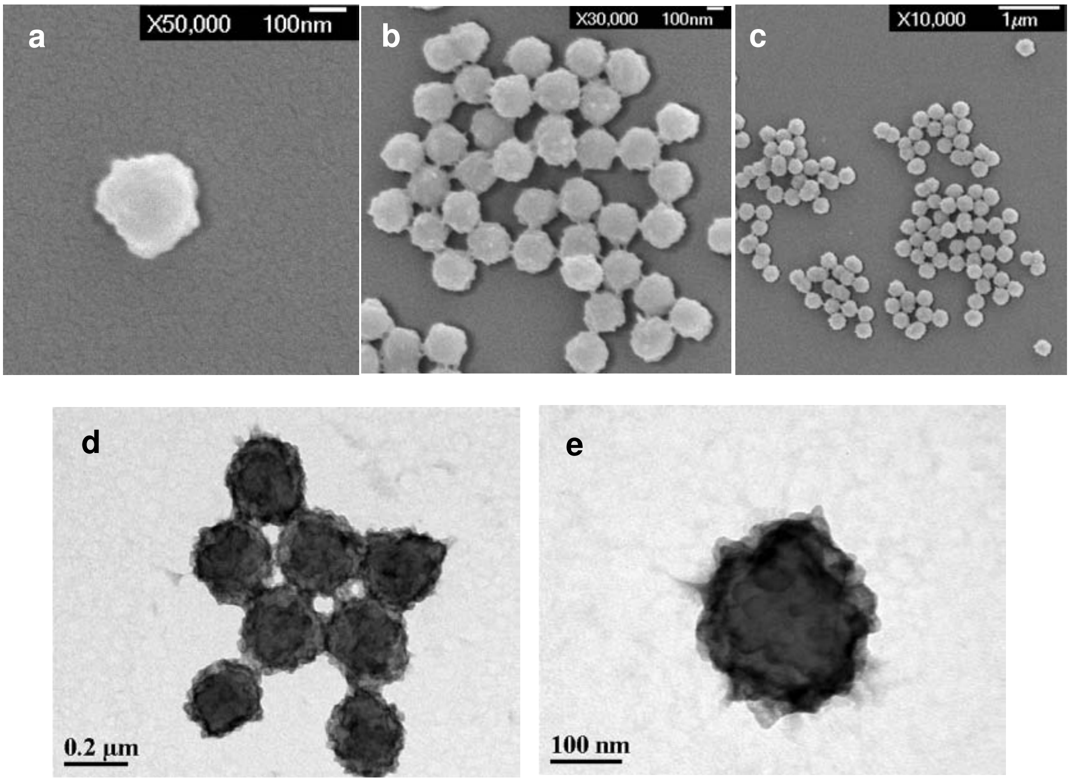

Figure 4.31 FE-SEM and TEM micrographs of PMMA/PVAm particles. (a-c): FE-SEM images; (d and e): TEM images of stained particles.

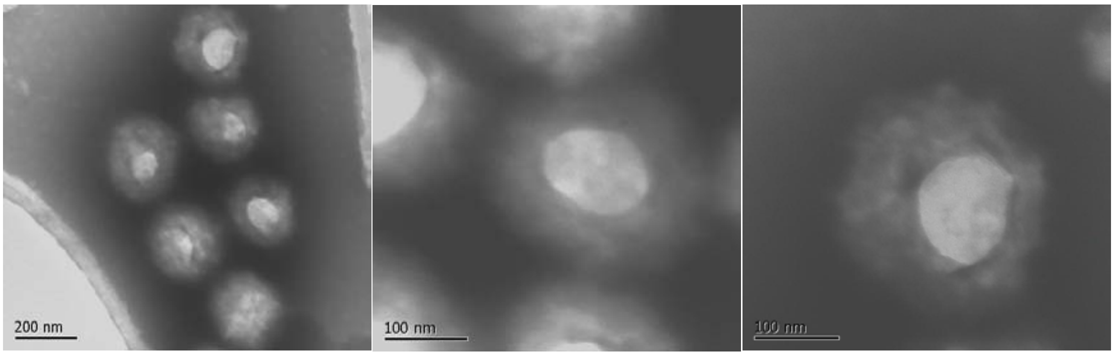

Figure 4.32 TEM images of the particles with well-defined PMMA cores (white part) and PVAm shells (darker part)

4.4 Conclusions

Amphiphilic PMMA/PVAm core-shell particles were synthesized via a direct graft copolymerization of MMA from PVAm induced by a small amount of TBHP in aqueous medium Amphiphilic graft copolymers and PMMA homopolymers were generated concurrently to form highly monodispersed particles with diameters in the range of 100-300 nm. The formation of graft copolymers and homopolymers was confirmed by FTIR. ζ-potential measurement suggested the formation of cationic PVAm shell. TEM micrographs revealed that the particle had a well-defined core-shell nanostructure. SEM images indicated that PMMA/PVAm particles displayed a raspberry-like morphology. The purified PMMA/PVAm particles possessed a pH-sensitive nature, coagulating at a pH higher than 10. The effects of reaction pH, TBHP concentration, weight ratio of PVAm to MMA, salt concentration, molecular weight of PVAm, amination degree of poly(NVA-PVAm) and crosslinking degree of PVAm have been systematically investigated with respect to the stability of the particles, the monomer conversion, particle size and size distribution, surface charge, grafting percentage and efficiency, and surface morphology. The stability of the particles was strongly dependent on the reaction pH, weight ratio of PVAm to MMA, salt concentration, molecular weight of PVAm. The particles could be synthesized in reaction medium with a salt concentration up to 0.5 M. But they could not be obtained if the Mw of the PVAm is less than 35000. The monomer conversion increased with the increase of reaction pH, weight ratio of PVAm to MMA, and amination of poly (NVA-PVAm) because of more available amino groups for graft copolymerization. The increase of TBHP concentration could also increase the monomer conversion slightly. The particle size and size distribution were able to be tuned by variation of the TBHP concentration and crosslinking degree of PVAm, while the surface functionality of the particles could be tailored by changing the amination of poly(NVA-VAm). It was also found that the grafting efficiency of the PMMA increased with the increase of reaction pH and decrease of TBHP concentration. Surface morphology studies suggested that the reaction pH had a strong influence on the surface morphology of the particles, while the other factors had little influence.

References:

1. Li, P.; Zhu, J. M.; Harris, F. W. Amphiphilic core-shell latexes. US. Patent 6,573,313, 2002.
2. Li, P.; Zhu, J.; Sunintaboon, P.; Harris, F. W., New Route to Amphiphilic Core-Shell Polymer Nanospheres: Graft Copolymerization of Methyl Methacrylate from Water-Soluble Polymer Chains Containing Amino Groups. *Langmuir* **2002,** 18, (22), 8641-8646.

3. Zhu, J.; Li, P., Synthesis and characterization of poly(methyl methacrylate)/casein nanoparticles with a well-defined core-shell structure. *Journal of Polymer Science, Part A: Polymer Chemistry* **2003,** 41, (21), 3346-3353.
4. Ye, W.; Leung, M. F.; Xin, J.; Kwong, T. L.; Lee, D. K. L.; Li, P., Novel core-shell particles with poly(n-butyl acrylate) cores and chitosan shells as an antibacterial coating for textiles. *Polymer* **2005,** 46, (23), 10538-10543.
5. Li, P.; Zhu, J.; Sunintaboon, P.; Harris, F. W., Preparation of latexes with poly(methyl methacrylate) cores and hydrophilic polymer shells containing amino groups. *Journal of Dispersion Science and Technology* **2003,** 24, (3 & 4), 607-613.
6. Leung, M. F.; Zhu, J.; Harris, F. W.; Li, P., Novel synthesis and properties of smart core-shell microgels. *Macromolecular Symposia* **2005,** 226, (Polymer Chemistry, Reactions and Processes), 177-185.
7. Leung, M. F.; Zhu, J.; Harris, F. W.; Li, P., New route to smart core-shell polymeric microgels: Synthesis and properties. *Macromolecular Rapid Communications* **2004,** 25, (21), 1819-1823.
8. Katchalsky, A.; Mazur, J.; Spitnik, P., Polybase properties of poly(vinylamine). *Journal of Polymer Science* **1957,** 23, 513-30, discussion 530-2.
9. Kirwan, L. J.; Papastavrou, G.; Borkovec, M.; Behrens, S. H., Imaging the Coil-to-Globule Conformational Transition of a Weak Polyelectrolyte by Tuning the Polyelectrolyte Charge Density. *Nano Letters* **2004,** 4, (1), 149-152.
10. Arote, R.; Kim, T.-H.; Kim, Y.-K.; Hwang, S.-K.; Jiang, H.-L.; Song, H.-H.; Nah,

J.-W.; Cho, M.-H.; Cho, C.-S., A biodegradable poly(ester amine) based on polycaprolactone and polyethylenimine as a gene carrier. *Biomaterials* **2007,** 28, (4), 735-744.

11. Lynn, D. M.; Langer, R., Degradable Poly(beta-amino esters): Synthesis, Characterization, and Self-Assembly with Plasmid DNA. *J. Am. Chem. Soc.* **2000,** 122, (44), 10761-10768.
12. Laue, T.; Plagens, A., *Named organic reactions*. 2nd ed.; Wiley: Chichester, 2005; p x, 310 p.
13. Liu, Y.; Wu, D.; Ma, Y.; Tang, G.; Wang, S.; He, C.; Chung, T.; Goh, S., Novel poly(amino ester)s obtained from Michael addition polymerizations of trifunctional amine monomers with diacrylates: safe and efficient DNA carriers. *Chemical Communications* **2003**, (20), 2630-2631.
14. Akashi, M.; Saihata, S.; Yashima, E.; Sugita, S.; Marumo, K., Novel nonionic and cationic hydrogels prepared from N-vinylacetamide. *Journal of Polymer Science, Part A: Polymer Chemistry* **1993,** 31, (5), 1153-60.
15. Kawahara, J.-I.; Ishikawa, K.; Uchimaru, T.; Takaya, H., Chemical cross- linking by glutaraldehyde between amino groups: its mechanism and effects. *Polymer Modification, [Papers presented at the Symposium on Polymer Modification], Orlando, Fla., Aug. 25-29, 1996* **1997**, 119-131.
16. Hayashi, T.; Ohta, Y.; Namiki, M., Electron spin resonance spectral study on the structure of the novel free radical products formed by the reactions of sugars with amino acids or amines. *J. Agric. Food Chem.* **1977,** 25, (6), 1282-1287.

17. Namiki, M.; Hayashi, T., Development of novel free radicals during the amino-carbonyl reaction of sugars with amino acids. *J. Agric. Food Chem.* **1975,** 23, (3), 487-491.
18. Roberts, R. L.; Lloyd, R. V., Free Radical Formation from Secondary Amines in the Maillard Reaction. *J. Agric. Food Chem.* **1997,** 45, (7), 2413-2418.

Chapter 5

Synthesis of PVAm from NVF and its Application in Synthesis of PMMA/PVAm Core-Shell Particles

5.1 Introduction

The synthesis of PVAm from *N*-vinylacetamide (NVA) and its application in the synthesis of PMMA/PVAm particles have been described in Chapter 3 and Chapter 4. *N*-vinylformamide (NVF), an isomer of acrylamide, is another important precursor which could be used for the synthesis of PVAm. NVA was first chosen to prepare PVAm due to its lower toxicity and easier handling than the NVF. However, it has several disadvantages comparing to NVF, as shown in Table 5.1. Perhaps the biggest drawback for the preparation of PVAm from NVA is its high cost. The NVA is more expensive than NVF. In addition, hydrolysis of NVA takes longer time and requires more drastic conditions than the hydrolysis of NVF. Therefore, NVF has been the most popular precursor for simple and economical production of PVAm in the last decade since its synthetic route had been developed commercially.[1-3]

Here we describe the synthesis of PVAm by the free radical polymerization of NVF to PNVF, followed by the acidic hydrolysis of the as-prepared PNVF. The PVAm prepared from PNVF was used for the synthesis of PMMA/PVAm core-shell particles.

Table 5.1 Comparison of NVA and NVF

	N-vinylacetamide (NVA) 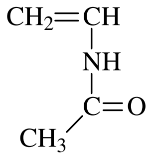	*N*-vinylformamide (NVF) 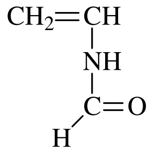
Advantages	● Stable ● No need to purify before use	● Cheaper than NVA ~HK$690/500ml, ~1/5 that of the cost of NVA ● PNVF is easier to be hydrolyzed (1) Conditions to achieve nearly 100% hydrolysis: at 80 °C for 4h in 3M HCl solution, (2) Hydrolysis of PNVF can be performed in both an acidic or a basic condition
Shortages	● More expensive than NVF ~HK$650/100g, 5-times that of NVF PNVA is harder to be hydrolyzed than PNVF Conditions to achieve nearly 100% hydrolysis: at 80 °C for 72h in 3M HCl solution, ● PNVA can not be hydrolyzed in a basic condition ● The commercial production of NVA has been discontinued in Aldrich	● Unstable (1) Decomposition of NVF is fast when temperature is higher than 90 °C (2) NVF must be purified before use under very high vacuum to ensure that the monomer can be distilled out at a temperature lower than 70 °C.

5.2 Experimental

5.2.1 Materials

N-vinylformamide (NVF) (98%, light-yellow liquid, MW=71.08, Aldrich) was purified by a vacuum distillation at a temperature lower than 70 °C and stored at -15

^{o}C. Methyl methacrylate (MMA) (colorless liquid, Mw=100.12, density=0.936 g/cm^3, Aldrich) was purified following a reported procedure.[4] It was first washed three times with 10 wt.% NaOH solution, then with de-ionized (DI) water until the pH of the water layer to 7. After that, the monomer was dried with anhydrous calcium chloride, followed by a vacuum distillation.

2,2'-Azobis(2-amidinopropane) dihydrochloride (V-50) (97%, faint yellow crystal, free radical initiator, $T_{1/2}$=56℃, MW=271.2, Wako), *tert*-Butyl hydroperoxide (TBHP) (70% aqueous solution, colorless liquid, MW=90.07; Aldrich), reagent grade of chloroform (aldrich), acetone (aldrich), hydrochloric acid (HCl) (37% Aldrich) and NaOH (Fluka) were all used as received. DI water was used as the dispersion medium.

5.2.2 Synthesis of PNVF

For a total weight of 250 g, NVF (50 g) was dissolved in DI water (200 g) in a three-neck flask equipped with a condenser and a nitrogen inlet. After purging the solution with nitrogen for 30 minutes, V-50 (0.3744g, 1.38 mmol) was added and polymerization was carried out at 60 ^{o}C for 24 hours. The product was purified by repeated dissolution-decantation-precipitation cycles with acetone and DI water to remove any unreacted monomer and oligomer. Finally, the purified PNVF was dried at 50 ℃ for 3 days in a vacuum oven. The yield of PNVF was calculated according to the following formula:

$$\text{Yield (\%)} = \frac{\text{Weight of PNVF obtained}}{\text{Weight of NVF added}} \times 100\%$$

5.2.3 Acidic hydrolysis of PNVF to poly(vinylammonium chloride) (PVAmHCl)

In a typical reaction, PNVF (5.0 g, amide units: 0.0703 mol) was dissolved in 3 M HCl solution (40 ml) in a three-neck flask equipped with a condenser and a nitrogen inlet. The mixture was then purged with N_2 for 30 minutes and stirred at 80℃ for 4 hours. The product was precipitated directly from water by dropwise addition of a concentrated HCl solution. It was further purified by repeated dissolution-decantation-precipitation cycles with water and acetone. Finally, the product was dried at 50 ℃ *in vacuo* for 3 days. The yield of PVAmHCl was calculated based on the following formula:

$$\text{Yield (\%)} = \frac{\text{Weight of PVAmHCl obtained}}{\text{Weight of theoretical yield}} \times 100\%$$

5.2.4 Synthesis of PVAm/PMMA core-shell particles

For a total weight of 50 g, PVAmHCl (0.25 g) was dissolved in DI water and the pH of the solution was adjusted to 12 with 10% NaOH solution. The solution was then mixed with purified MMA (1 g) in a three-necked water-jacketed flask equipped with a thermometer, a reflux condenser and a nitrogen inlet. The stirred mixture was purged with nitrogen for 30 minutes. A diluted TBHP solution (0.5 mL of 10 mM solution) was added and the mixture was stirred at 80 ℃ for 3 hours. After the reaction, the monomer conversion was determined gravimetrically. The particle dispersion was purified by repeated centrifugation-decantation-dispersion cycles using DI water.

5.2.5 Measurement and characterization

Infrared spectra were recorded on a Nicolet Avatar 360 FT-IR spectrophotometer using KBr disks. The ^{1}H NMR spectra were recorded on a Bruker advance DPX-400 (400 MHz) instrument. The particle size and size distribution were measured with a Coulter LS230 Particle Size Analyzer. The ζ-potential of the particles was measured with a Malvern Zetasizer 3000HS (Malvern, UK) in 1 mM NaCl solution. The surface morphologies of the particles were examined by field emission scanning electron microscopy (FE-SEM, JEOL JSM 6335F). Samples were prepared by coating the dried particles spread over a glass surface with a thin layer of gold to a depth of ca. 5 Å. under vacuum.

5.3 Results and Discussion

5.3.1 Synthesis of PVAm

The free radical polymerization of NVF to PNVF could be easily carried out by bulk, solution, precipitation or inverse emulsion polymerization using an oil-soluble or water-soluble initiator.[5-7] Here PNVF was prepared by a free radical solution polymerization of NVF in water using V-50 as a free radical initiator, followed by purification of PNVF via repeated precipitation-decantation-dissolution cycles with acetone and DI-water (as shown in Scheme 5.1). A colorless polymer with a yield up to 85% was obtained.

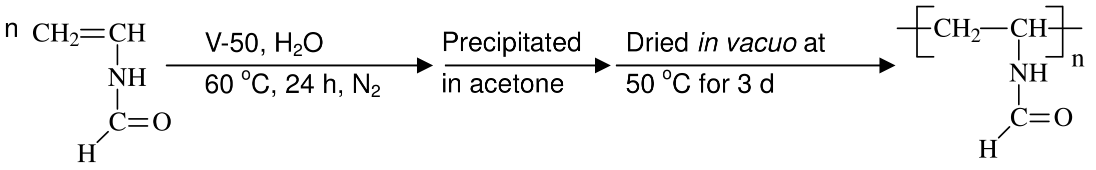

Scheme 5.1. Synthesis of PNVF

The product was characterized with FT-IR and ^{1}H-NMR spectroscopes. It is expected that the absorbance of the C=C double bond from NVF was greatly reduced or completely disappeared in the spectrum of the product. In the FTIR spectrum of NVF (Figure 5.1a), the peak at 1645 cm^{-1} was attributed to the presence of C=C double bond. It disappeared in the FTIR spectra of PNVF (Figure 5.1b), indicating that there is no unreacted NVF in the purified PNVF sample. In the FT-IR spectrum of PNVF (Figure 5.1b), a peak at 3275 cm^{-1} is attributed to the N-H stretching vibration, the peak at 1683 cm^{-1} is assigned to C=O stretching vibration (amide I), the peaks at 1516 cm^{-1} is donated by N-H (amide II). All these peaks indicate the existence of amide groups.

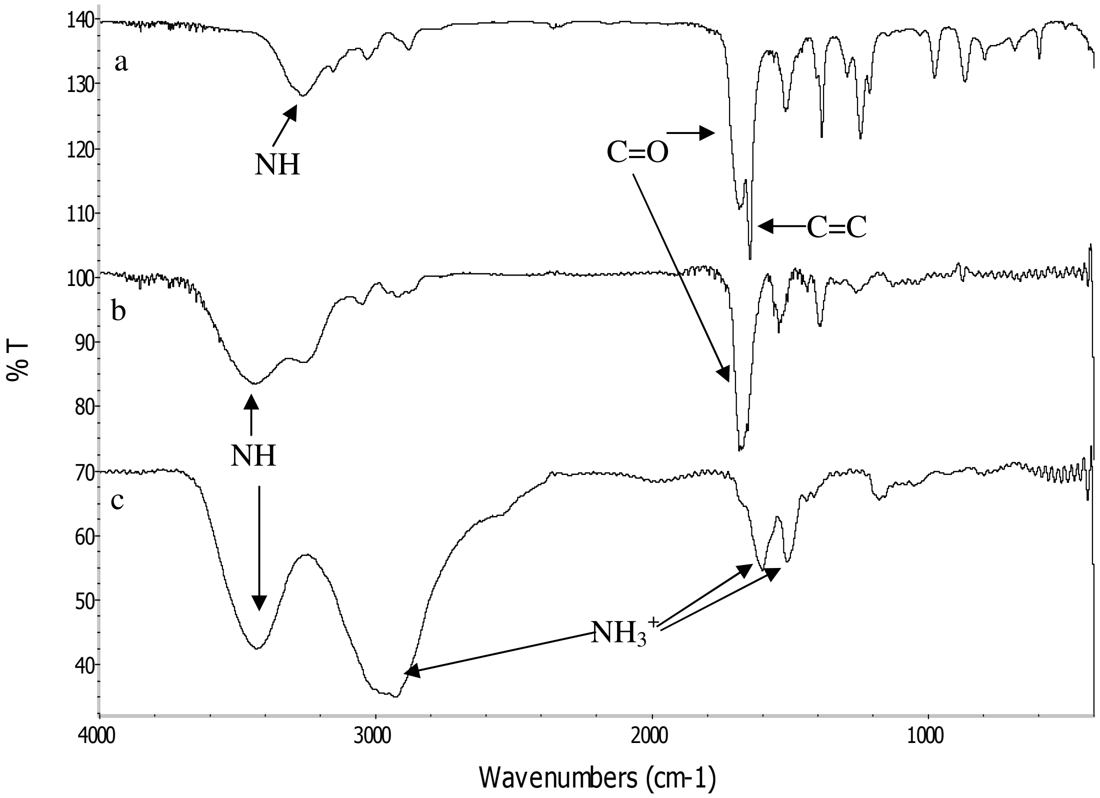

Figure 5.1 FTIR Spectra of a) NVF; b) PNVF; and c) PVAmHCl

The ^1H NMR spectra of NVF and PNVF were recorded in D_2O. In the NMR spectrum of NVF (Figure 5.2a), the peaks at 8.2~7.97 ppm are assigned to the proton on –CHO group, The peaks at 6..9~6.5 ppm are attributed to the proton on =CH group, while the peaks at 4.9~4.4 ppm are donated by the protons on $=CH_2$ group, which are overlapped with the peak of H_2O in D_2O. These peaks disappeared in the NMR spectrum of PNVF (Figure 5.2b), while new peaks at 1.9~1.4 and 4.0~3.2 ppm, which are donated to the protons on $–CH_2$ and –CH- groups of PNVF respectively,[8] were observed. The results clearly show that there is no unreacted monomer in the product. This is in accordance with the conclusion obtained from the FT-IR analysis. In the NMR spectrum of PNVF, the resonance of the amide protons appeared at 8.1~7.6 ppm.

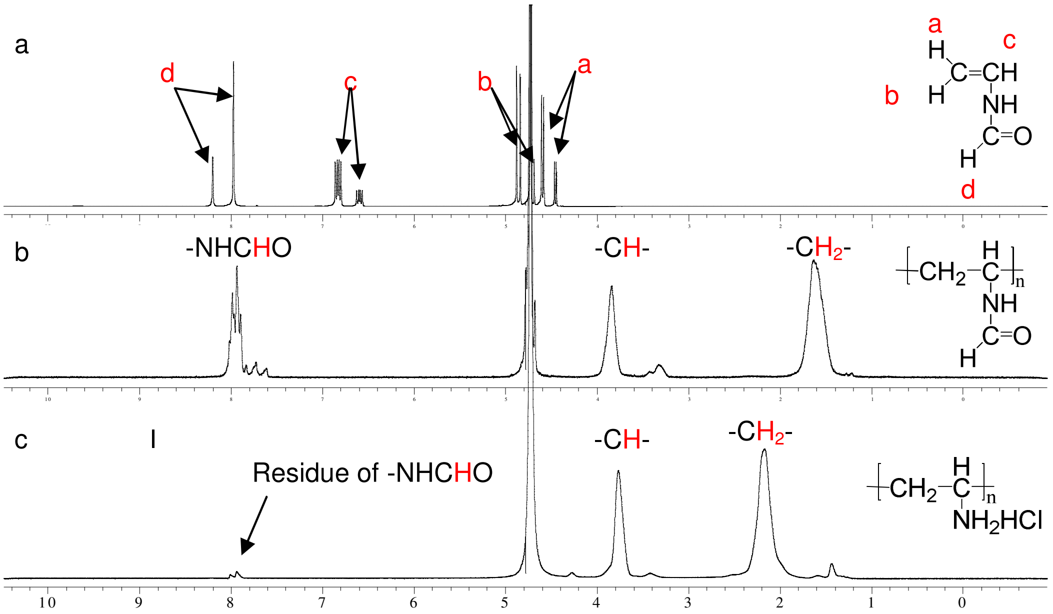

Figure 5.2 ^{1}H NMR spectra of a) NVF; b) PNVF and c) PVAmHCl

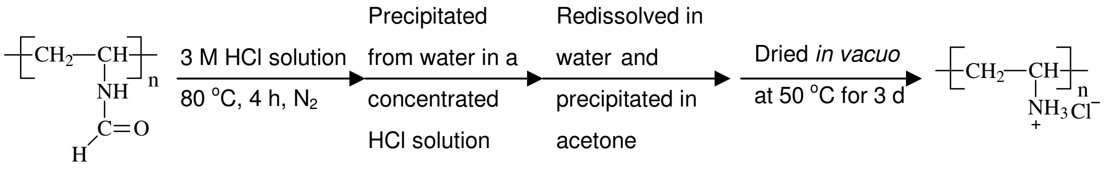

Scheme 5.2 Acid-hydrolysis of PNVF to PVAmHCl

PNVF can be easily converted to PVAm through hydrolysis in either acidic or alkaline solutions.[7] Here PNVF was hydrolyzed in 3 M HCl solution as shown in Scheme 5.2. A slight-yellow product with a yield up to 89% was achieved. The product was identified with FT-IR and ^{1}H NMR spectra.

In the IR spectrum of PVAmHCl (Figure 5.1c), no peaks attributed to the amide groups were observed, suggesting that PNVF molecules have been almost completely hydrolyzed. The IR spectrum of PVAmHCl shows the typical characteristics peaks of the primary ammonium. The broad absorption at 3200-2400 is attributed to the NH_3^+

asymmetric stretching, while the peaks at about 1621 and 1519 cm^{-1} are donated to NH_3^+ asymmetric and symmetric deformation, respectively. The peaks at about 3431 and 1177 cm^{-1} are assigned to N-H and C-N stretching.

In the ^{1}H NMR spectra of PVAmHCl (Figure 5.2c), the peak attributed to the proton of $-CH_2-$ moves slightly downfield to 2.17 ppm, while the peak donated to the proton in –CH- shifts to 3.77 ppm. The amination of the hydrolyzed product can be determined by monitoring the change in the amide group peak area (8.1-7.6 ppm). Eq 5.1 gives the calculation of the amination.

$$\text{Amination (\%)} = \left(1 - \frac{2 \times \text{amide group peak area}}{-CH_2-\text{ peak area}}\right) \times 100 \qquad (\textbf{Eq. 5.1})$$

Here, the amination of the product was about 96%. In other words, 96% of the amide groups have been converted to amine groups under this hydrolysis condition.

5.3.2 Synthesis of PMMA/PVAm particles

Scheme 5.3 shows the procedure for the synthesis of the amphiphilic PMMA/PVAm core-shell particles. PVAmHCl was first converted to PVAm by reacting with 10% NaOH solution. Then the PVAm was treated with a small amount of TBHP at 80 °C in the presence of MMA to generate PMMA/PVAm particles.

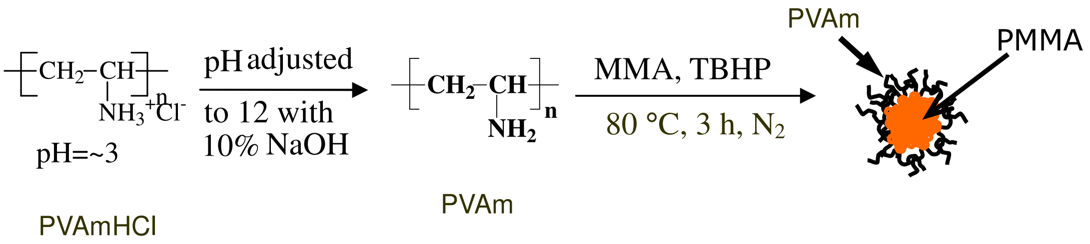

Scheme 5.3 Synthesis of PMMA/PVAm particles

However, the first attempt to synthesize PMMA/PVAm failed when using the PVAmHCl prepared from NVF (Table 5.2, P168). To ensure that there was no problem with the materials other than PVAmHCl, a control experiment was carried out using a previously synthesized PVAmHCl from PNVA. The control experiment was successful with a monomer conversion up to 80%, indicating that it was the PVAmHCl prepared from PNVF, which caused the failure to form the particles.

Table 5.2 Synthesis of PMMA/PVAm particles using PVAmHCl from NVF[a]

Items	PVAmHCl from	Observation	Conversion
control	PNVA	Particles formed	80%
P168	PNVF	No particles formed	0
P170[b]	PNVF	No particles formed	0
P186[c]	PNVF	Particle formed	67%

[a] Reaction conditions: PVAmHCl : 0.25g; MMA: 1g; [TBHP]: 0.1 mM; Solid content : 2.5%; Total weight: 50g; Reaction time: 3 h; Temperature: 80 °C; Reaction pH=12.

[b] The PVAmHCl was repurified to ensure no impurities existing in the polymer.

[c] The PVAmHCl was further hydrolyzed to ensure complete hydrolysis.

The failure of particle formation might be attributed to the impurities existing in the PVAmHCl. Thus the PVAmHCl was carefully re-purified by repeated dissolution-decantation-precipitation cycles with DI water and acetone. Then the synthesis of PMMA/PVAm particles was performed again (Table 5.2, P170). Again the polymerization failed, indicating that the problem might be from the PVAmHCl chains that could interfer with the particle formation.

It has been reported that the oxidative amidation of aldehydes with amine hydrochloride salts can be highly efficient in the existence of TBHP and copper ion (Eq. 5.2).[9] TBHP can also added to a carbonyl group (Eq. 5.3).[10] For example, formaldehyde could react with TBHP to give *tert*-butylperoxymethanol, and the reaction enthalpy is -66.5 kJ mol^{-1}.

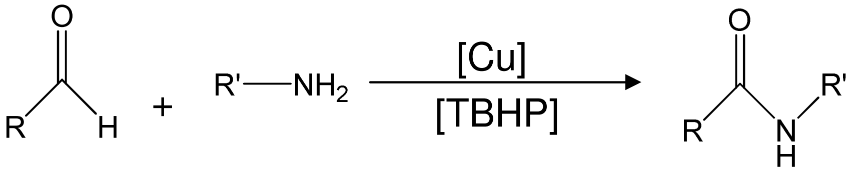

(Eq. 5.2)

$$>C{=}O + t\text{-BuOOH} \longrightarrow >C(OH)(OOBu\text{-}t) \qquad \text{(Eq. 5.3)}$$

Therefore, it was suspected that the residual aldehyde groups in the PVAmHCl chains might prevent the initiation of the graft copolymerization of MMA form PVAm. Therefore, the PVAmHCl was further hydrolyzed in a 3 M HCl solution for 12 hours to ensure the complete hydrolysis of the polymer. The product was identified with ^{1}H NMR spectroscopy. As shown in Figure 5.3, the peak area attributed to the residue of –CHO groups was significantly reduced after re-hydrolysis comparing to the former product.

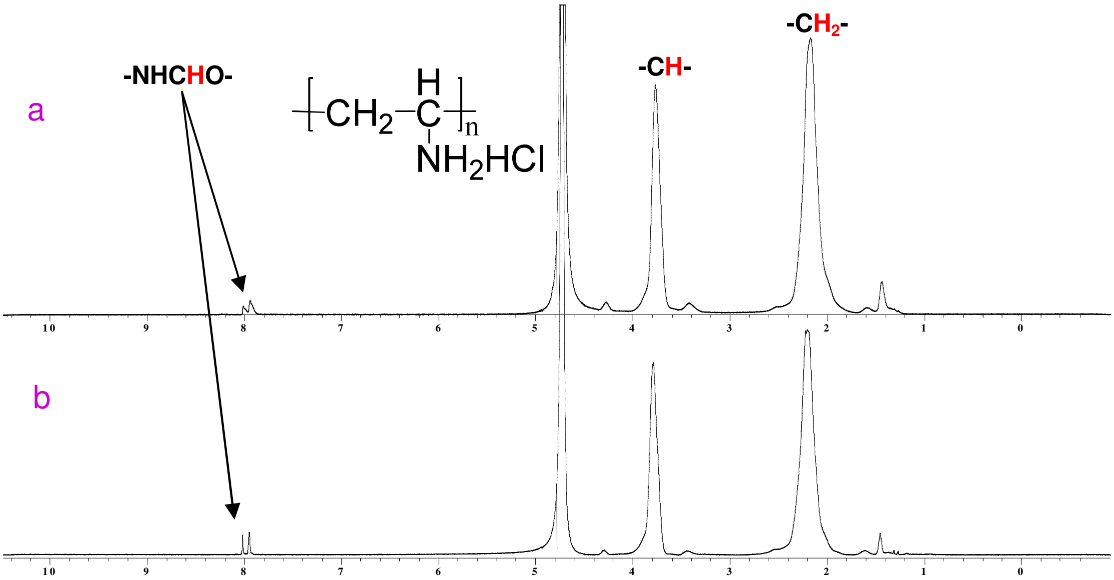

Figure 5.3 ^{1}H NMR spectra of a) before; and b) after re-hydrolysis

PMMA/PVAm particles were successfully prepared with the re-hydrolyzed product. Stable and uniform particles were obtained with a monomer conversion up to 67% (Table 5.2, P186), which is comparable with the result using the PVAmHCl prepared from PNVA. The volume and number average diameters (D_v and D_n, respectively) of the particles were 214 and 196 nm respectively, with a narrow size distribution (PDI=1.09) (Figure 5.4). ζ-potential measurement showed that the surface charge of the particles was +46.9 mV, suggesting the formation of cationic PVAm shells. FE_SEM images of the particles (Figure 5.5) showed that the particles were spherical with uneven surfaces.

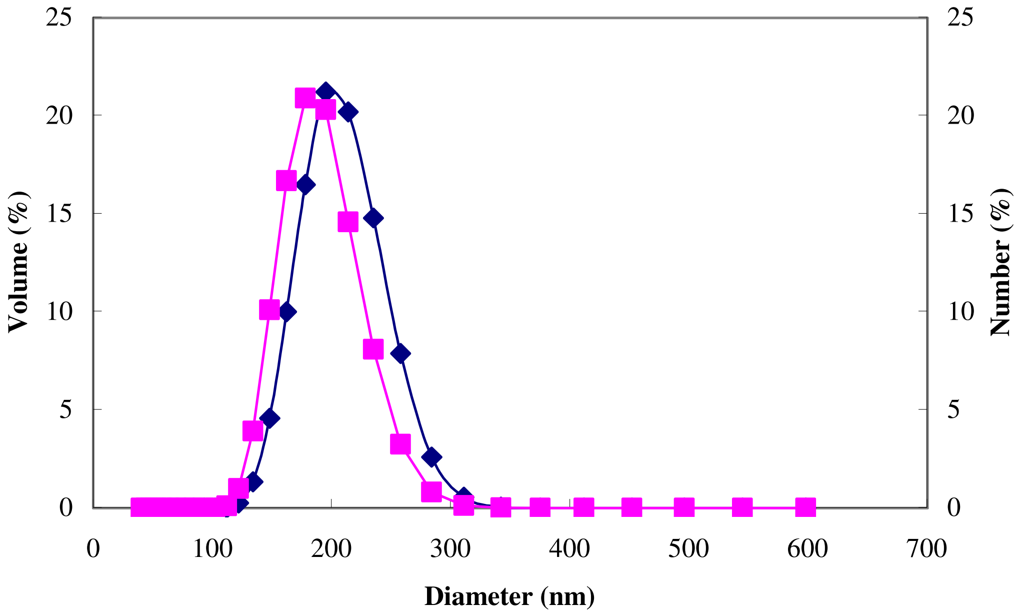

Figure 5.4 Particle size and size distribution of the PMMA/PVAm particles. (◆) D_v = 214 nm; (■) D_n = 196 nm; PDI = 1.09 (D_v/D_n).

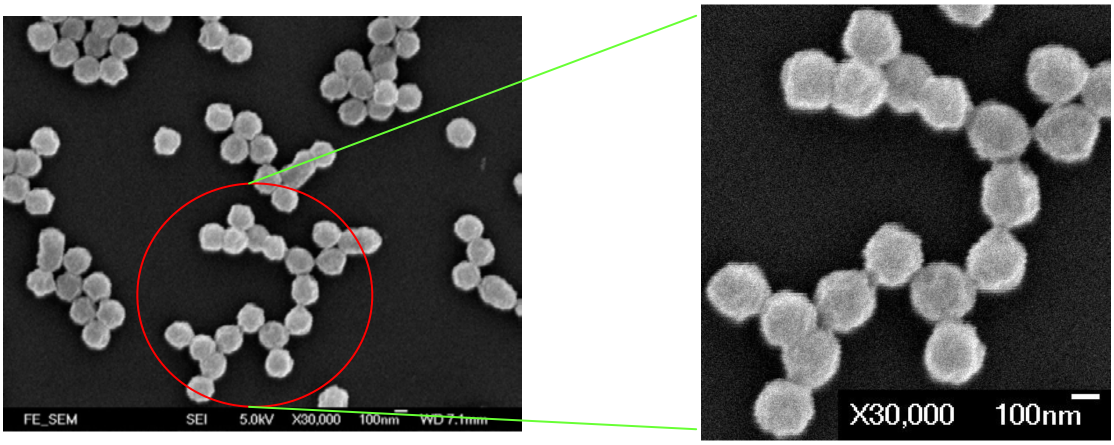

Figure 5.5 FE-SEM micrographs of the PMMA/PVAm particles

5.4 Conclusions

PVAmHCl was synthesized from NVF through a free radical polymerization of NVF in water using V-50 as an initiator, followed by hydrolysis of the preformed

PNVF in 3 M HCl aqueous solution. The successful synthesis was confirmed by IR and ^1H NMR spectra. Because aldehyde groups can react with TBHP and amino groups, thus preventing the initiation of graft copolymerization of MMA from PVAm, the hydrolysis of PNVF must achieve complete conversion. The as-prepared PVAmHCl was used for the synthesis of PMMA/PVAm particles, giving a monomer conversion up to 67%. The PMMA/PVAm particles prepared have a diameter about 196 nm with a very narrow size distribution (PDI=1.09). ζ-potential measurement identified the formation of cationic PVAn shells. FE-SEM images showed that the particles were spherical with uneven surface morphology. These results are comparable with the PMMA/PVAm particles prepared using PVAmHCl form NVA under the same conditions as described in Chapter 4.

References:

1. Xu, J.; Barros Timmons, A.; Pelton, R., *N*-Vinylformamide as a route to amine-containing latexes and microgels. *Colloid and Polymer Science* **2004,** 282, (3), 256-263.
2. Shi, L.; Boduch-Lee, K. A.; Henssler, J. T.; Beckman, E. J.; Chapman, T. M., Synthesis and characterization of alkylated N-vinylformamide monomers and their polymers. *Journal of Polymer Science, Part A: Polymer Chemistry* **2004,** 42, (19), 4994-5004.
3. Kroner, M.; Dupuis, J.; Winter, M., *N*-vinylformamide - syntheses and chemistry of a multifunctional monomer. *Journal fuer Praktische Chemie (Weinheim,*

Germany) **2000,** 342, (2), 115-131.

4. Li, P.; Zhu, J.; Sunintaboon, P.; Harris, F. W., Preparation of latexes with poly(methyl methacrylate) cores and hydrophilic polymer shells containing amino groups. *Journal of Dispersion Science and Technology* **2003,** 24, (3 & 4), 607-613.
5. Gu, L.; Zhu, S.; Hrymak, A. N.; Pelton, R. H., Kinetics and modeling of free radical polymerization of N-vinylformamide. *Polymer* **2001,** 42, (7), 3077-3086.
6. Gu, L.; Zhu, S.; Hrymak, A. N.; Pelton, R. H., The nature of crosslinking in N-vinylformamide free-radical polymerization. *Macromolecular Rapid Communications* **2001,** 22, (3), 212-214.
7. Gu, L.; Zhu, S.; Hrymak, A. N., Acidic and basic hydrolysis of poly(*N*-vinylformamide). *Journal of Applied Polymer Science* **2002,** 86, (13), 3412-3419.
8. Yamamoto, K.; Imamura, Y.; Nagatomo, E.; Serizawa, T.; Muraoka, Y.; Akashi, M., Synthesis and functionalities of poly(*N*-vinylalkylamide). XIV. Polyvinylamine produced by hydrolysis of poly(*N*-vinylformamide) and its functionalization. *Journal of Applied Polymer Science* **2003,** 89, (5), 1277-1283.
9. Yoo, W.-J.; Li, C.-J., Highly Efficient Oxidative Amidation of Aldehydes with Amine Hydrochloride Salts. *Journal of the American Chemical Society* **2006,** 128, (40), 13064-13065.
10. Rappoport, Z., The chemistry of peroxides. John Wiley & Sons: Chichester, **2006**; Vol. 2, Part 1, P157.

Chapter 6

Synthesis and Characterization of PS/PVAm Core-shell particles

6.1 Introduction

Different types of core-shell particles can provide various properties, such as different T_g and hardness for a wide range of applications. In order to extend .the scope of core-shell particles with polyvinylamine (PVAm) shells, different types of particles with PVAm shells and various cores were developed to meet the requirements for specific applications. The effects of different reaction parameters on the graft copolymerization of MMA from PVAm have been investigated in Chapter 4. However, the optimized polymerization conditions for the synthesis of PMMA/PVAm particles could not been directly applied to other monomers, such styrene (St), *n*-butyl acrylate (BA) because of their different natures.

Our approach to prepare well-defined amphiphilic core-shell particles via the direct graft copolymerization of vinyl monomers from water soluble polymers containing amino groups is based on the reaction between alkyl hydroperoxides and amino groups of the water soluble polymer in water in the presence of dispersed vinyl monomers. During polymerization, the graft copolymerization of the monomer from the water soluble polymer and the homopolymerization of the monomer are initiated concurrently to generate amphiphilic graft copolymers and hydrophobic homopolymers respectively. The amphiphilic copolymers generated *in situ* act as polymeric surfactants, self-assembling to form micelle-like microdomains, which assist the emulsion polymerization of the vinyl monomer(s). This process can be divided into 4 stages: (1) The hydroperoxide (ROOH) initially interacts with amino groups on the polymer backbone, forming redox pairs to generate amino radicals and alkoxyl radicals (RO •); (2) Amino radicals initiate the graft copolymerization of monomer soluble in water to form amphiphilic graft copolymers, which can act like polymeric surfactants, while alkoxyl radicals can either abstract a hydrogen atom from the polymer backbone to generate backbone radicals that can also initiate the graft copolymerization of monomer soluble in water, or initiate homopolymerization of monomer like dispersion polymerization; (3) The amphiphilic graft copolymers self-assemble to form micelle-like microdomains when hydrophobic graft chains are long enough; (4) The graft copolymerization and homopolymerization are carried out in the micelle-like microdomains similar to the emulsion polymerization. During this particle formation process, solubility of the monomer in water has a significant influence on stage 2 and stage 3. If the monomer is too hydrophobic, the amphiphilic copolymer would be difficult to form because little monomer is available in water to under the graft copolymerization. But if it forms, self-assembling would occur quickly with a short grafted hydrophobic chain. On the contrary, if the monomer is too hydrophilic, the graft copolymerization would easily occur, but it would be difficult to reach the hydrophobic/hydrophilic balance, resulting in poorer micellar formation.

Styrene has a lower solubility in water (310 μg/ml) than MMA (16 mg/ml), thus it is more hydrophobic than MMA. It was found that the graft copolymerization of styrene from PVAm was quite different from that of MMA. Here we describe the synthesis and characterization of amphiphilic polystyrene (PS)/PVAm core-shell particles.

6.2 Experimental

6.2.1 Materials

Styrene (St) (a colorless liquid, Mw=104.15, density=0.909 g/cm^3, Aldrich) was purified first by washing it three times with a 10 wt.% sodium hydroxide (NaOH) aqueous solution to remove the inhibitor, then with di-ionized water until the pH of the water layer to neutral. Finally, the monomer was dried with anhydrous calcium chloride, followed by vacuum distillation. *tert*-Butyl hydroperoxide (TBHP) (70% solution in water, Aldrich) was used as received. De-ionized (DI) water was used as the dispersion medium.

Poly(*N*-vinylamine) (PVAm) solution (12 wt%) was prepared through neutralization poly(*N*-vinylammonium chloride) (PVAmHCl) solution with NaOH to pH 12, followed by purification using repeated cycles of precipitation-decantation-dissolution using freshly distilled acetone and DI water and concentration via vacuum distillation, as described in detailed in Chapter 3. The PVAm has a molecular weight of 320 kD as measured viscometrically.

6.2.2 Synthesis of PS/PMMA core-shell particles

For a total weight of 50 g, PVAm solution (2.1~14.0 g, 12 wt%) was first diluted in water (pH of the PVAm solution was 10.5) and charged into a water-jacketed flask equipped with a thermometer, a condenser, a mechanical stirrer and a nitrogen inlet and purged with nitrogen under stirring for 30 minutes. Styrene (1~6 g) was then charged into the reactor under stirring, followed by an addition of an appropriate amount of TBHP solution (5.0×10^{-6}~3.0×10^{-4} mol). The mixture was then kept at 80 ^{0}C for an appropriate time (2~12 h) under stirring. After the reaction, the particle dispersion was carefully purified by repeated centrifugation-decantation-dispersion cycles using DI water to remove unreacted water soluble polymer.

6.2.3 Measurement and Characterization

Monomer conversion was determined gravimetrically. The graft copolymers and homopolymers were isolated by Soxhlet extractions with chloroform for 48 hours. The grafting efficiency (GE%) was calculated as follows:

$$\text{GE \%} = \frac{\text{Weight of the grafted PS}}{\text{Weight of the total polymerized St}} \times 100$$

IR spectra were recorded on a Nicolet Avatar 360 FT-IR spectrophotometer using KBr disks. ^{1}H-NMR spectral determination was made on a Bruker Advance DPX-400 using D_2O as a solvent Particle size and distribution were measured on a Coulter LS230 Particle Size Analyzer. The ζ-potential of the particles was determined with a

Malvern Zetasizer 3000HSA (Malvern, UK) in a 1.0×10^{-3} M NaCl solution. The surface morphologies of the particles were observed with a JEOL JSM 6335F Field Emission Scanning Electron Microscope (FE-SEM). Samples were prepared by coating the dried particles spread on a glass surface with a thin layer of gold to a depth of ca. 5 Å. under vacuum. Transmission Electron Microscopy (TEM) micrographs were obtained with a JEM 100 CX transmission microscope at an accelerating voltage of 100 kV. Each sample was prepared by wetting a carbon-coated grid with a small drop of dilute particle dispersion. The dried particles were directly observed by TEM or treated with a small drop of phosphotungstic acid (PTA) solution (2 wt.-%) for 40 minutes, then dried at room temperature before the observation.

6.3 Results and discussions

6.3.1 Synthesis of PS/PVAm core-shell particles

Scheme 6.1 shows the reaction for the synthesis of amphiphilic PS/PVAm core-shell particles. The PVAm solution was treated with a small amount of TBHP in water at 80 ^{o}C in the presence of styrene to generate PS/PVAm particles. Stable particles were produced in the absence of surfactant because the PVAm provided not only reactive primary amino group for generating macroinitiator, but also electrosteric stabilization for the particles.

To obtain PS/PVAm particles with narrow size distribution, the effects of various reaction parameters such as reaction time, TBHP concentration and solid content

(SC%) on the formation of PS/PVAm particles have been investigated.

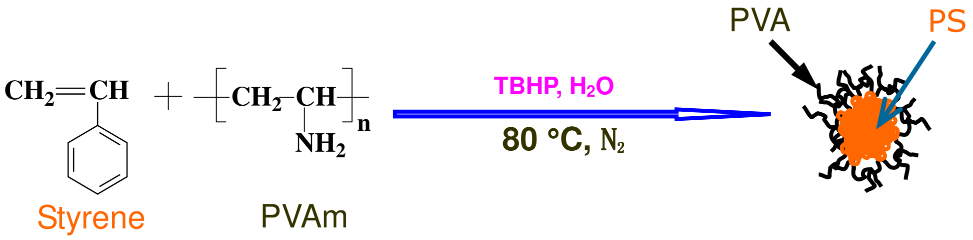

Scheme 6.1. Synthesis of PS/PVAm core shell particles

6.3.2 Effect of reaction time

The synthesis of PS/PVAm core-shell particles was first carried out using optimum reaction conditions for the synthesis of PMMA/PVAm particles ([TBHP]= 0.1 mM, reaction for 2 hours at 80 °C at pH 10.5 with 2.5% solid content as shown Table 6.1, P56). The particles produced had a number average diameter about 141 nm with a very narrow size distribution (PDI=1.11) (Figure 6.1a). However, the conversion was only 15% and the particles formed were coagulated quickly because of a large amount of unreacted St remaining in the dispersion. Therefore, the pH of the particle dispersion obtained had to be adjusted to 7 after polymerization to increase the surface charge density of the particles to keep them stable.

To increase the monomer conversion, the reaction time was increased from 2 to 12 hours (Table 6.1, P71). A higher monomer conversion up to 72 % was obtained. However, the particle size became much larger (D_n=569 nm) and the particle size distribution was broader (PDI=1.49) than before, as shown in Figure 6.1b. In addition, a lot of precipitates were obtained during the graft copolymerization of St from

PVAm. The increase of particle size and size distribution might be attributed to the secondary nucleation during the polymerization, which might be induced by the homopolymerization of styrene at 80 °C under a longer reaction time. The results indicate that the low monomer conversion might be due to the low polymerization rate of styrene during the reaction.

Table 6.1 Effect of reaction time on the graft copolymerization of St from PVAm[1]

Entry	Time (h)	Observation	Conv. (%)	D_v (nm)	D_n (nm)	PDI
P56	2	A lot of precipitate	15	156	141	1.11
P71	12	a lot of precipitate	72	846	569	1.49

[1] Other conditions: Temperature=80 °C; [TBHP]=0.1 mM; SC%=2.5; Reaction pH=11; Weight ratio of PVAm to styrene=1:4; Total weight=50 g

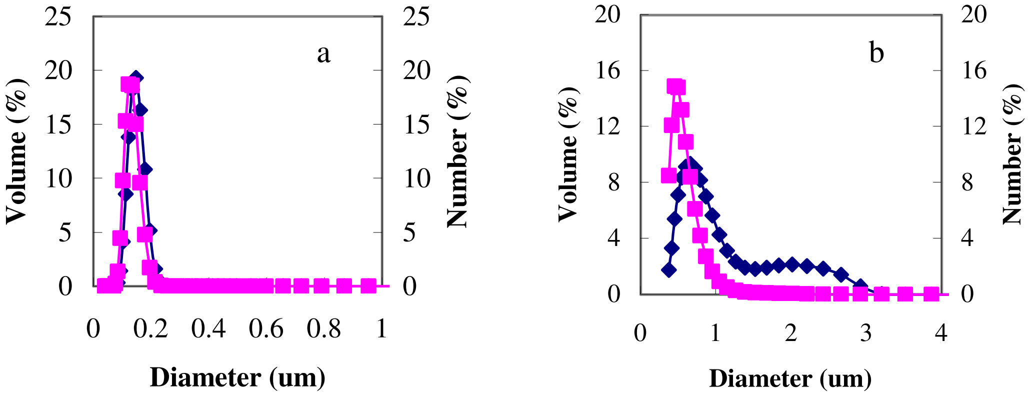

Figure 6.1 Effect of reaction time a) 2 h; b) 12 h on the particle size and size distribution. D_v (◆); D_n (■).

6.3.3 Effect of TBHP concentration

It is well known that the increase of initiator concentration can significantly increase the polymerization rate. Because the amount of TBHP used in the previous reactions were much less than that of the amino groups on the PVAm chains (1:1000 in mole ratio) in our system, increasing TBHP concentrations were expected to increase the radical concentrations, thus resulting in the increase of polymerization rate of styrene and monomer conversion.

Table 6.2 Effect of TBHP concentration on the graft copolymerization of styrene from PVAm[1]

Entry	[TBHP] (mM)	Reaction time (h)	Observation	Conv. (%)	Dv (nm)	Dn (nm)	PDI
P72	0.1	12	A lot of precipitation	55	1029	726	1.42
P75	0.2	12	A lot of precipitation	62	1066	778	1.37
P92	0.5	12	A lot of precipitation	71	565	86	6.59
P95	1	5	A lot of precipitation	66	637	165	3.87
P96	2	5	Stable	100	204	187	1.09

[1] Other conditions: Temperature=80°C; SC%=5; Reaction pH=11; Weight ratio of PVAm to styrene=1:4; Total weight=50 g.

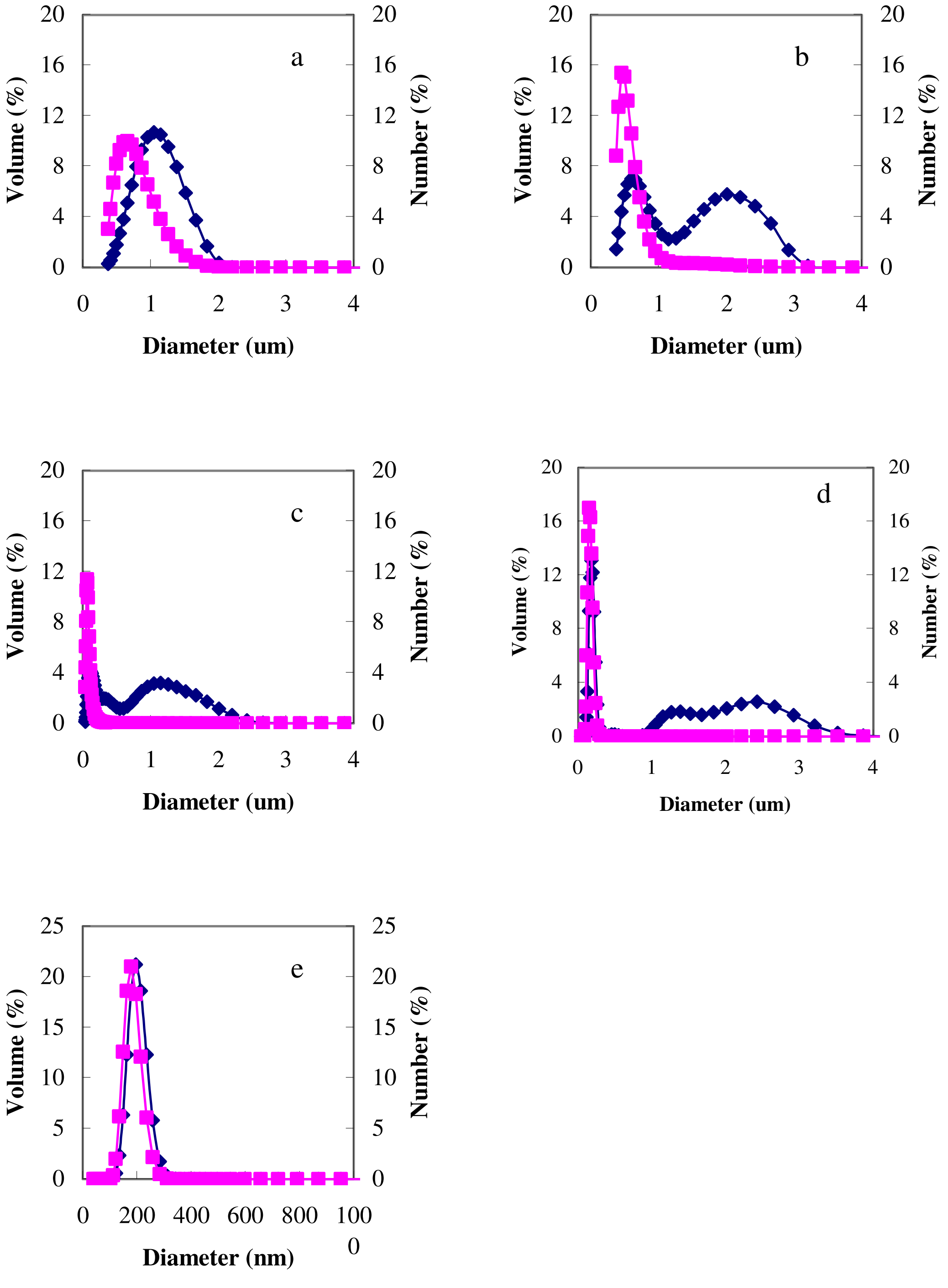

Figure 6.2 Effect of TBHP concentration on the particle size and size distribution. D_v (◆); D_n (■). TBHP concentration: a) 0.1 mM; b) 0.2 mM; c) 0.5 mM; d) 1 mM; e) 2 mM

Table 6.2 and Figure 6.2 summarize the effect of TBHP concentration on the graft copolymerization of St from PVAm. When the TBHP concentration was increased from 0.1 to 0.5 mM with a reaction time of 12 hours (P72, P73, P92,), the monomer conversion increased slightly from 55 to 70%. However, all of the three particles obtained had a large particle size (D_v >500 nm) and a broad size distribution (PDI>1.37) (Figure 6.2a, b and c). Further increase of the TBHP concentration to 1 mM while reducing the reaction time to 5 hours slightly reduced the monomer conversion to 66% (P95, Table 6.2) and the particles were still had a large size (D_v=637 nm) with a multi-model size distribution (PDI=3.87) (Figure 6.2d). A lot of precipitates were formed during polymerization in all of the four reactions. When the TBHP concentration was further increased to 2 mM, stable and highly uniform particles were produced (D_v=204 nm, PDI=1.08, Figure 6.2e). The monomer conversion was nearly 100% without any precipitate. The high monomer conversion was attributed to the high polymerization rate at a high TBHP concentration. These results suggest that the monomer conversion and particle size and size distribution are strongly dependant on the TBHP concentration.

6.3.4 Effect of solid content

A latex with high solid content (SC%) is favorable for the reason of economy and transportation in industry. Thus the effect of solid content on graft copolymerization of MMA from PVAm was investigated.

Table 6.3 Effect of solid content on the graft copolymerization of St from PVAm[1]

Entry	SC%	[TBHP] (mM)	Observation	Conv. (%)	Dv (nm)	Dn (nm)	PDI
P98	2.5	1	Stable	99	291	276	1.05
P95	5	1	A lot of precipitate	66	637	165	3.87
P96	5	2	Stable	100	204	187	1.09
P117	10	4	Stable	100	152	138	1.10
P107	15	6	Too viscous	100	195	172	1.13

[1] Other conditions: Temp.=80 ^{o}C; Reaction pH=11; reaction time=5 h; Weight ratio of PVAm to styrene=1:4; Total weight=50.

Table 6.3 shows the effect of solid content on graft copolymerization of styrene from PVAm. When the solid content of the reaction system was 2.5% (P98, Table 6.3), high monomer conversion up to 99% could be achieved at a TBHP concentration of 1 mM, producing stable and uniform (PDI=1.05) particles with a number average diameter (D_n) of 276 nm. When the solid content was increased to 5% while keeping the TBHP concentration at 1 mM (P95, Table 95), the monomer conversion was only 66% and the particles were unstable and had a larger size with a very broad size distribution (PDI=3.87). These results strongly suggest that the ratio of TBHP and monomer must be kept at a certain ratio to assure a successful polymerization. When the TBHP concentration was increased in proportion with the increase of the solid content, stable and uniform particles with comparable particle sizes were obtained with solid content up to 15% (P117 and P107, Table 6.3). All of the monomer conversions reached 100%. The findings indicate that this could be a commercially viable route.

When the solid content reached 15%, the particle dispersion obtained was so viscous that it almost lost its fluidizability. Hence, the maximum solid content for the batch synthesis of PS/PVAm particles under these conditions might be 15%.

6.3.5 Composition of PS/PVAm particles

The PS/PVAm particles were composed of both amphiphilic PVAm-g-PS graft copolymers and hydrophobic PS homopolymers. The graft copolymers and homopolymers were separated by Soxhlet extraction of the resultant polymers with chloroform for 48 hours. The compositions of the homopolymers obtained from the organic layer and the insoluble graft copolymers were determined gravimetrically. It was found that the grafting efficiency of polystyrene was only 15%, in other words, 85% polystyrene in the particle was in the form of homopolymer. Such high percentage of homopolymer formation might be attributed to the higher TBHP concentration (2 mM for 5% solid content reaction system) used for the polymerization, thus resulting in higher *tert*-butoxy and hydroxyl radical concentrations through thermal decomposition. These reactive radicals could initiate the homopolymerization of styrene. Structures of PVAm, homopolymer and graft copolymer isolated were identified with FTIR spectroscopy (Figure 6.3). The FT-IR spectrum of the PS/PVAm particles shows some typical peaks of PS at 3002-3103 cm^{-1} (C-H aromatic stretching vibration), 1601 cm^{-1} (C-C stretching frequency of ring in plane), 1493 cm^{-1} (C-H stretching vibration of ring in plane) as well as 751 and 695 cm^{-1} (C-H out-of-plane bending vibration of ring).[1-3] The peaks at about 3433 cm^{-1} and 1644 cm^{-1} corresponded to the amine groups of PVAm. Therefore, FT-IR spectra confirmed that the particles consisted of both grafted amphiphilic copolymer and homopolymer.

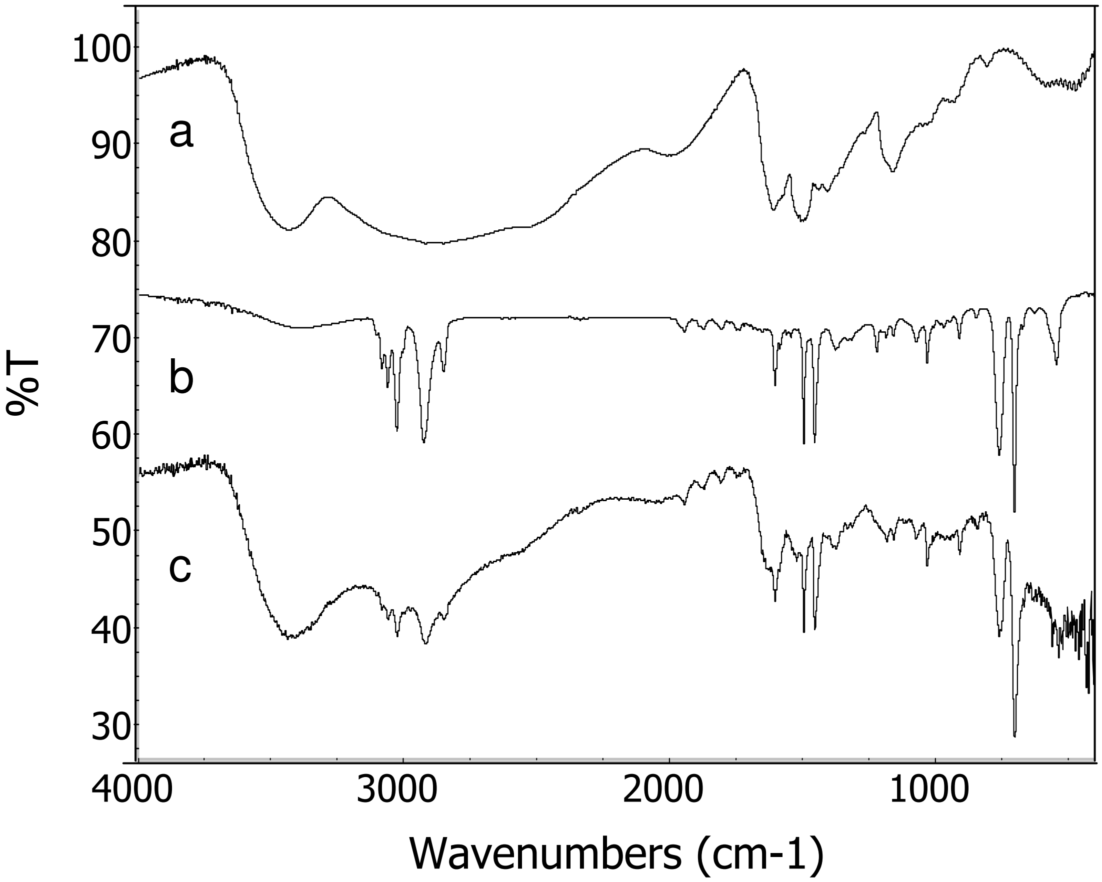

Figure 6.3 Comparison of FTIR spectra of (a) PVAmHCl; (b) PS homopolymer isolated from PS/PVAm particles; (c) PVAm-g-PS graft copolymer.

6.3.6 Morphology of PS/PVAm Particles

The morphologies of the PS/PVAm particles were studied with FE-SEM and TEM. Both the particles with or without staining with PTA solution were observed with TEM. The TEM pictures reveal that the particles have a core-shell structure with thin shells. The FE-SEM micrograph (Figure 6.4a) and TEM images of the particles without staining (Figure 6.4b) show that the PS/PVAm particles are highly mono-dispersed and the particle sizes are in accordance with above results. They also show that PS/PVAm particles are spherical with a smooth surface, which is quite different from that of the PMMA/PVAm particles. The variation in particle morphology might be attributed to the large difference in the grafting efficiency between the two particles and the side reactions between monomer(s) with PVAm during the polymerization. PMMA/PVAm particles had a much higher grafting efficiency than PS/PVAm particles (76% versus 15%). The high content of the PVAm-g-PMMA graft copolymer could promote the compatibility between PVAm and the PMMA homopolymers, thus lowering the interfacial tension at the polymer–polymer interface and increasing the amount of PMMA in the PVAm phase. Meanwhile, there are three side reactions occurring when MMA was graft-copolymerized to PVAm at pH 12: (1) Michael addition between PVAm and MMA, (2) hydrolysis of MMA, and (3) 1,2-addition between and MMA, as described in detail in Chapter 4. Both the hydrolysis of MMA to MAA, which further form a salt with PVAm, and 1,2-addition to MMA monomer result in introducing carbon double bonds as the side chains of the PVAm polymer, thus increasing the graft efficiency of MMA. These two reactions and the Michael addition of PVAm to MMA all lead to the hydrophobic modification of the PVAm. The hydrophobically modified PVAm could also lower the interfacial tension at the polymer–polymer interface and improve the solubility of PMMA in PVAm phase or itself might be phase separated to form uneven surface on the PVAm shells.

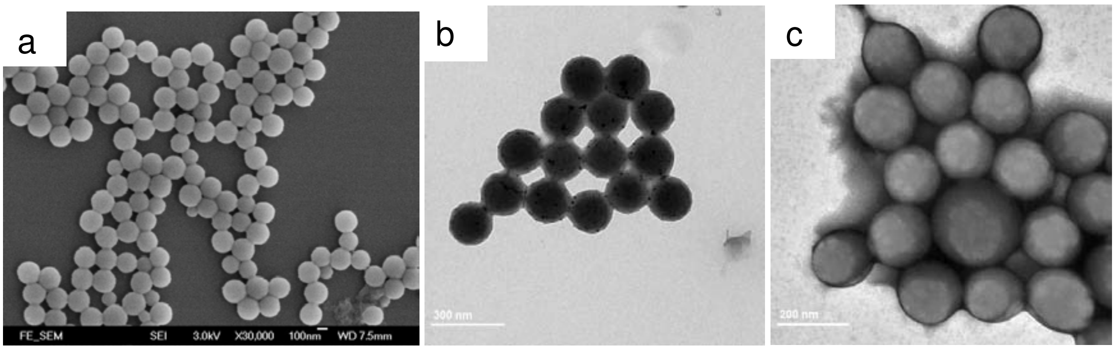

Figure 6.4 FE-SEM and TEM pictures of PS/PVAm particles (P96). (a) FE-SEM; (b) TEM (particles without staining); (c) TEM (particles stained with 2% PTA solution for 40 minutes).

To find out if there are side reactions between PVAm and styrene during the graft copolymerization of styrene from PVAm, PVAm was reacted with styrene at pH 12 at 80 ^{o}C for 3 hours in the absence of TBHP. After the reaction, the pH of the mixture was about 11.3, and adjusted to 2 with 6M HCl. Finally, the mixture was extracted with toluene to remove unreacted styrene and, if any, homopolymerized PS (Scheme 6.2). The product obtained was characterized with ^{1}H NMR spectroscopy. In the ^{1}H NMR spectrum of the product of styrene and PVAm (Figure 6.5), there is a weak peak at about 7.42 ppm which attributed to the protons on phenyl groups. The NMR result indicates that the Michael addition of PVAm onto styrene can also occur. However, the peak is very weak, suggesting that the Michael addition is very minor. Therefore, for PS/PVAm particles, the low grafting efficiency and minor reaction between styrene and PVAm resulted in poorer compatibility between PS and PVAm. Because polystyrene is more hydrophobic than PMMA, it should be more spherical in order to reduce interfacial tension between PS-water and PS-PVAm interfaces.

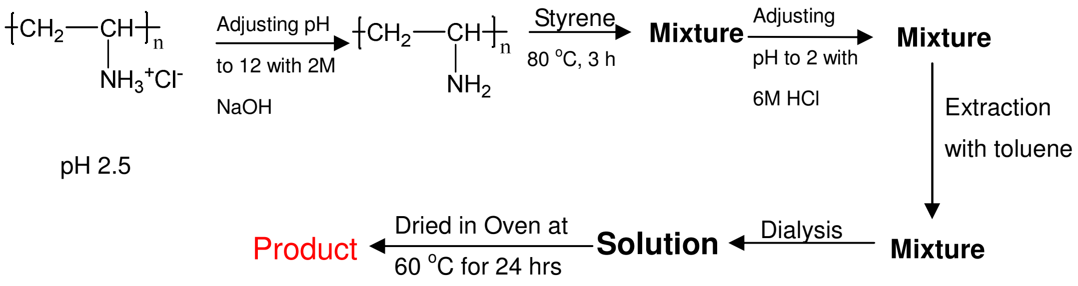

Scheme 6.2 Procedure for reaction between PVAm and styrene at pH 12 for 3 hours, followed by purification

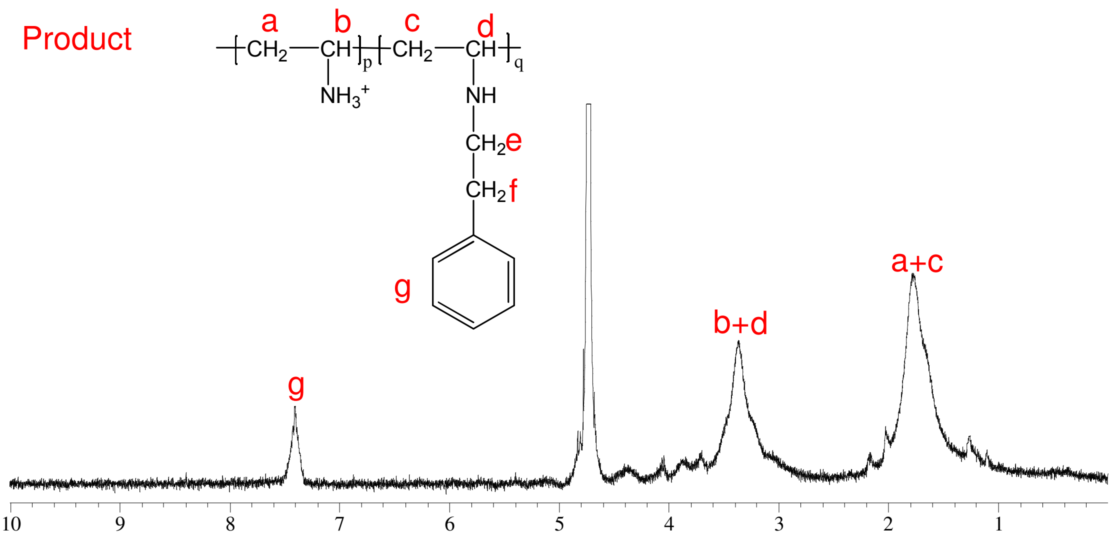

Figure 6.5 ^{1}H NMR spectrum in D_2O of the product of styrene and PVAm at pH 12 at 80 °C for 3 hours

6.4 Conclusions

Amphiphilic PS/PVAm core-shell particles were synthesized by a direct graft copolymerization of styrene from PVAm in water induced with a small amount of TBHP. Amphiphilic graft copolymers and PS homopolymers were generated concurrently to form highly monodispered particles with diameters in the range of

100-300 nm. Comparing with the synthesis of PMMA/PVAm core-shell particles, a higher TBHP concentration was required in the synthesis of PS/PVAm particles to achieve high monomer conversion and narrow particle size distribution. The formation of graft copolymers and homopolymers were confirmed by FTIR. FE-SEM studies indicated that PS/PVAm particles were spherical with smooth surface morphology, while TEM investigation revealed that they have a core-shell structure with thin shells. The particles could be produced up to 15 wt.% solid content, indicating that the process is amenable to commercial production.

References:

1. Bhutto, A. A.; Vesely, D.; Gabrys, B. J., Miscibility and interactions in polystyrene and sodium sulfonated polystyrene with poly(vinyl methyl ether) PVME blends. Part II. FTIR. *Polymer* **2003,** 44, (21), 6627-6631.
2. C. Y. Liang, S. K., Infrared spectra of high polymers. VI. Polystyrene. *Journal of Polymer Science* **1958,** 27, (115), 241-254.
3. Huang, Z.-L.; Liu, L.-X.; Lei, H.; Zhao, Y.-D., Vibrational spectroscopic encoding of polystyrene resin bead: a combined FT-IR and computational study. *Journal of Molecular Structure* **2005,** 738, (1-3), 155-159.

Chapter 7

Synthesis and Characterization of Poly(BA-MMA)/PVAm Core-Shell Particles

7.1 Introduction

n-Butyl acrylate (BA) is an important and commonly used monomer in polymer synthesis. It has a very poor solubility (0.14 g/100ml) in water at 25 °C when compared to methyl methacrylate (MMA) (1.6 g/100 ml), and its homopolymer, poly(*n*-butyl acrylate) (PBA), has a much lower glass transition temperature (Tg ≈ -54 °C) than poly(methyl methacrylate) PMMA (Tg ≈ 106 °C) and polystyrene (PS) (Tg ≈ 100 °C). Through copolymerization with MMA, styrene and other functional monomers, BA can form copolymers to alter the Tg and other properties in order to meet specific requirements. Thus it has been widely used in latexes, coatings, adhesives, leather finishing, paper-making and so on.

PMMA/PVAm and PS/PVAm core-shell particles which have hard cores have been successfully prepared through the direct graft copolymerization of MMA or Styrene from PVAm as described in previous chapters. Here, we describe the synthesis and characterization of PVAm-based particles with poly(BA-MMA) copolymer as the cores. The core composition was varied to consist of 60% BA and 40% MMA with a Tg at about -10 °C. Another core was composed of 25% BA and 75% MMA with a Tg at about 47 °C. The two cores have different Tg and hardness, thus they can provide different mechanical properties to meet specific requirements.

7.2 Experimental

7.2.1 Materials

Both *n*-Butyl acrylate (BA) (Aldrich) and methyl methacrylate (MMA) (Aldrich) were purified by first washing the monomers three times with a 10 wt.-% NaOH solution, then with de-ionized (DI) water until the pH of the water layer to neutral. The monomers were dried with anhydrous $CaCl_2$, followed by vacuum distillation.

tert-Butyl hydroperoxide (TBHP) (70% solution in water, Aldrich), glutaraldehyde (GA) (50 wt.-% aqueous solution, Aldrich), reagent grade of hydrochloric acid (HCl) (37%, Aldrich) and NaCl (Fluka) were all used as received. DI water was used as the dispersion medium.

Poly(*N*-vinylamine) (PVAm) solution (10.5 wt%) was prepared through neutralization poly(*N*-vinylammonium chloride) (PVAmHCl) solution with NaOH pellets to pH 12, followed by purification with repeated cycle of precipitation-decantation-dissolution using freshly distilled acetone and DI water, followed by concentration via vacuum distillation, as described in Chapter 3. The PVAm has a molecular weight of 340 kD as measured viscometrically.

7.2.2 Graft copolymerization of BA and MMA from linear PVAm

For a total solution of 50 g with a solid content (SC%) of approximately 2.5~5 wt.-%, a PVAm aqueous solution (2.4~4.8 g, 10.5 wt%) was first diluted in DI water (pH of the PVAm solution was 10.5), and the solution pH was adjusted to an appropriate value (8.5~12). The solution was then mixed with an appropriate amount of NaCl (up to 0.7313 g) and purified BA (0.25~1.2 g) and MMA (0.4~1.5 g) in a three-necked water-jacketed flask equipped with a thermometer, a reflux condenser, a magnetic stirrer, and a nitrogen inlet. The stirred mixture was degassed for 30 min under nitrogen. An appropriate amount of TBHP (0.063~0.625 mL of 8 mM aqueous solution) was then added and the mixture was kept at 80 ^{o}C for 2 hours under stirring.

7.2.3 Graft copolymerization of BA and MMA from crosslinked PVAm

PVAm was slightly crosslinked by using an appropriate amount of glutaraldehyde (GA) prior to the polymerization. A detailed description of the procedure is as follows. For a total solution of 80 g with a SC% of approximately 5 wt.-%, linear PVAm aqueous solution (7.6 g, 10.5 wt.-%) was diluted in DI water, and the pH of the solution was adjusted to 8.0 with 3 M HCl solution. The solution was then mixed with an appropriate amount of GA solution (up to 2 mL, 5 wt.-%) in a water-jacketed flask equipped with a thermometer, a condenser, a magnetic stirrer and a nitrogen inlet. The mixture was stirred overnight at room temperature, and then heated at 80 ^{o}C for 2 hours. A small amount of MMA (about 0.5 g) was first mixed with PVAm solution at 80 ^{o}C for 30 minutes. The remaining monomers (2.7 g) and diluted TBHP solution (1.2 mL of 2.0×10^{-2} M solution) were added and the polymerization was carried out at 80 ^{o}C for 3 hours under nitrogen atmosphere.

7.2.4 Measurement and Characterization

The monomer conversion was determined gravimetrically. The graft copolymers and homopolymers were isolated by Soxhlet extractions with chloroform for 48 hours. The grafting efficiency (GE%) was calculated as follows:

$$\text{GE\%} = \frac{\text{Weight of the grafted}}{\text{Weight of the total polymerized}} \times 100$$

IR spectra were recorded on a Nicolet Avatar 360 FT-IR spectrophotometer using KBr disks. ^{1}H-NMR spectral determination was made on a Bruker Advance DPX-400 using D_2O as a solvent. Particle size and size distribution were measured on a Coulter LS 230 Particle Size Analyzer. The ζ-potential of the particles was determined with a Malvern Zetasizer 3000HSA (Malvern, UK) in a 1.0×10^{-3} M NaCl solution. The surface morphologies of the particles were observed with a JEOL JSM 6335F Field Emission Scanning Electron Microscopy (FE-SEM). Samples were prepared by coating the dried particles spread on a glass surface with a thin layer of gold to a depth of ca. 5 Å. under vacuum. Transmission Electron Microscopy (TEM) micrographs were obtained with a JEM 100 CX transmission microscope at an accelerating voltage of 100 kV. Sample was prepared by wetting a carbon-coated grid with a small drop of dilute particle dispersion. After absorption of water, the wet particles were treated with a small drop of phosphotungstic acid (PTA) solution (2 wt.-%) for 3 minutes, then dried at room temperature.

7.3 Results and Discussions

7.3.1 Graft copolymerization of BA and MMA from linear PVAm

Synthesis of poly(BA-MMA)/PVAm particles was first attempted by direct graft copolymerization of a mixture of BA and MMA from linear PVAm using the same procedure for the synthesis of PMMA/PVAm or PS/PVAm particles, as illustrated in Scheme 7.1.

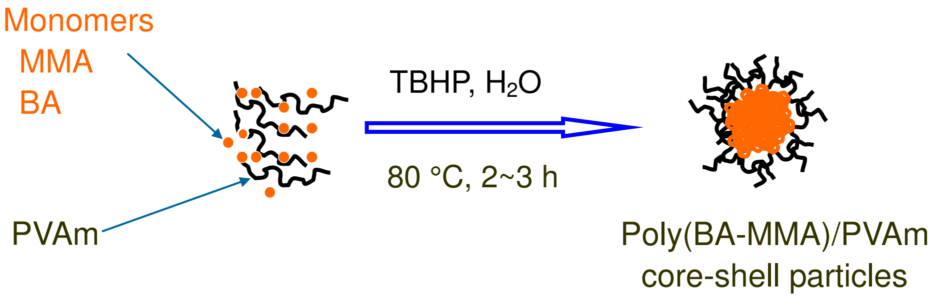

Scheme 7.1 Synthesis of poly(BA-MMA)/PVAm particles from linear PVAm

The reaction parameters for the formation of poly(BA-MMA)/PVAm particles were first optimized using a monomer weight ratio of BA to MMA at weight ratio of 60:40 [BA(60)/MMA(40)). The graft copolymerization of BA/MMA from PVAm was carried out at pH 12 using optimum reaction conditions for the synthesis of PMMA/PVAm particles ([TBHP] = 0.1 mM**,** reaction for 2 hours at 80 ^{o}C at pH 12 with 2.5% solid content (SC%) as shown in Table 7.1, P66). A monomer conversion up to 64% was obtained. However, gelation was observed after the copolymerization started for about 10 minutes. The gel formation was first attributed to the poor electrostatic repulsion between the PVAm molecules at pH 12. Therefore, the graft copolymerization of BA/MMA was carried out again at a lower pH (8.5 instead of 10.5) in order to increase the charge repulsion on PVAm. As shown in Table 7.1, comparable monomer conversions were obtained. However, the gel formation still occurred in these conditions, indicating that the poly(BA-MMA)/PVAm particles could not be obtained by simply adjusting the solution pH to enhance the electrostatic repulsion.

Table 7.1 Effect of pH on the graft polymerization of BA/MMA from PVAm[1]

Entry	Reaction pH	Conv. (%)	Observation
P66	12	64	Gel formation and severe phase separation
P55	10.5	74	A clear white-blue gel, a little phase separation
P73	9	77	A clear gel, which can not flow
P90	8.5	78	A clear gel, which can not flow

[1] Other conditions: Temperature=80 ^{o}C; Reaction time=2 h; Weight ratio of PVAm to monomers=1:4; [TBHP]=0.1mM; Total weight=50 g; SC%=2.5

Table 7.2 Effect of TBHP concentration on the graft polymerization of BA/MMA from PVAm[1]

Entry	[TBHP] (mM)	Conv. (%)	Observation
P55	0.1	73.8	A clear white-blue gel; a little phase separation
P67	0.05	55	A clear gel, which can not flow
P80	0.01	62.5	A clear gel, which can not flow

[1] Other conditions: Temperature=80 ^{o}C; Reaction time=2 h; Reaction pH=10.5; Weight ratio of PVAm to monomers=1:4; [TBHP]=0.1 mM; Total weight= 50 g; SC%=2.5

Since poly(BA-MMA)/PVAm particles could not be obtained by lowering the reaction pH to enhance the electrostatic repulsion, it was suspected that the gel formation might be induced by the fast polymerization rate of BA during the graft copolymerization. Thus the graft copolymerizations of BA/MMA from PVAm were performed using lower TBHP concentration (0.01 mM) (Table 7.2, P67 and P80). However, gel formation still occurred in this case, suggesting that the TBHP concentration was not the reason for the gel formation.

Table 7.3 Effect of salt concentration on the graft polymerization of BA/MMA from PVAm[1]

Entry	[NaCl] (M)	SC %	Conv. (%)	Observation
P55	0	2.5	73.8	A clear white-blue gel; a little phase separation
P59	0.1	2.5	68.9	A gel; severe phase separation
P62	0.2	2.5	53	A semi-transparent dispersion, some gel D_v=1427nm, D_n=580nm, PDI=2.46
P77	0.25	2.5	63	A semi-transparent dispersion Some gel formed in reactor; D_v=135nm, D_n=106nm, PDI=1.27
P82	0.1	5	--	A gel, which could not flow
P86	0.125	5	--	Particles coagulated
P85	0.15	5	--	Particles coagulated
P84	0.2	5	--	Particles coagulated
P81	0.25	5	--	Particles coagulated

[1] Other conditions: Temperature=80^{o}C; Reaction time=2h; Reaction pH=10.5; Weight ratio of PVAm to monomers=1:4; [TBHP]=0.1 mM; Total weight=50 g.

It is well known that electrolytes in polymer solution can reduce the solubility of the polymer, thus the graft copolymerization of BA/MMA from PVAm was carried out at different NaCl concentrations and results are summarized in Table 7.3. When the solid content of the reaction system was 2.5%, gel formation occurred at the salt concentration lower than 0.1 M (Table 7.3, P55 and P59). Semi-transparent dispersions were formed when the salt concentrations were up to 0.25 M (P62 and P77). The particle sizes were about 106 nm in diameter with a PDI about 1.27. However, stable particles were unable to obtain with the salt concentration ranging from 0.1 to 0.25 M when the solid content of the reaction system was increased to 5%. These results show that changing salt concentration still could improve the formation of poly(BA-MMA) particles.

Because the synthesis of PMMA/PVAm particles was successful, while poly(BA-MMA) particles could not be obtained under the same reaction conditions, it was obvious that of the presence of PBA caused the formation of gels, which might be due to its low Tg. Thus a seed polymerization procedure was developed to address the problem of gel formation. As shown in Scheme 7.2, PVAm was first treated with a small amount of TBHP in water at 80 ^{o}C for 15~30 minutes in the presence of MMA to generate PMMA/PVAm seed particles. Then BA was then charged into the reaction system to perform a seed polymerization for 2.5 hours and produce poly(BA-MMA)/PVAm particles. It was expected that BA would be polymerized in the core of PMMA/PVAm particles, thus preventing the gel formation.

$$\begin{array}{c}\text{PVAm}\\+\\\text{MMA}\end{array}\xrightarrow[80\ ^{o}\text{C, N}_2\text{, 15\textasciitilde 30 min}]{\text{TBHP, H}_2\text{O}}\begin{array}{l}\text{PMMA/PVAm}\\\text{seed particles}\end{array}\xrightarrow[\substack{\text{seed polymerization}\\\text{2.5 h}}]{\text{BA}}\begin{array}{l}\text{P(BA-MMA)/PVAm}\\\text{core shell particles}\end{array}$$

Scheme 7.2 Synthesis of poly(BA-MMA)/PVAm particles by seed polymerization

Table 7.4 Synthesis of poly(BA-MMA)/PVAm particles by seed polymerization[1]

Entry	Reaction pH	SC %	Conv. (%)	Observation
P105	10.5	2.5	--	BA was fed after formation of particles. A gel formed in 30 minutes after addition of BA.
P110	8.5	5	53.5	A semi-transparent dispersion was obtained, forming gel after one day.

[1] Other conditions: Temperature=80°C; reaction time=3h; weight ratio of PVAm to monomers=1:4; [TBHP]=0.1mM; Total weight=50 g.

The seed polymerization was first performed at pH 10.5 with a solid content of 2.5% (Table 7.4, P105). Unfortunately, gel formation occurred in 30 minutes after the addition of BA. Another experimental was carried out at pH 8.5 with a solid content of 5% (P110). A semi-transparent dispersion was obtained. The product changed to a gel in 24 hours after the polymerization. Based on these results, it was concluded that the linear PVAm was unable to provide enough stability for the production of stable poly(BA-MMA)/PVAm particles.

7.3.2 Graft copolymerization of BA and MMA from GA-crosslinked PVAm

Increasing electrostatic or steric interaction or a combination of both is considered to be one of the solutions to address the gel formation problem. The linear PVAm was slightly crosslinked by treatment with glutaraldehyde (GA) before polymerization to provide better steric stabilization. The reaction between GA and PVAm has been described in detail in Chapter 4. The crosslinking degree (CD%) was expressed as a percentage of the molar ratio of –CHO groups of the GA and $-NH_2$ groups of the PVAm. The crosslinked PVAm was less soluble than the linear PVAm in water, thus possibly promoting the micellar formation during the graft copolymerization.

7.3.2.1 Synthesis of poly[BA(60)-MMA(40)]/PVAm core-shell particles

The synthesis of poly(BA-MMA)/PVAm particles using GA-crosslinked PVAm was first attempted by treating PVAm with 5% GA at pH 10.5 at 80 ^{o}C for 10-120 minutes (Scheme 7.3). Then BA and MMA were charged into the reaction system and the mixture was purged with N_2 for 30 minutes to remove oxygen. Finally, TBHP was added into the reaction system to induce the graft copolymerization (Table 7.5, P99, P100 and P104). However, gel formation occurred in 20 minutes after addition of monomers before adding the TBHP in all cases. It was suspected that the crosslinking reaction between PVAm and GA at 80 ^{o}C would initiate the polymerization of monomers.

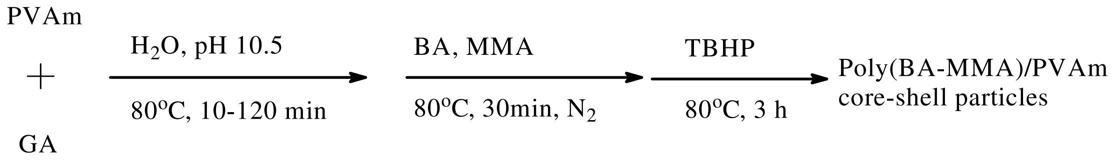

Scheme 7.3 Procedure 1 designed for the synthesis of poly(BA-MMA)/PVAm core-shell particles

Table 7.5 Synthesis of poly(BA-MMA)/PVAm core-shell particles using Scheme 7.3[1]

Entry	CD (%)	SC (%)	Reaction time of PVAm and GA before addition of monomers	Observation
P99	1	2.5	10 min	A gel formed in 20 min after addition of monomers
P100	1	2.5	40 min	
P104	5	5	120 min	

[1] Other conditions: Temperature=80°C; Weight ratio of PVAm to monomers=1:4; [TBHP]=0.1 mM; Total weight=50 g.

To avoid gel formation, the reaction time for crosslinking PVAm with GA was extended to 12 hours under room temperature (Scheme 7.4). The reaction pH was also changed to pH 8 to promote the crosslinking according to a literature report.[1] However, as shown in Table 7.6, gel formation occurred in 15 minutes after the addition of BA and MMA again prior to the addition of TBHP.

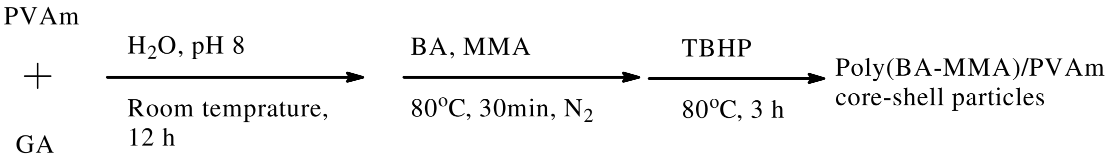

Scheme 7.4 Synthesis of poly(BA-MMA)/PVAm core-shell particles (procedure 2)

Table 7.6 Synthesis of poly(BA-MMA)/PVAm core-shell particles using Scheme 7.4[1]

Entry	CD (%)	SC (%)	Observation
P108	5	2.5	A gel formed in 15 min after addition of monomers

[1] Other conditions: Temperature=80°C; Weight ratio of PVAm to monomers=1:4; [TBHP]=0.1 mM; Total weight=50 g.

It has been reported that free radicals are generated when heating the products of the amino-carbonyl reactions between sugars or related carbonyl compounds and amino acids or amines [2, 3] (Eq. 7.1), or the Maillard reaction between glycolaldehyde or glyceraldehydes and *N, N*-dialkylethylenediamine (alkyl = methyl, ethyl, *iso*-propyl, *tert*-butyl)[4] (Eq.7.2). Thus, the gel formation before the addition of TBHP was probably initiated by the free radicals generated during heating the reaction mixture containing GA and PVAm.

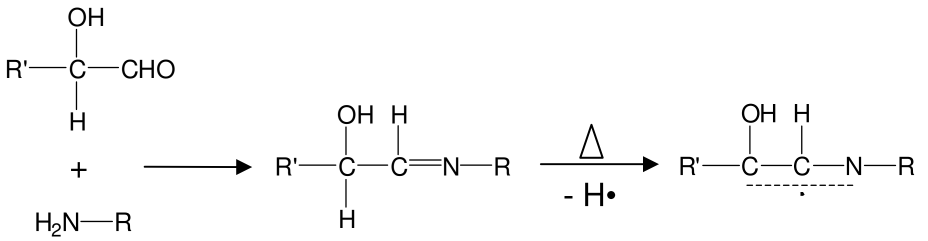
(Eq.7.1)

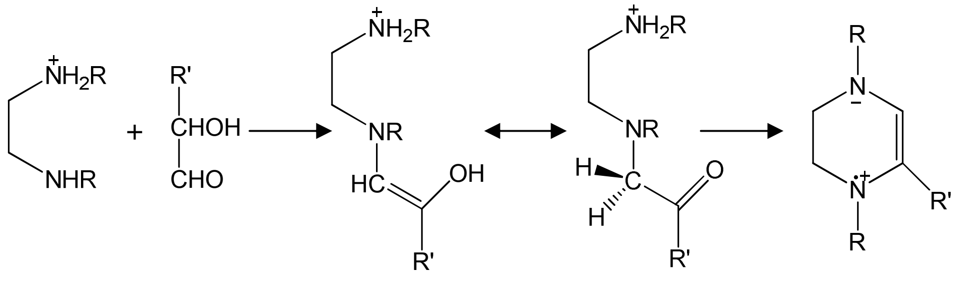
(Eq.7.2)

The gel formation occurred when BA was introduced into the reaction system, while no gel was formed when only MMA was used. Thus to avoid the gel formation by the polymerization of BA initiated by the free radicals generated via heating the product of aldehyde and amine redox reaction, MMA was first added into the reaction system after PVAm was crosslinked overnight at pH 8 under room temperature, and the reaction mixture was kept at 80 °C for 2 hours to consume most of radicals.

Finally BA and TBHP were charged and the polymerization was carried out at 80 °C for 3 hours to generate poly(BA-MMA)/PVAm core-shell particles (Scheme 7.5).

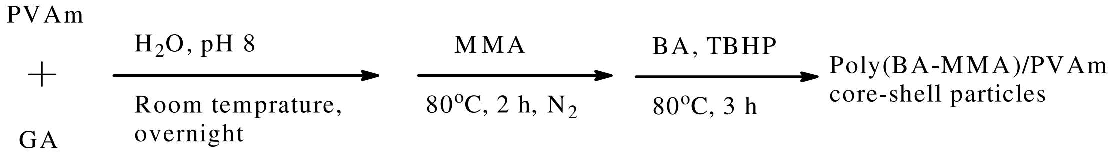

Scheme 7.5 Synthesis of poly(BA-MMA)/PVAm core-shell particles (procedure 3)

When the TBHP concentration was 0.1 mM (Table 7.7, P113), stable and uniform particles were produced with a number average diameter (D_n) of about 112 nm and a PDI of about 1.06. However, the monomer conversion was only 37%, which was much lower than that without crosslinking. This result indicated that the crosslinking of PVAm with GA had some negative effect on the graft copolymerization of the monomers from PVAm. Increasing the TBHP concentration from 0.1 to 0.2 mM significantly increased the monomer conversion from 37% to 73% (Table 7.7, P114), while the particle size (D_n=102 nm) and size distribution (PDI=1.10) were comparable. The monomer conversion was further increased to 79% (Table 7.7, P115) when a small amount of salt (0.1 M) was introduced into the reaction system to encourage the self-assembling of the graft copolymers to form particles. Particle size (D_n=112 nm) and size distribution (PDI=1.08) were almost no change. When the TBHP concentration was increased to 0.3 mM, the monomer conversion was further increased to 89%.

Table 7.7 Synthesis of poly(BA-MMA)/PVAm core-shell particles using Scheme 7.5[1]

Entry	SC (%)	[TBHP] mM	[NaCl] M	Conv. (%)	D_v (nm)	D_n (nm)	PDI	Observation
P113	5	0.1	0	37	119	112	1.06	stable
P114	5	0.2	0	73	112	102	1.10	stable
P115	5	0.2	0.1	79	121	112	1.08	stable
P118[2]	5	0.3	0.1	89	235	72	3.29	Particles formed before addition of BA and TBHP

[1] Other conditions: CD%=5; Temperature=80°C; Weight ratio of PVAm to monomers=1:4; Total weight=50 g; Reaction pH=8.0.

[2] P118: The total weight is 80g.

Although poly(BA-MMA)/PVAm particles had been successfully prepared via Scheme 7.5, it was found that sometimes the PMMA/PVAm particles were formed before addition of BA and TBHP (P118). The preformed particles were generated via the graft copolymerization of MMA from PVAm initiated by the radials generated from heating the crosslinked mixture of GA and PVAm. However, control experiment showed that the monomer conversion of the graft copolymerization of MMA from PVAm induced by 5% GA was lower than 30% when the polymerization was carried out at 80 °C for 12 hours. It suggested that these free radicals were relatively stable, and could not effectively initiate the graft copolymerization of MMA from PVAm. In addition, the unexpected formation of particles caused the formation of larger particles and a broad size distribution (PDI=3.29).

To avoid the pre-formation of the PMMA/PVAm particles, it was critical to exclude the free radicals generated from heating the mixture of GA and PVAm before the addition of MMA and BA. Thus the procedure in scheme 7.5 was further modified. As shown in Scheme 7.6, two approaches were adopted to consume the radicals: (1) The mixture of PVAm and GA was kept at 80 °C for 2 hours after PVAm was treated with GA overnight in water; (2) A few MMA (less than 0.5 g) was first charged into the reaction mixture and kept at 80 °C for 30 minutes. Since the amount of MMA added was very little, the pre-formation of PMMA/PVAm particles was avoided. The preformed graft copolymers of PVAm-g-oligo-PMMA generated from the graft copolymerization of MMA from PVAm initiated by the free radicals, if any, would assist the formation of micellar domains in the next stage. Finally, the remaining monomers and TBHP were charged and the polymerization was carried out at 80 °C for 3 hours to produce poly(BA-MMA)/PVAm particles.

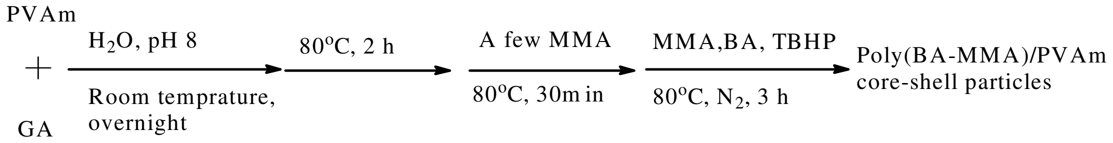

Scheme 7.6. Synthesis of poly(BA-MMA)/PVAm core-shell particles (Procedure 4)

The conditions for the synthesis of poly[BA(60)-MMA(40)]/PVAm core-shell particles according to the Scheme 7.6 and the results are listed in Table 7.8. Stable particles were obtained with a monomer conversion up to 73%. The surface charge of the particles was +39.8 mV, suggesting the formation of cationic PVAm shells. The volume and number average diameters of the particles were 128 and 119 nm, respectively, while the size distribution of the particles was very narrow (PDI=1.08), as shown in Figure 7.1.

Table 7.8 Synthesis of poly[BA(60)-MMA(40)]/PVAm core-shell particles using Scheme 7.6[1]

Entry	SC (%)	[TBHP] (mM)	[NaCl] (M)	Conv. (%)	GE (%)	ζ-potential (mV)
P120	5	0.3	0.1	73	80	+39.8

[1] Other conditions: CD%=5; Temp.=80°C; weight ratio of PVAm to monomers=1:4; Total weight=80; Reaction pH=8.0.

7.3.2.2 Synthesis of poly[BA(25)-MMA(75)]/PVAm core-shell particles

The synthesis of poly(BA(25)/MMA(75)/PVAm particles was performed following the same procedure as shown in Scheme 7.6.

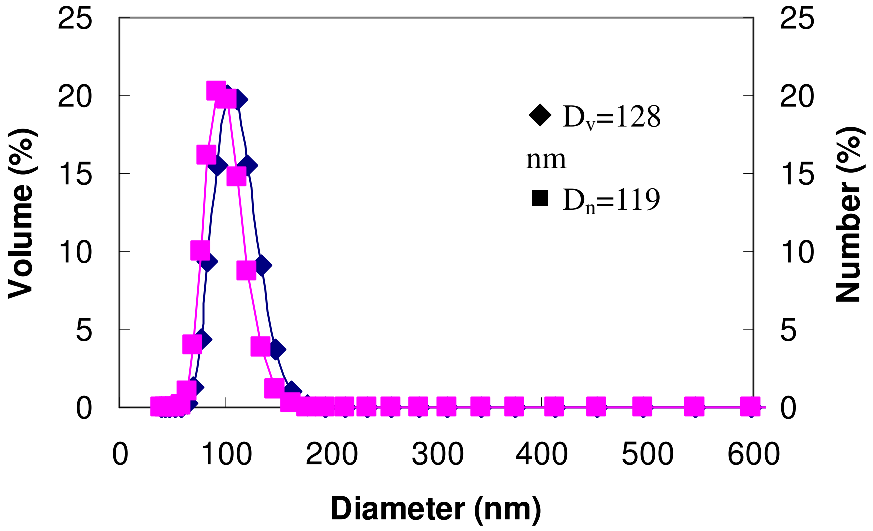

Figure 7.1 Particle sizes and size distributions of poly[BA(60)-MMA(40)]/PVAm amphiphilic core-shell nanoparticles.

Table 7.9 shows the detailed conditions and results for the synthesis of poly[BA(25)-MMA(75)]/PVAm core-shell particles. Stable particles with a monomer conversion up to 89% were obtained. The surface charge of the particles was +35.5 mV, suggesting the formation of cationic PVAm shells. The volume and number average diameters of the particles were 132 and 124 nm, respectively, while the size distribution of the particles was very narrow (PDI=1.06), as shown in Figure 7.2. These results are comparable with that of poly[BA(60)-MMA(40)]/PVAm particles.

Table 7.9 Synthesis of poly[BA(25)-MMA(75)]/PVAm core-shell particles using Scheme 7.6[1]

Item	SC (%)	[TBHP] (mM)	[NaCl] (M)	Conv. (%)	GE (%)	ζ-potential (mV)
P121	5	0.3	0.1	89	73	+35.5

[1] Other conditions: CD%=5; Temp.=80 ^{o}C; Weight ratio of PVAm to monomers=1:4; Total weight=80; Reaction pH=8.0.

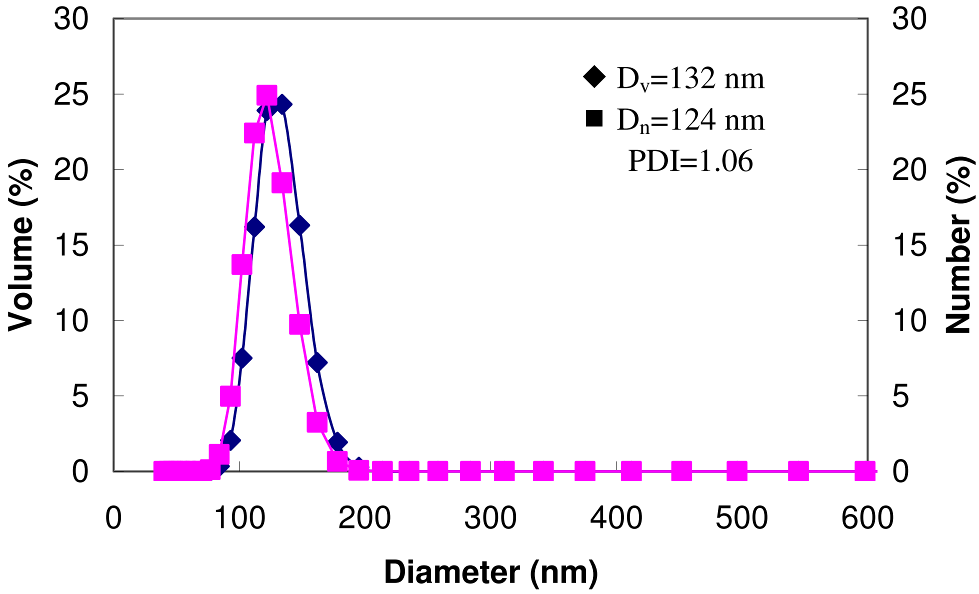

Figure 7.2 Particle sizes and size distributions of poly[BA(25)-MMA(75)]/PVAm amphiphilic core-shell nanoparticles.

7.3.3 Composition of the poly(BA-MMA)/PVAm particles

The poly(BA-MMA)/PVAm particles were composed of both amphiphilic graft copolymers and hydrophobic homopolymers. The graft copolymers and homopolymers were separated by Soxhlet extraction of the resultant polymers with chloroform for 48 hours. Compositions of the homopolymers obtained from the organic layer and the insoluble graft copolymers were determined gravimetrically (Table 7.7 and 7.8). It was found that grafting efficiencies of poly[BA(60)-MMA(40)] and poly[BA(25)-MMA(75)] were 80% and 73%, respectively. In other words, less than 27% of poly(BA-MMA) in the core was in the form of homopolymer. The structures of both homopolymers and graft copolymers isolated were identified with FTIR spectroscopy (Figure 7.3). Spectra of PVAm-g-P(BA-co-MMA)s show a strong

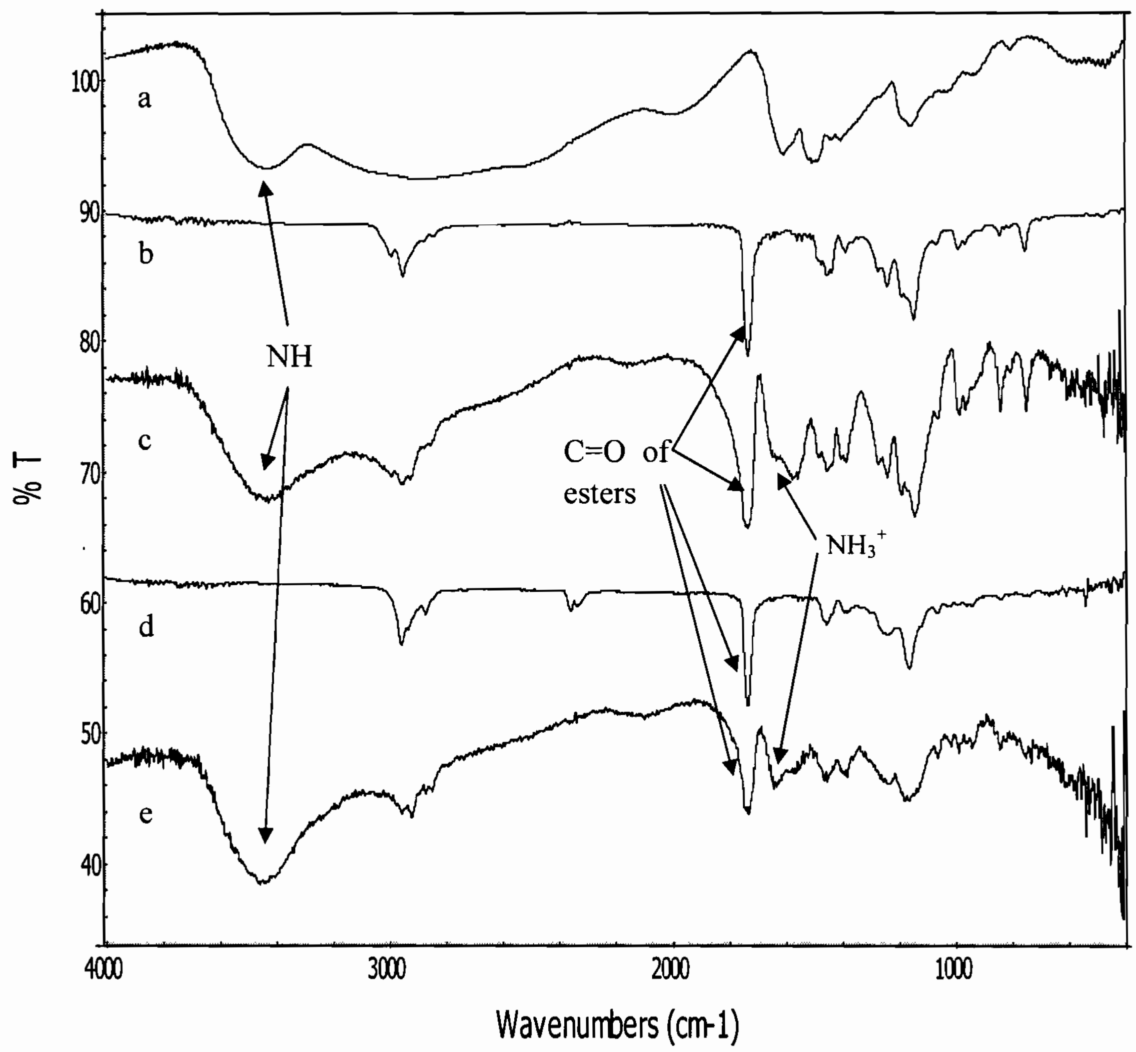

Figure 7.3. Comparison of FTIR spectra of various polymers: (a) PVAmHCl; (b) P[BA(25)-co-MMA(75)] isolated from P[BA(25)-co-MMA(75)]/PVAm particles; (c) PVAm-g-P[BA(25)-co-MMA(75)]; (d) P[BA(60)-co-MMA(40)] isolated; (e) PVAm-g-P[BA(60)-co-MMA(40)].

7.3.4 Morphologies of the poly(BA-MMA)/PVAm particles

Surface morphologies of the poly(BA-MMA)/PVAm particles were studied with a Field Emission Scanning Electron Microscopy (FE-SEM). Figure 7.4 shows that P[BA(25)-co-MMA(75)]/PVAm particles display uneven surfaces (Figure 7.4a and b), which is similar to that of PMMA/PVAm particles. In the case of

P[BA(60)-co-MMA(40)]/PVAm particles, discrete particles were difficult to observe because the soft PBA cores resulted in film formation (Figure 7.4c and d).

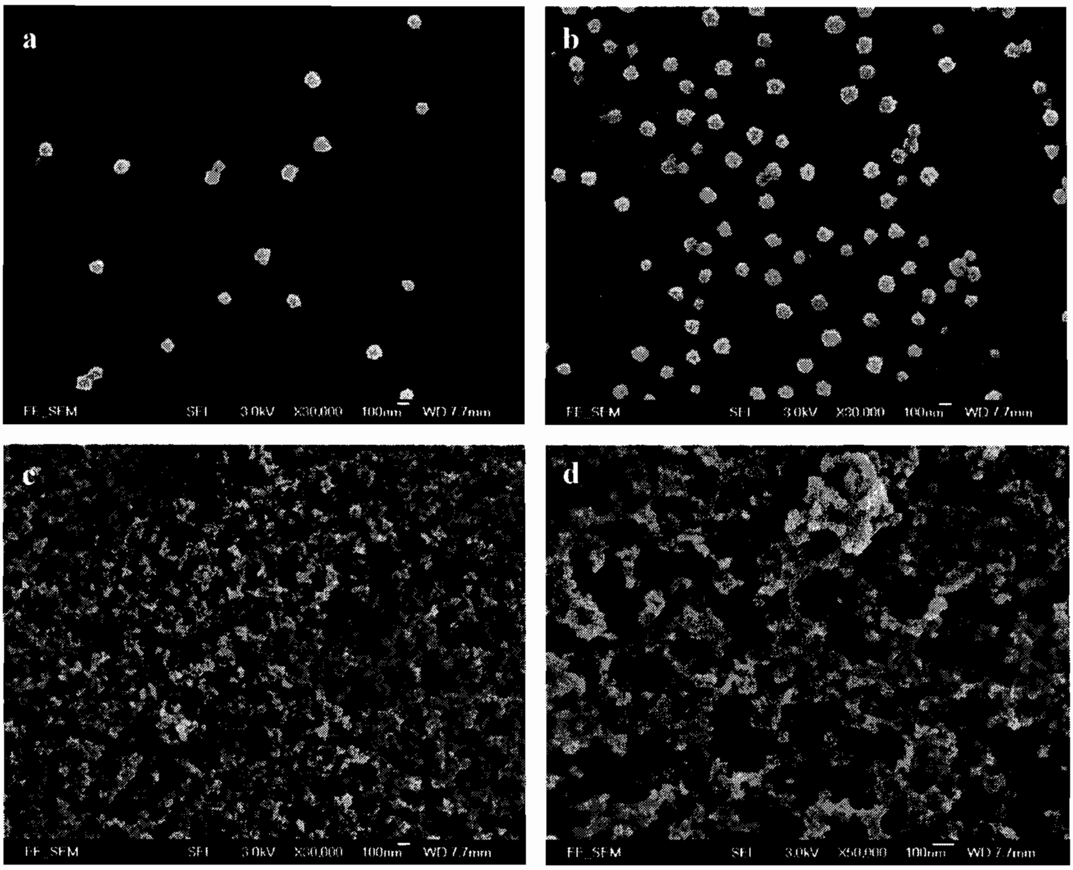

Figure 7.4. FE-SEM pictures of a) and b): poly(BA(25)-MMA(75))/PVAm particles; c) and d): poly(BA(60)-MMA(40))/PVAm particles.

The formation of rough surface morphology of the poly(BA-MMA)/PVAm particles is likely the consequence of phase separation of the hydrophobic segments. The hydrophobic segments might be attributed to the high grafting efficiency of poly(BA-co-MMA) and the side reaction during the polymerization. The high grafting efficiency of poly(BA-co-MMA) to PVAm improves the compatibility between PVAm and poly(BA-co-MMA), resulting in more poly(BA-co-MMA) dissolved in the PVAm shell. In addition, BA and MMA can react with PVAm via Michael addition to form amine esters (Eq. 7.3 and 7.4). To identify the occurrence of the Michael addition, PVAm was reacted with BA or MMA at pH 7 at 80 °C for 3 hours (Scheme 7.7). After purification by dialysis, the products of Michael addition were characterized by ^{1}H NMR using D_2O as a solvent (Figure 7.5).

In both the two spectra of the products of MMA (Figure 7.5a) and BA (Figure 7.5b) with PVAm, the peaks at about 1.95 and 3.53 ppm are attributed to the $-CH_2-$ and -CH- groups of the main chain of PVAm, respectively. In the spectrum of the product of MMA with PVAm, the peaks at about 1.10, 2.51, and 2.92 ppm are attributed by the protons of $–CH_3$, -CH- and $–CH_2-$ groups of the amine ester groups. In the spectrum of the product of BA with PVAm, the peaks at about 0.89, 1.32, 1.60 and 4.11 ppm are attributed by the protons of $-CH_3$, and $-CH_2-$ groups of the *n*-butoxyl groups, and the peaks at about 2.60 and 3.1 ppm are corresponding to the protons of the two $-CH_2-$ groups of the amine ester groups. These peaks clearly show that the Michael addition of PVAm to the double bond of BA or MMA occurs during the experiment. The Michael addition of BA and MMA to PVAm leads to hydrophobic modification of the PVAm. These hydrophobic segments in PVAm chains might also cause phase separation on the PVAm shell to generate a rough surface morphology. The peaks attributed to the protons of amine ester groups of the product of BA with PVAm are stronger than that of the reaction product of MMA with PVAm, suggesting that BA is much easier reacting with PVAm than MMA. The easier reaction between BA and PVAm might be the reason that the poly(BA-co-MMA)/PVAm has a rougher surface morphology than PMMA/PVAm particles.

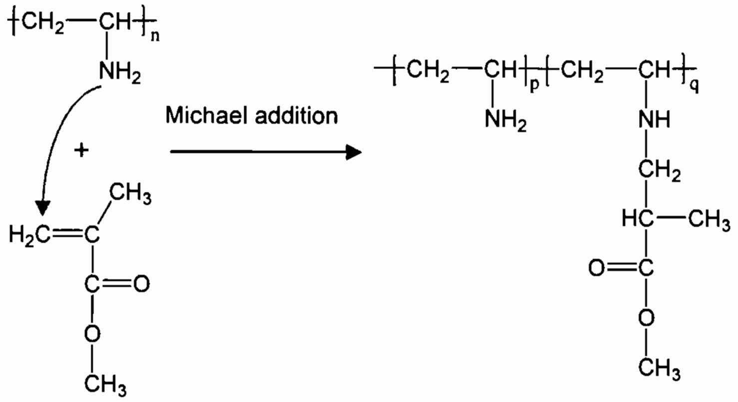

(Eq.7.3)

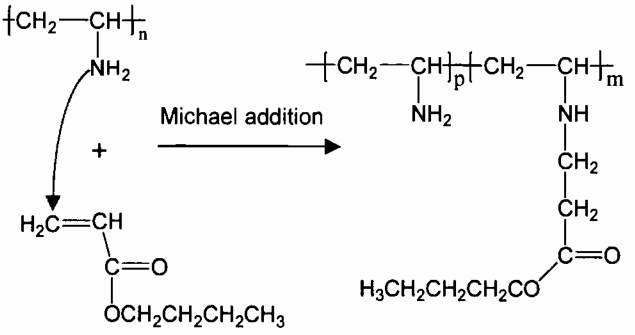

(Eq.7.4)

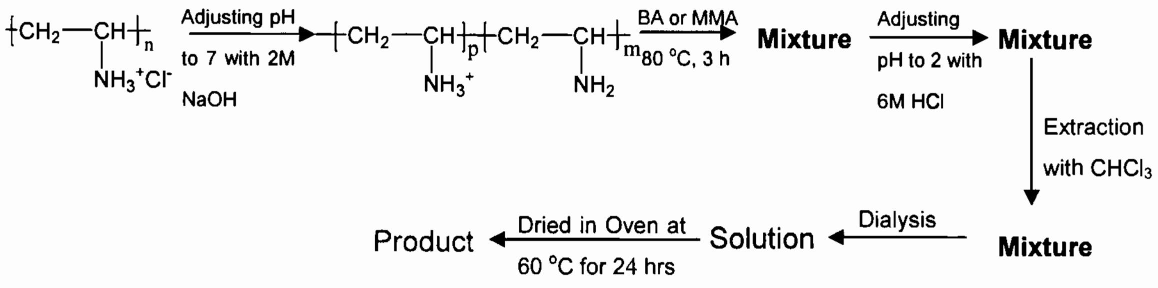

Scheme 7.7. Procedure for the reaction between PVAm and BA or MMA at pH 7 at 80 °C for 3 hours, followed by purification

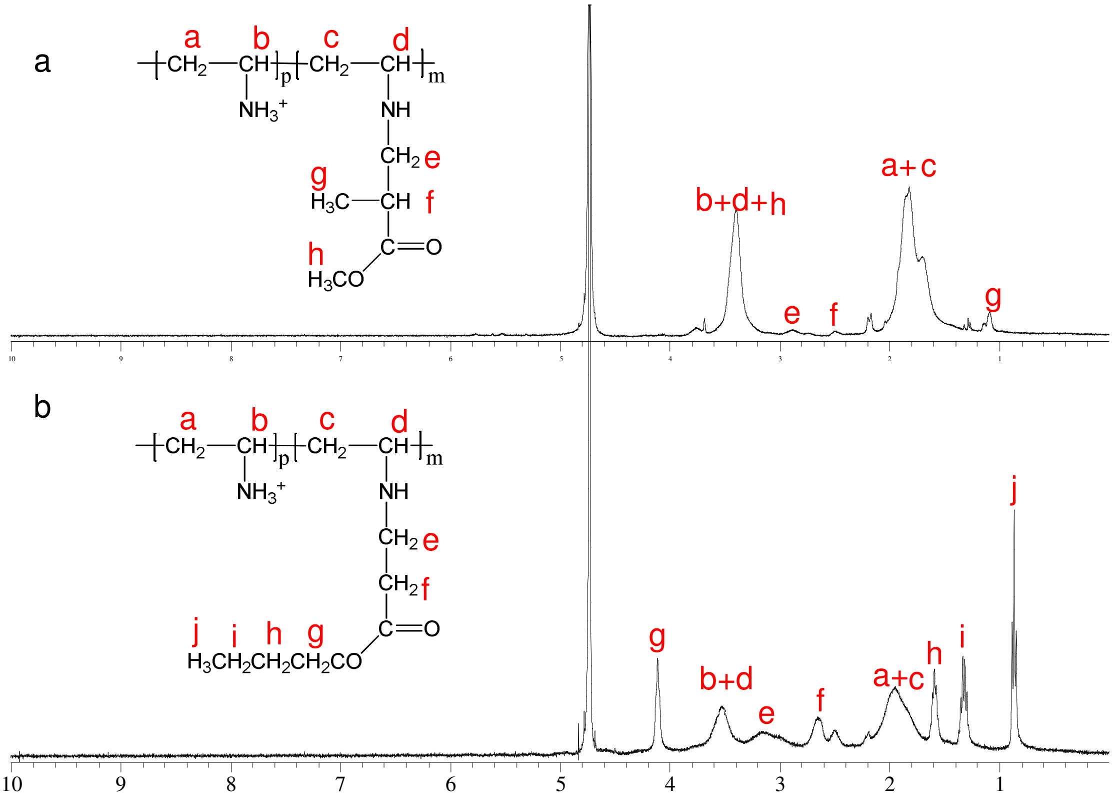

Figure 7.5 ^{1}H NMR spectra in D_2O of the products of the Michael additions of (a) MMA and (b) BA to PVAm at pH 7 at 80 °C for 3 hours.

Figure 7.6 shows TEM pictures of poly(BA(25)-MMA(75))/PVAm particles (Figure 7.6a) and poly(BA(60)-MMA(40))/PVAm particles (Figure 7.6b). They were stained with a 2 wt.-% phosphotungstic acid solution for 3 minutes, wherein poly(BA(60)-MMA(40))/PVAm particles were stained before drying to avoid film formation during drying. The TEM images clearly revealed that these two kind of particles had core-shell structures, where poly(BA-co-MMA) cores (white part) were coated with thick and hairy PVAm shells (darker part).

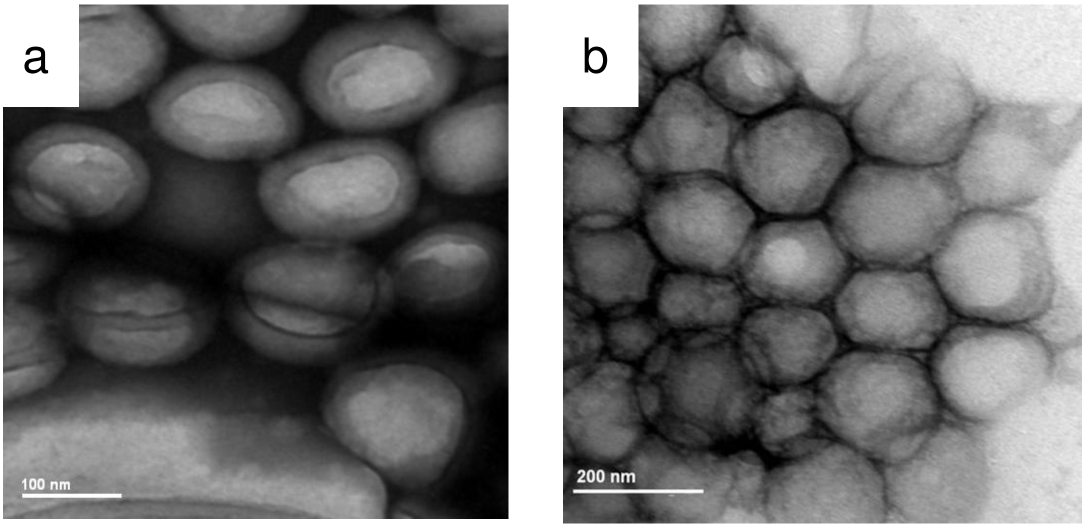

Figure 7.6 TEM pictures of a) poly(BA(25)-MMA(75))/PVAm particles; b): poly(BA(60)-MMA(40))/PVAm particles.

7.4 Conclusions

Amphiphilic poly[BA(25)-MMA(75)]/PVAm and poly[BA(60)-MMA(40)]/PVAm core-shell particles have been synthesized via a two step reaction: 1) crosslinking linear PVAm with GA; 2) graft copolymerization of BA and MMA from the crosslinked PVAm in water induced by a small amount of TBHP. The poly(BA-MMA)/PVAm particles could not be obtained directly using linear PVAm because the linear PVAm was unable to provide sufficient stability for the particles. Amphiphilic PVAm-g-poly(BA-MMA) graft copolymers and poly(BA-MMA) homopolymers were generated concurrently to form highly monodispered particles with diameters of about 120 nm, which were much small than that of PMMA/PVAm and PS/PVAm particles. The formation of graft copolymers and homopolymers were confirmed by FTIR. ζ-potential measurements revealed that the particles possess a cationic surface, suggesting the formation of PVAm shells. Morphology studies indicated that poly[BA(25)-MMA(75)]/PVAm particles displayed a spherical shape with rough surface morphology while poly[BA(60)-MMA(40)]/PVAm particles were difficult to observe because the soft PBA cores result in film formation. TEM studies revealed that they had a core-shell structure.

References:

1. Kawahara, J.-I.; Ishikawa, K.; Uchimaru, T.; Takaya, H., Chemical cross- linking by glutaraldehyde between amino groups: its mechanism and effects. *Polymer Modification, [Papers presented at the Symposium on Polymer Modification, Orlando, Fla., Aug. 25-29, 1996]* **1997**, 119-131.
2. Hayashi, T.; Ohta, Y.; Namiki, M., Electron spin resonance spectral study on the structure of the novel free radical products formed by the reactions of sugars with amino acids or amines. *Journal of Agricultural and Food Chemistry* **1977,** 25, (6), 1282-1287.
3. Namiki, M.; Hayashi, T., Development of novel free radicals during the amino-carbonyl reaction of sugars with amino acids. *Journal of Agricultural and Food Chemistry* **1975,** 23, (3), 487-491.
4. Roberts, R. L.; Lloyd, R. V., Free Radical Formation from Secondary Amines in the Maillard Reaction. *Journal of Agricultural and Food Chemistry* **1997,** 45, (7), 2413-2418.

Chapter 8

Synthesis and Characterization of Bi-functional Poly(methyl methacrylate)/Poly(vinyl alcohol-vinylamine) Core-Shell particles

8.1 Introduction

In chapter 4, the effect of amination of PVAm on the graft copolymerization has been investigated. A series of poly(*N*-vinylacetamide-vinylamine) [poly(NVA-VAm)] copolymers were synthesized through hydrolysis of poly(*N*-vinylacetamide) (PNVA) for specific times and used to prepare poly(methyl methacrylate) (PMMA)/poly(*N*-vinylacetamide-vinylamine) [poly(NVA-VAm)] core-shell particles. The successful preparation of PMMA/poly(NVA-VAm) core-shell particles shows that the graft copolymerization can be achieved if the water-soluble polymer contains certain amount of amine groups. Thus, to further explore the scope of this graft polymerization approach, synthesis of amphiphilic core-shell particles containing bi- or multi-functional surface groups using a copolymer containing amine and other functional groups was investigated.

Poly(vinyl alcohol) (PVA) is the largest synthetic water-soluble polymer produced in the world and its excellent chemical resistance and physical properties lead to broad industrial applications in textile sizing, adhesives, protective colloids for emulsion polymerization, fibers and paper sizing.[1] Numerous vinyl alcohol copolymers have also been prepared. One of the important vinyl alcohol copolymers is vinyl alcohol-vinylamine copolymer [poly(VA-VAm)], which possesses unique features due to its combination of the amine and hydroxyl groups. Thus the poly(VA-VAm) copolymer has been widely applied in various fields, such as in paper making,[2,3] coatings,[4-6] ink-jet recording media,[7,8] waster-water treatment,[9], hair-styling preparations,[10] protective colloid stabilizers,[11] drug formulation,[12] delivery of oligonucleotides,[13] and so on. However, in our knowledge, preparation of well-defined core-shell particles containing poly(VA-VAm) shells has never been reported. Because the core-shell particles often exhibit improved physical and chemical properties over their single-component counterparts, and have a broader range of applications, it is of interest to develop an efficient approach to synthesize core-shell particles containing poly(VA-VAm) shells.

In this chapter, the synthesis of core-shell particles bearing poly(VA-VAm) shells will be reported first, which are based on our recent work on the synthesis of a variety of core-shell particles.[14] Because the vinylamine and vinyl alcohol are not available to be used to directly synthesize the poly(VA-VAm), due to their tautomerization to acetaldehyde imine and aldehyde, poly(VA-VAm) has to be prepared indirectly via either acidic or basic hydrolysis of a copolymer of vinyl acetate and *N*-vinylalkylamides, such as *tert*-butyl-*N*-vinylcarbamate,[15] *N*-vinylacetamde (NVA),[16] and *N*-vinylformamide (NVF).[17-21] In our study, the poly(VA-VAm) copolymers were synthesized by a free radical copolymerization between vinyl acetate (VAc) and NVA, followed by acidic hydrolysis. The well-defined PMMA/poly(VA-VAm) core-shell particles were subsequently prepared by a direct graft copolymerization of MMA from poly(VA-VAm) initiated with a small amount of *tert*-butyl hydroperoxide (TBHP).

8.2 Experimental

8.2.1 Materials

Vinyl acetate (VAc) (a colorless liquid, Mw=86.09, density=0.934 g/cm^3, Aldrich) and methyl methacrylate (MMA) (a colorless liquid, Mw=100.12, density=0.936 g/cm^3, Aldrich) were purified following a reported procedure.[22] It was washed three times with 10 wt.-% sodium hydroxide (NaOH) aqueous solution, then with distilled water until the pH of the water layer to 7. After that, the monomer was dried with anhydrous calcium chloride followed by vacuum distillation.

N-Vinylacetamide (NVA) (97%, a white crystal, hygroscopic, MW=85.11, Aldrich), 2,2'-Azobis(2-amidinopropane) dihydrochloride (V-50) (97%, a faint yellow crystal, an free radical initiator, $T_{1/2}$=56℃, MW=271.2, Woko), *tert*-Butyl hydroperoxide (TBHP) (70% aqueous solution, colorless liquid, MW=90.07, Aldrich), reagent grade of chloroform (aldrich), acetone (aldrich), hydrochloric acid (HCl) (37% Aldrich) and NaOH (Fluka) were all used as received. De-ionized (DI) water was used as the dispersion medium.

8.2.2 Synthesis of poly(vinyl acetate-co-*N*-vinylacetamide) copolymer

For a total weight of 100 g, NVA (5 g), VAc (5 g) and DI water (90 g) were mixed in a three-necked water-jacket flask equipped with a condenser and a nitrogen inlet and purged with nitrogen for 30 minutes. V-50 (0.0694 g) was then added and the polymerization was carried out at 60 °C for 12 hours. After polymerization, the monomer conversion was determined gravimetrically. Most of water in the product was removed by a rotary evaporator, followed by washing with acetone three times. Finally, the purified poly(vinyl acetate-co-*N*-vinylacetamide) [poly(VAc-NVA)] was dried at 60 ℃ for 3 days in a vacuum oven. The yield was calculated according to the following formula:

$$\text{Yield (\%)} = \frac{\text{Weight of polymer obtained}}{\text{Weight of monomers added}} \times 100\%$$

8.2.3 Hydrolysis of poly(VAc-co-NVA) to poly(VA-co-VAm)

Poly(VAc-co-NVA) (4.7 g) was dissolved in 3 M HCl solution (36 mL) using H_2O/ethanol (V/V =1:1) mixture as a solvent in a three-necked flask equipped with a condenser and a nitrogen inlet. The mixture was purged with N_2 for 30 minutes, followed by stirring it at 80 ℃ for 66 hours to give a poly(vinyl alcohol-co-vinylammonium chloride) (poly(VA-co-VAmHCl). The hydrolyzed polymer was precipitated directly from water by dropwise addition of a 12 M HCl solution. The precipitate was further purified by repeated dissolution-precipitation-decantation cycles with water and acetone. Finally, the product was dried at 50 ℃ *in vacuo* for 3 days. The yield of product was calculated based on the following formula:

$$\text{Yield (\%)} = \frac{\text{Weight of product obtained}}{\text{Weight of theoretical yield}} \times 100\%$$

8.2.4 Synthesis of PMMA/poly(VA-co-VAm) core-shell particles

For a total weight of 50 g, poly(VA-co-VAmHCl) (0.25 g) was dissolved in DI water and the pH of the solution was adjusted to 12 with 10% NaOH solution. The solution was then mixed with purified MMA (1 g) in a three-necked water-jacketed flask equipped with a thermometer, a reflux condenser and a nitrogen inlet, and purged with nitrogen for 30 minutes. A diluted TBHP solution (0.5 mL of 10 mM solution) was added and the mixture was stirred at 80℃ for 3 hours. After the reaction, the monomer conversion was determined gravimetrically. The particle dispersion was purified by repeated centrifugation-decantation-dispersion cycles using DI water.

8.2.5 Measurement and characterization

The graft copolymers and homopolymers were isolated by Soxhlet extraction with chloroform for 48 hours. The grafting efficiency (GE%) was calculated as follows:

$$\text{GE \%} = \frac{\text{Weight of the grafted}}{\text{Weight of the total polymerized}} \times 100$$

^{1}H NMR spectra were recorded on a Bruker advance DPX-400 (400 MHz) instrument using D_2O or DMSO-d_6 as a solvent. The particle size and size distribution were measured with a Coulter LS230 Particle Size Analyzer. The ζ-potential of the particles was measured with a Malvern Zetasizer 3000HS (Malvern, UK) in 1.0×10^{-3} M NaCl aqueous solution The surface morphologies of the particles were examined by field emission scanning electron microscopy (FE-SEM, JEOL JSM 6335F). Samples were prepared by coating the dried particles, which were spread on a glass surface, with a thin layer of gold to a depth of ca. 5 Å. under vacuum. Transmission Electron Microscopy (TEM) micrographs were obtained with a JEOL 2010 transmission microscope at an accelerating voltage of 200 kV. Sample was prepared by wetting a carbon-coated grid with a small drop of dilute particle dispersion. The dried particles were treated with a small drop of phosphotungstic acid (PTA) solution (0.5 wt.-%) for 3 minutes, then dried at room temperature.

8.3 Results and Discussions

8.3.1. Synthesis and characterization of poly(VA-co-VAm) copolymer

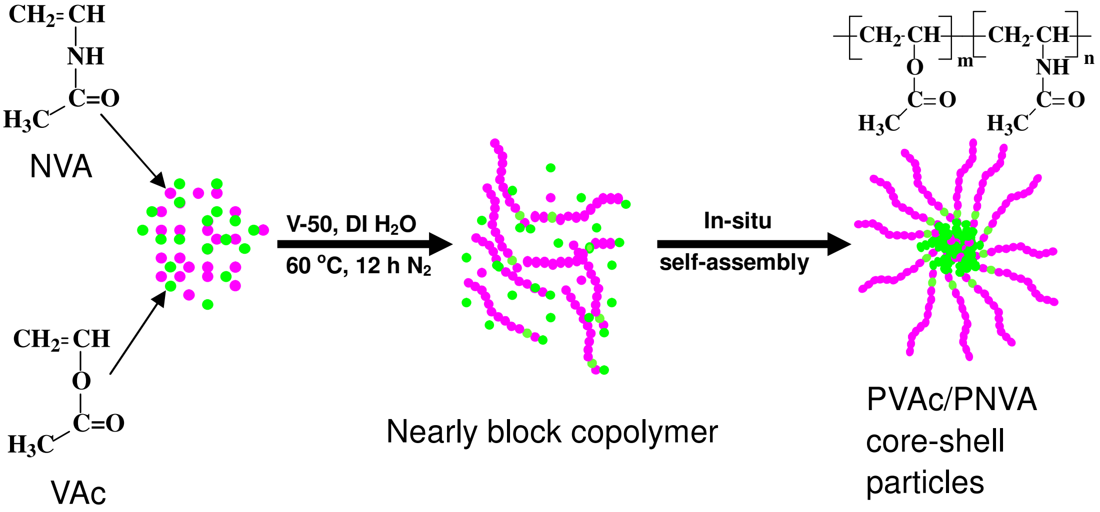

Scheme 8.1 Synthesis of poly(VAc-NVA) copolymer through a soap-free emulsion polymerization

The poly(VA-co-VAm) copolymer was synthesized via a two-step reaction: 1) Preparation of poly(VAc-co-NVA) copolymer through a soap-free emulsion polymerization of VAc and NVA; 2) Acidic hydrolysis of poly(VAc-co-NVA) to poly(VA-co-VAm). The soap-free emulsion polymerization of NVA and VAc (molar ratio=1:1) was carried out at 60 ^{o}C for 12 hours in water using V-50 as a free radical initiator, as shown in Scheme 8.1. The detailed reaction conditions and experimental results are summarized in Table 8.1. Yamamoto et al[23] have performed an detailed study on the free radical copolymerization of NVA and VAc in methanol and determined the monomer reactivity ratios as r_1=5.8 and r_2=0.68 (M_1=NVA, M_2=VAc), The values suggest that the growing NVA radical propagates more favorably than VAc monomer, and the copolymerization tends to yield a nearly block amphiphilic copolymer. When the free radical copolymerization of NVA and VAc was carried out in water, because NVA is soluble in water while VAc is not, it is more favorable to polymerize NVA first, thus resulting in a block amphiphilic copolymer of NVA and VAc. The block amphiphilic copolymers would self-assemble *in situ* in water to give PVAc/PNVA core-shell particles. In fact, a milky latex was obtained after the polymerization with a monomer conversion up to 85%。The latex was concentrated using a rotary evaporation precipitated in acetone. A colorless polymer with an isolated yield of 47% was obtained. The low yield might be attributed to the high solubility of PVAc in acetone.

Table 8.1 Copolymerization[a] of NVA with VAc and hydrolysis[b] of the as-prepared copolymer

Charging molar ratio of NVA to VAc	Conv. (%)	Isolated Yield after purification (%)	Molar ratio of NVA to VAc in purified poly(VAc-co-NVA) [c]	Yield after hydrolysis (%)
50:50	85%	47	70:30	71

[a] Reaction conditions for copolymeization: temperature: 60 °C; reaction time: 12 hours; molar ratio of monomers to initiator (V-50): 500:1; solid content: 10%; reaction media: DI H_2O; total weight: 100g.

[b] Reaction conditions for hydrolysis: temperature: 80 °C; reaction time: 66 hours; HCl concentration: 3 M; reaction media: ethanol/H_2O mixed solvent (V:/V 1:1).

[c] Measured by ^1H NMR

The structure of the copolymer was identified with ^1H NMR spectroscopy in DMSO-D_6 as shown in Figure 8. In the spectrum of NVA, the peaks at 6.72-6.78 ppm are attributed to the vinylic protons (=CH), the peaks at 4.71-4.75 and 4.47-4.50 ppm are donated to the protons of $=CH_2$ groups, and the peaks at 1.97 ppm are assigned to protons of $–CH_3$. In the spectrum of VAc, the peaks at 7.17-7.32 ppm are attributed to protons of =CH groups, the peaks at 4.8-5.0 and 4.6-4.8 ppm are due to protons of $=CH_2$, and the peaks at 2.1-2.3 ppm are assigned to protons of $–CH_3$ groups. Those peaks indicating the existence of C=C double bonds which disappeared in the spectrum of poly(VAc-NVA).

In the spectrum of poly(VAc-co-NVA), the peaks at about 4.63-4.89 and 3.47-3.91 ppm are attributed to the protons of the –CH- next to the ester groups and -CH- next to the amide groups, respectively. Their chemical shifts are exactly the same with their homopolymers, indicating that the copolymer has nearly a block copolymer structure. Thus the molar ratio of the VAc unit and NVA unit in the copolymer could be calculated from the peak areas attributed to the protons of PVAc and PNVA. The calculated molar ratio of VAc unit and NVA unit of the poly(VAc-co-NVA) copolymer is 30:70, which confirms that the propagation of NVA monomer is preferable than VAc monomer in the free radical polymerization. The peaks at about 1.7-1.9 and 1.9-2.07 ppm are attributed to protons of $–CH_3$ groups and the peaks at 1.2-1.7 ppm are attributed to protons of $–CH_2-$ groups. These three peaks are partially overlapped. In all three spectra, the peaks at about 3.36 and 2.54 ppm are attributed by H_2O and DMSO, respectively.

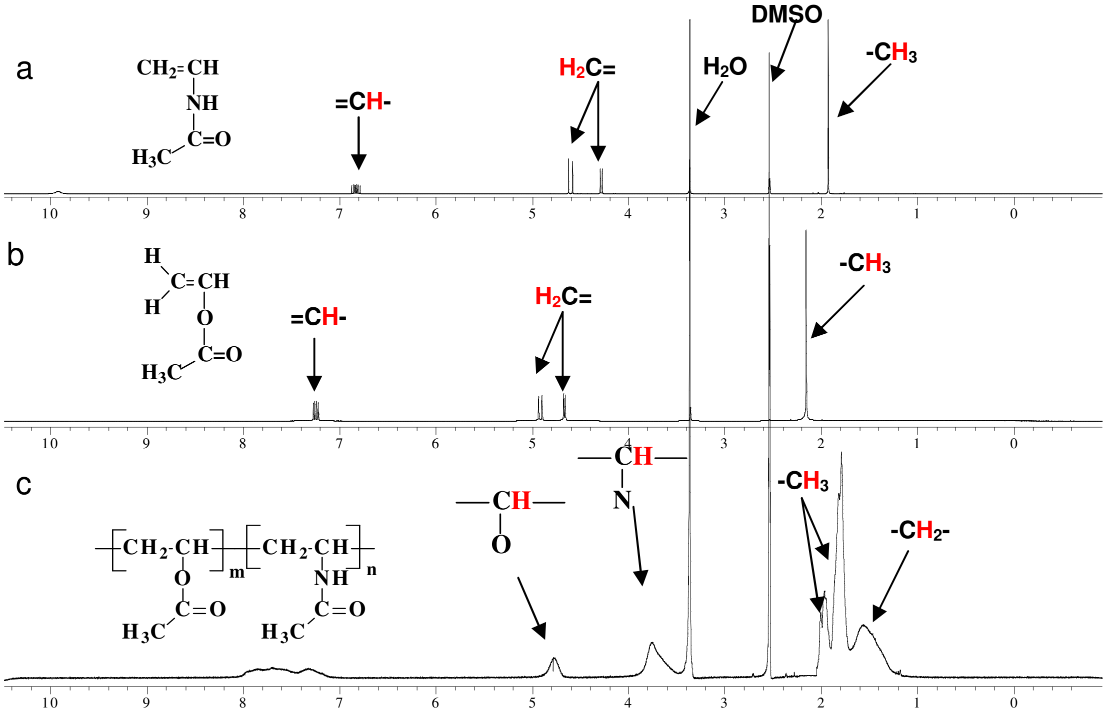

Figure 8.1 ^1H NMR spectra of a) NVA; b) VAc and c) poly(VAc-VAmHCl) in DMSO-D_6

Because PVAc is insoluble in water, the poly(VAc-co-NVA) was hydrolyzed to poly(VA-co-VAm) at 80 °C for 66 hours in 3 M HCl solution using a water/ethanol mixed solvent as a reaction media (Scheme 8.2). After hydrolysis, the product was precipitated with concentrated HCl from the reaction media and purified by repeated dissolution-precipitation-decantation cycles using H_2O and acetone. A slightly yellowish polymer was obtained with a yield up to 71% after drying the products at 60 °C under vacuum.

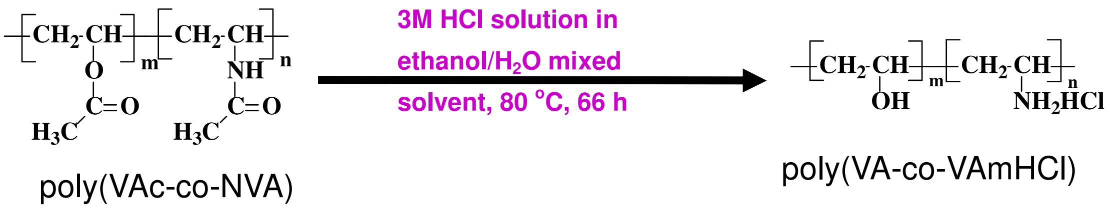

Scheme 8.2. Acid-hydrolysis of poly(VAc-co-NVA) to poly(VA-co-VAmHCl)

The hydrolyzed products were identified with ^1H NMR spectroscopy in D_2O. As shown in Figure 8.2, the peaks at about 3.0-3.8 ppm are attributed to protons of –CH- next to $–NH_3Cl$ groups, indicating the hydrolysis of amide groups. The peaks at about 3.9-4.2 ppm are attributed to protons of –CH- next to –OH groups, indicating the hydrolysis of ester groups. The little peaks at 4.2-4.4 ppm are attributed to protons of –CH- groups next to the unhydrolyzed amide groups. By calculating the peak areas attributed to protons of –CH- groups next to the unhydrolyzed amide groups and the $–NH_3Cl$ groups, it was found that up to 94% of the amide groups had been hydrolyzed. The peaks attributed to protons of –CH- groups next to the unhydrolyzed ester groups are overlapped with the H_2O peaks, thus can not be seen in the spectrum. However, the ratio between the peak area of protons of –CH- next to the –OH groups and the peak area of protons of –CH- next to the $–NH_3Cl$ groups in the hydrolyzed product was almost the same as the ratio between VAc and NVA units in poly(VAc-NVA) copolymers, indicating that almost all the VAc units had also been hydrolyzed. The peaks of protons of other $–CH_2-$ and $–CH_3-$ groups are overlapped between 1.2-2.4 ppm, as shown in Figure 8.2. Thus these results identified the formation of poly(VA-co-VAm), which containing the unhydrolyzed NVA and VAc units less than 6%.

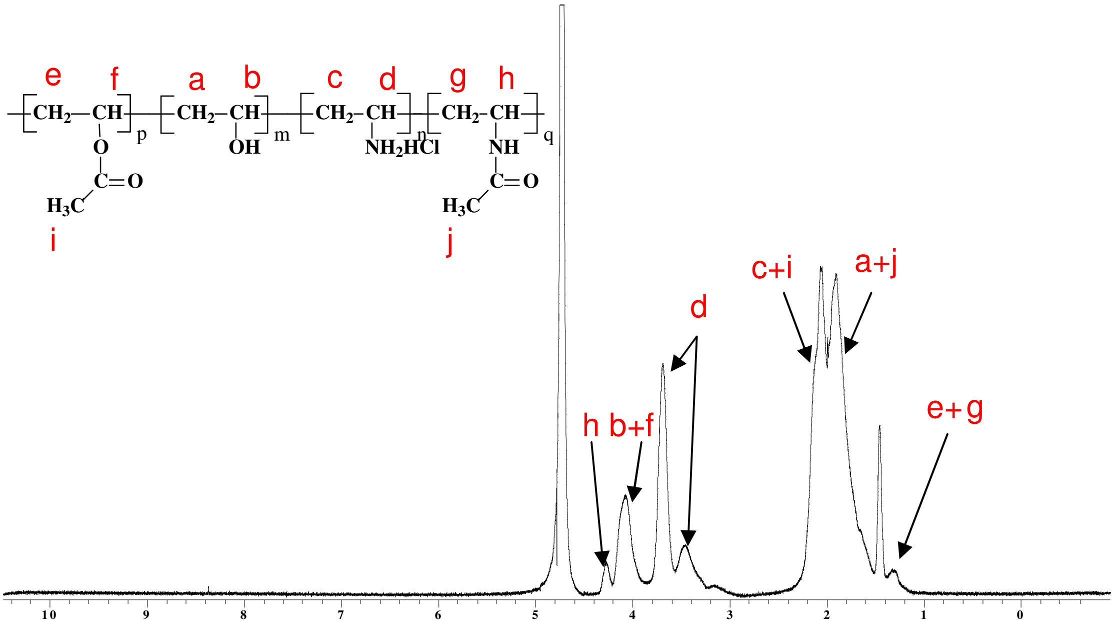

Figure 8.2 ^1H NMR spectra of hydrolyzed product in D_2O

8.3.2 Synthesis and characterization of PMMA/poly(VA-co-VAm) core-shell particles

Scheme 8.3 shows the reactions for the synthesis of amphiphilic

PMMA/poly(VA-co-VAm) core-shell particles, which has the same procedure as the synthesis of PMMA/PVAm particles discussed in Chapter 4. The pH of poly(VA-co-VAmHCl) solution was first adjusted to pH 12 with 10% NaOH solution, followed by treating it with a small amount of *tert*-butyl hydroperoxide (TBHP) at 80 °C in the presence of MMA to generate PMMA/poly(VA-co-VAm) particles. During the polymerization, graft copolymerization of MMA from poly(VA-co-VAm) and the homopolymerization of MMA were initiated concurrently. The amphiphilic graft copolymers generated *in situ* acted as polymeric surfactants and self-assembled to form micelle-like microdomains, which promotes the emulsion polymerization of MMA in water.

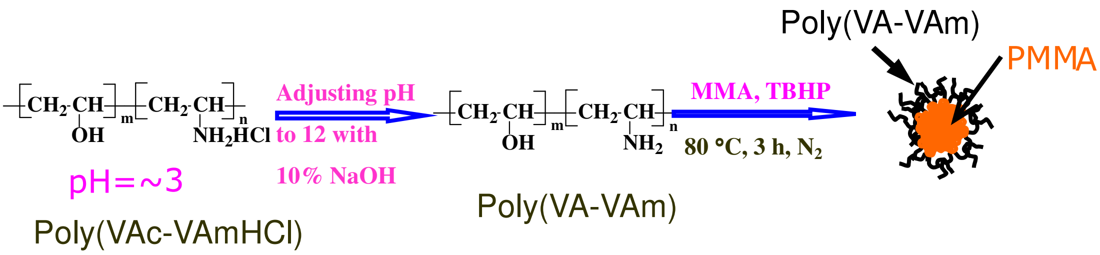

Scheme 8.3 Synthesis of PMMA/Poly(VA-co-VAm) core-shell particles

A reasonable monomer conversion up to 73% was obtained under very low TBHP concentration (0.1 mM) (Table 8.2). This result is comparable with the conversion for the synthesis of PMMA/PVAm particles, thus indicating that the existence of OH groups does not have negative effect on the graft polymerization. ζ-potential measurement showed that the surface charge of the particles was +46.8, indicating the formation of cationic poly(VA-co-VAm) shells. Dynamic light scattering measurement indicated that the volume average diameter (D_v) and number average diameter (D_n) were 211 and 192 nm, respectively. Figure 8.3 shows that the particles have a very narrow size distribution with polydispersity index (PDI=D_v/D_n) around 1.1.

Table 8.2 Synthesis of PMMA/P(VA-co-VAm) particles from poly(VA-co-VAm)[a]

Conversion	D_v (nm)	D_n (nm)	PDI	GP%	GE%	ζ-potential (mV)
73%	211	192	1.1	244	45	+46.8

[a]Reaction conditions: poly(VA-VAmHCl): 0.25g; MMA: 1g; [TBHP]: 0.1 mM; solid content : 2.5%; total weight: 50g; reaction time: 3 h; temperature: 80 °C; Reaction pH=12.

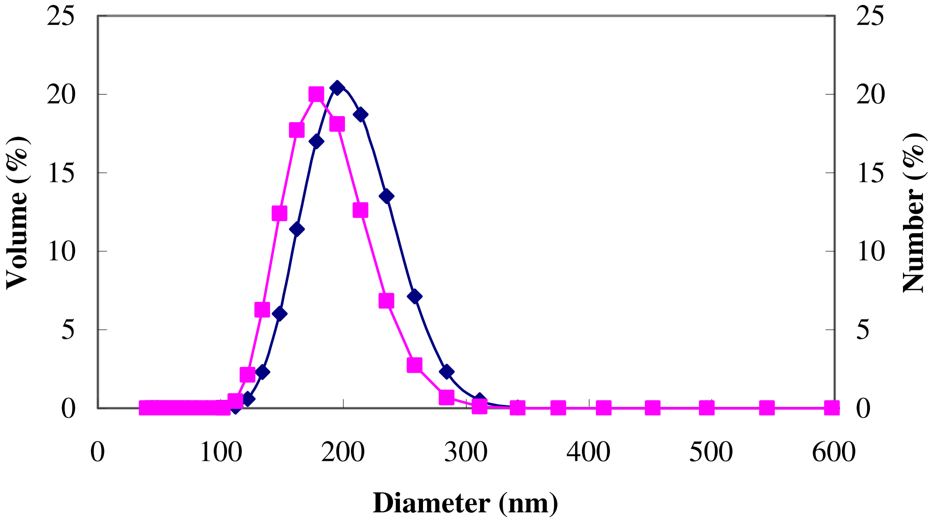

Figure 8.3 Particle size and size distribution of the PMMA/poly(VA-VAm) particles. (◆) D_v; (■) D_n.

The PMMA/poly(VA-co-VAm) core-shell particles were composed of both amphiphilic grafted copolymers and hydrophobic homopolymers, which were separated by Soxhlet extraction of the resultant polymers with chloroform for 48 hours. Compositions of the homopolymers obtained from the organic layer and the insoluble graft copolymers were determined gravimetrically (Table 8.2). It was found that the grafting percentage and efficiency were 244% and 45%, respectively. In other words, more than half of PMMA in the core was in the form of homopolymer.

The morphologies of the PMMA/poly(VA-co-VAm) core shell particles were observed with FE-SEM and TEM. FE-SEM micrographs (Figure 8.4a and 8.4b) reveal that the particles were spherical with rough surfaces, while the TEM picture (Figure 8.4c) (particles were stained with 0.5% PTA for 3 minutes) confirms that the particles have a well-defined core-shell structure, where PMMA cores (white part) are coated with thick and hairy poly(VA-co-VAm) shells (darker part). These results are similar to PMMA/PVAm core shell particles.

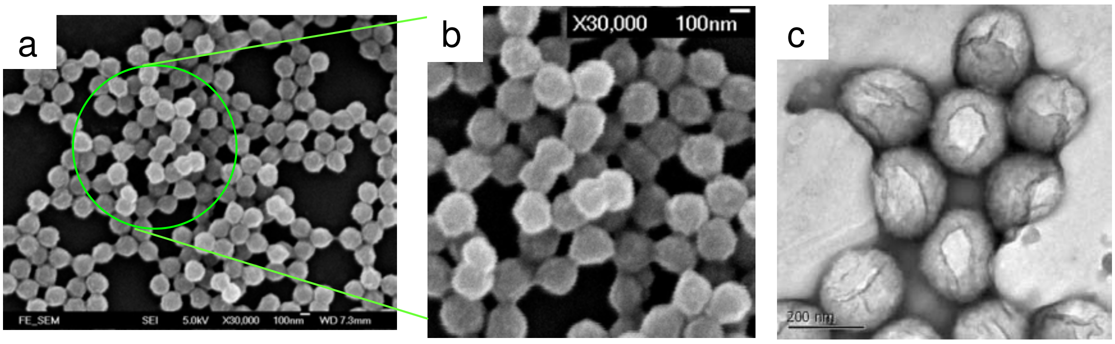

Figure 8.4. FE-SEM and TEM micrographs of the PMMA/poly(VA-co-VAm) particles. (a and b): FE-SEM images; (c): TEM image.

8.4 Conclusions

Poly(VA-co-VAm) was synthesized by the free radical copolymerization of VAc and NVA in water using V-50 as an initiator, followed by acidic hydrolysis of the preformed poly(VAc-co-NVA) copolymer in 3 M HCl water/ethanol solution. The successful synthesis of poly(VA-co-VAm) copolymer was confirmed by ^{1}H NMR spectroscopy. The obtained copolymer was had a almost block copolymer structure. The synthesis of amphiphilic PMMA/poly(VA-co-VAm) core-shell particles was realized by direct graft copolymerization of MMA from poly(VA-co-VAm) using TBHP as an initiator. Stable and uniform particles with diameter of 192 nm were obtained with monomer conversion up to 73%. ζ-potential measurement revealed that the surface charge of the particles was positive. Morphology study showed that the PMMA/poly(VA-co-VAm) particles were spherical with a well-defined core-shell structure and a rough surface, which are similar to PMMA/PVAm particles. Since the poly(VA-co-VAm) prepared contains 70% vinylamine and 30% vinyl alcohol units, variation of the ratio between vinyl alcohol and vinylamine units should be carried out in the future.

These results show that it is possible to synthesis bi- or multi-functional amphiphilic core-shell particles containing amine-rich shells. Since various PVAm-based random, block or graft copolymers can be synthesized through copolymerization of *N*-vinylalkylamides with other functional monomers. followed by hydrolysis or modification of PVAm, this approach could be amenable to produce a wide variety of novel amphiphilic core-shell particles, providing specific surface functionalities such as pH-sensitive, thermo-sensitive, photo-sensitive or bio-compatible properties.

References:

1. Marten, F. L., Vinyl Alcohol Polymers. *Wiley-Interscience, Encyclopedia of Polymer Science and Engineering.* **2003,** 8, 399-437.
2. Beckman, E. J.; Carroll, W. E.; Chapman, T.; Minnich, K. E.; Sagl, D.; Goddard, R. J. Compositions of amine-containing hydrophilic polymers and reducible saccharides for increasing paper strength. USP 2004050513, **2004**.
3. Smigo, J. G.; Robeson, L. M.; Davidowich, G.; Miller, G. D.; Carroll, W. E. Crosslinked vinyl alcohol-vinylamine copolymers for treating paper. USP 5281307, **1994**.
4. Posey, R. G. Coated polymeric film with oxygen barrier properties at high relative humidity. WO 2007002322, **2007**.
5. Fitch, J. Thermoplastic film with barrier layer having enhanced adhesive properties. WO 2006138597, **2006**.
6. Aoyama, M.; Sawa, K. Water soluble resin composition, gas barrier film and packaging material employing it. EP 1661925, **2006**.
7. Osborn, J. J.; Upton, A. M.; Wraith, M. A. Ink-jet recording materials. GB 2400335, **2004**.
8. Renz, W. L.; Ravichandran, R.; Naisby, A. J.; Suhadolnik, J.; Wood, M. G.; Xiong, R. Poly(vinyl alcohol)-co-poly(vinylamine) copolymers bearing functional moieties for ink jet recording media. WO 2003054030, **2003**.
9. Sommese, A. G.; Chung, D. K. Use of polymers containing vinylamine/vinylformamide for the treatment of food processing wastewater. USP

6280631, **2001**.

10. Omura, T.; Nanba, T. Hair-styling preparations containing vinyl alcohol-vinylamine copolymers, amino- or ammonium-containing silicones, and acids. JP 2001064128, **2001**.
11. Bott, R. H.; DiStefano, F. V., Synthesis and application screening of emulsions stabilized using salts of poly(vinyl alcohol-co-vinylamine) as the protective colloid. *Polymeric Materials Science and Engineering* **1999,** 80, 508-509.
12. Shumikhina, K. I.; Panarin, E. F.; Ushakov, S. N., Penicillin polymer salts. *Antibiotiki* **1966,** 11, (9), 767-70.
13. Goldenberg, M. S.; Beekman, A. C. Cationic copolymers of vinylamine and vinyl alcohol for the delivery of oligonucleotides. WO 9622792, **1996**.
14. Li, P.; Zhu, J.; Sunintaboon, P.; Harris, F. W., New Route to Amphiphilic Core-Shell Polymer Nanospheres: Graft Copolymerization of Methyl Methacrylate from Water-Soluble Polymer Chains Containing Amino Groups. *Langmuir* **2002,** 18, (22), 8641-8646.
15. Brouwer, W. M.; Piet, P.; German, A. L., Copolymers of vinylamine and vinyl alcohol by acid hydrolysis of poly(tert-butyl *N*-vinylcarbamate-co-vinyl acetate): evaluation of reactivity ratios. *Journal of Polymer Science, Polymer Chemistry Edition* **1984,** 22, (10), 2353-62.
16. Hoover, M. F.; Guilbault, L. J. Preparation of polymers containing primary pendant amino groups and their use in hair conditioning products. USP 4713236, **1987**.

17. Itou, Y.; Aoyama, M.; Sawa, K. Amine-functional copolymer and process for producing the same. WO 2003102036, **2003**.

18. Minagawa, M.; Shibuya, M.; Kitamura, K. Manufacture of vinyl alcohol-vinylamine copolymer. JP 2002069124, **2002**.

19. Mori, Y.; Sato, K.; Ueno, N. Preparation of water-soluble vinylamine-vinyl alcohol copolymer powders by hydrolysis of vinylamide-vinyl acetate copolymers and their uses. EP 1178056, **2002**.

20. Mori, K.; Sato, K.; Ueno, N. Hydrolysis of *N*-vinylamide-vinyl acetate copolymers and their uses. JP 2000219706, **2000**.

21. Pinschmidt, R. K., Jr.; Lai, T. W. Method for preparing poly(vinyl alcohol)-co-poly(vinylamine) via a two-phase process. USP 5300566, 1994.

22. Li, P.; Zhu, J.; Sunintaboon, P.; Harris, F. W., Preparation of latexes with poly(methyl methacrylate) cores and hydrophilic polymer shells containing amino groups. *Journal of Dispersion Science and Technology* **2003,** 24, (3 & 4), 607-613.

23. Yamamoto, K.; Serizawa, T.; Akashi, M., Synthesis and functionalities of poly(*N*-vinylalkylamide). XIV. Synthesis and thermosensitive properties of poly[(*N*-vinylamide)-co-(vinyl acetate)]s and their hydrogels. *Macromolecular Chemistry and Physics* **2003,** 204, (7), 1027-1033.

Chapter 9

PMMA/PVAm Core-Shell Particles as a Potential Carrier for Enzyme Immobilization

9.1 Introduction

Immobilized enzymes have several advantages over their soluble counterparts because of their improved recovery, reusability and stability. [1, 2] Thus, they have been widely applied in diverse areas, for example, as reusable heterogeneous biocatalysts, stable and reusable devices for analytical and medical applications, selective adsorbents for purification of proteins and enzymes, fundamental tools for solid-phase protein chemistry and effective micro-device for the controlled release of protein drugs, etc. [3]

Amphiphilic core-shell particles are suitable materials for enzyme and protein immobilization because of their large surface area, nano-scaled dimension and surface functionality.[4, 5] The immobilization can be achieved by different methods, such as adsorption, entrapment or encapsulation, covalent bonding, crosslinking or a combination of these methods.[6] For instance, Caruso et al[7, 8] encapsulated enzyme through the sequential adsorption of oppositely charged polyelectrolytes onto enzyme crystal templates and found that the encapsulated enzyme were well preserved for their activity. The enzyme stability against protease degradation was also improved. However, the encapsulation through layer-by-layer assembly is a very time-consuming and multi-step process. Hong et al[9] covalently bound α-chymotrypsin onto amine-functionalized magnetic nanogels using carbodiimide method and the bound enzyme exhibited improved thermal stability, storage stability and reusability. However, the maximal specific activity of the bound enzyme was only 59.3% of the free counterpart. Recently, polyelectrolyte brushes were found very suitable for the immobilization of enzymes in a simple procedure of absorption without a significant loss of enzymatic or biological activity.[4, 10-13] Haupt et al[14] investigated the enzymic activity of glucoamylase and β-glucosidase adsorbed on colloidal particles with spherical polyelectrolyte brushes and the results showed that up to 600 mg of enzyme was adsorbed on per g of the carrier particles and both enzymes kept nearly their full activity. Our group[15] has found that poly(methyl methacrylate) (PMMA)/polyethyleneimine (PEI) core-shell particles possess high immobilization capacity (up to 340 mg/g) of cellulase upon physical adsorption and the absorbed enzyme retained its activity up to 90%. It has been found that the main driving force is the electrostatic interaction between the polyelectrolyte chains and the protein molecule.[16]

Polyvinylamine (PVAm), one of the strongest cationic polyelectrolytes, possesses a much higher positive charge density than PEI. Thus it is expected to be more efficient for the immobilization of enzyme through either covalent bonding or electrostatic interaction. Here, we demonstrate the synthesis of amphiphilic PMMA/PVAm core-shell particles and its application in enzyme immobilization.

9.2 Experimental

9.2.1 Materials

Poly(vinylammonium hydrochloride) (PVAmHCl) was prepared through acidic hydrolysis of poly(*N*-vinylacetamide) as described in Chapter 3. The molecular weight of polyvinylamine (PVAm) was about 190 K Delton based on viscometrical measurement. Methyl methacrylate (MMA) (Aldrich) was purified by first washing the monomers three times with 10 wt.-% NaOH solution, then with de-ionized (DI) water until the pH of the water layer dropped to 7. It was then dried with anhydrous $CaCl_2$ followed by vacuum distillation.

tert-Butyl hydroperoxide (TBHP) (70% solution in water, Aldrich), bovine serum albumin (BSA) (protease free, Acros), sodium carbonxy methyl cellulose (CMC) powder (Sigma), coomassie brilliant blue G250 (CBB) (Sigma), 3,5-dinitrosalicylic acid (DNS) (Sigma), D-glucose (hydrolyzed product of CMC catalyzed with cellulose) (Sigma), potassium sodium tartrate-4-hydrate ($KNaC_4H_4O_6 \cdot 4H_2O$)(Riedel-de Haën), sodium hydroxide (NaOH) (Riedel-de Haën), potassium hydroxide (KOH) (Riedel-de Haën), acetic acid (Riedel-de Haën) and phosphoric acid solution (85 w/v%, Beijing Chemical Works) were all used as received. De-ionized (DI) water was used as the dispersion medium. The protein concentration of cellulase solution (from *Aspergillus sp*, Aldrich) was 7.16 mg/ml determined with Braford protein method using BSA as a standard.

9.2.2 Synthesis of PMMA/PVAm core-shell particles

For a total weight of 50 g, PVAmHCl (0.25 g) was dissolved in DI water and the pH of the solution was adjusted to 12 with 10% NaOH solution. The solution was then mixed with purified MMA (1 g) in a three-necked water-jacketed flask equipped with a thermometer, a reflux condenser and a nitrogen inlet and purged with nitrogen under stirring for 30 minutes to remove oxygen. A diluted TBHP solution (0.5 mL of 10 mM solution) was added and the mixture was stirred at 80℃ for 3 hours. After the reaction, the monomer conversion was determined gravimetrically. The particle dispersion was carefully purified by repeated centrifugation-decantation-dispersion cycles using DI water to remove unreacted water-soluble polymer and unreacted monomer and other low molecular weight of impurities. The solid content of the purified PMMA/PVAm core-shell particle dispersion was 1.49% w/w.

9.2.3 Characterization of PMMA/PVAm core-shell particles

The graft copolymers and homopolymers were isolated by Soxhlet extraction with chloroform for 48 hours. The grafting efficiency (GE%) was calculated as follows:

$$\text{GE}\,\% = \frac{\text{Weight of the grafted}}{\text{Weight of the total polymerized}} \times 100$$

Particle size and size distribution were measured on a Coulter LS 230 Particle Size Analyzer. The ζ-potential of the particles was determined with a Malvern Zetasizer 3000HSA (Malvern, UK) in a 1 mM NaCl solution. The surface morphologies of the particles were examined with a JEOL JSM 6335F Field Emission Scanning Electron Microscopy (FE-SEM). Samples were prepared by spreading dilute particle dispersion on a glass surface, followed by coating the dried particles with a thin layer of gold to a depth of ca. 5 Å. under vacuum.

9.2.4 Protein assay

Protein concentration was estimated by the Bradford protein assay method using BSA as a standard.[17]

9.2.4.1 Preparation of dye stock solution

Coomassie brilliant blue G-250 (CBB, 85.4 mg) was dissolved in 90% ethanol (40 mL). The solution was mixed with phosphoric acid solution (85 w/v%, 83 mL), then diluted to 500 mL with DI-water and stored at room temperature (used within one month).

9.2.4.2 Preparation of stock standard solution of BSA

BSA (about 100 mg) was dissolved in DI water (100 mL) at room temperature and stored below 4 °C (used within one month). The exact concentration of the BSA standard solution was determined with Bradford protein method.

9.2.4.3 Calibration of BSA stock standard solution

The calibration curve was established as follows. For a total volume of 3 mL, dye stock solution (2 mL), DI water (1.00~0.90 mL) and BSA standard solution (0.00~0.1 mL, 1 mg/mL) were mixed thoroughly in eleven test tubes, respectively, and kept at room temperature for 5 minutes to allow complete reaction between BSA and the dye. Finally the solutions were measured at a maximum absorbance of 595 nm on a UV/VIS spectrophotometer (Perkin-Elmer Lambda 35).

Figure 9.1 shows a calibration curve of BSA standard solution with the amount of protein from 10 to 100 μg. The calibration curve has a linear relationship with the equation of $y=0.0158x-0.2317$ ($R^2=0.9878$). To determine the protein concentration of an unknown sample, the sample (0.05 mL), the dye solution (2 mL) and DI-water (0.95 mL) were mixed and reacted as described above. Then the maximum absorbance of the mixture was determined at 595 nm on a UV/VIS spectrophotometer and the amount of protein in solution was calculated from the calibration curve of BSA solution. If the concentration was too high, the sample should be diluted to an appropriate concentration.

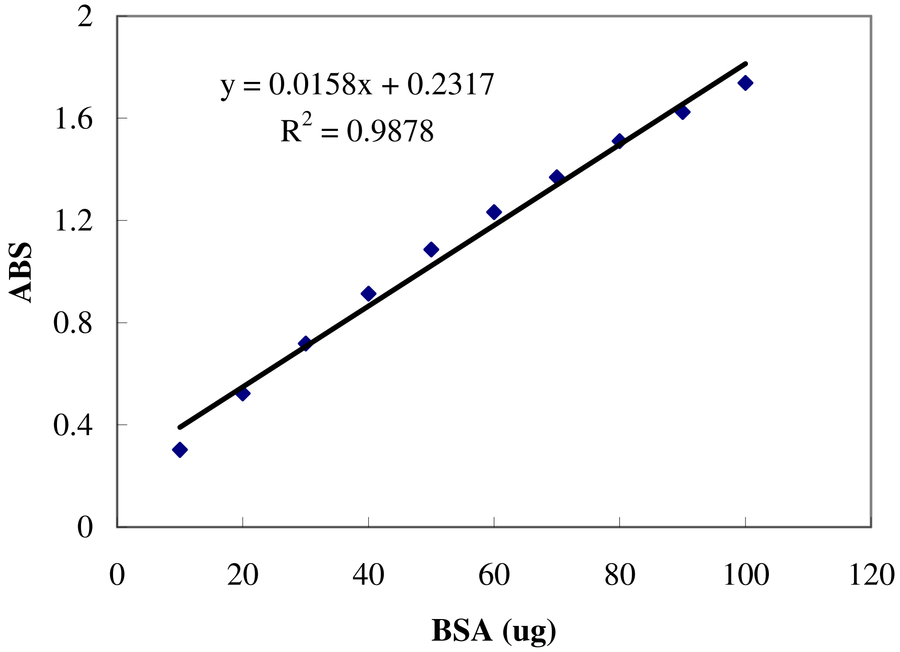

Figure 9.1 Calibration curve of BSA standard solution

9.2.5 Immobilization of enzyme

For a total volume of 2 mL, particle solution (14.9 mg/mL) (500 μL), cellulase solution (7.16 mg/mL) (50~1500 μL) and distilled water (1450~0 μL) were mixed in nine tubes, respectively, and the mixtures were shaken for 4 hours at room temperature. Then the enzyme-support complex was separated by centrifugation at 13000 rpm for 10 minutes, followed by washing three times with distilled water (1.0 mL per time). The amount of un-immobilized enzyme in supernatant was determined using the protein assay as described above.

9.2.6 Determination of loading amount of enzyme

The loading amount of enzyme is defined as the amount of enzyme immobilized onto per gram of particles. It is calculated as follows:

$$\text{Loading amount (mg/g)} = \frac{\text{Total amount of immobilized enzyme (mg)}}{\text{Total amount of particles added (g)}}$$

9.2.7 Determination of immobilization efficiency

The immobilization efficiency is defined as the percentage of enzyme immobilized onto the particles. It is calculated according to the following equation:

$$\text{Immobilization efficiency \%} = \frac{\text{Total amount of immobilized enzyme}}{\text{Total amount of enzyme added}} \times 100$$

9.2.8 Cellulase assay

9.2.8.1 Reagents:

(1). NaOH/KOH solution (4 M NaOH and 4 M KOH) (I)

NaOH (16 g) and KOH (22.4 g) were dissolved in DI water (80 mL) and the solution was diluted to 100 mL.

(2) 3,5-Dinitrosalicylic acid (DNS) reagent (stop solution)

DNS (2.0 g) was dissolved in DI-water (120 mL) at 50 ^{o}C. The NaOH and KOH solution (I) (20 mL) was then added dropwise into the solution under stirring, followed by the addition of potassium sodium tartrate tetrahydrate (60 g) under stirring at 50 ^{o}C. Finally the solution was cooled down to room temperature, diluted to

200 mL and stored at room temperature under dark environment.

(3) Buffer solutions

Acetate/acetic acid buffer (0.2 mM)

Table 9.1. Preparation of Acetate/acetic acid buffer

200 mM NaAc solution (mL)	200 mM HAc solution (mL)	Total volume (mL)	pH
18	82	100	4.0
49	51	100	4.6
70	30	100	5.0

Sodium acetate (NaAc) trihydrate (2.722 g) and anhydrous acetic acid (HAc) (1.17 g) were separately dissolved in DI water (100 mL) to give a 200 mM NaAc solution and a 200 mM HAc solution respectively. Acetate/acetic acid buffers with pH ranging from 4.0 to 5.0 were prepared according to the formulations listed in Table 9.1.

Borate buffer

Table 9.2. Preparation of borate buffer

200 mM borax solution (mL)	100 mM HCl solution (mL)	100 mM NaOH solution (mL)	DI water (mL)	Total volume (mL)	pH
50	4.60	/	45.4	100	9.0
50	/	18.3	31.8	100	10.0

Borax ($Na_2B_4O_7$) (0.2515 g) was dissolved in DI water (50 mL) to give a 25 mM borax solution. Two borate buffers with pH at 9.0 and 10.0 respectively were prepared according to the formulations listed in Table 9.2.

Phosphate buffer (0.2 M)

Table 9.3. Preparation of phosphate buffer

200 mM NaH_2PO_4 solution (mL)	200 mM Na_2HPO_4 solution (mL)	Total volume (mL)	pH
87.7	12.3	100	6.0
39	61	100	7.0
5.3	94.8	100	8.0

Sodium dihydrogen orthophosphate (NaH_2PO_4) (3.121 g) and disodium hydrogen phosphate 12-hydrate ($Na_2HPO_4 \bullet 12H_2O$) (7.164 g) were separately dissolved in DI water (100 mL) to give a 200 mM NaH_2PO_4 solution and a 200 mM Na_2HPO_4 solution respectively. Phosphate buffers with pH ranging from 6.0 to 8.0 were prepared according the formulations listed in Table 9.3.

(4) Substrate for cellulase

Sodium carboxy methyl cellulose powder (CMC, 4.0 g) was dissolved in acetate buffer (50 mL) at 100 ^{o}C and the solution was diluted to 100 mL with DI water.

(5) Glucose stock standard solution (100 mM)

S-glucose (1.8000 g) was dissolved in DI water (20 mL) in a 100 mL volumetric flask and the solution was diluted to 100 mL with DI water. The stock solution was stored at room temperature in darkness (used within one month).

9.2.8.2 Calibration of glucose solution

The calibration curve was established as follows. D-glucose stock solution (0~60 μL) was charged separately into thirteen test tubes, and each of the solution was diluted to 330 mL with DI water (330~270 μL). The stop solution (DNS solution, 0.15 mL) was then charged into each of the tube. The mixture in each tube was shaken thoroughly. After incubation in boiling water for 10 minutes, the solution was cooled down quickly in an ice-bath for 5 minutes, followed by addition of DI water (1.5 mL). Finally the solution was measured for its maximum absorbance at 530 nm on an UV/VIS spectrophotometer with the solution without D-glucose as a blank solution.

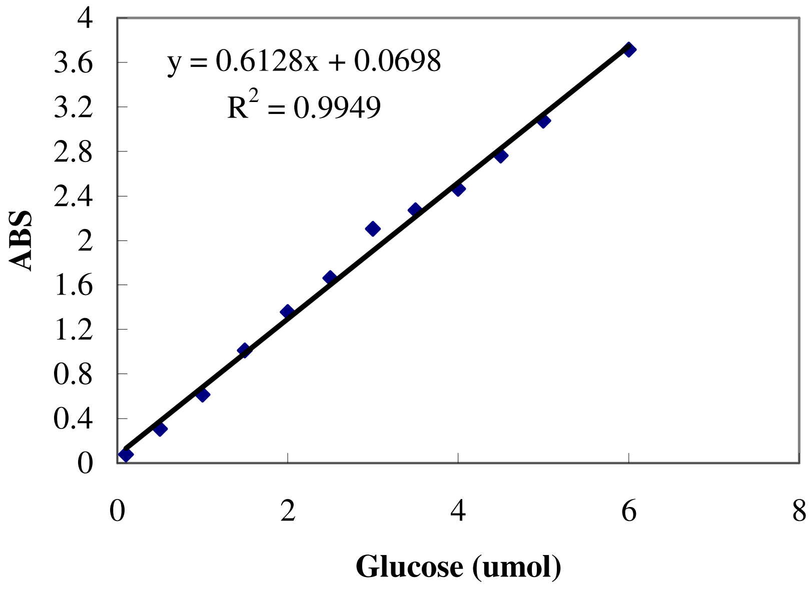

Figure 9.2. Calibration curve of glucose standard solution

Figure 9.2 shows a calibration curve of D-glucose standard solution with the amount of glucose from 0.1 to 6.0 μmol. The calibration curve has a linear relationship with the equation of y=0.6128x-0.0698 (R^2=0.9949). The amount of glucoses in solution could be calculated from the calibration curve of glucose solution and then the activity of cellulose could be calculated based on the equation in 9.2.9.

9.2.9 Determination of activity of free and immobilized enzyme

The enzymatic activity on CMC was determined using 3,5-dinitrosalicylic acid (DNS) reagent as a stop reagent according to a literature method.[18] The activity was calculated as follows:

$$\text{Activity of cellulase (IU/g])} = \frac{\text{Amount of produced glucose (μmol)}}{W \times t}$$

The amount of glucose (μmol) produced was calculated from the calibration curve. W is the amount of enzyme (g), while t is the time of reaction. One international unit (IU) is the amount of enzyme that releases 1 μmol of reducing glucose per minute from the CMC under the assay conditions.

9.2.10 Measurement on activity of enzyme

Cellulase solution (5~50 μL) or PMMA/PVAm particle-enzyme complex samples (50 μL) was charged in a tube and heated for 5 minutes at 50 ^{o}C in a water bath. Substrate solution (0.15 mL) and pH buffer (0.13 mL) that had been pre-heated to 50 ^{o}C were reacted with the cellulose solution at 50 ^{o}C for 20 minutes precisely. Then the stop solution (0.15 mL) was added to terminate the reaction and the mixture was incubated in boiling water for 10 minutes. The mixture was cooled down quickly in an ice-bath for 5 minutes, followed by addition of DI water (1.5 mL). Finally the maximum absorbance of the mixture at 530 nm was measured on an UV/VIS spectrophotometer using the solution without D-glucose as a blank and the amount of glucose produced was calculated from the standard curve.

9.2.11 Determination of efficiency of immobilization (E_{imm})

Efficiency of immobilization is obtained by comparing the activity of the immobilized enzyme to the total activity of original free enzyme under the same conditions. It was calculated according to the following equation:

$$E_{imm}\ \% = \frac{\text{Actual activity of immobilized enzyme}}{\text{Total activity of original enzyme solution used}} \times 100$$

9.2.12 Determination of specific cellulase activity (E_{spe})

Immobilized specific cellulase activity is obtained by comparing the activity of the immobilized enzyme to the activity of the free enzyme under the same condition. It was calculated according to the following equation:

$$E_{spe}\ \% = \frac{\text{Actual activity of immobilized enzyme}}{\text{Theoretical activity of immobilized enzyme}} \times 100$$

9.2.13 Statistical data analysis

Statistical data analysis was performed using the *t*-test with $p < 0.05$ as the minimal level of significance.

9.3. Results and Discussion

9.3.1 Synthesis and characterization of PMMA/PVAm core-shell particles

As shown in Scheme 9.1, amphiphilic PMMA/PVAm core-shell particles were prepared via a direct graft copolymerization of MMA from PVAm in water using TBHP as an initiator. The PVAmHCl was first converted to PVAm by adjusting the pH of PVAmHCl solution to 12 with 10% NaOH solution. Then the PVAm solution was treated with a small amount of TBHP at 80 ^{o}C in the presence of MMA to generate PMMA/PVAm core shell particles.

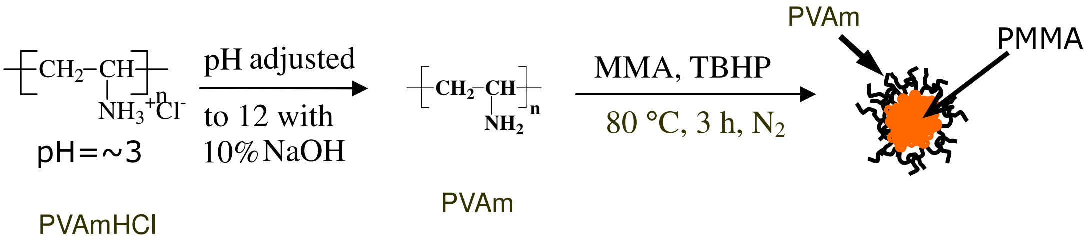

Scheme 9.1 Synthesis of PMMA/PVAm particles

Table 9.4 Synthesis and properties of PMMA/PVAm particles [a]

Conversion	Dv (nm)	Dn (nm)	PDI	Grafting efficiency (%)	ζ-potential (mV)
69%	262	186	1.41	59	+44.6

[a] Reaction conditions: PVAmHCl: 0.25g; MMA: 1g; [TBHP]: 0.1 mM; solid content : 2.5%; total weight: 50g; reaction time: 3 h; temperature: 80 ^{o}C; Reaction pH=12.

A monomer conversion up to 69% was obtained under a very low TBHP concentration (0.1 mM) (Table 9.4). ζ-Potential measurement showed that the surface charge of the particles was +46.8 mV, indicating the formation of cationic PVAm shells. Dynamic light scattering measurement indicated that the volume average diameter (D_v) and number average diameter (D_n) were 262 and 186 nm, respectively with a relatively broad size distribution (PDI=1.4). The slightly broad size distribution might be due to the use of lower molecular weight of PVAm (190K Delton), which had poor steric stabilization for the particles during the particle formation.

The PMMA/PVAm core-shell particles were composed of both amphiphilic grafted copolymers and hydrophobic homopolymers, which were separated by Soxhlet extraction of the resultant polymers with chloroform for 48 hours, as described in Chapter 4. Compositions of the homopolymers obtained from the organic layer and the insoluble graft copolymers were determined gravimetrically. It was found that the grafting efficiency were 59% (Table 9.4). In other words, more than half of PMMA in the core was attached to the water soluble polymer.

The surface morphologies of the PMMA/PVAm core shell particles were observed with FE-SEM. Figure 9.3 shows that the particles were spherical with uneven surfaces. This uneven surfaces might increase the specific area of the particles, thus is favorite for immobilization of enzymes.

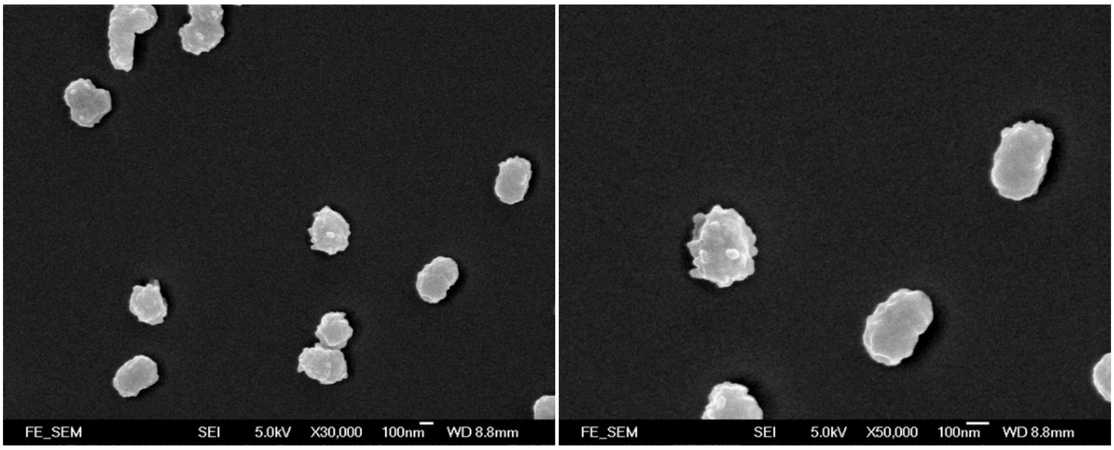

Figure 9.3. FE-SEM micrographs of the PMMA/PVAm particles

9.3.2 Enzyme immobilization

Cellulase was used as a model enzyme to examine the bio-immobilization ability of the PMMA/PVAm particles. There are three method that can be used to achieve the immobilization: (1) Direct contact of enzyme with the nanoparticles (physical adsorption); (2) Crosslinking of the enzyme adsorbed onto the nanoparticles (crosslinking method); and (3) Activation of the nanoparticles prior to immobilization (covalent method). Among them, physical adsorption is the simplest process and the enzyme absorbed on the particles would have little lose of their biological activity. Thus physical adsorption was adopted to immobilize the cellulase on the PMMA/PVAm particles.

The immobilization of cellulase on PMMA/PVAm particles was achieved by mixing the particle solution with the cellulase solution for 4 hours at room temperature. Scheme 9.2 demonstrates the use of PMMA/PVAm particles as a carrier for enzyme immobilization. Cellulase molecules were adsorbed spontaneously from solution onto the surface of the spherical particles. The main driving force for the interaction between particles and enzyme molecules were expected to be the positive-negative charge interaction between the cationic polyelectrolyte chains and the enzyme molecules.[4, 15]

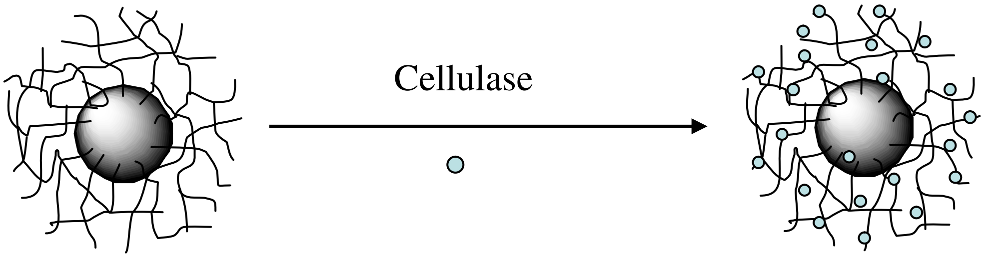

Scheme 9.2 Adsorption of cellulase on PMMA/PVAm particles.

The absorption of cellulase was carried out under different cellulase concentrations. The unabsorbed cellulase was collected and determined by protein assay based on the calibration curve. The loading amount of enzyme and the immobilization efficiency as functions of the enzyme concentration are shown in Figure 9.4. The loading amount of enzyme increased rapidly from about 48 to 192 mg/g as the enzyme concentration increased from 0.18 to 0.72 mg/mL, while the immobilization efficiency was almost 100%. In other word, almost all the enzyme molecules in the solution were absorbed onto the particle surface during this stage. Further increase of the concentration of enzyme up to 5.4 mg/mL had little effect on the loading amount. However, the immobilization efficiency quickly decreased from 100% to 18%. These results show that the maximum immobilization capacity of the particles was achieved at enzyme concentration ranging from 0.72~1.44 mg/mL. Thus the maximum loading amount of enzyme for the PMMA/PVAm particles used here was about 200 mg/g. This value was much less than that for the PMMA/PEI particles which we have reported (530 mg/g).[15] The relatively low immobilization capacity might be due to two reasons: (1) Thinner PVAm shell due to lower weight ratio (MMA : PVAm = 7.5 :1) used in the synthesis of the particles. (2) Some of the amino groups in the shell of the particles reacted with CO_2 during the purification process, thus losing partially its activity in absorption of enzyme molecules. Therefore, the pH of the particle dispersion should be adjusted to 2~3 to eliminate the CO_3^{2-} ions formation before the purification.

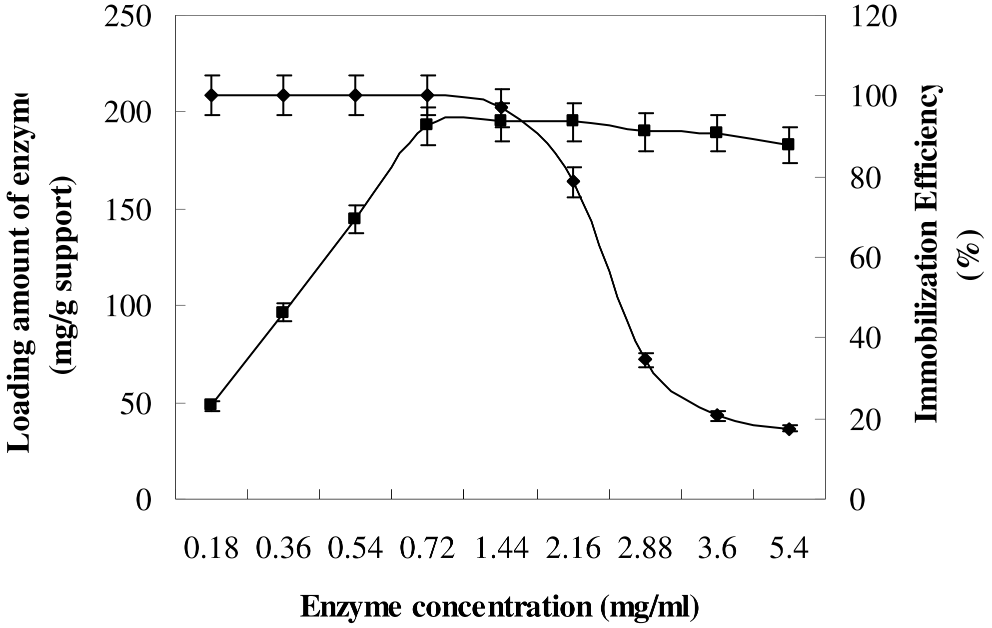

Figure 9.4 Loading amount and Immobilization efficiency as a function of enzyme concentration. (■) loading amount of enzyme; (◆) immobilization efficiency.

Sodium carboxy methyl cellulose (CMC) was used as a substrate for study of cellulase activity. Cellulase hydrolyzes CMC to D-glucose which subsequently was monitored by UV/VIS spectroscopy. The data obtained from the bound enzyme were compared with the results obtained from the free cellulase. The efficiency of immobilization (E_{imm}) and the specific cellulase activity (E_{spe}) were then calculated based on these results.

Figure 9.5 shows the effect of enzyme concentration on the E_{imm} and the E_{spe}. It is well known that enzyme would lose some of its activity during the immobilization. Therefore the initial E_{imm} and E_{spe} with the enzyme concentration of 0.18 mg/mL were low. When the concentration of enzyme increased, the free enzyme molecules in the solution would counteract the de-activity of the enzyme molecules immobilized, thus decrease the percentage of the de-actived enzyme molecules over the total enzyme molecules charged. Thus both the E_{imm} and the E_{spe} increased rapidly at first from 36% to 69% as the enzyme concentration increased from 0.18 to 0.36 mg/mL.,Further increasing the enzyme concentration to 1.44 mg/mL had little effect on the E_{imm} and the E_{spe} which was because almost all the enzyme molecules were immobilized on the particles. When the enzyme concentration increased to upto 5.4 mg/mL, however, the E_{imm} decreased rapidly while the E_{spe} increased to nearly 100%. The quick decrease of E_{imm} was due to the sharp decrease in immobilization efficiency, while the increase in E_{spe} was due to the existence of large amount of excess enzyme in solution counteracted the loss of enzyme activity during the immobilization.

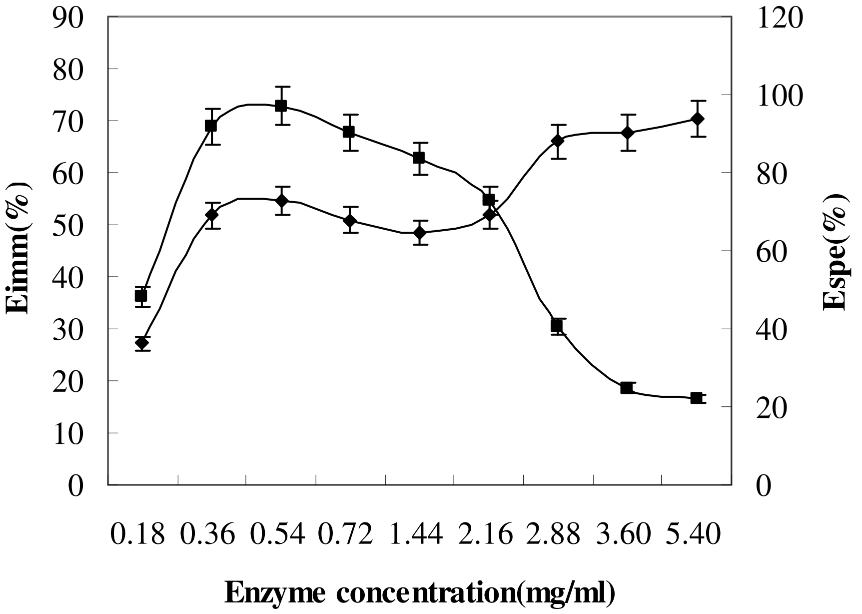

Figure 9.5 E_{imm} and E_{spe} as a function of enzyme concentration. (■) Efficiency of immobilization (E_{imm}); (◆) Specific activity (E_{spe}).

9.4 Conclusions

In conclusion, we demonstrated that PMMA/PVAm core-shell particles could immobilize an enzyme with high capacity (up to 200 mg/g) and the activity of immobilized enzyme could be preserved (94%). The capacity of immobilization of enzymes might be improved by further optimizing the conditions for the synthesis of PMMA/PVAm particles. Thus future studies will be directed to investigation of conditions on PMMA/PVAm particles and subsequently on the immobilization of enzymes.

References:

1. Mateo, C.; Palomo, J. M.; Fernandez-Lorente, G.; Guisan, J. M.;

Fernandez-Lafuente, R., Improvement of enzyme activity, stability and selectivity via immobilization techniques. *Enzyme and Microbial Technology* **2007,** 40, (6), 1451-1463.

2. Wilhelm, T.; Frank, W., *Immobilized Enzymes: Methods and Applications*. 1999; p 95-126.
3. Cao, L., *Carrier-bound immobilized enzymes : principles, applications and design*. Wiley-VCH: Weinheim, 2005; p xv, 563.
4. Neumann, T.; Haupt, B.; Ballauff, M., High activity of enzymes immobilized in colloidal nanoreactors. *Macromolecular Bioscience* **2004,** 4, (1), 13-16.
5. Yasuda, M.; Kobayashi, M.; Kotani, T.; Kawahara, K.; Nikaido, H.; Ueda, A.; Ogino, H.; Ishikawa, H., Synthesis of amphiphilic polymer particles by seed polymerization and their application for lipase immobilization. *Macromolecular Chemistry and Physics* **2002,** 203, (2), 284-293.
6. Panesar, P. S.; Kennedy, J. F., *Carrier-bound Immobilized Enzymes: Principles, Application and Design, by L. Cao, Wiley-VCH Verlag, GmbH & Co. KGaA, Weinheim, Germany: 2005*. 2006; Vol. 64, p 603.
7. Caruso, F.; Trau, D.; Moehwald, H.; Renneberg, R., Enzyme Encapsulation in Layer-by-Layer Engineered Polymer Multilayer Capsules. *Langmuir* **2000,** 16, (4), 1485-1488.
8. Caruso, F.; Schuler, C., Enzyme Multilayers on Colloid Particles: Assembly, Stability, and Enzymatic Activity. *Langmuir* **2000,** 16, (24), 9595-9603.
9. Hong, J.; Xu, D.; Gong, P.; Sun, H.; Dong, L.; Yao, S., Covalent binding of

[alpha]-chymotrypsin on the magnetic nanogels covered by amino groups. *Journal of Molecular Catalysis B: Enzymatic* **2007,** 45, (3-4), 84-90.

10. Wittemann, A.; Haupt, B.; Ballauff, M., Polyelectrolyte-mediated protein adsorption. *Progress in Colloid and Polymer Science* **2006,** 133, 58-64.
11. Cooper, C. L.; Dubin, P. L.; Kayitmazer, A. B.; Turksen, S., Polyelectrolyte-protein complexes. *Current Opinion in Colloid & Interface Science* **2005,** 10, (1-2), 52-78.
12. Jackler, G.; Wittemann, A.; Ballauff, M.; Czeslik, C., Spherical polyelectrolyte brushes as carrier particles for proteins: An investigation of the structure of adsorbed and desorbed bovine serum albumin. *Spectroscopy (Amsterdam, Netherlands)* **2004,** 18, (2), 289-299.
13. Wittemann, A.; Haupt, B.; Ballauff, M., Adsorption of proteins on spherical polyelectrolyte brushes in aqueous solution. *Physical Chemistry Chemical Physics* **2003,** 5, (8), 1671-1677.
14. Haupt, B.; Neumann, T.; Wittemann, A.; Ballauff, M., Activity of Enzymes Immobilized in Colloidal Spherical Polyelectrolyte Brushes. *Biomacromolecules* **2005,** 6, (2), 948-955.
15. MAO, X.; HUANG, J.; LEUNG, M. F.; DU, Z.; MA, L.; HUANG, Z.; LI, P.; GU, L., Novel Core-Shell Nanoparticles and Their Application in High-Capacity Immobilization of Enzymes. *Applied Biochemistry and Biotechnology* **2006,** 135, (3), 229-246.
16. Wittemann, A.; Haupt, B.; Merkle, R.; Ballauff, M., Interaction of dissolved

proteins with spherical polyelectrolyte brushes. *Macromolecular Symposia* **2003,** 191, (Molecular Order and Mobility in Polymer Systems), 81-88.

17. Bradford, M. M., A rapid and sensitive method for the quantitation of microgram quantities of protein utilizing the principle of protein-dye binding. *Analytical Biochemistry* **1976,** 72, (1-2), 248-254.
18. Miller, G. L., Use of Dinitrosalicylic Acid Reagent for Determination of Reducing Sugar. *Analytical Chemistry* **1959,** 31, (3), 426-428.

Chapter 10 Conclusions

Novel routes have been developed to synthesize various amphiphilic core-shell particles that consist of well-defined hydrophobic polymer cores and polyvinylamine (PVAm)-based shells via direct graft copolymerization of vinyl monomer(s) from PVAm-based water soluble polymers, such as polyvinylamine, poly(vinylalcohol-co-vinylamine) and poly(*N*-vinylacetamide-co-vinylamine) using *tert*-butyl hydroperoxide as an initiator in aqueous system.

The PVAm-based water soluble polymers were synthesized through a two-step reaction: 1) The free-radical polymerization of *N*-vinylacetamide (NVA), or *N*-vinylformamide (NVF) with/without vinyl acetate in water to generate a poly(*N*-vinylalkylamide)-based polymer; 2) The hydrolysis of the preformed poly(*N*-vinylalkylamide)-based polymer to PVAm-based polymer under acidic conditions. When NVF was used, the hydrolysis of poly(*N*-vinylformamide) (PNVF) must achieve complete conversion in order to avoid the existence of residual aldehyde groups, which can react with TBHP to inhibit the initiation of the graft copolymerization of MMA from PVAm.

The PVAm-based water soluble polymers were treated with a small amount of *tert*-butyl hydroperoxide (TBHP) in aqueous to generate free radicals that were able to initiate both the graft- and homo-polymerization of vinyl monomer(s) such as *n*-butyl acrylate (BA), methyl methacrylate (MMA) and styrene to generate the amphiphilic core-shell particles. Stable and highly mono-dispersed particles were produced in high yield with diameter in the range between 100 and 300 nm. The formation of graft copolymers and homopolymers was confirmed by Fourier Transform Infrared spectroscopy (FT-IR). ζ-Potential measurement confirmed the formation of cationic PVAm-based shells. The purified PMMA/PVAm particles possess a pH-sensitive property.

The reaction conditions were optimized via systematical investigation on reaction pH, initiator concentration, weight ratio of PVAm to MMA, salt concentration and solid content. Tailoring the shell thickness and surface functionality of particles were carried out via variation of molecular weight and functionality of PVAm-based polymers as well as their polymeric architectures (crosslinking degree of PVAm) with respect to the particle stability, monomer conversion, particle size and size distribution, surface charge density, grafting percentage and efficiency, and surface morphology.

The formation of stable particles was strongly dependent on the reaction pH, weight ratio of PVAm to MMA, salt concentration and molecular weight of PVAm. With the increase of reaction pH (from 7 to 12), weight ratio of PVAm to MMA (from 1:16 to 1:4) and molecular weight of PVAm (from 35 K to 400 K Delton), the stability of particles generated increased because less precipitate were formed during the graft copolymerization. In addition, the particle dispersion could be stable up to a salt concentration of 0.5 M.

The monomer conversion increased with the increase of reaction pH, initiator concentration, weight ratio of PVAm to MMA, and amination degree of poly

(NVA-co-VAm). The grafting efficiency of the PMMA increased with the increase of reaction pH and the decrease of TBHP concentration.

The particle size and size distribution were could be controlled through variation of the TBHP concentration and crosslinking degree of PVAm. The particle size decreased with the increase of TBHP concentration and crosslinking degree of PVAm.

The surface functionality of the particles could be controlled by tailoring the functionality of the PVAm-based polymer. Multi-functional particles such as poly(vinylalcohol-co-vinylamine) and poly(*N*-vinylacetamide-co-vinylamine) be obtained by controlling the functionalities of the water-soluble polymer containing amino groups.

Stable and highly uniform PMMA/PVAm particles could be obtained with a high monomer conversion of up to 81% through the graft copolymerization of MMA from linear PVAm at 80 ^{o}C for 3 h at pH 11 using very low TBHP concentration (2.0×10^{-4} M), while PS/PVAm particles need a higher TBHP concentration (2.0×10^{-3} M) and a longer reaction time (up to 5 h) to achieve a complete styrene conversion. This effect may be attributed to poorer water solubility and lower propagation rate of styrene than MMA. However, when BA was used, stable particles could not be formed using linear PVAm, and the poly(BA-MMA)/PVAm particles obtained using slightly crosslinked PVAm were about 120 nm in diameter, much smaller than PS/PVAm (about 190 nm) and PMMA/PVAm (about 240 nm) particles.

Transmission Electron Microscopy (TEM) micrographs of the particles revealed that they had well-defined core-shell nanostructures with thick and hairy PVAm shells. Surface morphology studies with Field Emission Scanning Electron Microscopy (FE-SEM) and particle size analysis with dynamic light scattering indicated that the structure of vinyl monomer and water-soluble polymer strongly influenced particle formation, size and morphology. The PS/PVAm particles were spherical with smooth surfaces, while the PMMA/PVAm and poly(BA-MMA) particles had rough surfaces. The variation in particle morphology might be attributed to the large difference in the grafting efficiency among the three types of particles and the side reactions between monomer(s) with PVAm during the polymerization. The grafting efficiencies of the PMMA/PVAm and poly(BA-MMA) particles (more than 76%) is much higher than PS/PVAm particles (about 15%). In addition, BA, MMA and styrene can reacted with PVAm through Michael addition. However, Styrene is more difficult to reaction with PVAm than MMA, while BA is easier than MMA. The hydrolysis of MMA and/or BA to methacrylic acid and/or acrylic acid, which further form salts with PVAm, also occurs when the polymerization is carried out at alkaline conditions. The hydrolysis and the Michael addition of PVAm to MMA lead to the hydrophobic modification of the PVAm. Both the high grafting efficiencies and the hydrophobic modification of PVAm can lower the interfacial tension at the polymer–polymer interface and improve the solubility of PMMA in PVAm phase. Thus, the rough particle surface of PMMA/PVAm and poly(BA-MMA) particles is likely the consequence of phase separation of the hydrophobic segments and/or PMMA in PVAm shells.

The application of PMMA/PVAm particles in enzyme immobilization was explored. PMMA/PVAm core-shell particles could immobilize cellulase with high capacity (up to 200 mg/g) and nearly full preservation of its activity (94%). Thus the PVAm-based core-shell particles are potential carrier for enzyme immobilization.

Chapter 11 Future Study

(1) Synthesis of various branched PVAm-based polymers and their applications in the synthesis of PVAm-based core-shell particles.

We have found that the crosslinking degree of PVAm has great influence on the particle formation, particle size and size distribution, surface morphology, etc. However, using glutaraldehyde to crosslink PVAm have some disadvantages: (1) the residual aldehyde groups may react with TBHP, preventing the initiation of the graft copolymerization of vinyl monomer(s) from PVAm; (2) the crosslinked product using glutaraldehyde is easy to become yellow, introducing an unpleasant color for the particles. Thus it is better to find an alternative way to crosslink the PVAm: (1) using other crosslinkers such as hexane diacid, (2) synthesis of crosslinked poly(*N*-vinylacetamide) or poly(*N*-vinylformamide), followed by hydrolysis.

(2) Design and synthesis of multi-functional random or block copolymers containing amino-groups and their applications in the synthesis of multi-functional core-shell particles.

We have demonstrated that it is possible to synthesize multi-functional core-shell particles through controlling the functionalities of PVAm-based polymers. It will be of great interest to design and synthesize various multi-functional core-shell particles to meet specific requirements.

(3) Application of PVAm-based core-shell particles in various areas.

PMMA/PVAm particles have showed its great potential in enzyme immobilization. However, the results are just preliminary. Thus systematic investigation of synthetic conditions, various immobilization strategies and activity of the immobilized enzyme are necessary. Other applications of the particles as composite materials, coating and adhesives should also be exploited.